An Evaluation of Thallium-201 as Tumour Imaging Agent

BY

DR. ALI MAHMOUD SEHWEIL

B.Sc., (Med) Gr. Board of Radiology & Radiotherapy

A Thesis presented for the Degree of Ph.D.,

Glasgow University

Nuclear Medicine Department, Glasgow University

and

Nuclear Medicine Department, Kuwait Cancer Control Center

Ministry of Public Health, Faculty of Medicine, Kuwait University

1988

Supervisors

James H. McKillop, FRCP., Ph.D.

Senior Lecturer

Glasgow University

Prof. Hussain Abdel Dayem, MD.

Chairman of Nuclear Medicine

Kuwait University

Dr. Yousuf T. Omar, FRCR

Director, Kuwait Cancer Control Centre, Kuwait

TABLE OF CONTENTS

CHAPTER IV: MECHANISM OF TL-201 UPTAKE IN TUMOURS

CHAPTER V: THALLIUM-201 CHLORIDE SCINTIGRAPHY IN THE DIAGNOSING AND STAGING OF MALIGNANT DISEASE

Note: Tables and figures relating to the individual chapters are placed at the end of that chapter.

LIST OF TABLES

ACKNOWLEDGMENT

I am deeply indebted to my supervisor, Dr. J.H. McKillop, Senior Lecturer in the Faculty of Medicine at Glasgow University, and Professor Hussain Abdel-Dayem, Chairman of the Department of Nuclear Medicine in the Faculty of Medicine and Ministry of Public Health, who always supervised and guided me at every stage of the work. In spite of their busy schedules, they found time to spare their ideas, comments and corrections. Without their inspiration, guidance and tolerance this work would not have been completed.

My thanks to Dr. H. Gray, Dr. Bassent and Dr. Milroy whose encouragement and assistance are deeply acknowledged.

Dr. Y.T. Omar, Director of the Kuwait Cancer Control Center, Ministry of Public Health, Kuwait, deserves my sincerest gratitude for arranging the study, allowing me to use the facilities of the Centre for the project, and his continuous support and encouragement. Thanks are also extended to my colleagues and staff both in Kuwait and Glasgow Royal Infirmary who constantly bore with me and took extra work during the project.

I must also acknowledge the British Council for its financial grant which enabled me to fulfill partially the university tuition fees.

Appreciation is also due to Mrs. Stephanie Atieh for her great efforts in typing this thesis.

Finally, to my wife, Mariam, and our children Reem, Nidal and Khalid, thank you for your love and support.

Parts of this work have been accepted for publication, oral presentation or poster discussion at international scientific meetings.

1. Sehwell A, El-Sayed M, Ziada G, Al-Huda F, Momarak L, Omar YT, Abdel-Dayem HM and McKillop JH: Thallium-201 Kinetics in malignant tumours. J Nucl Med 1986; 27:1033.

   This abstract was accepted as a poster presentation in the 33rd Annual Meeting of the Soiciety of Nuclear Medicine, June 22-25, 1986, Washington, D.C.

2. Same abstract was accepted for oral presentation in the European meeting of the Society of Nuclear Medicine, Goslar, 4 September 1986.

3. Sehwell A, Milroy R, McKillop JH, Abdel-Dayem HM, Al-SAyed M, Ziada G, Banham SW, Davidson KG: Thallium-201 chloride in the staging of lung cancer.

   This abstract was accepted for oral presentation at BNMS Annual Meeting, 13 - 15 April 1987, London.

4. Sehwell A, McKillop JH, Ziada G, Al-Sayed M, Abdel-Dayem H and Omar YT: The optimum time for tumour imaging with Thallium-201.

   This abstract was accepted for oral presentation at BNMS Annual Meeting, 13 - 15 April 1987, London.

5. Sehwell A, El-Sayed M, Ziada G, Abdel-Dayem H, and McKillop JH: Thallium-201 chloride in brain and soft tissue tumours.

   This abstract was accepted for oral presentation at BNMS Annual Meeting, 13 - 15 April 1987, London.

6. Sehwell AM, McKillop JH, Abdel-Dayem H, El-Sayed M, Omar YT: Thallium-201 chloride imaging in the tumours of the liver.

This abstract was accepted for oral presentation at BNMS Autum Meeting, 2 October 1987, Oxford.

7. Sehwell AM, McKillop JH, Milroy R, Wilson R, Abdel-Dayem HM: Mechanism of Thallium-201 uptake in tumours.

This abstract has been accepted for oral presentation at the Society of Nuclear Medicine 35th Annu7al Meeting, June 14-17 1988, San Francisco, California.

8. Sehwell A, McKillop JH, Ziada G, Al-Sayed M, Abdel-Dayem H and Omar YT: The optimum time for tumour imaging with Thallium-201. Eur J Nucl Med 1988; 13:527-529.

9. El-Gazzar AH, Sehwell A, Zaki O, Mahmoud A, Omar YT, Abdel-Dayem HM: Tl-201 uptake in lymphangitis carcinomatosis. Case Report. Nuc Compact 1988; 19:28-29.

10. El-Gazzar AH, Malki AA, Sehwell A, et al.: Role of thallium-201 in etiologic classification of solitary bone lesions (SBL).

This abstract has been accepted for oral presentation at the Society of Nuclear Medicine 35th Annual Meeting, June 14-17 1988, San Francisco, California.

11. McKillop JH, Sehwell A, Abdel-Dayem HM et al.: Thallium Imaging and Tumours.

This abstract has been accepted at the Australian and New Zealand Nuclear Medicine Society Meeting, Sydney, May 1988.

SUMMARY

I evaluated thallium-201 chloride as a tumour imaging agent.

I studied the time course of Tl-201 uptake in various tumours in order to establish the best time for imaging tumours following injection of the tracer. The results show that uptake occurs rapidly in tumours with a peak value obtained 8 to 20 minutes post-injection in various tumours studied. The mean time of tumour uptake (±SD) was 11.2 (±3.34) minutes for lung carcinoma, 11.21 (±1.88) minutes for breast carcinoma and 11.76 (±3.25) minutes for lymphoma. There were no significant differences in different tumour types.

Tumour to background ratios also rapidly attained peak values and remained relatively constant over the hour following injection. The mean (±SD) time of maximal tumour/background activity was assessed and found for lung cancer to be 18.3 (±0.59) minutes, breast cancer 13.0 (±1.16) minutes, and lymphoma 16.7 (±1.04) minutes. The mean tumour to background ratios did not change significantly over the first hour once the peak value was obtained at around ten minutes.

The tumour to background ratios were also compared in the early and four hours delayed ten minutes and found to be mean (±SD) 1.8 (±0.30) for the initial image and 1.67 (±0.33) for the delayed image. These values are not significantly different.

From these data I concluded that tumour imaging with Tl-201 is best performed 20 to 60 minutes post injection. I did not find any evidence that delayed four hour imaging was advantageous because tumour to background was not significantly changed and the count in tumour decreased.

I studied the mechanism of tumour uptake of Tl-201 by in vivo and in vitro studies.

In a series of patients with lung cancer (n=50), breast cancer (n=24), and mediastinal lymphoma (n=13), the time course of tumour uptake of Tl-201 paralleled that in the myocardium with almost identical times being obtained in tumours and myocardium. The time from injection to peak myocardial activity ranged from 8 to 20 minutes. The mean time to peak myocardial activity ($\pm$SD) was 11.61 ($\pm$ 3.25). The mean ($\pm$SD) washout of Tl-201 from the tumour over four hours post injection was 25.4 ($\pm$ 33.5) percent of the activity present in the early static image. The mean washout of Tl-201 from the myocardium over four hours was 29.7 ($\pm$16.7).

In a patient with hepatic metastases from colonic cancer undergoing laparotomy, TC ^{99m} labeled microspheres and Tl-201 were injected into the hepatic artery and biopsies of metastatic and normal liver tissue obtained. The tumour to normal liver tissue activity ratios for Tl-201 were one-tenth of those for TC^{99m} microspheres.

Measurement of Tl-201 activity was made under control conditions and after digoxin intervention in non-small cell lung cancer line SK-MTS. The cells were incubated for 30 minutes with Tl-201 and without the addition of digoxin, which acts as a sodium-potassium pump blocker. The cells exposed to digoxin showed markedly decreased uptake of Tl-201 compared to the cells not exposed.

Results of the studies indicate that Tl-201 uptake in tumours in not a purely flow dependent process. The mechanism of intracellular uptake of Tl-201 demonstrates the viability and metabolic activity of the pathological cells. It appears to be similar to the myocardium by substitution of Tl-201 for potassium in the ATP-ase dependent sodium-potassium pump.

I carried out a clinical evaluation of Tl-201 chloride in the diagnosis and staging of various common malignancies.

I evaluated the ability of Tl-201 chloride to detect primary lung cancer (n=147) and to demonstrate mediastinal spread of the disease. Thallium-201 images were compared with the results of CT Scanning and surgical mediastinal exploration. Thallium-201 was accurate in locating 126 of 147 of the primary lung tumours (86%) but disappointing in detecting mediastinal tumour spread (15%).

Ten patients with benign lung disease were examined. Tl-201 chloride was also found to concentrate in active sarcoidosis (one case) and active TB (two cases). The specificity of 70 percent was obtained. Forty-five patients with histologically proven lung cancer underwent Tl-201 and Ga-67 studies.

Thirty-nine (87%) showed positive uptake of Tl-201 into the primary tumour, while 36 (80%) had positive Ga-67 uptake in the tumour. Ga-67 was superior over Tl-201 in detecting mediastinal spread of the disease in 16 out of 28 (58%) patients with mediastinal gallium uptake, while five out of 28 (18%) patients showed positive Tl-201 uptake. I concluded that Tl-201 chloride concentrates in both malignant and benign active metabolic tissue. Tl-201 is highly sensitive in locating primary lung cancer but lacks sensitivity in determining mediastinal spread of the disease.

I evaluated Tl-201 chloride in patients with breast cancer (n=26) and in patients with malignant lymphoma (n=15), and found that Tl-201 is highly sensitive in detecting primary tumours and disappointing in detecting nodal spread of the disease.

Thallium-201 was also evaluated in patients with bone and soft tissue tumours (n=9), brain tumours and in patients with mass lesions of the liver.

Thallium-201 was found to be useful in detecting bone and soft tissue tumours (100% sensitivity), brain tumours (100%) and was not affected by steroid therapy. Thallium-201 was found to be equally useful to gallium-67 for imaging primary hepatomas. It surpasses gallium-67 imaging in distinction of pseudotumours of the liver. In addition, it has the advantage over gallium-67 of early imaging.

Finally, sequential Tl-201 scans were found to be useful in evaluating patients with malignant disease and determining local tumour response after anti-tumour therapy, especially when the scan was positive pre-treatment. There was a good correlation between the changes in Tl-201 uptake and the change in the primary tumour size after treatment as determined radiographically.

CHAPTER I

A HISTORICAL REVIEW OF THE APPLICATION OF THALLIUM-201 IN VIVO

I(1) Introduction

The first application of radioactive tracers in man was in the field of cardiovascular disease, when Blumgart and colleagues in 1927 injected radium C into the vein of an arm to measure the transit time through the heart to an arterial site in the other arm. The arrival of the tracer was detected with a cloud chamber [1]. A longer than normal circulation time was found in patients with auricular fibrillation or "myocardial degeneration" [2].

Following the development of the first cyclotron by Lawrence and Livingston, 1932 [3] and its later improvement by Lawrence and Cooksey 1936 [4]. Hamilton, 1938 described the artificial radioisotope potassium-42 which was suitable for biological use [5]. Three years later Noonan, Fenn and Haege demonstrated rapid accumulation of potassium-42 in the myocardium of rats following intraperitoneal injection [6].

In the early 1950's, work by Burch and his associates demonstrated that while radioactive rubidium and potassium do not have identical kinetics they are sufficiently similar to allow rubidium to be used in making generalisation concerning certain aspects of Kaliokinetic phenomena in man. The two tracers behaved similarly during the 120 minutes following intravenous administration. The partitioning of potassium-42 and rubidium-86 in the intra- and extravascular compartments also was similar [7]. Similar properties were also found for radioactive caesium-134 [8].

The studies of Burch and his colleagues which indicated rapid uptake of rubidium-86 by the myocardium suggested the possibility of demonstrating the myocardium by photoscanning after administration of this radioisotope. Carr and his associates showed the feasibility of demonstrating the myocardium of the beating heart of living dogs by this technique. Furthermore, in photoscintigrams they found 'cold areas' of relatively decreased uptake of rubidium-86 in hearts previously subjected to coronary artery ligation, but these defects could only be identified reliably after excision of the heart [9]. They, therefore, considered this isotope unsuitable for in vivo imaging of the myocardium and turned their attention to caesium-131. Using a rectilinear scanner and intravenously injected caesium-131, they reported the first successful radioisotope imaging of the human myocardium in vivo, and they were able to demonstrate decreased isotope uptake corresponding to areas of

infarcted myocardium. In the same publication they also reported that ischaemic tissue in dogs showed an uptake of caesium less than that of normal tissue but greater than that of infarcted tissue [10].

Over the next ten years a number of diffusible monovalent cationic extractable indicators were used clinically as myocardial imaging agents, notably potassium-42 and potassium-43, rubidium-81 and rubidium-82, caesium-129 and caesium-131, and nitrogen-13 labeled ammonia. None of them ever became available for widespread use and they did not reach the clinical arena. These radionuclides had major disadvantages as myocardial imaging agents, namely, their low myocardial extraction, low target organ/background ratio, and high photon energies, which made imaging with a conventional gamma camera difficult [11] [12]. The situation was changed by the introduction of thallium-201 in 1974 [13]. This radionuclide has been extensively evaluated in both clinical and laboratory studies and has been applied particularly in asymptomatic and symptomatic patients [11]. Thallium-201 currently has replaced the other radionuclides as the myocardial imaging agent of choice.

Radionuclides for myocardial imaging are generally injected as the chloride salt in the ionic state. The biological behaviour of the radionuclides of potassium, rubidium, caesium and thallium vary in detail with respect to dosimetry, blood clearance, duration of uptake in target organ, and target to non-target ratios. Different radionuclides of a specific element, such as potassium, demonstrate the same biological behaviour. However, radionuclides of a given element will not have

the same dosimetry because each radionuclide has different decay characteristics. All of the elements mentioned tend to localise in viable tissue, e.g., the myocardium, resulting in cold spot images of infarcted or ischaemic areas [14]. The property is dependent on broadly similar physiological behaviour between potassium and other elements, which are viewed as potassium analogues.

Potassium is a major cationic constituent of the body. The intracellular content of potassium ion is much higher than that in the extracellular spaces. This gradient is maintained by an energy expending process which is oxygen dependent, and even transient periods of hypoxia lead to immediate loss of intracellular ion [15]. If this efflux could be measured, a very sensitive method for the rapid detection of the regional hypoxia would be provided. Of course, the label would have to be in the cell prior to the hypoxic insult. Radiopotassium has only been used as a regional flow indicator. On a single passage through the heart, over 70 percent of available K^+ ions in the plasma will enter myocardial cells [16]. An equal number of intracellular ions will leave the cell, but as the concentration of intracellular K^+ to extracellular K^+ is very large, the turnover rate of the radioactive ions is slow enough to permit acquisition of an image that initially represents the distribution of regional blood flow. Over a period of several hours, the radioactive and non- radioactive potassium will come into equilibrium, and the distribution of the radioactive potassium then reflects

the potassium pool, not regional perfusion. The most reliable determination of regional perfusion will be obtained in the first few minutes following injection [17].

I(2) The physical and biological properties of Thallium-201

I(2)(a) Physical Properties

In 1861, the English chemist William Crookes noted the occurence of a brilliant green line in the spectrum of some selenium residues whilst examining them for tellurium. He confirmed that the green line was due to a new element, probably a higher member of the sulphur, selenium and tellurium group, possessing well defined characters. He proposed for it the name of Thallium (Symbol Tl), from the Greek θαλλός, or Latin thalius, "a budding twig - a word which is frequently employed to express the beautiful green tint of young vegetation, and which I chose on account of the green line which it communicated to the spectrum recalling with peculiar vividness the fresh colour of early spring" [18].

Thallium (atomic number 81) is a metallic element of group IIIA of the periodic table. It belongs to a different element group from potassium, rubidium and caesium.

The use of radiothallium in nuclear medicine was first suggested by Kawana et al, 1970 [19]. Using thallium-199 they demonstrated the possibility of imaging the human myocardium, but the images they obtained

were of poor quality because of contaminating high energy gamma rays causing excitation of the lead in the collimator and they suggested that thallium-201 might be a more suitable radiopharmaceutical. Workers at Brookhaven National Laboratory in the U.S.A. developed a method for producing the radionuclide in a form suitable for human use [20] [13]. Thallium-201 was produced by irradiating a natural thallium target in the external beams of the Brookhaven cyclotron with 31 MeV protons. The nuclear reaction is $^{203}Tl_{(p,3n)} \rightarrow {}^{201}Pb$. Lead-21 has a half-life of 9.4 hours and is the parent of ^{201}Tl. The thallium-201 is separated from the lead by a process involving dissolving the target in nitric acid and passing the solution through several resin exchange column stages [13]. Thallium-201 has a physical half-life of 73 hours, and decays by electron capture, emitting a small yield of gamma rays (135 to 167 keV) in ten per cent total abundance. In addition, the daughter nuclide mercury-201 emits X-rays with an energy of 69 to 83 keV. These X-rays occur in 98 percent of thallium-201 disintegrations [13]. The thallium-201 is contaminated with a small amount of thallium-202 (half-life 288 hours) [21].

The gamma rays emitted by thallium-201 have suitable energies for scintillation camera imaging, but as they are not significantly abundant the mercury daughter X-rays are usually utilized. Atkins et al found that the X-rays gave count rates during myocardial imaging which were seven times greater than those from the gamma rays [22]. Because of the inherent low energy of the X-rays utilized for thallium-201 images, the energy signal is poorly determined statistically by the scintillation

camera and this results in relatively poor spatial and contrast resolution in the image. Contrast resolution is further degraded by the Compton scattered photons from the gamma ray fraction. The half-value layer in tissue equivalent of Hg-201 X-rays is about 4 cm. so that about 50 percent to 70 percent of the emitted photons are absorbed in patients[23]. Tissue attenuation can produce thallium defects. An apparent decrease in radioactivity in the septum or lateral wall may occur secondary to breast attenuation [24]. The diaphragm has been shown to attenuate photons originating from the inferior myocardial segment when the patient is in the supine position for the left lateral view. This difficulty may be overcome by imaging with the patient lying on his or her right side [25].

I(2)(b) Mechanism of cellular uptake of thallium

In 1960, Mullins and Moore noted that the crystal radius of Tl^+ (1.44A) is between that of K^+ (1.33A) and Rb^+ (1.49A), and thus expected that Tl^+ would behave as do these alkaline ions. Working with the isolated frog sartorius muscle preparation, they found "results which were consistent with the view that the muscle fibre membrane cannot distinguish between the toxic heavy metal Tl^+ and K^+ provided that the concentrations of the former ion are kept low". The efflux of Tl^+ is increased during stimulation to at least the same extent as is that of K^+ in stimulated muscle [26].

The biological similarities between potassium and thallium were confirmed by Gehring and Hammond working firstly with rabbit erythrocytes[27] and later with biodistribution studies in rats and dogs[28]. They demonstrated that "activation of the Na and K activated adenosine triphosphatase by the substitutions of thallium for potassium supports the belief that the mechanism involved in the active transport of potassium cannot differentiate between potassium and thallium". The cellular uptake of Tl^+ was inhibited by ouabain and sodium fluoride, which block the $Na^+ - K^+$ pump [28]. Britten and Blank working in rabbit kidney also confirmed that the cellular uptake of thallium is due to activation of the sodium-potassium ATP-ase system, but their results suggested that the mechanism of uptake was not identical with thallium binding on two sites in the enzyme system compared to one for potassium [29].

Gilbert and co-workers, 1976, investigated myocardial uptake of Tl^+ with a canine infarct model and reported that thallium-201 concentration in myocardial biopsies correlated with both perfusion and regional ATP-ase activity [30]. This has led other investigators to postulate that the reduction of thallium uptake in ischaemic myocardium is primarily due to a decrease in ATP-ase activity [31] [32].

Several studies have shown that the distribution of thallium is a flow-dependent process [33] [34] [35]. To assess the role of ATP-ase in thallium uptake, studies were performed in arrested dog hearts after introducing ouabain. The coronary sinus blood thallium activity was in-

creased approaching arterial activity, and the myocardial extraction ratio fell markedly. It was concluded that myocardial thallium uptake is mediated by ATP-ase [35]. The myocardial distribution of potassium analogues is also dependent on regional blood flow. Prokop et al, 1974, compared the regional distribution of ionic potassium-43 with that of radioactive microspheres administered into the left atrium in three groups of dogs as an indicator of blood flow. The regional myocardial distribution of potassium was similar to that of microspheres under normal conditions, during experimental ischaemia and after complete coronary arterial occlusions. These data suggest that the major determinant of ionic tracer distribution is blood flow [36]. Similar investigation has been performed with thallium. Strauss et al, 1975 [37], and Nielsen et al, 1980 [38], demonstrated that the distribution of thallium in the canine myocardium following intravenous administration is proportional to the regional flow as measured with labeled microspheres although the relationship to blood flow is not linear over all flow rates. Similarly, Weich et al, 1977 [32], found that the initial extraction of thallium in canine hearts is proportional to myocardial blood flow.

Many of the current methods for measuring blood flow with radioactive tracers are based on the fractionation principle of Sapirstein [39], or on the recording of myocardial washout of diffusible indicators injected into a coronary artery [40].

According to the Sapirstein fractionation principle, if an indicator is uniformly mixed with blood at the left ventricular outlet the fraction of the administered dose distributed to the myocardium during the first circulation equals the fraction of cardiac output that perfuses cardiac muscle. This applies both to particulate indicators that do not re-circulate [41], and to re-circulating indicators with high extraction rates during the first circulation, such as potassium and other cationic tracers as long as the amount of non-extracted indicator leaving the myocardium is exactly balanced by the amount that re-enters the coronary arteries with re-circulation [42]. Under these conditions, when the fraction of the indicator in the myocardium can be measured as a fraction of the injectate, one can calculate total myocardial blood flow (or the fraction of cardiac output that perfuses the myocardium) [40].

According to the "Washout principle", one can calculate myocardial blood flow per unit mass of myocardium, when the mean washout time of the indicator can be determined, the space of distribution of the indicator is confined to the myocardium and its tissue/blood partition coefficient is known [43]. Nishiyama et al, 1982 [44], studied myocardial uptake and washout of thallium-201 in an experimental dog model, and found that thallium uptake and washout was directly related to blood flow. With reactive hyperaemia, there was a rapid and absolute increase in uptake followed by rapid washout; with ischaemia, there was slow and decreased uptake followed by a slow washout. They found significant differences in washout slopes, compared to control dogs after reactive hyperaemia, and after transient ischaemia, with half-washout times of 5.3 hours, 3.4

hours and 11.0 hours respectively. These data suggest that both the initial excess in the hyperaemic area and the decreased uptake in the ischaemic area are corrected by different washout rates of ischaemic and hyperaemic cells during re-distribution [44].

In clinical practice, myocardial blood flow is likely to be the main determinant of regional myocardial distribution of thallium-201, but some experimental data suggest that thallium accumulation becomes abnormal only when decreased perfusion results in myocardial ischaemia, that is disordered metabolism [45]. Experimental animal studies have demonstrated that the myocardial distribution of intravenously injected thallium-201 reflects myocardial blood flow [37]. The relationship, however, is not linear, with increase in perfusion producing a proportionally smaller augmentation of tracer accumulation [37] [46]. Trapping of the thallium-201 within the myocardial cell involves a dynamic process of Na-K pump [30]. The process consists of continuous extraction and release of ionic thallium by viable myocardial cells [47]. The changes in the thallium distribution observed on serial images reflect both regional perfusion and myocardial cell metabolism [11]. Though myocardial blood flow is usually the main determinant of the initial distribution of thallium-201, any process causing an abnormality of the Na-K pump could impair myocardial uptake of thallium-201 [11].

I(2)(c) Biodistribution of thallium-201

Following intravenous administration, thallium-201 is distributed to the entire body, and is extracted in multiple organs. Bradley-Moore et al, 1975 [48], working in goats found that the greatest concentrations of thallium-201 were in kidney, heart and liver, and that the activity remained high in these organs for at least two hours. Maximum myocardial and renal uptake were achieved by ten minutes. The organ distribution of thallium in animal species has been reported to be similar in mice [37], in goats [48], in rats and dogs [49], and in man [22] [50].

The rate of blood disappearance is extremely rapid. Bradley-Moore et al, 1975 [48], working with goats found the half-time clearance from blood of intravenously injected thallium was less than one minute. Similar rapid rates of clearance were reported by Shelbert et al (1976) [49] and by Strauss and Pitt (1977) [51]. Nishiyama et al, 1976 [52], working with dogs, found slightly slower clearance which occurred in biexponential fashion with the half-time of the fast component being 2.9 minutes. Atkins et al, 1977 [22], also investigated the blood clearance in humans, and reported that at five minutes after intravenous administration only five to eight percent of the injected activity remained in the blood. A biexponential disappearance curve was obtained with 91.5 percent of the blood radioactivity disappearing with a half-time of about five minutes. The remainder had a half-time of about 40 hours. The majority of the slower clearing component was within the red

blood cells, the plasma fraction varying from 28 percent to 50 percent[22]. Strauss and Pitt, 1977 [51], found this residual blood concentration is in equilibrium between red cells (33%) and plasma (66%). The whole body retention of thallium-201 was measured in three volunteers by Atkins et al, 1977 [22], using a whole body counter. They found a mean whole body disappearance half-time of 9.8 days (range 7.4 - 12.4 days). A repeat study with potassium loading showed no significant change, the half-time being 11.0 days (range 8.1 - 15.1 days).

Bradley-Moore et al reported that the maximum uptake of thallium-201 by the myocardium was approximately 3.7 percent of the injected dose at 10-25 minutes [48], a finding subsequently confirmed by others[50] [46] [53]. Schelbert et al, 1976 [49], demonstrated that myocardial uptake in rats was significantly higher for thallium than for rubidium. The thallium concentration in the liver and blood were either lower or fell more rapidly than those of rubidium resulting in higher target to background ratios [49]. Nishiyama et al, 1976, found both K-43 and Tl-201 surpass Cs-129 in terms of rapidity of radionuclide concentration in the myocardium. Furthermore, Tl-201 is superior to Cs-129 and K-43 in target to non-target ratio [52] [54]. Atkins et al, 1977 [22], found that the myocardial uptake of thallium-201 did not significantly change from five to 60 minutes after injection in human subjects. Throughout this period the blood activity is sufficiently low to enable myocardial imaging[22]. Bradley-Moore et al, 1976 [48], reported that the loss of thallium-201 from the myocardium had two components with half-times of 4.4 hours (78%) and 40 hours (22%) respectively.

Abbate, Maseri, Biagini et al, 1977 [55] estimated the first pass myocardial extraction of thallium-201 to be 83 percent whilst Pitt and Strauss, 1976 [54], quote a first pass extraction of 85 percent of the tracer. Grunwald et al (1981) [34] investigated myocardial extraction efficiency of Tl-201 at varying coronary artery perfusion pressures and concluded that the extraction of thallium by the myocardium is not significantly altered at various levels of flow reduction [34].

Myocardial distribution of thallium-201 is uneven. This was first observed in the goat heart [48]. Similar regional differences in myocardial thallium concentration were found in the dog heart, higher concentration being found in the free LV wall and in the intraventricular septum than in the free RV wall [49]. Strauer et al (56), 1977, working in cats found that the highest thallium-201 concentration per gram of muscle weight was in the inner LV layer and in the LV papillary muscle, the out layer containing ten to 15 percent less radioactivity per gram than the inner layer. The total RV thallium accumulation was found to be 40 percent less than that in the whole of the left ventricle [56]. Hamilton et al, 1978 [50], found that right ventricular activity was about 75 percent of left ventricular activity. These differences are likely to reflect differences in regional myocardial perfusion since they correspond closely to the distribution of radioiodinated macroalbumin particles [57]. The lower thallium concentration in the RV myocardium explains why the thin walled RV often is not visualized on scintigraphy.

Drugs may alter the tissue distribution and, in particular, the myocardial uptake of thallium-201. Dipyridamole following intravenous administration can increase coronary blood flow to three to four times resting levels [58], with a 60 percent increase in myocardial thallium-201 concentration [50] [46]. Gould et al, 1978, concluded that myocardial images equal in quality to those obtained when thallium-201 was administered during treadmill stress could be obtained using Dipyridamole infusion [59]. The optimal technique comprised of intravenous Dipyridamole at a dose of 0.142 mg/Kg for four minutes with the thallium-201 injected in the third and fourth minute after completion of the infusion, with the patient upright, walking in place. In a group of patients who had both exercise and Dipyridamole imaging performed, the sensitivity and specificity of the two techniques for detection of coronary artery disease was identical [60]. The satisfactory sensitivity and specificity of Dipyridamole imaging have been confirmed by Harris et al, 1980 [61]. Thus, "pharmacological stress" imaging with Dipyridamole has potential clinical value, especially in patients who are unable or unwilling to exercise adequately.

Digoxin and propranolol produce a small reduction in left ventricular thallium-201 concentration, but this does not seem to affect the quality of image obtained [50]. Acidosis and hypoxia both induced a fall in extraction efficiency in parallel with an increase in coronary blood flow [47].

Sodium bicarbonate has been shown to enhance the myocardial concentration of thallium-201 in rabbits and goats [62]. The suggestion that this could be used clinically to improve the quality of myocardial images has not been attempted.

Renal uptake occurs rapidly being maximal 10 minutes after injection into goats [48] and between ten and 20 minutes after injection in mice[37]. Four hours after injection of the tracer, the ratio of renal to background activity is reduced from that shortly after injection but some accentuation of renal uptake can still be seen on images performed five days after injection [22]. The renal excretion rates for thallium-201 are low [49] [22]. Faecal excretion has also been found to be insignificant [22].

The uptake in the abdominal organs was approximately 20 percent of the injected dose. The large bowel shows considerable uptake of thallium-201 and, as in the kidneys, there is prolonged retention of activity[22]. Liver uptake is marked when the tracer is injected into animals at rest [48] [49], but in clinical studies liver uptake can be considerably reduced by injecting the radionuclide with the patient standing and fasting [22]. Colonic, hepatic and splenic uptake are reduced by injecting the tracer during exercise, which also produces a better myocardial to lung activity ratio [63] [21]. Testicular tissue was found to accumulate 0.15 percent of the injected dose in man.

Studies on a female beagle showed the total amount in ovaries and uterus was 0.2 percent of the injected, but in human ovaries the uptake could not be estimated due to high uptake in the gut and pelvic organs [22].

The thyroid accumulates 0.2 percent of the injected dose, but this activity disappears within 24 hours [22].

Two mechanisms have been postulated for the concentration of thallium in the thyroid. First, the formation of a complex anion, thallous dichloride ($TlCl_2^-$) which could behave as an iodide analogue (based on its postulated ionic radius and charge), or secondly, the substitution of thallium for potassium in the sodium-potassium ATP-ase pump in which case the thyroid distribution of thallium should parallel blood flow rather than iodide concentration [64].

The changes in thyroidal iodide concentration in perchlorate treated rats with little change in the thallium concentration [64], and the inverse relationship between serum potassium level and thyroidal thallium uptake [65] all suggest that thyroidal thallium uptake reflects the state of sodium-potassium ATP-ase system - the cationic side of the pump - rather than anionic side.

Pulmonary extraction fraction of thallium-201 during the first transit was estimated to be about nine percent of the injected dose [66]. Initially the lung activity received scant attention in the interpretation of thallium-201 studies, although this contributes a considerable por-

tion of the background activity of the heart [67]. Increased pulmonary thallium-201 concentration has been observed in exercise stress thallium perfusion imaging in patients with coronary artery disease [66] [70] [69] [68] [71]. This increased lung uptake after stress has been associated with the presence of severe coronary artery disease [68].

The exact mechanism of increased lung thallium-201 uptake following exercise is incompletely understood [71]. Boucher et al, 1980, showed a direct relation between exercise-induced increased in pulmonary capillary wedge pressure and increased lung thallium-201 uptake in patients with significant coronary artery disease [68]. In addition, Bingham et al, (1978) [72], using an open chest dog model, showed that increased extraction of thallium-201 in the lung can result from increases in left arterial pressure. It may be postulated that increased thallium-201 lung activity results from transient, exercise-induced left ventricular dysfunction with a concomitant increase in interstitial lung water. Because thallium is injected intravenously and initially traverses the pulmonary vascular bed during a period when left ventricular filling pressure is elevated, transudation of water with radiotracer into the interstitial compartment would occur [70].

Increased lung uptake of thallium-201 is likely to result from left ventricular dysfunction of any cause, including cardiomyopathy as well as valvular and congenital heart disease [71], and the calculated in-

dices of increased thallium-201 lung uptake and lung clearance have been suggested as useful indices for assessing the severity of exercise-induced left ventricular dysfunction [73].

There is considerable thallium uptake by the skeletal muscles if thallium-201 is injected during exercise [21], and leg muscle uptake during walking on a treadmill has been applied to the assessment of patients with arterial disease [74]. This technique has not found general clinical application.

1(2)(d) Radiation Dosimetry

The whole body radiation dose from thallium-201 has been variously estimated as 0.07 to 0.24 rads per millicurie [75] [13] [48] [76] [77]. The critical organ for radiation exposure is the kidney with an average radiation dose of 0.52 rads per millicurie. The renal medulla where thallium concentrates receives a dose of 1.1 rads per millicurie [48]. This dose is unlikely to cause renal damage as no significant long term functional or anatomical effects were observed in dog kidneys irradiated with 400 rads [49].

1(2)(e) Toxicology of Thallium

In common with other heavy metals, thallium is potentially toxic. The main effects are seen on the gastrointestinal tract and nervous system[78] [79] [80].

The minimum fatal dose of thallium for man is thought to be 8 to 12 milligram per kilogram body weight [81], or a tissue concentration of 0.5 mg percent elemental thallium [49]. Toxicity in higher animals and man has been reported at a dose of 0.1 milligram per kilogram [48]. Schelbert et al calculated the dose ~~administrated~~ administered. in diagnostic studies using two millicuries to be of order 0.07 to 0.15 nanogram per kilogram body weight, and blood levels averaged 0.0017 nanogram per 100 ml [49]. Even for minimal toxicity, the required dose of thallium is about 10.000 times greater than the dose of thallium given as radiopharmaceutical[48]. As yet, there have been no reports of ill effects following administration of the radiopharmaceutical of thallium as a diagnostic imaging agent either in animal studies or for human use.

1(3) Thallium-201 myocardial imaging

1(3)(a) Introduction

The main use of Tl-201 imaging until now has been in the detection of coronary artery disease. In this application, stress myocardial imaging is especially important. Various studies have shown that regional myocardial perfusion may not be significantly changed at rest in spite of coronary artery disease (CAD) [82] [83] [31].

In 1973, Zaret et al [84] reported that the administration of potassium-43 at peak exercise to detect exercise-induced perfusion defects in 28 of 34 patients with coronary artery disease. No defects were seen in 12 out of 12 patients without CAD. Strauss et al, 1973, demonstrated that images obtained after injection of potassium-43 during exercise were abnormal in CAD patients with normal rest studies [85]. CAD is typically a segmental disease with varying degrees of obstruction in different coronary arteries. During exercise, increased myocardial oxygen consumption requires an increase in coronary blood flow. In situations of increased myocardial oxygen demand or during pharmacological hyperaemia, the coronary flow increases in non-obstructed coronary arteries but does so to a lesser extent in arteries with significant stenosis. This impairment with stress hyperaemia was seen distal to occlusions of 50 percent or more of the luminal diameter [59]. If thallium-201 is injected at peak exercise, the increased flow in normal

vessels leads to greater thallium-201 concentration in their territory. At the same time, areas perfused by diseased vessels do not receive such an increase in flow, and a difference in tracer concentration results[37].

At rest, areas of decreased myocardial Tl-201 uptake have been shown to correlate usually with myocardial fibrosis or necrosis [86]. This has lead to the classification of Tl-201 defects as fixed or irreversible. Areas of abnormal tracer uptake on the stress study not seen on the rest study, "reversible defects", are taken to indicated viable but ischaemic myocardium, while defects which are unchanged from rest to stress "fixed defects" are taken to indicated non-viable tissue [87] [88] [89] [90].

In 1977, Pohost et al observed that certain zones of decreased myocardial thallium uptake present on immediate post-stress images resolved, while other defects persisted. The transient defects appeared to correspond to zones of transient ischaemia, while the persistent defects appeared to correspond to zones of previous myocardial infarction [47]. The mechanism of redistribution appears to be a combination of uptake of thallium from the blood pool by the previously ischaemic zone and a loss of isotope from the non-ischaemic area which has an estimated biologic half-time of 4.5 and seven hours [91] [47]. The resulting image represents the net effect of thallium uptake by the previously ischaemic zone and loss from the non-ischaemic zone [92]. This was confirmed in experimental studies by Grunwald et al, 1981 [93], who measured the intrinsic myocardial washout rate of thallium in the absence of systemic

recirculation. At anytime after i.v. injection of the tracer the myocardial concentration of thallium-201 depends upon the net balance between continuing myocardial extraction from low levels of recirculating thallium in the blood compartment and the net rate of efflux of thallium from the myocardium into the extracardiac blood pool [93].

Experimental studies were performed by Khan, Strauss, Pohost et al, 1983, in animals with acute coronary occlusion to compare the distribution of radiolabeled antimyosin antibody (AM-Fab) with immediate and delayed distribution of thallium-201. Cardiac myosin-specific antibodies labeled with iodine-125 localize in necrotic myocytes and are highly specific markers for myocardial infarction. Thallium-201 distribution correlated closely with microsphere regional blood flow, but an inverse exponential relation to iodine-125 antimyosin antibody (AM-Fab) uptake was found. They concluded that immediate thallium-201 distribution at five minutes after injection is flow-limited and an indicator of relative blood flow. Delayed thallium-201 distribution reflects cell viability and is flow independent [94].

The abnormalities observed in early post stress images can be due to either exercise-induced in homogenity of perfusion or to previous areas of myocardial scarring or infarcts. A second study is necessary to determine whether the area with decreased perfusion is irreversibly damaged (scar tissue) or is ischaemic but viable. Since the half-life of thallium-201 is 74 hours, a repeat study should be done five to seven days later at rest. If the images are similar during exercise and rest,

a diagnosis of old scar is made. IF the images are abnormal during exercise but normal at rest, the diagnosis of exercise-induced perfusion abnormality is made. The need for two separate studies is uncomfortable for the patient and adds to both the rediation dose and the expense of the test [95] [11] [12]. Pohost et al, 1977 [47], have shown that the perfusion abnormality will tend to normalize if a repeat study is done three to six hours after the initial exercise images. This is termed a redistribution (delayed) study, or the single dose technique.

It is now generally accepted for clinical purposes, stress and redistribution imaging rather than separate stress and rest studies is satisfactory [12].

1(3)(b) Acquisition of myocardial images

Three types of myocardial imaging are mainly used in clinical practice, namely, (1) rest, (2) exercise or stress, and (3) redistribution images. Some studies are combined with dypyridamole vasodilation [11].

Recently, there has been marked improvement in the technical aspects of thallium-201 myocardial imaging especially in imaging systems, computer application, tomographic techniques and quantitative analysis of thallium-201 distribution.

1(3)(b)(1)Thallium-201 imaging at rest

Rest studies are performed by injecting the tracer as a bolus intravenous injection in a standard dose of 1.5 to two mCi after the patient has been sitting quietly for some time. The splenic uptake can be minimized by having the patient fast prior to the injection [11] [12].

1(3)(b)(2)Exercise myocardial thallium-201 imaging

Stress Tl-201 imaging should always be performed by a physician who is experienced in exercise testing. Any contra-indication to exercise testing such as arrhythmias, unstable angina decompensated cardiac failure and severe, uncontrolled hypertension should be excluded by history and examination. Whenever possible, nitrates are withheld for at least four hours prior to the test. The other cardiac medications such as beta-blockers, calcium antagonists, other vasodilators, digitalis, diuretics, or antiarrhythmic drugs are not discontinued routinely. It must be kept in mind that the administration of beta-blockers will frequently result in suboptimal exercise test results because of lesser heart rate increases, and this may decrease the sensitivity of the test[12].

After detailed explanation of exercise procedures to the patient, a medium-sized angiocatheter is secured to an antecubital vein and attached to a solution of dextrose and water. A 12-lead ECG is recorded at rest.

For the exercise test a Bruce multistage treadmill exercise protocol or bicycle ergometric exercise may be used. Blood pressure is measured with sphygmomanometer at the midpoint of each stage. At peak exercise level, a dose of 1.5 to two mCi of thallous chloride Tl-201 is injected intravenously and flushed with dextrose and water. The patient is requested to continue exercising for 30 to 60 seconds more. An ECG is recorded immediately upon termination in the standing and supine position. The precordial leads are removed, the patient is positioned under the gamma camera, and acquisition is usually started within two to three minutes of termination of exercise.

The method of thallium administration and timing of scintigraphy are important in detecting stress-induced myocardial ischaemia. If exercise is not maintained after thallium administration, the distribution of the radionuclide may not reflect the heterogeneity of exercise induced perfusion abnormalities. If the exercise is submaximal (less than 85% of predicted maximal heart rate) there may be insufficient differences in myocardial perfusion to be detected by scintigraphy [23]. McLaughlin et al, 1977 [96], have demonstrated that of the thallium perfusion defects seen after maximal exercise, only 53 percent were present after submaximal exercise.

The images collected shortly after exercise are representative of the myocardial perfusion during stress. If scintigraphy is delayed or prolonged after exercise, the distribution of thallium in the myocardium may be influenced by a redistribution of the radionuclide, and the image obtained does not reflect myocardial perfusion during exercise, and stress-induced abnormalities may be missed [47].

1(3)(b)(3)Redistribution Images

Pohost et al, 1977, demonstrated that following exercise injection of thallium-201, delayed imaging in patients without infarction but with exercise induced ischaemia revealed disappearance of initial perfusion defects. These authors observed that pictures taken two to four hours apart in dogs with complete coronary ligation were similar. On the other hand, when pictures were taken two to four hours after the release there was a substantial difference with a "redistribution" or "filling in" in the regions displaying perfusion defect in the early images. This method of the single dose" was clinically useful especially in the distinction between ischaemia and infarction [47].

It was initially believed that redistribution of thallium might be secondary to reactive hyperaemia in previously ischaemic areas following exercise. However, redistribution has also been observed after injec-

tion at rest in patients with severe fixed coronary stenosis without infarction and without evidence of internal changes in myocardial perfusion between the time of injection and delayed imaging (97) (98).

1(3)(b)(4) Imaging system

Thallium-201 images can be recorded with either a rectilinear scanner or scintillation camera but the latter is almost universally used now. The energy window of choice for clinical thallium imaging is a 20 per cent window centered on the abundant 69-83 keV mercury X-ray photopeak (22). In systems with multi-pulse height analyzers, the use in addition of the less abundant 135 and 167 keV photopeaks may be desirable in order to improve counting sensitivity and spatial resolution. Gamma cameras with at least 37 photomultiplier tubes are used, preferably those with 1/4 inch thick crystals with significant improvement in intrinsic and system resolution and negligible loss in sensitivity.

Standard field of view cameras are most commonly fitted with a low energy all purpose or high sensitivity collimator. A high resolution collimator may be used, but myocardial motion and degradation of the image by tissue absorption tend to cancel any gain in resolution. A converging collimator will magnify the size of the myocardial image but may produce distortion of the image and loss of contrast, and so have not gained wide acceptance except when a wide field of view camera is being used (51) (23) (11). To adequately delineate the left ventricular myocardium multiple projections are taken, usually anterior, one or more

left anterior oblique (LAO) images and a left-lateral. The precise anatomical areas seen in each projection will depend somewhat on the orientation of the heart [25]. In thallium-201 images, the areas of the left ventricular myocardium best seen in any projection are those perpendicular to the front of the camera face [61].

The computer plays an important role in thallium acquisition, processing and display. The gating of Tl-201 image acquisition may improve the quality of the images by removing the blurring induced by cardiac motion [50] [99] but is doubtful if this significantly improves diagnostic yield[100].

Tomographic techniques have been utilized for displaying the radioactivity in a section of the myocardium at a given depth.

Vogel et al, 1979, have described the use of a 7-pinhole collimator to produce myocardial tomograms with thallium-201. In a series of 65 patients in whom both 7-pinhole and planar images were obtained, they demonstrated improvement in accuracy of detection of coronary artery disease over non-tomographic methods [101]. Similar results were reported by Francisco et al, 1979 [103]. However, Ritchie et al, 1981 [104], found that 7-pinhole collimator tomography had no advantage over planar imaging for detecting prior myocardial infarction.

Single photon emission tomography with a rotating gamma camera does give tomographic slices with little interplanar propagation [105] [106]. Tamaki et al, 1981, [107], found that the sensitivity of diagnosing prior myocardial infarctions by thallium-201 single photon emission tomography (SPECT) was 96 percent compared with 75 percent by standard planar imaging. Maublant et al, 1981 [108], also found that SPECT increased the sensitivity for diagnosing prior myocardial infarction. Nohara et al, 1984 [109], compared exercise SPECT with planar scintigraphy in patients with CAD. The sensitivity and specificity of SPECT in detecting disease in each coronary artery was 96 and 87 percent for the right coronary, 88 and 89 percent for LAD, and 78 and 199 percent for LC arteries. Those are higher than the corresponding figures for planar imaging (85 and 87% for right coronary artery, 73 and 89% for LAD, and 39 and 100% for LC).

1(3)(c) Interpretation of myocardial images

The aim of using different techniques in thallium scintigraphy is to enhance the sensitivity and specificity or overall accuracy in diagnosing coronary artery disease by minimizing the differences in image contrast, and the role of the observer in interpretation. Computer processing of thallium images has been directed toward image enhancement and quantitation. Two types of image enhancement are mainly used, namely background subtraction and image filtering.

Until now, there is no generally accepted method for background substraction. In some studies no background subtraction was used[110] [111] [112].

Two methods of background correction commonly being used are either simple threshold subtraction [113] [44] [114], or bilinear interpolative background substraction [116] [116].

The final thallium-201 myocardial images are still most commonly analyzed visually. Leaners et al, 1977 [117], used a combined visual and quantitative technique by generating myocardial isocount lines and considered areas falling below the 75 percent level as abnormal. Fletcher et al, 1978 [110], derived an index of "perfusion in homogenity" by computer analysis of the activity in each matrix element occupied by the myocardial image. Wainwright et al, 1977 [118], used a regional count density profile to analyze the image. Meade et al, 1978 [119], Burrow et al, 1979 [112], and McKillop et al, 1978 [120], described different versions of producing circumferential activity profiles on thallium images. McKillop et al, 1980 [116], compared the visual and semi-quantitative analysis of stress thallium-201 myocardial images in 79 patients with suspected coronary artery disease. With the semi-quantitative method they achieved the highest accuracy for the classification of patients as either having or not having coronary artery disease. Garcia et al, 1981 [121], and Maddahi et al, 1981 [122], using a computer-mapping technique that combined circumferential

activity profiles between stress and redistribution demonstrated increased sensitivity with coronary artery disease, particularly in patients with multiple vessel disease.

Various quantitative methods and semi-quantitative techniques have been found to have greater accuracy for the detection of coronary artery disease than visual analysis of the same image [117] [123] [124] [116] [12]. However, Gould, 1982 [125], reviewing the literature on quantitative imaging in nuclear cardiology concluded that while these computerized mapping techniques may add impartiality and ease of interpretation to these studies, they have not been proven yet to improve diagnostic accuracy[125].

Intra- and interobserver variation influence the interpretation of thallium scintigraphy, and thus the accuracy of detecting coronary artery disease. Hamilton et al, 1977 [126], reported 90 percent complete intraobserver agreement in 30 rest thallium scintigrams and in the other ten percent only minor disagreement. The same was reported by Botvinick et al, 1978 [127], when exercise and rest scans were compared in 50 patients.

Several studies have reported interobserver variability in thallium scan interpretation [86] [90] [117] [128] [126] [129] [130] [100]. The incidence of disagreement varied between 11 percent and 21 percent.

The inter observer variation is acceptable and is no worse than reported for in the interpretation of coronary angiogram [131] [132]; chest X-ray[133]; and liver scan [134].

I(3)(d) Sensitivity and specificity in the diagnosis of coronary artery disease

Sensitivity is defined as patients with true positive results divided by all patients with coronary artery disease, and specificity as patients with true negative results divided by all patients without coronary disease. A review [135], summarizing data on 1,817 patients including most of the reported series with exercise thallium-201 scintigraphy shows a range of sensitivity (from 66 to 100%) and specificity (75 to 100%). The average values for the 24 published series were 82 percent sensitivity and 90 percent specificity. Within these series, the overall sensitivity and specificity of the electrocardiographic exercise test for coronary artery disease was 60 percent and 81 percent respectively[135]. The thallium-201 exercise study has been found particularly useful in patients with equivocal electrocardiographic tests because of hyperventilation, drug effect, ventricular hypertrophy, intraventricular conduction delay and bundle branch block, pre-excitation syndrome or previous myocardial infarction [127] [136].

The sensitivity of thallium-201 exercise test for coronary disease increases with increasing extent of diseased vessels and increasing severity of stenosis [123] [128]. The scintigraphic sensitivity is also

high for left main coronary artery disease but similar appearances may be seen with other coronary artery lesions [137]. Sensitivity decreases in the presence of coronary collateral vessels [138] and in patients taking propranolol with a negative electrocardiographic exercise test[139].

Generally, there is an inverse relationship between the sensitivity and specificity. An increase in sensitivity which can be achieved by less stringent criteria is followed by a decrease in specificity (more 'false positive' cases are reported). An increase in specificity (which can be achieved by using more stringent criteria) is usually accompanied by a decrease in sensitivity; fewer "false positive" cases will result [12].

1(3)(e) Thallium-201 imaging in prediction of the extent of coronary artery disease

There is a fairly constant anatomic relation between individual coronary arteries and myocardial regions. The anterior, anterolateral and septal regions are predominantly perfused by the left anterior descending artery. The inferior and posterior walls are perfused by the left anterior descending artery. The inferior and posterior walls are perfused by the posterior descending artery which is a branch of the right coronary artery in the remaining ten percent. The postero-lateral wall is perfused by the circumflex artery [12].

In patients with coronary artery disease, the number of vessels involved is prognostically significant [140]. Because mortality from coronary artery disease is associated directly with the magnitude and extent of disease, patients with triple vessel disease or occlusions of the main left coronary artery have an especially bad prognosis. A number of investigators have examined the use of stress thallium-201 imaging for identifying such high risk individuals. Rigo et al, 1980 [141], reported that the sensitivity for detection of individual involved arteries diminishes as the number of vessels involved increases. With single-vessel disease, 80 percent of the left anterior descending, 54 percent of the right coronary artery, and 33 percent of the circumflex lesions were detected. In patients with triple vessel disease, only 63 percent of the left anterior descending, 50 percent of the right coronary artery and 16 percent of the circumflex arteries were identified. Similarly, Leaners, 1979 [142], detected disease of the left anterior descending coronary artery in 83 percent of cases, the right coronary artery in 63 percent, and the left circumflex coronary artery in 48 percent of cases. Similar results were reported by McKillop et al, 1979 [124], and Massie et al, 1979 [123]. In each of these series, high grade stenoses of 90 to 100 percent were more commonly detected than were stenoses of lesser magnitude. Dash et al, 1979 [143], in a small series of patients with left main coronary disease and a larger series of patients with three vessel coronary artery disease showed only 43 percent of patients with triple-vessel or left main coronary artery disease, were identified as such. Leppo et al, 1979 [128], studied a group

of 30 patients with three vessel coronary disease and exercise electrocardiographic signs of ischaemia and showed that only two thirds of this subset had perfusion abnormalities.

Recent studies employing semi-quantitative computerized analysis of thallium-201 washout in the four to six hours after isotope injection suggest that the accuracy of detection of individual stenotic arteries is improved [144] [145]). Maddahi et al, 1981 [122], using computerized quantitative analysis of both perfusion defects and redistribution images, were able to detect 64 percent of the involved arteries in patients with double-vessel disease and 84 percent of the involved vessels in patients with triple-vessel disease. They found, overall, the quantitative analysis detected 70 percent of vessels with stenosis between 50 and 75 percent of vessels with stenosis greater than 75 percent. Thus, computer mapping, semi-quantitative techniques and quantitation techniques with the use of computerized tomographic methods are promising and may allow more frequent identification of the anatomic site of each lesion [12], enabling detection of high risk patients.

I(3)(f) Coronary Artery Spasm

Coronary arterial spasm has been recognized as a very important phenomenon, capable of leading to severe myocardial ischaemia in some patients, with or without underlying atherosclerotic coronary lesions. During a spontaneous attack, there is transient transmural reduction of myocardial blood flow which can be demonstrated using thallium-201 imag-

ing [146] [147]. Fuller et al, 1980 [148], have also demonstrated Tl-201 perfusion defects and abnormal radionuclide ventriculograms during exercise in patients with angiographically proven exercise-induced coronary artery spasm. Similar reduction in myocardial perfusion can be demonstrated when attacks are induced in affected subjects by the administration of the vasospastic agent ergonovine maleate, and thallium-201 imaging has been used to evaluate patients suspected of having coronary spasm and to assess the value of proposed therapies [96]. Because of the potential hazard of coronary spasm, drug provocation tests are usually confined to the catheterization laboratory.

I(3)(g) Thallium scintigrams in acute and old myocardial infarction

Thallium-201 imaging has been proposed as an additional method of assessing patients with a suspected acute myocardial infarction [149].

Wackers et al, 1976 [87], have demonstrated that rest thallium-201 scintigrams have high sensitivity for the demonstration of acute myocardial infarction. This sensitivity appears to be extremely dependent on the time when the images are done. Within six hours of the onset of symptoms, image defects were demonstrated in all 44 patients studied. When imaging was delayed more than 24 hours from the onset of symptoms, only 72 percent of patients had an abnormal result. The frequency of false negative studies was greater in patients with non-transmural or biochemically small infarctions. Because of the very high sensitivity in the early hours of myocardial infarction, thallium-201 may be used

when deciding whether or not to admit a patient suspected of having acute myocardial infarction to a coronary care unit, since a negative thallium-201 scintigram in this setting is strong evidence against the diagnosis of myocardial infarction (150). Such a policy, however, has not been widely employed due to the difficulties and expense of having radiopharmaceutical constantly available. There are also problems when thallium-201 images are obtained some days after admission in an attempt to clarify equivocal E.C.G. and enzyme results. In this setting, a positive scintigraphic study does not distinguish between recent and remote myocardial infarction, while a normal study does not exclude small, or possibly even a moderate sized infarct (120).

Thallium-201 imaging, although quite sensitive for the presence of acute myocardial infarction, is not specific because one cannot distinguish old scarring resulting from old infarction or cardiomyopathies from recent necrosis. In addition, some patients with angina without infarction may also have an abnormal rest scan (97).

Thallium-201 imaging has an important contribution in the delineation of prognosis in patients at high risk following recent myocardial infarction. Silverman et al, 1980 (151), examined 42 patients with acute infarction with 15 hours of the onset of symptoms. Patients with shock or frank pulmonary-oedema were excluded. The site of the thallium-201 defects was determined in three projections and expressed as a summed

defect score. During the in-patient hospital stay and a mean follow up of nine months, the thallium-201 score was a potent indicator of short and mid term prognosis.

The use of thallium-201 imaging to identify individuals at high risk after recovery from acute infarction was also evaluated by Turner et al, 1980 (152). In a group of 32 patients exercise and redistribution, thallium-201 imaging were performed three weeks after acute infarction. Each patient also underwent coronary angiography and biplane cine left ventriculography at the same time. The scintigraphic study proved much more reliable than clinical findings in identifying patients as being at high risk due to the presence of multi-vessel coronary artery disease and residual jeopardized myocardium.

The reported incidence of positive thallium-201 scans with previous myocardial infarction varies from 37 percent to 91 percent. Hamilton et al, 1977 (126), reported positive rest scans in ten out of 11 patients with old infarctions who had rest and exercise scintigraphy. Verani et al, 1979 (111), observed complete "filling in" of exercise-induced perfusion defects at delayed imaging in only five out of 27 patients and, in 22 patients, the remote infarction was still demonstrable. Blood et al, 1978 (90), found perfusion defects in 15 rest studies and 26 redistribution studies, each performed in 28 patients with prior infarcts. Wackers et al, 1979 (150), obtained positive rest scans in nine of 24 patients with old infarction.

Thallium-201 imaging is of limited value in the diagnosis of old infarction. Not infrequently, the images return to a normal pattern a variable time after healing occurs. This later normalization of scintigrams may be more common with inferior infarcts and subendocardial infarcts. The finding of a normal thallium-201 scan in patients known to have had a myocardial infarction may still have important prognostic implication, especially in evaluating the extent of viable myocardial tissue remaining [111]. The use of rest and redistribution imaging for evaluation of myocardial viability has recently been subjected to pathological verification [153]. In a group of cardiac transplant recipients, preoperative myocardial images were compared to pathological examination of the heart following its removal at the time of grafting. Fixed rest defects were both sensitive and specific for areas of myocardial fibrosis. Some reversible rest defects in this group corresponded to areas of myocardium showing an admixture of fibrotic and viable myocardium. These results confirmed the usefulness of rest with redistribution myocardial imaging as a non-invasive method of studying myocardial viability [153].

I(3)(h) Thallium-201 scintigraphy in anginal syndromes

Stress thallium-201 imaging is not useful in most patients with typical angina pectoris. The group as a whole has a high prevalence of coronary artery disease (around 90%). So thallium-201 imaging is diagnostically useful in such patients only if it reliably predicts the extent of coronary artery disease [124].

The patient with atypical angina has a probability of coronary artery disease of around 50 percent, and thus, from Bayesian analysis, is precisely the individual in whom stress thallium-201 imaging is valuable, especially if the stress electrocardiogram is negative or equirocal [11]. Several investigators found that thallium-201 imaging during an anginal attack would result in a high percentage of scintigraphic defects [40] [89].

However, positive thallium-201 imaging in patients with unstable angina provides additional information that acute coronary insufficiency is present and identifies potential high risk groups. One third of these patients may be at risk for a complicated course [47].

I(3)(i) Stress thallium-imaging in patients with equivocal stress electrocardiogram

In a considerable number of patients the stress electrocardiogram may be either uninterpretable or nondiagnostic. Inconclusive exercise ECGs are caused by a number of factors including conduction disturbances[11]. Exercise thallium-201 imaging is useful in patients with inconclusive exercise ECGs. McCarthy et al, 1979 [154], have reported the sensitivity, specificity and diagnostic accuracy of exercise imaging in 39 patients with inconclusive ECGs to be 81 percent, 69 percent and 71 percent respectively. Botvinick et al, 1978 [127], studied 19 patients with inconclusive ECGs who underwent both stress thallium-201 imaging

and selective coronary arteriography. The radionuclide images were abnormal in all 12 patients with coronary artery disease and normal in five of seven with no significant coronary lesions. Similar sensitivity and specificity were reported by Tweddel, Pearson, McKillop et al, 1980 (155). When the results of exercise imaging are compared with the diagnostic results of exercise ECGs (that is, either positive or negative), the sensitivity of both tests have been found to be equal (129) (156). The value of exercise ECGs in patients with inconclusive or slightly abnormal exercise images has not been studied.

I(3)(j) Screening for coronary disease in patients with valvular heart disease

Data in the literature is conflicting about the value of thallium-201 imaging in mitral valve prolapse (157). These patients usually experience angina-like chest pain or resting ST-segment and T-wave abnormalities; many have exercise-induced ST-segment depression. The exact cause of chest pain in these patients in the absence of associated coronary artery disease is not well understood. Positive stress thallium-201 images in approximately two thirds of patients with mitral valve prolapse had been reported by some authors (158) (159) (160) while others suggest that thallium-201 exercise-induced defects are rare in such patients in the absence of obstructive coronary disease (161) (162).

Patients with aortic stenosis may have angina pectoris. In this group of patients, symptomatic and electrocardiographic evaluation is unreliable. Bailey et al, 1977 [86], and McKillop et al, 1979 [124], found an unacceptably high rate of both false positive and false negative results, and demonstrated that thallium-201 exercise imaging was unsuitable in predicting associated coronary artery disease in patients with aortic stenosis.

I(3)(k) Exercise thallium-201 in evaluation of coronary artery bypass graft surgery and transluminal coronary angioplasty

Thallium-201 exercise imaging has been studied to evaluate the early and long-term follow up of patients receiving coronary artery bypass graft surgery. Normalization of preoperative perfusion defects correlates highly with patent graft [129] [163] [164]. Exercise imaging in the post operative patient combined with the results of preoperative coronary angiograms offers a unique non-invasive and reliable method, especially if preoperative exercise images are also available for comparison [165]. Verani et al, 1976 [166], found that 70 percent of the preoperative underperfused myocardial segments showed improved perfusion post operatively, and 85 percent of the patients who submitted to saphenous bypass graft had marked improvement in regional myocardial perfusion. Also, they found that patients with previous myocardial infarction had a slightly higher prevalence of post-operative residual abnormalities in

their perfusion scans. Although patients usually show marked clinical improvement post-operatively, some residual thallium-201 imaging abnormalities are common.

When considering the post operative use of myocardial imaging, it is usual to compare its results to arteriographic evaluation of graft patency. The anatomical site of the graft and myocardial perfusion are not necessarily synonymous. Thus, it is possible for patent grafts to supply areas of myocardial infarction [167], which could be abnormal on myocardial images. Conversely, though a graft is occluded, myocardial perfusion may be maintained due to collaterals either from native vessels or from other grafts [168].

Several investigators have been less sure of the value of thallium-201 imaging following revascularization of the myocardium. These studies have indicated that myocardial imaging is more accurate in predicting graft patency than graft occlusion [169] [170] [171] [172].

Similarly to coronary artery bypass surgery, thallium-201 imaging has been assessed in the evaluation of transluminal coronary angioplasty. Although the short term results of transluminal coronary angioplasty are excellent, a significant number of re-stenosis occur with time. Thallium-201 imaging has a major potential contribution in the identification of significant stenosis which may occur in asymptomatic patients [173] [174] [175].

CHAPTER II

THALLIUM-201 AS TUMOUR IMAGING AGENT

II(1) Introduction: Scintigraphic techniques for tumour detection

Various radiopharmaceuticals have been investigated for their "tumour affinity". There is hope that specific localization in malignant lesions will be useful in detecting the primary tumour, its metastatic extension or to monitor response to various anti-tumour therapies. The success rate of all these radiopharmaceuticals is variable, and none has been completely successful due to biological, physical or economic problems.

Gallium-67 citrate, the most commonly used radiopharmaceutical for tumour localization, lacks specificity for malignant lesions. Many reports of gallium uptake in benign, inflammatory, granulomatous or autoimmune disease have been presented in the literature (176) (177) (178) (179).

Gallium-67 is cyclotron produced by proton bombardment of Zn-67 or deuteron bombardment of Zn-66. Ga-67 decays with a 77.9 hour half-life to Zn-67 by electron capture. It has four primary gamma emissions of 93 keV (38%), 184 keV (24%), 300 keV (16%), and 393 keV (4%) with no primary particulate radiation.

The absorbed dose varies somewhat in different body tissues. The target organ is the large bowel which receives 0.9 rads/mCi. The total body dose is 0.26 rads/mCi. The bone marrow dose is estimated to be 0.58 rads/mCi. Based on the usual dose range of three to eight mCi, the total body and gonadal exposure is 0.78 - 2.08 rad. The radiopharmaceutical is most commonly used as the citrate at a neutral pH. Most preparations contain less than one mg of citrate per cubic centimeter.

Numerous imaging methods have been employed with Ga-67. In the past, dual probe rectilinear scanner with a wide window setting encompassing ~~either~~ the 184 keV and 93 keV photopeaks was used for total body imaging. Some centers have utilized rectilinear scanners with summation of the output of two pulse height analyzers with windows set around the 93 and 184 or 184 and 300 keV photopeaks. Whole body or spot view imaging with a gamma camera is most successful when dual or triple pulse height analyzers are available so that a 20 percent window can be set about each principal photopeak. A medium energy collimator, preferably designed for Ga-67 rather than I-131, should be used. With either camera or rectilinear scanner, an information density of 400-600 counts per square centimeter should be obtained.

The normal Gallium scan shows the greatest accumulation of the radiopharmaceutical in the liver and throughout the skeleton and bone marrow. Skeletal localization is particularly notable in the spine and pelvis. The spleen may show minimal activity but is frequently not visualized. Other organs in which normal accumulation can be noted include the nasopharynx, lacrimal glands, salivary glands and external genitalia [180].

Uptake has been noted in the human breast and breast milk during pregnancy, lactation and exogenous estrogen administration [181].

Gallium-67 citrate is bound in blood to transferrin. Within 24 hours after the intravenous injection, approximately ten to 20 percent of gallium is excreted through the gastrointestinal tract, mainly through the bowel wall. Another approximate ten to 20 percent is excreted via the kidneys [178]. Clearance of activity from the blood is slow, and the background activity is high resulting in low target to nontarget ratios. A delay of 48 to 72 hours is necessary post-injection before images can be obtained, and the patient has to come two or three times to the nuclear medicine department to complete the investigation.

In addition to transferrin, other iron-binding proteins in plasma, such as lactoferrin and ferritin, have been shown to bind Ga-67 . At physiologic pH, lactoferrin has a higher affinity for Ga-67 than transferrin [182]. The role of lactoferrin and ferritin in the transport of Ga-67 in the circulation is not clear [183].

The localization of Ga-67 in tumours and abscesses, as well as in most normal tissues, appears to occur in at least two phases. During the early phase of up to six hours, the Ga-67 that has localized in the tissue can be extracted by iron-binding chelats such as Desferal [184]. However, when Desferal is administrated 24 hours after Ga-67, it is no longer capable of leaching the radionuclide from most tissues [184]. This suggests that Ga-67 localizes by an early weak binding or diffusion followed by a firmer intercellular binding phase [185].

At least three mechanisms by which Ga-67 may localise in infections have been postulated. These include leukocyte labeling [186], Lactoferrin binding at the site of infection [187], and direct bacterial uptake [188]. Increased availability of Ga-67 at sites of inflammation can easily be explained by increased vessel permeability at such sites [185].

Proposed mechanisms of Ga-67 localization in tumour are controversial. There is some agreement that the highly permeable walls of tumour vessels, combined with the large extracellular fluid space of tumours play an important role in the initial localization of Ga-67 at the site of tumours [189].

Hayes et al, 1976 [190]; 1977 [191]; 1981 [192]; suggest that Ga-67 enters tumour cells, presumably by simple diffusion, as a result of the hyperpermeability of the tumour cell membrane. However, English et al, 1977 [193], have shown that several types of tumour cells do not significantly accumulate Ga-67 unless the plasma membrane permeability barrier is disrupted as in nonviable cells.

Anghileri et al, 1971; [194]; 1974 [195]; and Anghileri 1977 [196] suggests a link between Ga-67 localization and calcium metabolism in tumours, the uptake of Ga-67 to calcium and magnesium-binding sites. This theory conflicts with the observation that Ga-67 uptake and Ca^{+2} content in tumours are not associated [185].

Hoffer et al; 1980 [185], proposed that binding of Ga-67 by lactoferrin present in some tumours is responsible for Ga-67 accumulation. Studies of Sephton and Harris, 1975 [197], and Larson et al, 1979 [198], suggested that human transferrin enhanced Ga-67 uptake by a number of tumour cell lines and proposed that Ga-67 accumulation in tumours was due to transferrin mediated uptake by tumour cells.

A number of in vivo and in vitro studies have been done attempting to elucidate the role of transferrin on the tumour uptake of Ga-67, and to determine the intracellular localization of Ga-67. The results of these studies are conflicting [199] [200] [201].

The exact mechanism of gallium localization in tumours and other tissues is not precisely known [180]. In view of the strong evidence available to support many of the competing theories for gallium localization in tumour, it is possible that more than one mechanism is operating [185] [202].

Since its introduction by Edwards and Hayes in 1969 [203], Ga-67 has become the most widely employed tumour imaging agent. It has been most useful for head and neck lesions and less effective in the abdomen because of its normal excretion into the gastrointestinal tract contents. Lymphomas, malignant melanomas, focal leukaemic masses, metastatic testicular malignancies, and Ewing tumours often have been well demonstrated. It has been less reliable for detection of breast, lung, gastrointestinal, and uterine malignancies. In the liver, it has demonstrated hepatomas or lymphomatous masses [204]. Clinically it has been employed widely for lymphoma. It has detected 70 percent of untreated Hodgkin's sites, 50 percent of irradiated sites, and 48 percent of abdominal sites [205]. The results have been poor for Non-Hodgkin's lymphoma, only 53 percent of untreated involved sites were positive[206].

Gallium imaging cannot be used to rule out site of malignancy, to differentiate benign from malignant lesions, or to distinguish neoplastic from inflammatory lesions [178] [207] [208].

Grove et al, 1974, investigated the chemotherapeutic agent bleomycin labeled with Indium-111 for tumour detection, but the results were inferior to those from Ga-67 citrate [209]. Another group of investigators tried Cobalt-57 bleomycin-A2 in doses of 40 MBq for localizing lung carcinoma. The sensitivity of detecting lung cancer varied from 83 percent to 96 percent in different series, and about 14 percent of benign tumours and non-neoplastic lesions produced positive images [210]. This agent has not been accepted widely because of the long physical half-life of cobalt-57 (272 days). About 80 percent of the activity is excreted in the urine by 24 hours, causing a waste disposal problem. Also, non-radioactive cobalt-bleomycin conjugated with a bifunctional chelating agent (BLEDTA) labeled with Indium-111 has been used for tumour localization, but lacks sensitivity and specificity for tumours[211].

Ohta et al, 1984, developed a pentavalent preparation of dimercaptosuccinic acid labeled with TC-99m at pH 8 - 8.5 with stannous chloride and sodium bicarbonate for tumour localization. This agent was rapidly excreted in the urine and did not accumulate in the renal cortex. Images were obtained two hours after intravenous injection of 370 MBq of the Tc-99m complex. It was proposed for the detection of medullary thyroid carcinoma [212]. Later, the same group of investigators claimed the new

agent did not concentrate in inflammatory lesions and obtained a sensitivity of 90 percent for detecting soft tissue tumours, mostly sarcomas of the limbs and extremities [212]. Recent work from some groups has yielded good results for tumour imaging [214], but others have been less successful [215].

Radioactive iodine is widely used in the diagnosis and treatment of certain functioning thyroid tumours [216].

Well differentiated papillary and follicular carcinomas represent 75 percent of all primary thyroid malignancies [217]. The primary treatment for thyroid cancer is surgery. After total or subtotal thyroidectomy, thyroid hormone replacement is withheld for six weeks. This will enhance endogenous thyroid-stimulating hormone stimulation of any remaining normal thyroid tissue in the thyroid bed and any functioning metastatic lesions. Whole body images are obtained one to five days after the oral administration of 5 to 10 mCi of I^{131}. Demonstrating metastatic uptake of radioactive iodine is difficult when there is a significant amount of residual thyroid tissue after thyroidectomy. If there is a significant amount of normal tissue in the thyroid bed or metastatic uptake, the remaining normal tissue can be ablated or the metastases treated by a therapeutic dose of 10 to 150 mCi of radioactive I^{131}.

In the patient with complete ablation of normal thyroid tissue, abnormal localization of I^{131} is specific for functioning carcinoma [218].

Radioiodinated metaiodobenzylquaidine (I ^{131} MIBG) has proved useful in localizing catecholamine producing tumours such as pheochromocytoma, neuroblastoma, as well as adrenomedullary hyperplasia, and primary medullary thyroid carcinoma which contained elevated tissue catecholamines (219) (220).

Shapiro et al, 1985, (219), reported their experience for locating suspected pheochromocytoma in 400 cases. They have shown that I ^{131} MIBG is a safe and efficacious means of localizing a wide range of pheochromocytomas. Radioiodinated metaiodobenzylquanidine scintigraphy proved to be more sensitive than conventional X-ray, especially in cases of recurrent disease, mediastinal tumours and in some malignant metastatic disease. Kalf et al, 1982 (221), also reported in 22 percent of cases with pheochromocytoma, conventional imaging techniques had failed to locate the lesions which were revealed by scintigraphy.

The specific accumulation of I ^{131} MIBG in the tumours suggested the treatment by therapeutic doses of I ^{131} MIBG. Such a treatment has been reported in both pheochromocytoma and neuroblastoma (222) (223).

In addition, Fieldman et al, 1984, reported that I ^{131} MIBG is also concentrated in normal platelets by neuronal-pump mechanism. This platelet uptake raised the possibility that I ^{131} MIBG might be useful for visualizing other tumours which have a neuronal ~~pick-up~~ pump mechanism such as carcinoid tumours (224). Fieldman et al, 1986 (225), reported that 13

of 23 patients (61%) with carcinoid tumours were visualized. Lewington et al, 1987 [226], reported 84 percent overall sensitivity of uptake in carcinoid tumours. Three patients have been treated with 5.5 GBq mIBG, symptoms relief occurred in one patient and reduction of five HIAA excretion in the other two patients [226]. While Clarke et al, 1986, reported that I ^{131} MIBG is an expensive radiopharmaceutical with poor imaging characteristics and has been shown to be taken up variably in patients with MCT with a significant false negative rate [227]. Poor results were also demonstrated by Hilditch et al, 1986 [215].

Conray et al, 1987, compared I ^{123} MIBG scanning with US and CT in 16 patients with neuroendocrine tumours. They found a good correlation between these imaging modalities in detecting the primary lesions. I ^{123} MIBG imaging demonstrated metastatic lesions not identified by CT or US. They suggested that I ^{123} MIBG imaging is the more appropriate initial imaging technique and provides more accurate information on the size and location of other metastatic lesions prior to surgery [228]. m IBG has has a recognised role in the staging and therapy of neuroblastoma.

Recently most research on tumour imaging agents has focused on radiolabeled monoclonal antibodies (Mabs).

Antibody molecules, or immunoglobulins, are produced by plasma cells in higher animals in response to the introduction of foreign substances (antigens) that are generally large molecules of 1,000 daltons or more. Immunoglobulins posses specific binding regions that recognize the shape of particular sites, or determinants, on the surface of the antigen.

An antigen may have several determinants, or epitopes, each of which can stimulate one or more B lymphocytes. Each B lymphocyte has the capacity to differentiate into plasma cells that secrete a single, specified immunoglobulin in response to one antigenic determinant, and each different antibody is produced by the family of plasma cells that stems from one of the B lymphocytes. Antigenic challenge thus evokes a heterogeneous antibody response resulting from a mix of antibody-producing plasma cells.

If a suitable animal recipient, typically a mouse or rabbit, is immunized with an antigenic agent, serum taken from the sensitized host will contain antibodies to different epitopes of the antigen. Since these antibodies are derived from a population of stimulated B lymphocytes and their daughter plasma cells, the term polyclonal antibodies is applied. However, if individual lymphocytes or plasma cells could be extracted and cloned in tissue culture, each clone would have the potential to manufacture a single species of antibody molecule, or a monoclonal antibody [229].

Technological improvement was made by Kohler and Milstein who developed the monoclonal antibodies and hybridoma technique in 1975 [230]. Monoclonal antibodies have largely replaced antisera raised in animals against human antigens because the former are highly specific, reproducible, and capable of being highly purified [231]. An extensive search has been made of murine Mabs to surface antigens unique to tumour

cells, such as anti-CEA labeled with I^{131} for detection of gastrointestinal tumours [232]; I^{131} antiferritin for hepatoma and Hodgkin's disease [233]; I^{131} anti P97 for melanoma [234]; and for choriocarcinoma, Tc-99m anti HCG [235].

Monoclonal antibodies can be labeled with gamma emitters for tumour immunoimaging. Several alpha and beta emitting radionuclides have potential for the radioimmunotherapy of cancer. Iodine-131 has most commonly been used [229]. Biodistribution studies performed with Mabs have allowed a reasonable estimation of dosimetry, and calculated that in a patient with good tumour uptake it would be possible to deliver 1000 rads to tumour per 70 mCi I^{131} labeled fab with 23 rads to marrow and 205 rads to liver [234].

Many labeled Mabs successfully image human tumour xenografts in mice, but the results are disappointing in human trials with poor sensitivity in detection of small tumours [236]. There are many problems in the use of labeled Mabs for tumour imaging. Mabs are very expensive to develop and screen. Protein impurities have been found in Mabs preparation. Most Mabs have been labeled with I^{131} or I^{123}, and often, promptly deiodinated in vivo. Mabs which are labeled with Indium 111 tend to have a higher hepatic uptake [234]. All Mabs must be screened for contamination by murine viruses before administration to humans. Using subtraction techniques, sometimes artifacts produced by blood activity mimicked positive tumour uptake and false positive results obtained[237]. In addition, there are many biological problems leading

to poor tumour visualization [238]. Mabs may be of considerable value in the future, but at present are not yet fully developed and are available only in a few centers for clinical trials.

Controversies continue between investigators regarding clinical research in this field. "Whither? back to basics and maybe the fog will clear", as postulated by Bradwell and Dykes [239] who gave little ground of encouragement due to many problems in radioimmunoscintigraphy (RIS) and wonder "Whither (or wither) tumour imaging using radiolabeled antibodies. While Britton and Granowska [240], concluded that each discipline of this complete technique is refining and improving its contribution to the methodology and clinical application of radioimmunoscintigraphy encourages for serious work to make (RIS) a major contribution of nuclear medicine in clinical practice.

II(2) Potassium analogues as tumour imaging agents

A possible alternative tumour imaging agent is the potassium analogue thallium-201 chloride.

Charkes et al, 1965 [241], reported that the potassium analogue caesium concentrated in tumour and in introducing thallium-201, Lebowitz et al, 1974 [13], suggested that it might be useful. for tumour localization in addition to its role as a myocardial and renal imaging agent.

The first description of tumour uptake of thallium-201 was by Cox, Belfer and Van der Pompe in 1976 [241]. They reported concentration of the tracer in the primary tumour of a man with bronchial carcinoma, and also showed that the nuclide was taken up by rehabdomyosarcoma implants in rats. Tonami, Michigishi, Bunko et al, 1977 [243], incidentally found a primary lung cancer clearly visualized on thallium-201 scintigrams taken for myocardial evaluation. This led them to investigate thallium-201 as a tumour imaging agent in man, and compared the detection rate of malignant lesions with Gallium-67. Of the 51 malignant lesions, 36 (71%) were visualized as positive with thallium-201, whereas 13 (72%) of 18 lesions were positively delineated with Gallium-67. In patients with thyroid nodules, 14 of 15 (95%) with thyroid cancer had a hot spot with thallium-201, but only six of 19 benign adenomas which were cold on technitium-99m imaging showed thallium-201 uptake. All of five chronic thyroiditis, and all of three hot nodules showed positive accumulation of thallium-201. In patients with lung cancer, ten of 14 (72%) were positive with thallium-201. Thallium-201 accumulation occurred in three of four patients (75%) with primary hepatoma, but none of eight patients with liver metastasis. On the basis of these findings, Tomami et al, 1977, suggested that thallium-201 imaging might be useful in differentiating hepatoma and secondary tumour in the liver. They also concluded that if a thyroid nodule does not accumulate thallium-201 then the probability of malignancy is very low.

Ochi, Sawa, Fukuda et al, 1982 [244], employed early and three to five hours delayed images of thallium-201 scintiscans in thyroid tumour, and were able to differentiate most malignant thyroid tumours from those which were benign. In 35 of 37 malignant tumours, thallium-201 accumulated in the cold nodule of the I^{123} thyroid scan on both early and delayed scans, and the delayed thallium-201 scans were negative in 35 out of 39 benign tumours [244]. Hoefnagel et al, 1985 [245], investigated the role of thallium-201 total body scintigraphy in 294 patients after total thyroidectomy for thyroid carcinoma. Results were correlated with I^{131} - scintigraphy and tumour marker levels (Thyroglobulin or calcitonin/CEA). Thallium-201 scintigraphy correctly detected tumour localization in 24 of 30 patients with I^{131} positive metastases. In 28 patients, thallium-201 total body scintigraphy revealed metastases which did not concentrate I^{131}. Histopathological examination confirmed thyroid carcinoma metastases in 16 patients and other pathology in five cases. Nine of 18 patient with medullary thyroid carcinoma (I^{131} negative) had elevated calcitonin/CEA levels. The thallium-201 scan was positive in eight of these patients. In 196 patients with no evidence of disease, whole body thallium-201 scan was negative. They concluded that thallium-201 total body scintigraphy is useful in the follow up of thyroid carcinoma, especially when a discrepancy of the other parameters exists and particularly in medullary carcinoma. They suggested that one could rely upon thallium-201 total scintigraphy in combination with tumour marker assays for long term follow up of patients successfully treated for thyroid carcinoma [245].

Terui, Oyameda, Nishikawa et al, 1984 [246], investigated thallium-201 as a tumour scanning agent in six patients with bone tumours (2 with Ewing's sarcoma, 3 with osteosarcoma and 1 with giant cell tumour), and three with soft tissue sarcomas (1 with liposarcoma and 2 with malignant fibrous histiocytoma). The distribution of thallium-201 in the tumours was similar to that of Gallium-67, but sometimes different from that seen on Tc-99m MDP bone scan. In all patients with Ewing's' sarcoma, the primary and the metastatic lesions were clearly visualized with thallium-201. In three patients receiving effective chemotherapy, a post-therapy scan showed reduction in thallium-201 uptake which was more marked than that on the Tc-99m bone scan. In a further patient who had no response to treatment, no changes were seen in the post therapy scan. On the basis of these findings they suggested that thallium-201 is a useful tumour imaging agent, and might be of clinical value in assessing the response of bone tumours to chemotherapy [246].

Kaplan et al, 1987, compared brain imaging using thallium-201, technetium-99m glucoheptonate and gallium-67 citrate with CT and neuropathological data in patients with gliomas. In seven patients for whom autopsy data were available, thallium-201 offered the most accurate correlation with viable tumour. Gallium-67 gave similar results in patients not receiving steroids. Tc-99m glucoheptonate scans could not accurately differentiate tumour from necrosis and oedema. Similarly, the CT scan could not differentiate between fibrotic, nonfibrotic, necrotic and neoplastic tissue. In 22 patients without autopsy data, Tl-201 scans commonly showed smaller and more focally abnormal when com-

pared to Tc-99m glucoheptonate and Ga-67 citrate scans. They concluded that thallium-201 scan reflected viable tumour burden more accurately than other radionuclide studies of brain tumours. It had the additional advantage that it could be performed immediately following tracer administration, was not affected by concomitant steroid administration and compliment the anatomic data obtained from CT scans [247].

II(3) Aims of the present thesis

The background of these isolated reports on Tl-201 tumour imaging led to the work described in this thesis, which attempts to evaluate more systematically the role of thallium-201 as a tumour imaging agent in conditions other than thyroid carcinoma. The major aims of the study were:

(1) To study the time course of thallium-201 uptake in order to assess the optimal time for tumour imaging with Tl-201.

(2) To establish the sensitivity and specificity of thallium-201 uptake in a variety of tumours and to compare it as a means of tumour staging with more standard methods.

(3) To investigate changes in tumour uptake following chemotherapy and radiotherapy and establish whether such changes were helpful in evaluating tumour response to therapy.

II(4) Materials and equipment for Thallium-201 as a tumour imaging agents

II(4)(a) Radionuclide

All studies described in this thesis were performed using thallous chloride (Tl-201) injection supplied by Amersham PLC, London. This isotope is supplied as a sterile isotonic solution in sodium chloride at a pH of five to seven. At the calibration time the solution contains one millicurie (37 MBq) of activity per millilitre, and is virtually carrier free with a specific activity of more than 500 millicuries of thallium. Radionuclide purity is also high with less than one percent thallium-200 and less than 0.5 percent thallium-202 at the calibration time.

Thallium-201 emits a small yield of gamma rays (135 to 167 keV in 10% total abundance) (see Chapter I). In addition, the daughter nuclide mercury-201 emits an X-ray with an energy of 69 to 85 keV in 98 percent of thallium disintegrations [13]. These X-rays are usually utilized for imaging. In the studies of the time-course of thallium-201 uptake by tumours, X-rays and both gamma ray photopeaks were used to increase the count ratio obtained. In studies of imaging only the X-rays alone 69 - 85 keV with a 20 percent window were used.

II(4)(b) Imaging Equipment

Thallium-201 kinetics and tumour images were obtained using wide field of view gamma cameras (General Electric 400A or General Electric 500 Maxi camera), fitted with a general purpose parallel hole, low energy collimator.

Various quality control checks were carried out daily including uniformity response using a flood source, energy settings of pulse height analyzers, visual inspection of image quality and electrical and mechanical safety inspections. In addition spatial resolution was obtained weekly using bar phantoms.

The gamma cameras were interfaced to a dedicated minicomputer (General Electric "Star" or Link "Maps"). The images could be viewed on either a black and white or colour television display. Digital images were subjected to contrast enhancement, but neither to smoothing nor background subtraction. Hard copy images were produced either on colour polaroid film or black and white film from the television screen or on X-ray film using a multimatrix imager.

Time activity curves and statistical analysis of the curves were obtained using standard programmes in the STAR computer. The STAR computer was linked with a printer and the curve points were printed. The studies were stored on magnetic tapes in unprocessed form.

II(3)(c) Patients

All our patients came through the Kuwait Cancer Control Centre or Glasgow Royal Infirmary with proven histopathological diagnosis.

The diagnosis are summarized in Table 1. More detailed descriptions of the patient population will be provided in the relevant sections of the thesis.

Table (1)

Summary of Patients

Breast	Carcinoma primary & metastatic	26
Lung	Cancer	147
	Carcinoid tumour	1
	Sarcoid	3
	Lung abcess	1
	T.B	3
	Fibrosing alveolitis	1
	Neurobl astoma excised	2
	Scar	1
Lymphoma	Mediastinal	13
	Abdominal	1
	Rectal	1
Bone	Primary & Soft tissue	9
Liver	Primary hepatoma	8
	Cirrhosis	5
	Hydatid cyst	1
	Metastases	5
Brain	Primary brain tumours	9
	Brain Metastases	6
	CVA	2
Post radiation therapay		35
Post chemotherapy		11
	Total	291

CHAPTER III

THE TIME COURSE OF THALLIUM-201 UPTAKE IN MALIGNANT TUMOURS

III(1) Introduction

Previous studies of thallium-201 imaging of tumours have not established the optimal time after injection of the tracer for obtaining the images. In the present study, therefore, the first step was to carry out an analysis of the time course of uptake of the radionuclide in various tumours.

The aim of this part of the study was to determine the time of maximal tumour uptake of the tracer, and to study changes in the tumour to background activity ratios in order to establish the optimal time for tumour imaging with Tl-201.

III(2) Patient Population

Ninety-seven patients with histologically proven malignant tumours have been examined. Fifty-six patients (47 male, 9 female) had lung carcinoma. Their mean age group (± SD) was 59.5 (± 11.3 years). Twenty-six patients (1 male, 25 female) had breast carcinoma. Their mean age

(± SD) was 44.9 (± 7.6) years. The remaining 15 patients (12 male, 3 female) had malignant lymphoma. The mean age of this group was 39.3 (±15.6) years.

The studies performed prior to radiation therapy or chemotherapy in 35 patients with lung carcinoma, 16 patients with breast carcinoma, and nine patients with malignant lymphoma. The rest of the patients had already started the first course of radiotherapy either alone or in combination with chemotherapy. Three patients of the lung cancer group were diabetics under medication. All other patients were on no therapy apart from analgesic. Patients on B-blockers or digoxin were excluded because of the known effects of these drugs on Tl-201 kinetics. However, all medication of the patients was not altered. All studies were performed at rest after four hours of fast.

III(3) Data Acquisition

A cannula was inserted into an antecubital vein and the patient placed supine under the gamma camera with the field of view centred over the primary tumour site. Two millicuries (75 MBq) Tl-201 were injected as a bolus via the cannula and flushed with 10 mls normal saline. Data was acquired as two "dynamic" studies covering the first hour after injection and a delayed static image as follows:

(1) For the first five minutes, data was acquired continuously as five second frames, using a 64 by 64 matrix.

(2) For the next 55 minutes, data was acquired continuously as 30 second frames using a 128 by 128 matrix. Data acquisition was then discontinued until four hours after injection.

(3) At four hours post injection, a ten minute long static image was acquired in a 128 by 128 matrix.

All data was stored on a computer in an unprocessed form.

III(4) Data analysis

The 60 frames of the initial dynamic study were summated to create one image. Then equally sized regions of interest (ROIs) were chosen over an area of the tumour site, background close to the tumour and the myocardium. Time activity curves were generated over these areas. The curves were displayed on the screen and recorded on polaroid pictures. The same procedure was followed with the second dynamic study. The frames were summated and the previously created ROIs over tumour, background and heart were assigned (Fig. 1). Activity time curves were generated and displayed on the screen and recorded on polaroid pictures. The processed data were stored on the disk. The computer was linked with a printer and curve points were printed.

For each patient the time activity curves were analyzed for the time of maximal tumour uptake of Tl-201. The time of maximal tumour uptake in the tumour was defined as the earliest time after injection at which peak uptake occurred.

Using the computer, the tumour time activity curve was divided by the background curve to yield the tumour to background ratios. The time of maximal tumour / background ratios was estimated in each patient.

For each patient the tumour to background activity ratios were calculated at 5, 10, 20, 30, 40, 50, and 60 minutes after injection to enable assessment of changes in tumour to background ratios.

The changes in thallium-201 concentration between early and four hours delayed images (wash out rate) were quantitatively assessed. An "early" static image was produced by summating the dynamic data obtained from 5 to 15 minutes following injection. Equal regions of interest over the tumour and surrounding background were generated, and total counts in the tumour and background were recorded. The same region of interests were transferred over the tumour site and surrounding background on the delayed four hours image (Fig. 2 - 3). The change of activity in the tumour between the early and delayed images was calculated, as were the tumour to background ratios.

III(5) Results

Abnormal Tl-201 uptake in the primary tumour occurred in 85 of the 97 patients studied (48 lung cancer, 24 breast cancer and 13 lymphoma patients, Table 2). Figures 4 through 6 show examples of Tl-201 uptake in a bronchial carcinoma, a breast carcinoma and a mediastinal lymphoma.

III(5)(a) Time course of tumour uptakes

Following intravenous administration, thallium-201 accumulated in tumours rapidly. Thallium-201 concentration in tumours increased gradually until it reached the time of maximum uptake and then did not change significantly during the first one hour.

Examples of curves from the initial and subsequent dynamic studies are shown for bronchial carcinoma, breast carcinoma and mediastinal lymphoma (Figs. 7 - 12).

III(5)(b) Time of maximal tumour uptake

The individual values for time of maximal tumour uptake in each of the tumour types studied are shown in Figure 13. The mean time of tumour uptake ($\pm$ SD) was 11.9 $\pm$ 3.34 minutes for lung carcinoma, 11.21 $\pm$ 1.88 minutes for breast carcinoma and 11.76 $\pm$ 3.25 minutes for lymphoma (Table 3).

III(5)(c) Time of maximal tumour / background uptake

The mean (± SD) time of maximal tumour / background activity was assessed and found for lung cancer to be 18.3 ± 0.59 minutes, breast cancer 13.0 + 1.16 minutes, and lymphoma mean 16.7 ± 1.04 minutes (Table 4). Tables 5 to 7 show the individual results of tumour to background ratios at 5, 10, 20, 30, 40 and 60 minutes. Figure 14 shows the individual values of maximal tumour / background ratio. Table 8 shows the summary of mean ± SD of tumour / background ratios at 5, 10, 20, 30, 40 and 60 minutes for each group of patients. The same results are shown in Figures 15 through 17. The mean tumour to background ratios do not change significantly over the first hour once the peak value is obtained at around ten minutes.

III(5)(d) Tumour uptake and tumour / background uptake at four hours versus the initial ten minutes image produced from the data obtained from five to 15 minutes post injection.

Four hours after administration of tracer, the background and tumour activities had decreased, but there is still clear visualization of the tumours.

The percentage of loss of tumour activity (wash out value) has been estimated in 46 patients with different tumour types, and expressed as a percentage of the activity present in the tumour in the initial (early)

static image. The individual values are shown in Table 9. For the whole group, the average (± SD) wash out was 25.4 (± 33.5) percent (Table 10).

The tumour to background ratios were also compared in the early and delayed 10 minutes and found to be (mean ± SD) 1.8 ± 0.30 for the initial image and 1.67 ± 0.35 for the delayed image.

These values are not significantly different ($P > 0.05$).

III(6) Discussion

The aim of the present study was to establish the best time for imaging tumours following injection of Tl-201. Our results show that uptake occurs rapidly in tumours with a peak value obtained ten to 15 minutes post injection in most cases. There were no significant differences in different tumour types.

Tumour to background ratios also rapidly attained peak values and remained relatively constant over the hour following injection. No significant change in tumour / background ratio was found in the four hour post injection images compared to one hour post injection data.

Previous studies of Tl-201 tumours imaging have utilized variable delays after injection. Kaplan et al, 1987 [247] started imaging brain tumours five minutes after injection of Tl-201. Senga et al, 1985 [248], studying thyroid tumours imaged at ten to 20 minutes post injection and reported that these early images produced a clearer scintigram than delayed studies. On the other hand, Ochi et al, 1982 [244], emphasized the importance of delayed imaging and concluded that three to five hours post injection was the most appropriate time for imaging.

From our own data we conclude that tumour imaging with Tl-201 is best performed 20 to 60 minutes post injection. Multiple views can be obtained in this period with no significant loss of lesion uptake. We did not find any evidence that delayed (4 hour) imaging was advantageous because tumour / background is not significantly changed and the count in tumour decreased. No tumour not seen in the early image was visualized at four hours. The short waiting period after injection with Tl-201 clearly offers a major potential advantage over alternative tumour imaging agents, such as Gallium-67 or radio-labeled monoclonal antibodies which require much longer delays from injection to image.

Table (2)

Abnormal Tl-201 uptake in the primary tumour occured in 85 of the 97 patients studied.

Group of patients	Positive with T1-201
Lung carcinoma	48/56
Breast carcinoma	24/26
Malignant lymphoma	13/15
Total	85/97

Table (3)

Time to maximal Tl-201 uptake (mins; mean ± SD) *

Lung carcinoma	11. 9 ± 3.34
Breast carcinoma	11.21 ± 1.88
Lymphoma	11.76 ± 3.25
Myocardium	11.61 ± 3.28

* Tumour uptake uncorrected for background activity.

Table (4)

Time of maximal tumour/background ratio (mins; mean ± SD) *

Lung carcinoma	18.3 ± 0.59
Breast carcinoma	13.0 ± 1.16
Lymphoma	16.7 ± 1.04

* Tumour uptake uncorrected for background activity.

Table (5)

Lung carcinoma patients individual values for tumour and back ground activities (counts/30 sec) and tumour to background ratios at varios intervals after injection of Tl-201 (Tumour activity not corrected for background)

Name		5 min	10 min	20 min	30 min	40 min	50 min	60 min
	T	283	296	313	332	317	315	320
F.G	BG	211	284	212	209	206	229	209
	Ratio	1.34	1.61	1.48	1.58	1.54	1.37	1.53
	T	1290	1500	1410	1430	1510	1460	1430
R.A	BG	816	754	712	720	767	726	740
	Ratio	1.58	1.99	1.98	1.98	1.96	2.00	1.93
	T	545	470	437	396	409	384	357
B.A	BG	293	251	245	251	239	246	227
	Ratio	1.86	1.87	1.78	1.57	1.71	1.56	1.57
	T	571	578	584	544	574	560	545
L.S	BG	309	329	281	282	290	259	295
	Ratio	1.85	1.76	2.08	1.93	1.98	2.16	1.85
	T	548	531	492	483	465	458	457
A.Y	BG	339	329	302	296	286	263	282
	Ratio	1.61	1.61	1.63	1.63	1.62	1.74	1.62
	T	711	700	680	640	602	610	570
M.F	BG	411	419	362	358	296	323	319
	Ratio	1.61	1.67	1.88	1.78	2.03	1.88	1.79
	T	226	226	231	185	205	193	204
S.A	BG	162	146	170	161	147	141	140
	Ratio	1.39	1.55	1.35	1.15	1.39	1.36	1.46
	T	317	263	237	238	235	216	216
H.J	BG	197	153	141	141	149	133	131
	Ratio	1.61	1.72	1.68	1.69	1.58	1.63	1.65
	T	160	168	163	144	144	106	
M.M	BG	147	117	135	128	123	76	
	Ratio	1.09	1.44	1.21	1.12	1.17	1.39	
	T	177	175	168	147	146	138	153
S.A	BG	113	107	82.8	96.6	111	86.8	92.9
	Ratio	1.57	1.64	1.93	1.52	1.31	1.59	1.64
	T	430	454	428	459	395	372	355
R.A	BG	283	270	271	257	244	237	240
	Ratio	1.52	1.68	1.58	1.67	1.62	1.57	1.48

Table 5: Lung carcinoma patients

Name		5 min	10 min	20 min	30 min	40 min	50 min	60 min
	T	117	101	94.1	94.4	79.4	87.6	87.8
R.S	BG	61.1	59.1	60.8	53.9	55.2	51.4	52.0
	Ratio	1.91	1.69	1.55	1.75	1.44	1.70	1.69
	T	164	214	211	213	205	160	163
K.A	BG	87.4	87.1	99.6	97.6	96.4	86.2	88
	Ratio	1.88	1.46	2.11	2.18	2.13	1.86	1.85
	T	238	229	226	213	224	202	196
H.A	BG	106	95.4	103	105	107	99	99
	Ratio	2.25	2.40	2.19	2.02	2.04	2.09	2.08
	T	247	245	249	244	246	239	241
A.O	BG	154	130	118	117	116	114	116
	Ratio	1.60	1.89	2.11	2.09	2.12	2.10	2.08
	T	384	379	380	372	369	366	352
A.A	BG	222	214	221	213	215	220	217
	Ratio	1.73	1.77	1.72	1.74	1.71	1.66	1.62
	T	170	168	168	166	154	162	144
M.H	BG	94.4	91.8	93.8	93.3	87	105	88.3
	Ratio	1.8	1.83	1.79	1.78	1.77	1.53	1.63
	T	81.6	100	88.8	83.6	73.1	86.8	90.9
W.A	BG	53.2	46.4	48.2	46.2	53.9	48.9	52.2
	Ratio	1.53	2.15	1.84	1.80	1.36	1.78	1.74
	T	564	464	375	462	453	489	436
A.M	BG	94.4	91.8	93.8	93.3	87	105	88.3
	Ratio	1.98	2.03	2.01	1.99	1.96	2.04	1.99
	T	915	1010	809	1018	987	884	878
M.A	BG	609	599	646	645	554	499	469
	Ratio	1.52	1.69	1.25	1.57	1.78	1.77	1.87
	T	345	309	325	316	299	293	286
A.N	BG	233	207	207	212	197	189	188
	Ratio	1.48	1.49	1.57	1.49	1.51	1.59	1.54
	T	119	109	105	98	101	97	89
A.F	BG	68	62	59	58.3	60.8	59	61
	Ratio	1.75	1.76	1.71	1.63	1.66	1.64	1.61
	T	739	698	692	660	653	624	598
A.T	BG	391	347	346	332	351	334	336
	Ratio	1.89	2.01	2.0	1.99	1.86	1.87	1.78

Table 5: Lung carcinoma patients

Name		5 min	10 min	20 min	30 min	40 min	50 min	60 min
	T	968	967	896	761	822	795	760
L.M	BG	457	430	433	416	413	398	422
	Ratio	2.12	2.25	2.07	1.83	1.99	2.00	1.80
	T	306	302	298	275	288	256	270
H.M	BG	268	238	177	199	188	182	221
	Ratio	1.14	1.27	1.68	1.38	1.53	1.41	1.22
	T	997	911	920	902	1003	893	898
F.A	BG	702	533	609	553	599	383	
	Ratio	1.42	1.71	1.51	1.63	1.72	1.49	1.54
	T	114	109	113	114	101	106	105
S.M	BG	46.6	44.5	69.7	72.7	48.9	43.3	51.5
	Ratio	2.44	2.65	1.34	1.57	2.23	1.90	2.05
	T	350	353	352	351	345	338	352
A.S	BG	245	239	205	220	218	226	224
	Ratio	1.43	1.48	1.72	1.6	1.79	1.5	1.57
	T	277	284	387	381	379	380	375
F.A	BG	244	241	269	270	243	240	280
	Ratio	1.13	1.17	1.43	1.41	1.54	1.58	1.33
	T	160	153	155	147	108	120	113
A.A	BG	92.8	84.4	94.9	86.8	73.4	88.4	84.0
	Ratio	1.64	1.81	1.63	1.69	1.47	1.42	1.35
	T	186	196	223	208	200	232	220
A.E	BG	93.3	95.9	92.3	92.7	101	119	116
	Ratio	1.99	2.05	2.41	2.24	1.98	1.94	1.89
	T	187	165	174	170	160	172	149
A.T	BG	111	84.5	89.8	88.2	90.2	91.9	101
	Ratio	1.68	1.94	1.76	1.92	1.77	1.87	1.47
	T	177	176	185	174	176	172	166
H.M	BG	94.2	92.8	98.6	95.4	97.2	96.3	89.8
	Ratio	1.87	1.89	1.87	1.82	1.81	1.78	1.84
	T	786	720	660	640	604	611	605
H.A	BG	444	395	344	365	336	330	336
	Ratio	1.77	1.82	1.91	1.75	1.79	1.85	1.80
	T	336	349	328	307	301	268	266
M.S	BG	302	277	250	244	230	213	221
	Ratio	1.11	1.25	1.31	1.25	1.30	1.25	1.20

Table 5: Lung carcinoma patients

Name		5 min	10 min	20 min	30 min	40 min	50 min	60 min
	T	1070	1020	1040	972	1040	1020	991
N.H	BG	493	453	453	464	469	461	476
	Ratio	2.04	2.25	2.3	2.09	2.21	2.21	2.08
	T	286	280	272	255	248	231	237
A.S	BG	161	134	131	135	131	126	138
	Ratio	1.7	2.09	2.08	1.90	1.90	1.83	1.78
	T	246	243	280	241	250	253	241
W.S	BG	195	157	146	159	179	159	172
	Ratio	1.26	1.55	1.91	1.51	1.39	1.59	1.40
	T	1030	965	967	839	822	775	757
K.K	BG	538	451	456	481	448	412	442
	Ratio	2.01	2.18	2.28	1.94	2.05	2.19	2.17
	T	267	270	226	261	244	258	230
I.S	BG	187	140	147	144	159	147	151
	Ratio	1.43	1.93	1.81	1.81	1.53	1.76	1.52
	T	138	136	130	119	132	132	129
S.S	BG	72.3	71.6	69	82.6	77.6	74.2	73.3
	Ratio	1.91	1.90	1.88	1.44	1.70	1.78	1.76
	T	432	440	418	402	397	382	366
L.A	BG	767	254	263	244	234	251	256
	Ratio	1.62	1.73	1.59	1.65	1.70	1.52	1.43
	T	498	480	472	433	438	435	442
M.L.	BG	398	329	335	316	304	315	289
	Ratio	1.25	1.46	1.41	1.37	1.44	1.38	1.51
	T	93.1	118	97.9	94.2	85.6	83.2	89.4
R.M	BG	58.2	67	56.3	63.6	50.4	58.6	58.4
	Ratio	1.60	1.76	1.74	1.48	1.70	1.42	1.53
	T	80.9	101	95.6	88.4	72.8	78.6	67.7
F.G	BG	42.6	42.3	47	42	40.3	36.8	39.3
	Ratio	1.90	2.39	2.03	2.10	1.81	2.16	1.72
	T	153	125	115	105	114	105	94
A.T	BG	94.8	75	68.3	66.0	69.9	64.2	59.4
	Ratio	1.61	1.66	1.68	1.59	1.63	1.64	1.58
	T	267	265	250	241	237	240	221
L.H	BG	205	198	201	197	187	190	192
	Ratio	1.30	1.34	1.24	1.22	1.27	1.26	1.15

Table (6)

Breast Carcinoma Patients

Individual values for tumour to background ratios (counts/30 secs) and tumour to background ratios (Tumour activity corrected for background) after injection of Tl-201. (Tumour activity not corrected for background).

Name		5 min	10 min	20 min	30 min	40 min	50 min	60 min
	T	159	148	145	153	151	177	155
F.Sh	BG	144	92.9	118	103	117	113	101.1
	Ratio	1.10	1.59	1.23	1.48	1.29	1.57	1.53
	T	513	510	487	475	418	469	422
H.J	BG	211	261	250	200	231	198	220
	Ratio	2.43	1.95	1.95	2.38	1.81	2.37	1.92
	T	501	472	428	432	455	462	405
H.M	BG	239	227	256	213	234	222	237
	Ratio	2.10	2.08	1.67	2.03	1.94	2.08	1.71
	T	188	165	175	180	188	148	181
M.M	BG	84.6	82.7	83.3	92.7	82.9	81.8	77.4
	Ratio	2.22	2.0	2.10	1.94	2.27	1.81	2.34
	T	197	244	250	250	249	231	224
M.S	BG	66.7	65.9	69.4	67.3	79.9	92.1	69.8
	Ratio	2.95	3.7	3.60	3.7	3.11	2.51	3.21
	T	153	137	133	139	145	160	152
M.L	BG	81.3	69.9	172	71.3	95.1	78.4	72.3
	Ratio	1.88	1.96	1.83	1.95	1.52	2.03	2.10
	T	117	96.3	78.4	94.4	77.4	87.6	87.8
R.S	BG	61.1	63.1	46.3	53.6	55.4	51.8	52.0
	Ratio	1.91	1.53	1.69	1.76	1.40	1.69	1.69
	T	164	196	211	213	205	160	163
K.M	BG	97.4	87.1	87.9	97.6	96.4	82.7	84.6
	Ratio	207	2.25	215	2.18	2.13	1.93	1.92
	T	71.3	61.1	53.9	92.3	73.6	96.8	
S.M	BG	58.5	54.6	42.8	55.7	47.2	44.3	
	Ratio	1.22	1.12	1.26	1.65	1.54	2.18	

Table 6 : Breast Carcinoma Patients

Name		5 min	10 min	20 min	30 min	40 min	50 min	60 min
	T	108	115	114	109	96	86	89
S.H	BG	91	87.2	88	84.2	76.3	70.4	71.1
	Ratio	1.19	1.32	1.29	1.30	1.26	1.22	1.25
	T	91.5	96.1	94.1	84.3	88.2	87.2	85.5
M.G	BG	96	95.1	96	84.2	89.1	85.5	85
	Ratio	0.95	1.01	0.98	1.00	0.99	1.02	1.01
	T	423	392	365	353	361	383	369
F.S	BG	270	363	225	232	235	206	223
	Ratio	1.57	1.52	1.82	1.52	1.54	1.86	1.65
	T	404	404	3663	363	383	346	
R.K	BG	250	207	224	220	240	219	
	Ratio	1.63	1.95	1.63	1.65	1.60	1.58	
	T	238	287	283	252	236	272	272
F.A	BG	162	153	170	181	184	158	178
	Ratio	1.47	1.87	1.66	1.39	1.28	1.72	1.52
	T	2350	2310	2300	2210	2222	2150	2160
F.Ah	BG	2080	1770	1890	1770	1720	1730	1650
	Ratio	1.13	1.31	1.21	1.24	1.29	1.23	1.30
	T	630	522	519	503	471	444	452
M.S	BG	315	318	360	329	341	322	308
	Ratio	2.0	1.64	1.44	1.53	1.38	1.38	1.48
	T	649	676	671	625	584	610	615
A.A	BG	312	338	348	324	321	301	289
	Ratio	2.08	2.0	1.93	1.93	1.82	2.03	2.13
	T	361	375	339	381	367	342	295
Z.S	BG	319	232	217	227	214	201	231
	Ratio	1.73	1.61	1.56	1.67	1.71	1.70	1.27
	T	264	256	262	239	260	263	247
F.M	BG	141	130	142	139	151	143	157
	Ratio	1.87	1.97	1.85	1.72	1.72	1.84	1.57
	T	1620	1530	1590	1330	1190	1110	1050
M.B	BG	782	694	678	620	561	567	577
	Ratio	2.07	2.20	2.34	2.15	2.12	1.95	1.82

Table 6: Breast Carcinoma Patients

Name		5 min	10 min	20 min	30 min	40 min	50 min	60 min
	T	282	278	303	283	278	303	316
F.B	BG	136	124	137	142	116	128	117
	Ratio	2.07	2.24	2.21	1.99	2.39	2.37	2.70
	T	595	635	589	589	603	639	567
K.N	BG	568	441	424	473	450	465	464
	Ratio	1.05	1.44	1.39	1.26	1.34	1.37	1.22
	T	732	757	682	661	669		
M.R	BG	562	521	486	471	465		
	Ratio	1.30	1.45	1.40	1.40	1.43		
	T	65.9	70	63.8	62.9	45.9	58.6	55.5
S.H	BG	47	43	44.8	41.5	37.9	41.6	35.6
	Ratio	1.40	1.63	1.42	1.51	1.21	1.41	1.56

Table 7

Malignant Lymphoma Patients

Individual values of tumour/background activities (background cs) and tumour to background ratios at various intervals after I-201.
(Tumour activity not corrected for background).

Name		5 min	10 min	20 min	30 min	40 min	50 min	60 min
	T	1070	1180	1100	1230	1170	1190	1210
T.M	BG	602	566	517	538	507	489	478
	Ratio	1.78	2.08	2.13	2.29	2.30	2.43	2.53
	T	818	853	863	881	900	830	841
K.Y	BG	500	503	511	530	535	532	539
	Ratio	1.64	1.70	1.69	1.66	1.68	1.56	1.65
	T	2320	2360	2410	2560	2540	2580	2660
B.A	BG	1180	1280	1270	1410	1350	1370	1370
	Ratio	1.97	1.84	1.90	1.82	1.88	1.88	1.94
	T	692	694	767	720	743	693	670
M.J	BG	207	167	223	212	207	217	215
	Ratio	3.34	4.15	3.44	3.40	3.59	2.19	3.11
	T	286	417	410	416	399	302	375
M.A	BG	279	248	230	257	255	225	280
	Ratio	1.38	1.68	1.78	1.63	1.56	1.34	1.34
	T	213	229	248	205	169	172	185
F.F	BG	141	160	178	147	124	123	151
	Ratio	1.51	1.43	1.39	1.39	1.36	1.40	1.23
	T	225	199	207	167	165	139	
D.M	BG	147	132	139	121	117	91.5	
	Ratio	1.53	1.51	1.49	1.38	1.41	1.52	
	T	170	172	168	149	146	161	141
V.K	BG	101	102	101	94.3	93	101	92
	Ratio	1.68	1.69	1.66	1.58	1.57	1.59	1.53
	T	115	111	114	116	103	107	108
M.A	BG	76.7	74.2	79.7	80.1	78.3	73.2	71.5
	Ratio	1.50	1.49	1.43	1.45	1.32	1.46	1.51

Table 7: Malignant Lymphoma Patients

Name		5 min	10 min	20 min	30 min	40 min	50 min	60 min
	T	165	157	152	147	118	136	117
S.A	BG	101	86.7	93	88	78	91.2	81.8
	Ratio	1.63	1.81	1.64	1.68	1.52	1.49	1.43
	T	603	635	592	576	531	513	511
B.G	BG	538	438	435	440	385	383	396
	Ratio	1.17	1.45	1.36	1.31	1.38	1.34	1.29
	T	284	253	270	224	198	183	193
S.K	BG	192	182	186	174	156	140	146
	Ratio	1.48	1.39	1.45	1.29	1.27	1.31	1.32
	T	115	113	83	101	93	97	85
M.S	BG	101	92	74	83	78	80	73
	Ratio	1.14	1.23	1.12	1.22	1.19	1.21	1.16

Table 8

Tumour to background ratios (mean ± SD) of T1-201 in the hour following injection.

(Tumour activity not corrected for background).

Name	5 min	10 min	20 min	background). 0 min	50 min	60 min
Lung Carcinoma	1.65	1.81	1.77	1.70	1.71	1.71	1.67
	±0.30	±0.19	±0.20	±0.27	±0.08	±0.26	±0.24
Breast Carcinoma	1.74	1.81	1.74	1.77	1.68	1.78	1.68
	±0.47	±0.51	±0.50	±0.41	±0.36	±0.37	±0.59
Lymphoma	1.67	1.80	1.73	1.70	1.69	1.67	1.67
	±0.55	±0.52	±0.57	±0.58	±0.64	±0.54	±0.59

Table 9

The washout rate between early and 4 hours delayed images in various tumours.
(Tumour activities are corrected for background).

Name	Early T/BG	Ratio	Delayed T/BG	Ratio	% Washout
M.M	5720/ 3788	1.51	5060/ 3530	1.43	20.81
S.A	6654/ 3520	1.72	5909/ 3410	1.90	-10.46
W.M	4192/ 2065	2.03	3847/ 2224	1.73	23.70
L.S	18261/ 9085	2.01	17949/ 7770	2.31	-10.93
A.Y	8500/ 4030	2.11	4800/ 3200	1.50	64.21
M.F	12180/ 6870	1.78	7670/ 4460	1.72	39.55
W.S	8773/ 4514	1.94	6730/ 4306	1.56	43.08
F.B	8355/ 4104	2.04	6506/33319	1.96	25.03
M.S	10532/ 4994	2.11	3053/ 2159	1.41	83.85
S.H	9768/ 4579	2.13	9150/ 5423	1.69	28.17
A.A	19695/11540	1.71	9810/ 6941	1.41	64.81
Z.H	5645/ 2610	2.16	5003/ 2448	2.04	15.81
K.N	5140/ 3292	1.56	3361/ 2965	1.13	78.57
A.M	10950/ 6260	1.75	5666/ 3522	1.61	54.28
F.A	6197/ 4201	1.48	3954/ 2816	1.40	42.98
S.A	8905/ 6850	1.30	5146/ 4253	1.21	56.54
H.M	10726/ 4915	2.18	1790/ 900	1.98	84.68
S.A	26790/16000	1.67	17000/11000	1.54	44.39
M.H	17000/ 9000	1.89	16000/12000	1.33	50.00
F.A	4330/ 3520	1.23	4136/ 2870	1.44	-56.30
M.S	15176/ 8980	1.69	10400/ 6342	1.52	42.58
M.J	13305/ 6000	2.22	13127/ 7100	1.84	17.49
A.A	5498/ 3899	1.41	4308/ 3122	1.38	25.82
M.K	462/ 382	1.21	551/ 477	1.15	7.50
M.L	3243/ 2100	1.54	5443/ 4165	1.30	-11.81
M.S	4518/ 2235	2.02	4588/ 1674	2.74	-27.64
R.A	9432/ 5639	1.67	7788/ 3793	2.05	- 5.30
H.A	14931/ 9450	1.58	10555/ 7486	1.41	44.06
M.S	15438/ 7903	1.95	10383/ 6300	1.65	45.81
K.N	13615/ 5360	2.54	12235/ 4894	2.50	11.07
A.O	24700/15470	1.60	24100/10955	2.19	-42.41
W.A	5850/ 3530	1.66	4032/ 1785	2.25	3.15
S.A	11630/ 6020	1.93	8560/ 4380	1.95	25.49
M.G	8350/ 5400	1.55	7900/ 4700	1.68	- 8.47
D.N	11012/ 4882	2.25	9281/ 4730	1.96	25.75
A.Y	9852/ 4975	1.98	7403/ 4569	1.62	41.89
N.H	10250/ 6313	1.62	8380/ 5624	1.49	29.99
S.J	13830/ 9763	1.62	11725/ 8450	1.39	46.02
A.S	24060/10020	2.40	18960/10744	1.76	41.86
A.T	3485/ 2041	1.71	4632/ 2405	1.92	-54.22

Table (9)

Name	Early T/BG	Ratio	Delayed T/BG	Ratio	% Washout
E.E	4962/ 3101	1.60	4778/ 3057	1.56	7.52
A.A	6785/ 4526	1.50	3524/ 2670	1.32	62.19
S.A	7945/ 4786	1.66	4830/ 3157	1.53	47.04
A.T	6961/ 3889	1.79	6052/ 3478	1.74	16.21
S.J	15830/ 9763	1.62	11725/ 8450	1.39	46.17
A.Ar	3841/ 2222	1.73	4824/ 2975	1.62	-14.21

Table 10

Mean (± SD) Tl-201 washout from tumour between 1 and 4 hrs post injection was 25.4% (± 33.5).

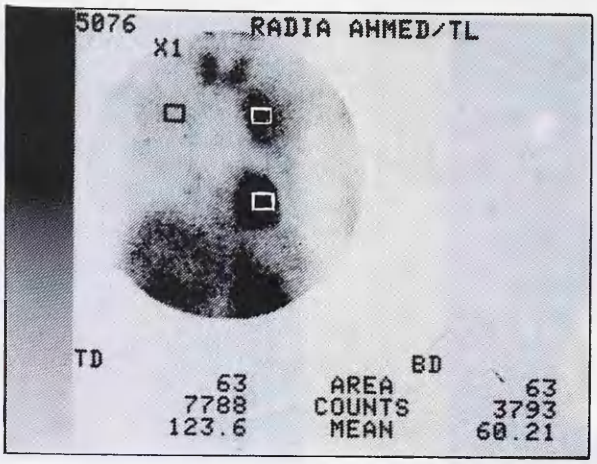

Figure (1): Regions of interest over the tumour, background and myocardium.

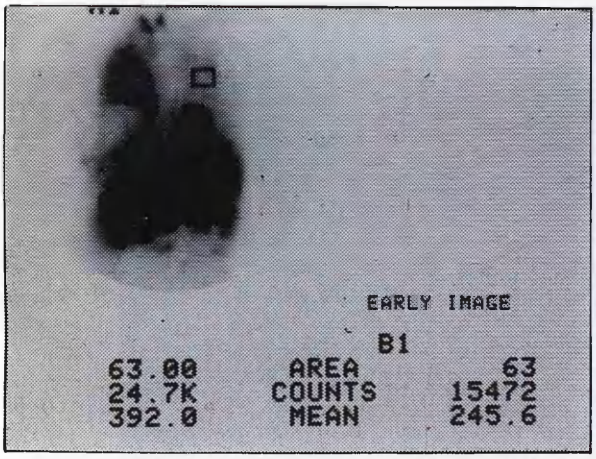

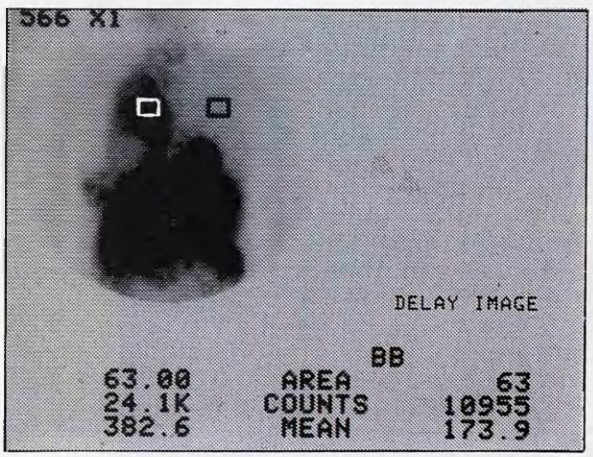

Figures (2 & 3): Regions of interest, over the tumour, background in early (figure 2) and delayed image (figure 3). The counts in each ROI were obtained and washout rate was calculated.

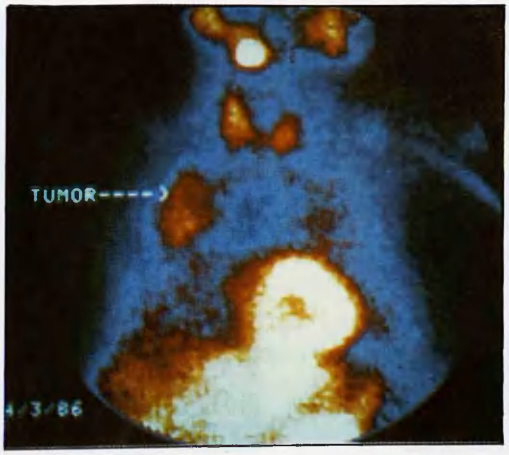

Figure (4): Abnormal Tl-201 concentration in the upper part of the Rt. lung in a patient with lung carcinoma.

Figure (5): Abnormal Tl-201 chloride concentration in the right breast in a patient with breast carcinoma.

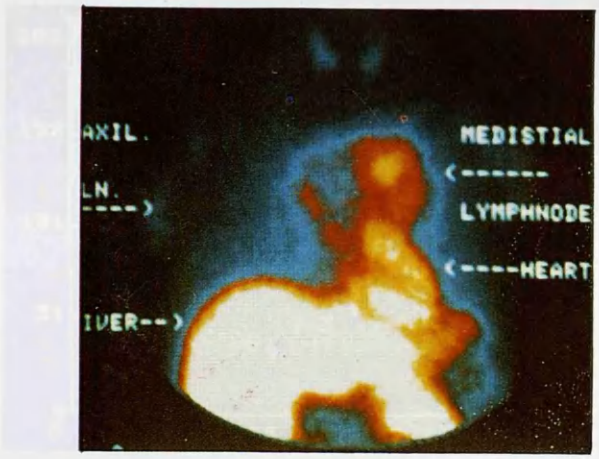

Figure (6): Abnormal Tl-201 concentration in the mediastinum in a patient with malignant lymphoma.

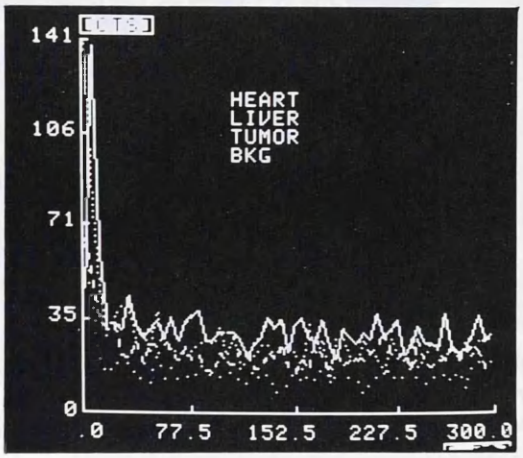

Figure (7): Flow I. The initial uptake immediately, after I.V. injection of Tl-201 by the heart, liver, tumour and background in a patient with lung carcinoma.

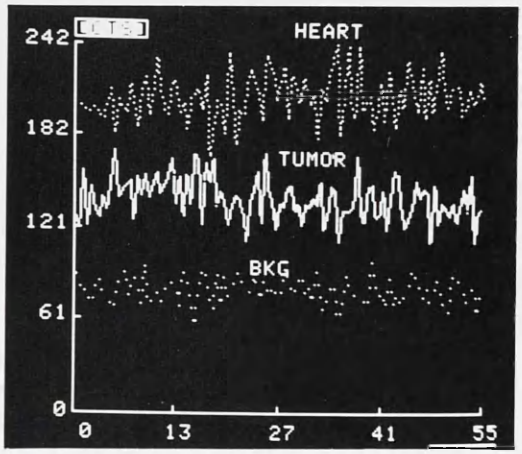

Figure (8): Flow II. Time activity curve until 55 minutes of the heart, tumour, and background in a patient with lung carcinoma.

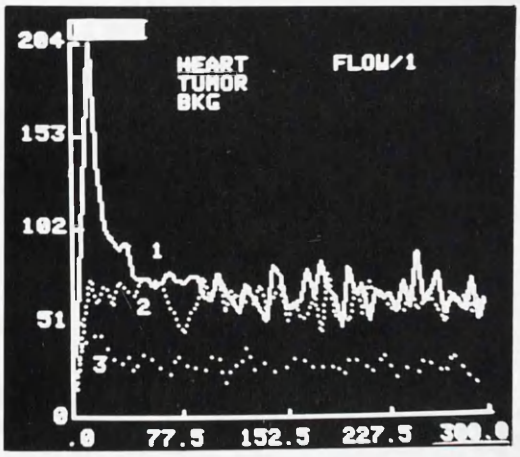

Figure (9): Flow I. The intiial uptake of Tl-201 by the heart, tumour and background in a patient with breast carcinoma.

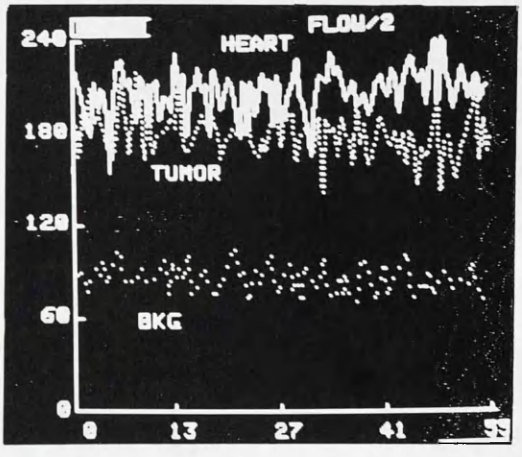

Figure (10): Flow II, time activity curve until 55 minutes of the heart, tumour and background in a patient with breast carcinoma.

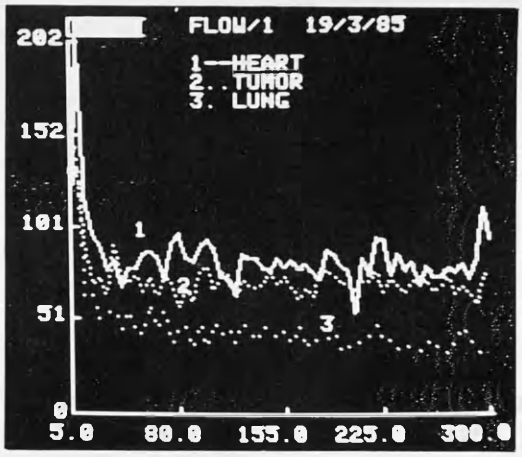

Figure (11): Flow I, the initial uptake of Tl-201 by heart, tumour and background (lung) in a patient with malignant lymphoma.

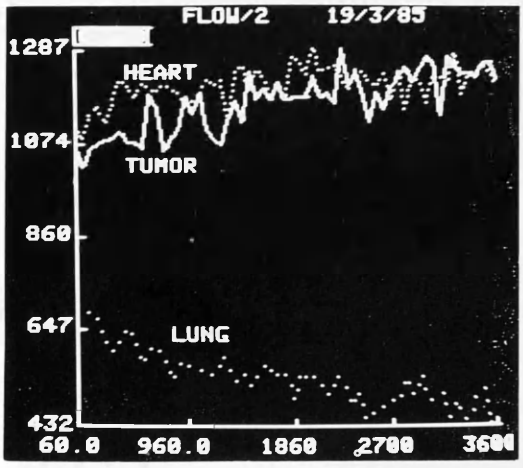

Figure (12): Flow II, time activity curve until 1 hour of the heart, tumour and lung (as a background) in a patient with mediastinal lymphoma.

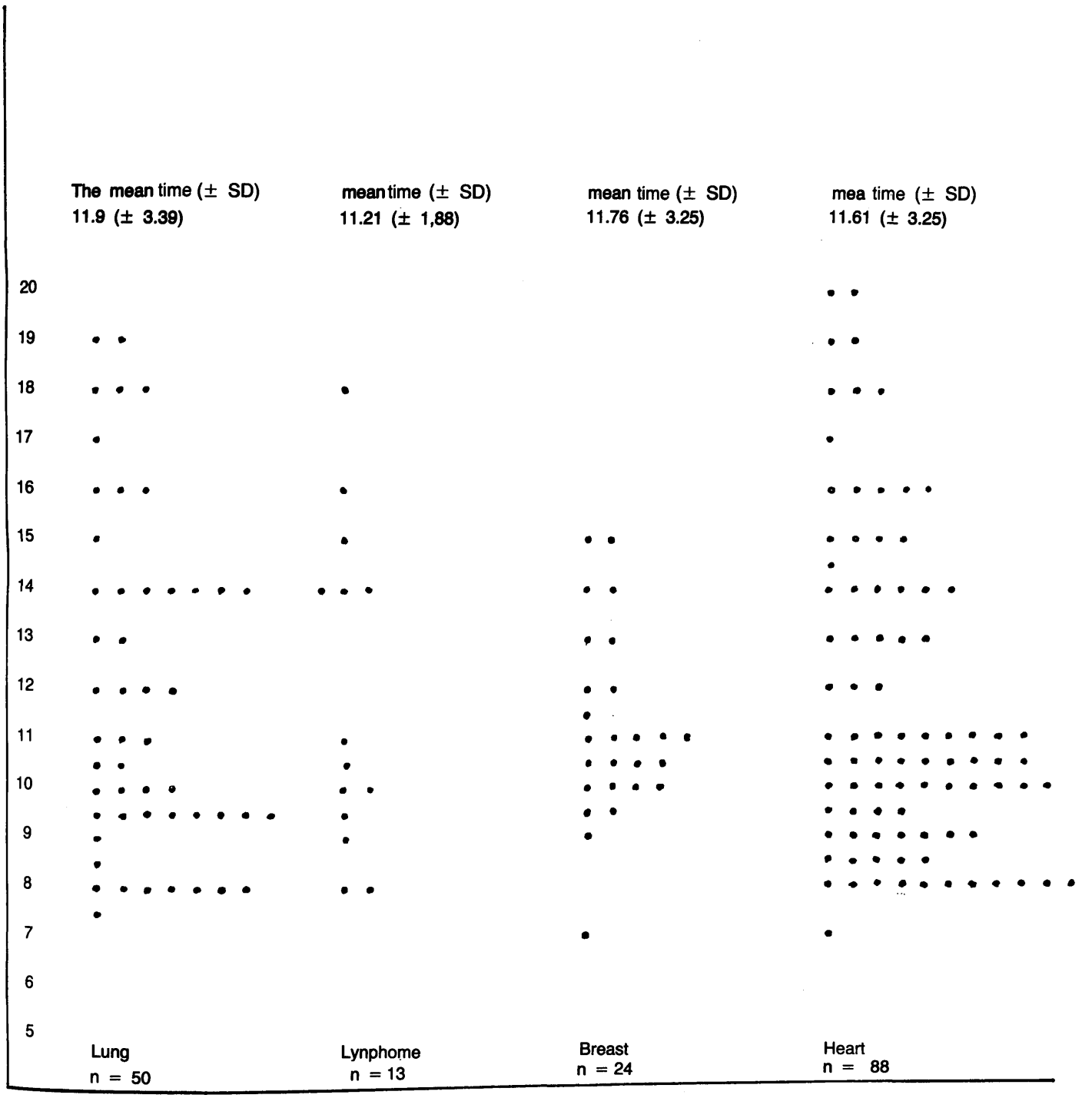

Figure (13): The individual values of maximal tumour uptake in lung cancer n=(50), lymphoma (n=13) breast cancer n=(24), heart n=(88).

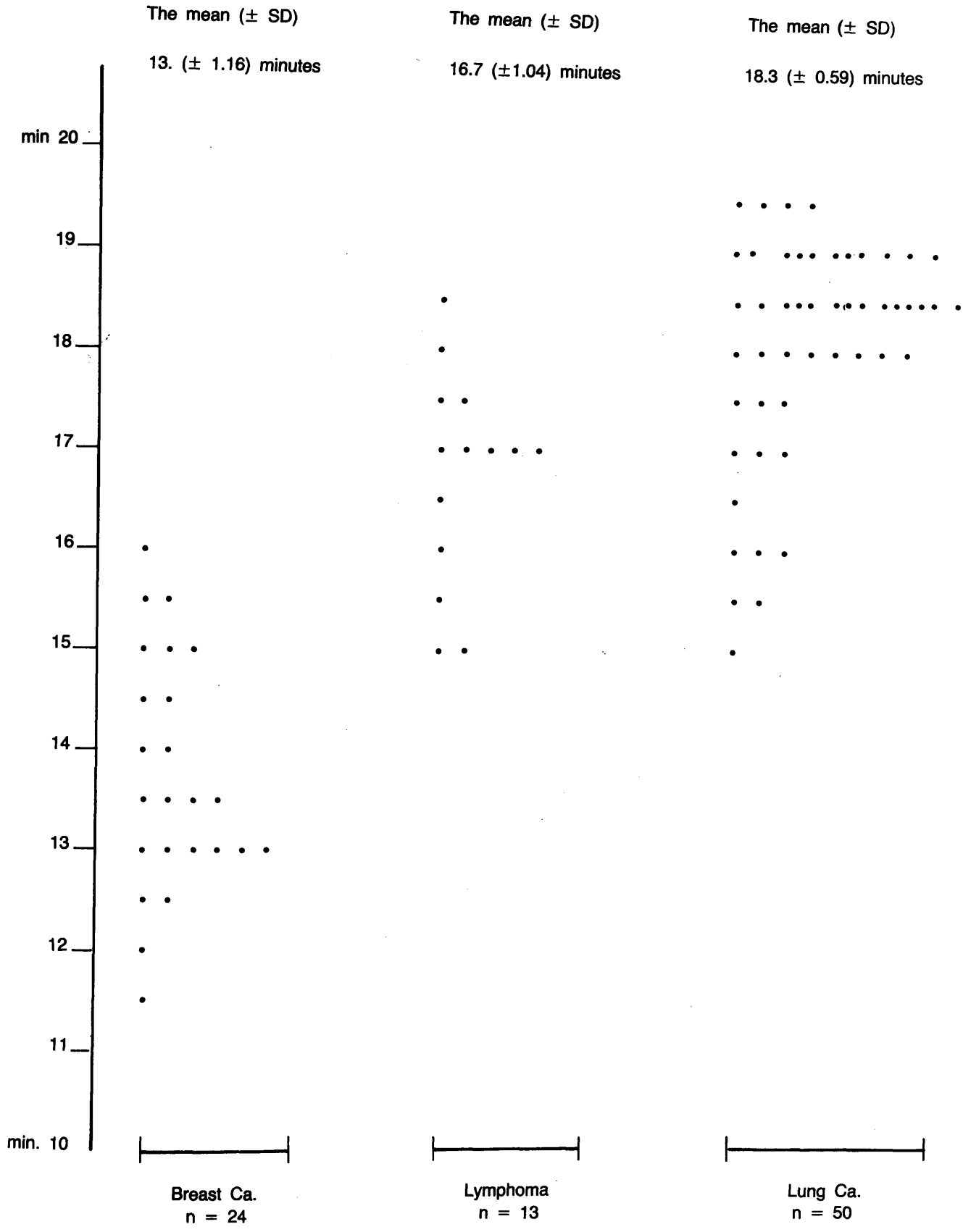

Figure (14) : The individual values of maximal tumour to background ratio in breast cancer (n=24), lymphoma (n=13) and lung cancer (n=50).

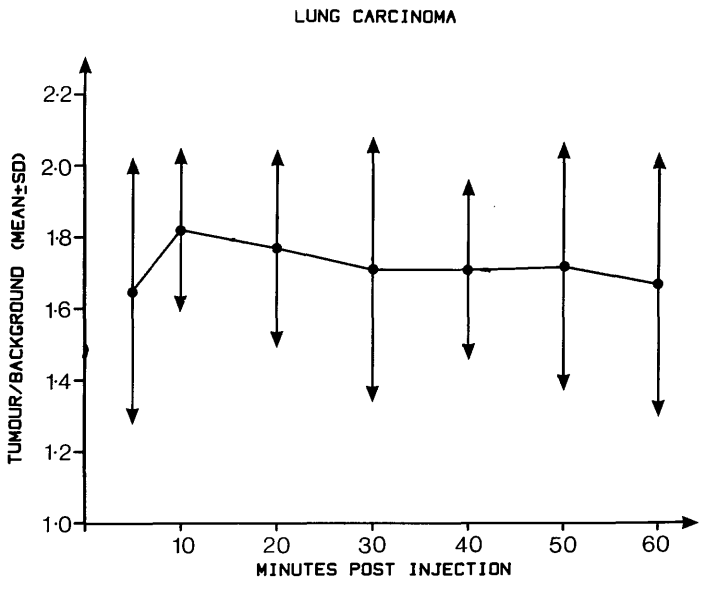

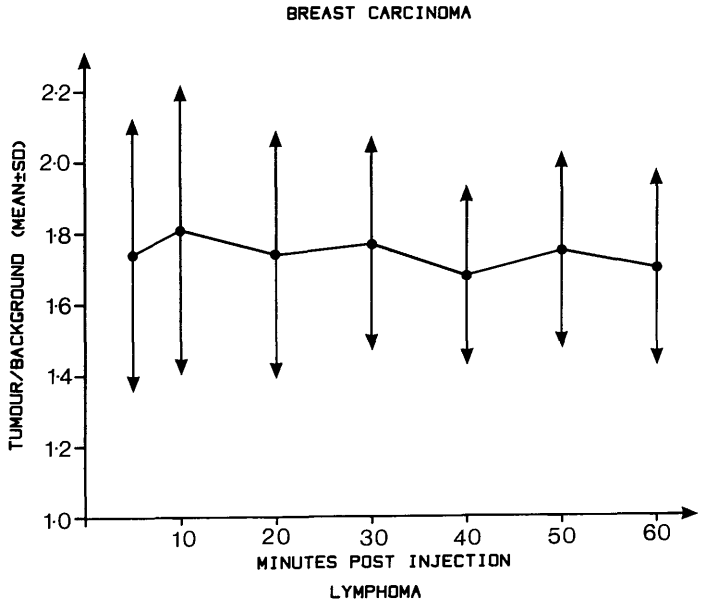

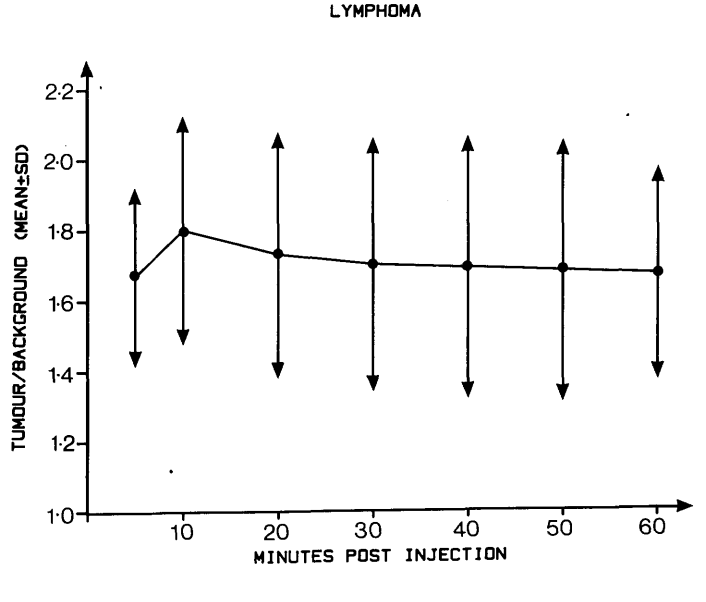

Figures (15-17): Tumour/background ratios (± SD) at intervals of 5, 10, 20, 30, 40, 50 and 60 minutes in patients with lung carcinoma, breast carcinoma and malignant lymphoma.

CHAPTER IV

MECHANISM OF Tl-201 UPTAKE IN TUMOURS

IV (1) Introduction

Thallium is a metallic element in group III-A of the periodic table. The use of Tl-201 as a myocardial imaging agent is dependent upon its similarities to ionic potassium in biologic systems. As a potassium analogue, thallium activates the sodium-potassium (Na-K) ATP-ase dependent pump and the cellular uptake of Tl is inhibited by ouabain and sodium floride which block the Na-K pump [28]. Update of Tl^+ and K^+ is not identical: Thallium appears to bind to two sites on the enzyme system compared to one for potassium [29]. This may explain the more prolonged clearance of thallium from the myocardium compared to potassium [51]. Thallium also has highly polarizable outer electron shells and readily complexes with water, and the membrane is almost equally permeable to Tl^+ as it is to K^+. It has been suggested that intracellular accumulation of thallium is driven by the transmembrane electropotential gradient [26].

Thallium and potassium belong to different groups in the periodic table. The biological similarities between thallium and potassium in terms of organ distribution have been explained by the fact that the hydrated

ionic radius of thallium lies between potassium and rubidium in size. This radius has been suggested as the essential property that determines passive penetration through a liquid layer and membrane [26] [249].

Mechanism of Tl-201 uptake in tumours has not been established. In the present study this mechanism was evaluated by a) comparison of the time course of Tl-201 uptake in tumours and myocardium; b) comparison of ratios of uptake of Tl-201 and $Tl^{(99m)}$-microspheres in tumour and normal tissues in a patient; and c) by in vitro studies of Tl-201 uptake by a tumour cell line.

IV(2) Comparison of tumour and myocardial uptake

IV(2)(a) Patients and Methods

As described in Chapter III, 97 patients with proven malignancy were examined for the optimal time for tumour imaging by Tl-201. Of these, 88 patients (53 with lung carcinoma, 24 with breast carcinoma and 13 with mediastinal lymphoma), had a comparative study was made of time course of tumour and myocardial uptake.

Also described in Chapter III, the data was acquired as two dynamic studies at five seconds intervals for five minutes then at 30 seconds intervals for 55 minutes. A ten minutes static image was obtained at four hours post injection. And after creating equally sized regions of interest over the tumour, background close to the tumour and myocardium,

activity time curves were generated from the two dynamic studies. These were analyzed for time course of uptake of Tl-201 in the tumour and myocardium.

The wash out rate between early and four hours delayed images was quantitatively assessed. An early static image was produced by summating the dynamic data obtained from five to 15 minutes following injection. Equal regions of interest over the tumour, myocardium, and surrounding background were recorded. The same region of interests were transferred over the tumour site, myocardium and surrounding background on the delayed four hours image. The change of activity in the tumour and myocardium between the early and delayed images was calculated.

IV(2)(b) Results

Following intravenous injection, Tl-201 uptake in the tumour and myocardium occurs rapidly. Figures 7 - 12 show typical activity time curves of the tumour and myocardium obtained from lung carcinoma, breast carcinoma, and mediastinal lymphoma.

In the whole series of patients the time from injection to peak tumour activity ranged from eight to 20 minutes. The mean time to peak tumour activity (ISD) was 11.9 ($\pm$ 3.34) minutes for lung carcinoma, 11.21 ($\pm$ 1.88) minutes for breast carcinoma and 11.76 ($\pm$ 3.25) minutes for lymphoma. These results were compared with the maximum time of myocardial

uptake and found to be similar. The time from injection to peak myocardial activity ranged from eight to 20 minutes. The mean time to peak myocardial activity (± SD) was 11.61 (±3.25).

The time course of tumour uptake paralleled myocardial uptake with almost identical times of peak uptake being obtained in tumour and myocardium.

Comparison of early "static" and four hours post injection images were possible in 46 patients (20 lung carcinoma, 17 breast carcinoma and 9 lymphoma). The mean (± SD) wash out of Tl-201 from the tumour over this period was 25.4 (±33.5) percent of the activity present in the early static image. The mean wash out of Tl-201 from the myocardium over four hours 29.7 (± 16.7) precent.

IV(3) Blood flow distribution of Tc 99m-microspheres versus Tl-201 in tumours

IV(3)(a) Introduction

As described previously (Chapter I) the uptake of Tl-201 in the myocardium reflects myocardial blood flow and Na-K pump activity. In view of the similarity of the time course of uptake of Tl-201 in the tumours and myocardium, the opportunity was taken of making a comparative study of the distribution of Tl-201 and Tc 99m - microspheres (reflecting blood flow) in tumour and normal tissues in a patient.

IV(3)(b) Methods

The subject was a 63 year old patient with known hepatic metastases from a carcinoma of colon who was undergoing a laparotomy for placement of a hepatic artery catheter for the purpose of regional chemotherapy.

Following insertion of the catheter, 20 MBq thallous chloride (Tl-201) and 40 MBq 99m-technetium microspheres were injected into the catheter. The microspheres were obtained from Sorin Biomedica (Italy) and had a particle size range of 23 to 45μ. Ten minutes after injection of the tracers biopsies were obtained from hepatic metastases and from normal liver. The lesion obtained was submitted to histological examination and to well counting for Tl-201 and Tc ^{99m}.

Three biopsies were taken, one gram of normal liver tissue, and two grams of tumour tissue. These samples were analyzed using a three channel Packard autogamma counter.

Channel 1 was set on Tc ^{99m} spectrum 120-160 kev. Channel 2 was set on Tl-201 spectrum 65-85 kev.

The samples were counted on day one and after five days (122.6 hours). The Tc-99m was decayed by more than 20 half-lives. The scattered radiation of both radionuclides were calculated and true count from each

radionuclide was obtained. The samples were weighted and counts per gram tissue for each radionuclide were obtained. The tumour/normal uptake ratio was calculated for both Tl-201 and and Tc-99m.

IV(3)(c) Results

Table 11 summarizes the weight of the samples and true count uptake of both radionuclides by the tumour, and normal liver tissues and counts per gram tissue for both Tc-99m and Tl-201 chloride.

The total tumour uptake of Tc-99m was found 4050 counts per gram.

The total tumour uptake of Tl-201 was found 1653 counts per gram.

The normal liver tissue uptake of Tc-99m was 66431 counts per gram and for Tl-201 was 297931 counts per gram.

Table 12 shows the ratio of uptake in tumour to normal liver tissue (per gram tissue) for the Tc-99m was 0.061, and for Tl-201 was 0.006.

Histology confirmed that no tumour was present in the area of macroscopically normal liver.

The tumour area was shown to contain a mixture of viable and necrotic tissue.

IV(3)(d) Comments

The distribution of thallium-201 within the tumours tissue is not proportional to the distribution of $^{Tc-99m}$ microspheres which reflects the regional blood flow of the liver deposits. These data suggest that Tl-201 chloride did not reflect the regional blood flow of the tumour. And I concluded that Tl-201 distribution in tumours is not purely a flow dependent process.

IV(4) In vitro studies: Thallium-201 uptake in non-small cell lung cancer

IV(4)(a) Aim of the Study:

To assess whether Thallium-201 uptake by tumour cells is dependent on the Sodium potassium ATPase pump, in a squamous carcinoma cell line SK-MES.

SK-MES cells grow as a monolayer in tissue culture flasks, grow in F10 DMEM and are trypsinized and passaged weekly.

IV(4)(b) Methods

Measurements of Tl-201 activity have been made under control conditions and after digoxin intervention in tumour cells. Five experiments were done, in each 5 cm^2 of cells incubated with Tl-201 without digoxin (control group) and 5 cm^2 of cells with digoxin.

The tumour Cell line is SK-MES (a squamous cell carcinoma). The mean cell count was 5 X 10^6 cells in 25 cm^2 flasks. The culture medium was F10-EM, supplemented with foetal bovine serum. Antibiotics were not added.

To 5 cm^2 sample added either o.1mg digoxin injectate BP in 0.4ml or 0.4ml saline to the control group.

Twenty minutes later, 3-4 MBq of Tl-201 chloride added and incubated for 45 minutes at 37^oC.

The cells were centrifuged down. The supernatant decanted and retained. Cells were resuspended in five ml saline, recentrifuged, supernatant separated and retained. The cells were resuspended in 5 ml saline and again centrifuged and the supernatant retained. Cells were resuspended in 5ml saline. The cells were trypsinized and harvested and the radioactive content of the cells was measured.

Counting was carried out in a gamma counter, for 60 seconds per tube. Blank tubes were used for background at beginning and end of counting the samples.

In each experiment two samples were treated with digoxin and two samples without digoxin. Each of 0.5ml samples of cells suspension, and o.5ml samples of mixed supernatant were counted separately.

Total activity in cellular and supernatant fractions calculated and cellular activity expressed as a percentage of total cellular and supernatant activity.

IV(4)(c) Results

The radioactive content of the cells was higher when incubated with Thallium alone (Table 13). The radioactive content of the supernatant was higher when the cells were incubated with Thallium and Digoxin. This suggests that Digoxin blocks the uptake of thallium by squamous lung carcinoma cells SK-MES.

IV(5) Discussion

The time course of tumour uptake paralleled myocardial uptake, with almost identical times of peak uptake being obtained in tumours and myocardium. The range of times to peak activity that I found in tumour and myocardium (8-20 minutes) is very similar to that reported by Bradley-Moore et al., 1975 [48] for Tl-201 myocardial uptake in an animal model.

The similarity in tumours and myocardial Tl-201 uptake may indicate a similar mechanism of tracer uptake. Myocardial Tl-201 uptake is generally accepted to reflect both blood flow and Na+ - K+ ATPase dependent pump activity [250].

There are conflicting reports in the literature concerning the exact role of blood flow in the extraction of Tl-201 by the myocardium. Abbate et al., 1977 [55], reported that the initial extraction of thallium by myocardium following bolus injection in man does not appear to be influenced by myocardial blood flow. On the other hand several studies have shown that the distribution of thallium is a flow dependent process[32] [251] [93] [250].

Other authors have reported that Tl-201 uptake in the tumours occurred rapidly, with a pattern of tissue distribution similar to that seen with potassium [247] [252]. This led them to postulate that the mechanism of thallium-201 uptake by the tumour cells is certainly related to a function of blood flow and the (Na-K)-ATP-ase cell membrane pump that is the same mechanism as Tl-201 myocardial uptake.

Tumours often have abnormal vascularity and Tl-201 may accumulate rapidly in the extra cellular space either due to the increased permeability of new vessels with large intracapillary pores [189] or simply to increased vascularity.

I was able to study in a single patient the role of blood flow in the initial distribution of Tl-201 in tumour cells. The data from this single patient suggest that the distribution of Tl-201 in tumour tissue

is not purely proportional to the microspheres distribution. I concluded that initial extraction of Tl-201 by tumour cells is not completely a flow dependent process.

According to the work of Mullins and Moore, 1960 [26], confirmed by Gehring and Hammond, 1964 [27] and 1967 with biodistribution studies in animal models, the mechanism involved in active transport of potassium cannot differentiate between potassium and thallium. The cellular uptake of Tl^{+} was inhibited by cardiac glycoside ouabain and sodium floride, which are well established selective Na^{+} K^{+} ATP-ase pump inhibitors [28]. Digoxin also has been postulated that blocks the sodium-potassium ATP ase in the cell membrane and decrease the extraction of Tl-201 [50].

The data obtained in my in vitro study showed a large decrease in extraction of thallium-201 by the tumour cell line following incubation with digoxin. The $Na^{(+)}$ $K^{(+)}$ ATP-ase pump activity inhibited following digoxin administration resulting in low extraction efficiency by the tumour cells. This indicates that the mechanism of intracellular tumour uptake is active transport through the cell membrane with influx of Tl-201 and it is mediated by Na+, K^{+} ATP-ase system.

The initial extraction after intravenous injection of thallium-201 does not remain fixed in the tumour. Most tumours showed considerable loss of Tl-201 activity by four hours post injection. The rate of Tl-201 loss we found is similar to that reported by Ziada et al, 1986, for myocardial volunteers studied at rest (28% $\pm$ 7) [253].

Areas of necrosis do not accumulate thallium-201, and this was proved clinically by imaging the tumours, and quantitatively using SPECT in some patients (Figure 19). The presence of necrotic tissue in the liver metastases is a possible explanation of the poor correlation between Tl-201 and Tc 99m microspheres uptake presented above. It may be due to non-functioning ATP-ase cell membrane pump activity, so that there is not active transport into the necrotic tumour cells. It appears thus that Tl-201 reflects the viability and metabolic activity of the tumour cells.

In conclusion, results of the studies indicate that Tl-201 uptake in tumours is not purely a flow dependent process. The mechanism of intracellular uptake of Tl-201 demonstrates the viability and metabolic activity of the pathological cells. It appears to be similar to the myocardium by substitution of Tl-201 for potassium in the ATP-ase dependent sodium-potassium pump.

Table 11

The weight of the samples and counts/gm of normal and tumour tissues for both Tc-99m and Tl-201 chloride.

	Weight gm	Counts Tc-99m	Count/gm	Counts Tl-201	Counts/gm
Total tumour	1.722	6,975	4,050	2,846	1,653
Normal liver	0.682	45,306	66,431	203,189	297,931

Table 12

Tumour/Normal uptake ratio (per gram) for Tl-201 and TC-99m

TC-99m = 0.061

Tl-201 = 0.006

Table 13

The percentage of total activity in cellular fraction after digoxin treated and without in tumour cells.

		Without digoxin	With digoxin
Experiment	1	11.3%	0.6%
	2	12.4%	0.4%
	3	10.7%	0.6%
	4	11.9%	0.5%
	5	12.5%	0.7%

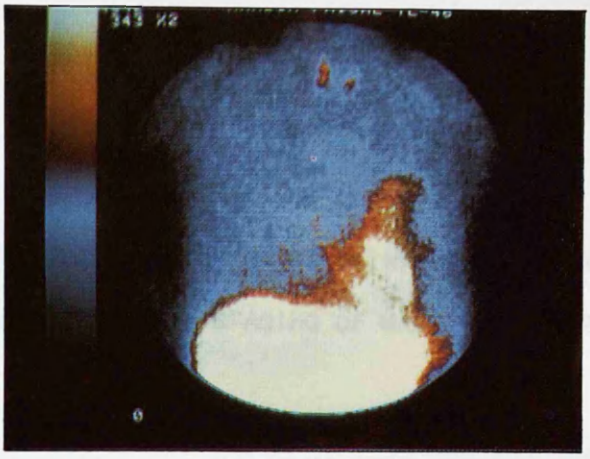

Figure (18) : Increased Tl-201 uptake in primary left lung carcinoma.

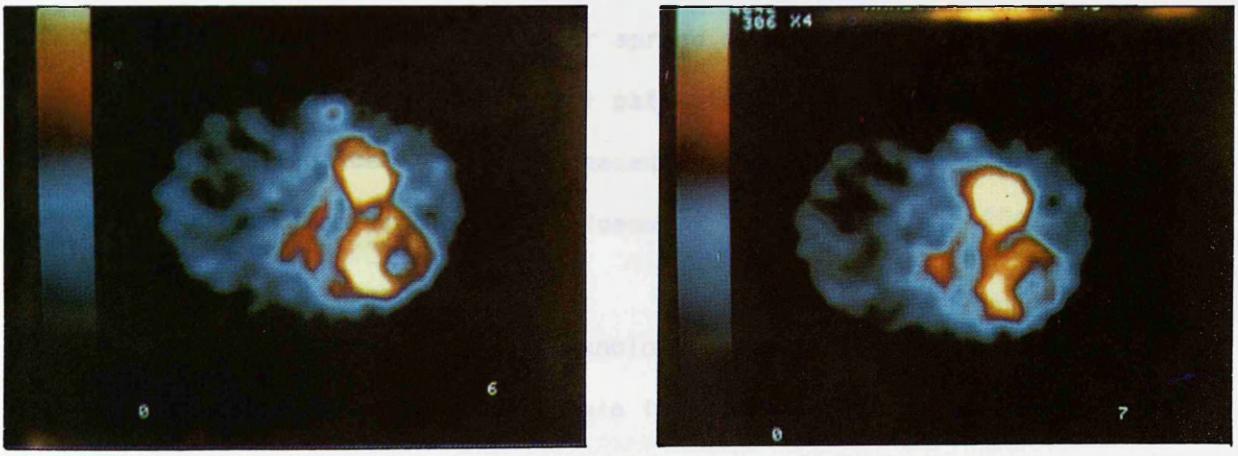

Figure (19) : Single photo emission computerized tomography (SPECT) transaxial cuts showed the tumour uptake with central photopenia.

CHAPTER V

THALLIUM-201 CHLORIDE SCINTIGRAPHY IN THE DIAGNOSING AND STAGING OF MALIGNANT DISEASE

V(1) Introduction

Establishing the extent of tumour spread is a major factor in choosing the most appropriate therapy for patients with malignancy. Staging is critical in treatment planning, because inadequate staging can result in less than optimum treatment or excessive local treatment (204).

Biochemical investigations, immunological markers, imaging tests and surgical procedures all play a role in this assessment. The information derived from such procedures influences the choice of therapy in many malignancies and in some tumours has been essential in improving survival (255). However many of these procedures have inherent limitations including morbidity, expense and failure to detect all tumour sites.

Noninvasive nuclear medicine procedures are easily performed, have no significant morbidity, and can be repeated safely.

With the current interest in thallium-201 chloride as a tumour imaging agent, we have carried out a clinical evaluation of this radionuclide in the diagnosis and staging various common malignancies.

In this chapter I will present the clinical results of Tl-201 imaging in this content. The chapter is divided into various sections, each dealing with a particular type of malignancy.

V(2) Thallium-201 chloride in the staging of lung cancer

V(2)(a) Aim of the study

The aim of study was to evaluate the ability of thallium-201 chloride to detect primary lung cancer and to demonstrate mediastinal spread of the disease.

Demonstrating whether or not there is mediastinal involvement in lung cancer is crucial as patients with disease spread to the mediastinum are generally held to have no chance of being cured by surgical resection [256]. Mediastinal spread can be established by preoperative mediastinoscopy but the technique is invasive causing a significant morbidity and is not completely accurate. A non-invasive method of establishing mediastinal involvement would spare patients this additional trauma and be extremely cost effective [256] [257]. To be effective, however, the

technique would need to be both sensitive, that is abnormal in a high proportion of patients with mediastinal involvement, and specific, i.e. yield a low rate of false positive results.

Preliminary reports have appeared in literature dealing with Tl-201 uptake in the primary lung cancer [258] [243] [259]. These initial studies yielded encouraging results but did not attempt to evaluate spread to mediastinal or hilar nodes. In a recent review of the use of radionuclide techniques in lung cancer, Waxman 1986, concluded that a large series with independent documentation of mediastinal status was required before the role of this radionuclide as a staging modality in lung cancer could be established [208]. The findings in such a series are now presented.

V(2)(b) Patient population

Two groups of patients with histologically proven lung cancer were examined. Group A, consisting of 72 patients (62 male, 10 female, age range 58.29 $\pm$ 13.34 years) with a diagnosis of irresectable lung cancer, had been referred to the radiotherapy department for radiotherapy or palliative treatment. Group B, consisting of 75 patients (53 male, 22 female, age range 59.6 $\pm$ 11.25 years) with potentially resectable lung cancer, had been referred to the cardiothoracic surgical unit. This group of patients underwent further staging procedures to establish whether surgery was feasible.

In addition, ten patients (7 male, 3 female, mean age $\pm$ SD = 51.5 $\pm$ 5.04 years), with proven benign lung disease were examined. Three had active sarcoidosis, one fibrosing alveolitis, two chronic obstructive airway disease (COAD), three tuberculosis (1 active, and 2 were inactive tuberculosis) and one lung abscess.

V(2)(c) Methods

All patients underwent routine staging by clinical examination, chest x-ray, CT scanning, routine biochemical and haematological screens, bronchoscopy, and relevant isotope organ scans if indicated.

CT scanning of the thorax was performed using an EMI 5005 2nd generation scanner with 20s scanning times and with slice thickness of 13 mm at slice distances of 15mm to the tracheal bifurcation and 15mm or 20mm more caudally. The matrix was a 320 x 320 with individual pixel size of one mm.

Thallium-201 images of thorax were performed 30 minutes after intravenous administration of 75 MBq of Tl-201 chloride, flushed with 10 ml. normal saline. The patients fasted for four hours before the injection. The medication of the patients were not altered. All the studies were carried out at rest. The patients were positioned under a large field of view gamma camera which was peaked on Tl-201 with a 20% window centered over the 69-80 keV x-rays. Static images were then acquired in anterior, posterior and both lateral views of the thorax, 500,000 counts

being obtained in each view. In 23 patients, an anterior view only was obtained with 15 minutes acquisition producing over 1500 K counts in the whole field of view.

Thallium-201 images were displayed on coloured polaroid images or on x-ray film and were interpreted independently of any other data including the extent of mediastinal disease apart from chest radiographs which were available in all cases.

Thallium-201 scanning was performed during the week before operation. CT scanning of the thorax also was performed during the same week.

All patients in the surgical group (B) had mediastinoscopy and/or surgical exploration of the mediastinum at thoracotomy, thus enabling histological verification of the mediastinal status. Patients with negative chest x-ray and CT examinations underwent thoracotomy without prior mediastinoscopy. Patients in whom radiology was suspicious for mediastinal involvement had preoperative mediastinoscopy and proceeded to thoracotomy if the mediastinoscopy failed to reveal histological evidence of tumour spread.

V(2)(d) Results

Abnormal thallium-201 uptake was seen in the primary tumour of 126 out of 147 (85.7%) patients examined (table 14). The primary tumour showed abnormal Tl-201 uptake in 90 of 99 (91%) squamous cell tumours, 21 of 25

(84%) adenocarcinoma, 7 of 11 (64%) small cell and 4 of 6 anaplastic tumours. Abnormal thallium-201 uptake also was seen in four out of six other tumours of the lung (1 neuroblastoma, 1 neurofibrosarcoma, and 4 carcinoma of the lung in which cell type could not confirmed).

The false negative results of Tl-201 chloride (14.5%) scans in patients with primary lung cancer may relate to the size of the tumours in six patients. Four tumours were 1.5 cm in diameter, 2 cm, and 2.5 cm in diameter for the other two tumours. No smaller tumour than 2.5 cm in diameter was seen. The size of other tumours with negative Tl-201 uptake ranged between 5-9 cm in diameter. These tumours had not received prior anti-tumour treatment. Two were in the posterior mediastinum, three were complicated with massive pleural effusions, and three in the lower base of the right lung with collapse of the right lower lobe. The remaining seven tumours were distributed in both lung fields and there was no apparent cause of false negative results.

Figure 20 showed abnormal Tl-201 uptake in the primary tumour of the lungs.

Of the ten patients with benign lung disease who were studied, seven showed no evidence of abnormal Tl-201 uptake (Table 15). Abnormal uptake of Tl-201 was seen in one patient with sarcoidosis and in two with active pulmonary tuberculosis. Figures 21 - 23 showed abnormal Tl-201 uptake in active tuberculosis and in sarcoidosis.

From these results, Tl-201 had a sensitivity of 85.5% for the detection of primary lung cancer and a specificity of 70%.

Thallium-201 images were correlated with the CT scanning findings in the mediastinum in the 72 patients in the radiotherapy group (Table 16). None of the 25 patients with negative mediastinal CT studies showed abnormal mediastinal Tl-201 uptake. Of the 47 patients with CT evidence of mediastinal involvement, nine (19%) showed mediastinal uptake of Tl-201 chloride. Figure 24 demonstrates abnormal Tl-201 uptake in the mediastinum. In the 75 patients in the surgical group, 24 (32%) had histological evidence of tumour spread to the mediastinum. The remaining (51) had negative mediastinal histology on the operative specimens. Of the 24 with mediastinal involvement, only three (12.5%) showed abnormal Tl-201 uptake in the mediastinum while 21 had a normal mediastinal appearance on Tl-201 imaging. CT imaging showed the presence of mediastinal involvement in 16 of these 24 patients. Of the 51 patients with negative mediastinal histology, none had abnormal mediastinal Tl-201 uptake but 14 had abnormal CT findings (Table 17). From these findings Tl-201 imaging had a sensitivity of 12.5% for detecting mediastinal spread and a specificity of 100%. For the CT the sensitivity was 67 and the specificity 70.5%. In 23 patients who underwent thoracotomy an anterior view only was obtained with 15 minutes acquisition containing more than 1,500,000 counts in the whole field of view in most of the patients. The results were also disappointing in that only one patient with histological evidence of mediastinal involvement had abnormal Tl-201 uptake in the mediastinum. Of these 23 patients, seven (30%) had histological

evidence of tumour spread to the mediastinum. From these findings Tl-201 imaging had a sensitivity of 14% for detecting mediastinal spread and a specificity of 100.

V(2)(e) Comparison of Thallium-201 chloride and Gallium-67 citrate imaging in lung cancer

Forty-five of the patients in the radiotherapy group (A) underwent both Tl-201 and Ga-67 citrate imaging. Five patients were female and 40 patients were male. The mean age group $\pm$ (SD) = 50.13 ($\pm$ 7.5) years.

Following completion of the thallium-201 imaging as described above 200 MBq gallium-67 citrate was injected into the patient.

Images were performed 48 hours post injection using a large field of view gamma camera interfaced to a mini- computer. The gamma camera was fitted with a high energy collimator. The 93, 184 and 296 keV photopeaks of gallium-67 were utilised. In all cases anterior, posterior and both lateral projections of the thorax were obtained with 500 K counts each view. Images were displayed on x-ray films or colour polaroid pictures. Images were interpreted visually independent of knowledge of the results of the radiology and Tl-201 imaging. In the group of 45 patients, 39 (87%) showed positive uptake of Tl-201 into the primary tumour, while 36 (80%) had positive Ga-67 uptake into the tumour (Table 18). The differences are not statistically significant.

The results for individual tumour types are listed in Table 18.

There is a marked discordance in the degree of abnormal Ga-67 uptake when compared to Tl-201 images. Only in eight patients both Tl-201 and Ga-67 images showed similar abnormal tracer uptake into the tumour. In four patients both Tl-201 and Ga-67 showed no abnormal tracer uptake into the tumour. Three patients had abnormal Tl-201 uptake and negative with Ga-67, while two patients were positive with Ga-67 and there is no abnormal Tl-201 uptake. Table 19 showed scintigraphic findings of T1-20 and Ga-67 imaging in tumours.

Of the 45 patients, CT scanning demonstrated 28 patients with evidence of mediastinal involvement. Five (18%) showed positive uptake of Tl-201 into the mediastinum, while 16 (58%) had mediastinal Ga-67 uptake (Table 20). The specificity was high (100%) for both radionuclides in comparison to the CT findings. No histological correlation was done in this group of patients.

V(2)(f) Discussion

There is a high correlation between survival in patients with lung cancer and the extent of metastatic spread from the primary lesion. Detection of metastatic spread is necessary to determine a rational approach for selecting patients for thoracotomy. In assessing suitability for surgical treatment, accurate staging and evaluation of mediastinal

tumour spread is of vital importance [260]. It has been shown that patients with mediastinal metastases treated surgically have a poor prognosis [261].

Noninvasive methods of mediastinal staging would be valuable in reducing the need for mediastinoscopy and in presenting inappropriate thoracotomies.

Since the resolution in routine chest radiographs for detection of primary lung cancer is 1.5 cm, radiography remains the preferred screening method for primary lung carcinoma [262]. However, it cannot be relied upon in all patients to preselect those who should undergo mediastinoscopy [263] [264].

Fosburg et al, (1979)[263] found the sensitivity of chest radiography in detecting mediastinal metastasis was 75% and mediastinal tomography 81%. Lunia et al, 1981[264] found the overall accuracy of the chest radiography for assessment of regional nodes to be 56%.

The value of the gallium-67 scan for the detection of hilar and mediastinal tumour spread is a controversial question. Alazraki et al, 1980[257], studied the value of Ga-67 imaging in detecting mediastinal disease in a group of patients with potentially resectable lesions. They reported a 100% sensitivity and 71% specificity for detection of mediastinal nodal involvement with gallium studies. Mc Meester et al, (1979)[265] demonstrated a 56% sensitivity and 94% specificity in the

detection of mediastinal tumour spread to the mediastinum with gallium scintigraphy. Richardson et al, (1980)[266] reported similar findings. Low sensitivity of 55% and poor overall accuracy was reported by Neumann et al, 1980[267].

Waxman et al, (1986)[208] evaluated 51 patients who underwent thoracotomy for primary lung cancer. They demonstrated the effect of tumour location and the criterion for a positive study on sensitivity and specificity of the gallium study. It was evident that when the mediastinum is evaluated selectively, the sensitivity for detection is low (56%), while the specificity is high (100%). If the hilum and mediastinum are considered together, the sensitivity of gallium study is high (91%), but the specificity falls considerably (58%).

Based on their findings of high sensitivity of a positive gallium scan for mediastinal spread of the disease, Alazraki et al, (1978)[256], recommended patients with negative gallium scans be considered candidates for thoracotomy without the necessity for mediastinoscopy. However, because of low specificity, patients with a positive or equivocal results were referred for mediastinoscopy. Conversely , McMeester et al, (1979)[265], demonstrated a low sensitivity and high specificity for mediastinal nodal detection and they recommended mediastinoscopy only when patients had a negative gallium study. Neumann et al, 1980[267], and Waxman et al, 1986[208] concluded that gallium-67 scin-

tigraphy is an insensitive and non-specific indicator for detection of nodal metastatic involvement of the mediastinum, and they suggested mediastinoscopy if the hilar regions were positive with Ga-67 study.

CT scanning has been found to substantially improve the resolution of possible mediastinal lesions. Hirleman et al, 1980[268] reported a sensitivity of 95% and specificity of 80% in predicting mediastinal metastases. CT scanning has the advantage of providing precise anatomical delineation of mediastinal structures, although it cannot differentiate between lymph nodes enlarged due to tumour infiltration or simple reactive inflammation resulting in false positive scans [269].

Richardson et al, (1980)[266] studied 96 patients with suspected bronchogenic carcinoma by prospectively performing mediastinal staging, including CT, Ga-67 scintigraphy, and surgical sampling of mediastinal tissues. Gallium was found to be highly specific for mediastinal disease: 31 of 32 patients with negative gallium scans of the mediastinum had no evidence of mediastinal metastasis at surgery. Specificity for CT was 81%. Of 18 patients who had proven metastatic disease in the mediastinum, only ten (55%) had a positive gallium scan, whereas 11 (61%) had a positive CT scan. Evaluation of the hilar regions using CT was difficult because of the super imposition of the great vessels. They concluded that CT scanning had little value in the staging of bronchogenic carcinoma, but the gallium scan was useful. Similar findings were reported by Julian et al, (1982)[270].

In a prospective study of preoperative staging of patients with lung carcinoma, Milroy et al (1986)[269] compared Ga-67, CT scanning and mediastinoscopy. They reported that gallium-67 imaging had a similar sensitivity with the CT scanning, (72%) versus (79%) for the mediastinoscopy in detecting mediastinal involvement. The Gallium-67 scan had a specificity of 85%, CT scanning 82% versus 100% to the mediastinoscopy.

We evaluated Tl-201 chloride in the detection of both primary lung cancer and mediastinal spread of the disease in 147 patients with histologically proven lung cancer. Of these, 45 patients underwent both thallium-201 and gallium-67 imaging. In addition, ten patients with benign lung disease were studied.

In the present series the sensitivity of thallium-201 in detecting primary lung cancer was 86% (124/147) and the specificity of 70%. Tonami and Hisada, (1977)[243], reported their experience of positive Tl-201 uptake in the primary tumour of lung cancer patients. Hisada et al, 1978[259], also reported that in 57 patients with known primary lung cancer, 49 (86%) were positive with Tl-201. The hilar and/or mediastinal involvement and the size of the primary tumours was not considered in this report.

Salvatore et al, 1976[258] reported that in 43 patients with metastasis, 20 of 23 patients demonstrated positive Tl-201 uptake of the hilum. Twenty had peripheral masses on x-ray, 18 of the 20 showed positive Tl-201 uptake.

Waxman 1986[208], showed an example of a patient with malignant thymoma in which a combined Tl-201 and Ga-67 study was performed. He reported that the extent of the tumour visualization, especially in the mediastinum, was better seen with Tl-201 scan. He also showed another example of lung cancer with metastasis to the mediastinum demonstrated at mediastinoscopy. The Tl-201 scan was accurate in determining the extent of mediastinal spread of the disease, but he stated that there was lack of information relative to the sensitivity and specificity of Tl-201 in detecting hilar and/or mediastinal involvement, and suggested continuing these studies especially with surgical documentation. Our results in 75 patients in the surgical group showed that Tl-201 chloride had a low sensitivity of 15% for the detection of mediastinal spread and a specificity of 100%. For the CT the sensitivity was 46% and the specificity 70%.

The sensitivity of Tl-201 scans in detecting primary tumours and its extension is highly dependent on the vascularity, the size and location of the lesion.

The anatomic site of the lesion affects the sensitivity of Tl-201, and Tl-201 may lack sensitivity in imaging of deeply sited tumours due to a short half value layer in tissue for its gamma and x-rays. (D 1/2 in tissue for its gamma rays at 167 keV is 4.95 cm, and for 135 keV and x-rays at 69-83 keV is 4.15 cm.) [22].

Thallium-201 imaging has poor intrinsic resolution and thus may limit the size of lesions visible. Okerlund et al, 1984[271], reported that 92% of parathyroid adenomas > 1.0 cm were located with Tl-201 as opposed to only 50% of those <0.7 cm. Single and multiple tumours and hyperplasia could be identified. Winzelberg, Hydovitz, (1985)[272], studied 31 cases of parathyroid adenoma with dual isotope subtraction technique and found the 73% of tumours weighing 499mg or less and 78% of tumours weighing 500 - 1499 mg were correctly identified, and 100% of adenomas weighing more than 1500 mg were detected.

In our clinical study, peripheral primary lung cancers smaller than 2 cm in diameter were not detected with Tl-201. In addition, diseased lymph nodes 2.5 cm in diameter in parahilar and mediastinal region were not detected by Tl-201 when compared to mediastinal exploration.

The false negative results of Tl-201 chloride scans in patients with large tumours of the lung may relate to poor viability of the tumours.

Twenty minutes following intravenous injection of thallium-201 chloride, the uptake by the tumour achieved peak values and remained constant during the first hour. Multiple views can be obtained with no significant change in target to back ratios throughout the time of imaging. Maximum information is obtained with a single anterior projection of the chest requiring 15 minutes of acquisition time. This method was performed on 23 patients obtaining more than 2000 k count per view. The aim of this study was to obtain more counts from the tumours and to detect smaller lesion in the mediastinum. But it has been shown that this method does not offer any advantage over the 500 k counts per-view. Only in one out of seven patients was mediastinal involvement detected in this study with a sensitivity of 14%. Lateral projections may be helpful, especially when the tumour is located in the lower base of the left lung, due to abnormally high tracer by the myocardium.

In the comparison study of Tl-201 and Ga-67, both radionuclides showed nearly similar sensitivity in detecting primary lung cancer, but Ga-67 showed higher sensitivity (57%) in determining mediastinal spread of the disease.

The detection rate of the tumours by thallium-201 may not be affected by the tumour cell type. Tumour uptake is different from one patient to another even within the same histopathological type. This was demonstrated by the wide variation in the tumour/background ratio.

Togawa, et al, (1985)[273], claimed that he could classify the lung cancer histologically by measuring the "crude uptake ratio" (CUR) of thallium-201 to gallium-67 citrate uptake. Patients received 2 mCi of Tl-201 chloride, followed by 2 mCi of Ga-67 one week later. Regions of interests of similar size were symmetrically created over the tumour and normal lung field on the same patient, and the mean counts of each region of interest were recorded. CUR for Tl-201 and Ga-67 was obtained by calculating (Tumour-Background) /Background. They found that adenocarcinoma had a CUR of 2 $\pm$ 1.55, epidermoidal carcinoma and oat cell carcinoma showed a CUR of 0.47 $\pm$ 0.30 and 0.37 $\pm$ 0.05 respectively, while adenosquamous carcinoma represented a CUR of 0.91 $\pm$ 0.15 intermediate between adenocarcinoma and epidermoidal carcinoma. These findings were not reliable because six patients with adenocarcinoma had greater gallium-67 citrate uptake than thallium-201 chloride, and one patient with oat cell carcinoma had greater thallium-201 uptake than gallium-67 citrate.

In the present series we compared thallium-201 uptake and gallium-67 citrate uptake in 45 patients with lung cancer. It was found that patterns of Tl-201 and Ga-67 accumulation in lung cancer differed among patients having the same histological type. In the same histological type, negative thallium-201 uptake and positive with gallium-67 were found on the one hand and positive thallium-201 uptake and negative gallium-67 citrate uptake on the other. The results obtained do not support these of Togawa et al[273] and suggest that Tl-201/Ga 67 differential uptake is not helpful in predicting cell type.

V(3) Thallium-201 chloride imaging in breast cancer

V(3)(a) Introduction

Various imaging techniques are used to demonstrate primary breast carcinoma and also to detect the extent of the dissemination of the disease.

In clinical practice, mammography is the best complementary method of examination of the primary site of breast carcinoma [274].

The demonstration of dissemination of breast carcinoma is important in the assessment and management of the disease. The detection of metastases, whether skeletal or in soft tissues, alters the primary surgical treatment and adds secondary therapeutic procedures when discovered on follow up examination.

Radiological, ultrasonic and scintigraphic techniques are used in the detection of distant metastases but fail in demonstrating nodal spread of the disease [274]. A test that could reduce the need for surgical sampling of the axilla and offer prognostic information would be of vital importance [275].

Ege (1978), developed a method of radiocolloid internal mammary lymphoscintigraphy, and reported that it is a useful, non-invasive method of evaluation of the parasternal nodes in the management of breast carcinoma [276], although the technique cannot replace lymph node sampling for patient staging [275].

Efforts to obtain useful demonstration of involved axillary lymph nodes by means of lymphoscintigraphy have been disappointing, mainly due to the relatively large numbers of axillary nodes and their wide drainage areas which require multiple injections. In addition, the test is non-specific with high false positive rate [277].

I examined Tl-201 chloride in detecting primary breast cancer and tumour spread.

V(3)(b) Patient population

Twenty six patients with histologically proven breast cancer were examined, one male patient and 25 patients were female. The mean age of the group (± SD) was 49.92 (± 7.6) years. Of the 26 patients, 20 were presenting with primary breast cancer and six had local recurrence following primary treatment.

Patients were studied after a four hour fast, at rest and medications of the patients were not altered.

V(3)(c) Methods

The patient was lying supine, under a large field of view gamma camera fitted with a low energy, high sensitivity collimator and interfaced to a mini-computer camera was positioned over the tumour site. Seventy-five MBq Tl-201 chloride were injected intravenously and flushed with 10 ml normal saline. Images were then acquired as follows: (A) 5 second frames for 5 minutes, 64 X 64 matrix size; (B) 30 seconds frames for 55 minutes 128 X 128 matrix. All images were stored on disc for subsequent analysis. An early static image was created from the dynamic data obtained from 5 to 15 minutes post-injection.

The static images were displayed on coloured polaroid pictures and interpreted visually. Results of Tl-201 scintigraphy were compared to clinical and surgical findings.

V(3)(d) Results

Thallium-201 chloride uptake occurred in all 20 patients with primary adenocarcinoma of the breast (Figure 33).

Of the six patients with recurrent disease, four showed abnormal Tl-201 uptake at the tumour site. The remaining two patients had normal Tl-201 images in spite of histological proof of tumour recurrence.

In five patients who had tumours with a necrotic center, a rim of increased Tl-201 uptake with central of photopenia was seen (Figure 34).

Thallium-201 chloride imaging was insensitive in detecting nodal spread of the disease. Of 14 patients with clinical evidence of nodal metastases, only three (21%) patients were detected on Tl-201 scans. One patient had a large mass in the right supraclavicular region, the second patient had a large mass in the left axillary region, and the last one had 2 1/2 X 2 1/2 cm in the right axilla. Each of the three patients also had multiple other small lymph nodes metastases not detected by Tl-201 scans.

Four patients underwent surgery within a week of the Tl-201 study. There was pathological evidence of metastasis in the axillary lymph nodes in all patients, none of which were demonstrated by Tl-201 scans.

Thallium-201 scan was accurate in locating brain lesions in two patients who had clinical evidence of brain metastasis. Lung metastasis were detected in two patients. In one patient a Tc $^{(99m)}$ MDP bone scan showed multiple areas of increased tracer uptake in the skull, lumbar spine and ribs.

Tl-201 scan detected the skull and lumbar spine lesion, but failed to demonstrate the rib lesions. This was due to high uptake in the heart, liver and lungs and poor resolution with Tl-201 chloride.

V(3)(e) Discussion

Thallium-201 scans were found to be highly sensitive in detecting the primary site of breast carcinoma. Twenty out of 20 malignant primary breast lesions took up Tl-201 focally at the primary site while abnormal uptake was seen in four out of six patients with recurrent disease.

In patients studied before surgery, the sensitivity in predicting nodal involvement was very poor. The sensitivity of Tl-201 scans was also very poor in comparison to the results of palpation in patients who had clinical evidence of nodal spread of the disease. The sensitivity of Tl-201 images in evaluation of local spread of the disease and nodal detection was disappointing. It failed to detect any lesions less than 2 1/2 cm in diameter but did show lesions larger than this. Thus, Tl-201 scan is not helpful in reducing the number of patients who needs lymph nodes sampling.

Tl-201 scans were not sensitive in demonstrating small distant metastasis, especially in the ribs, lungs and mediastinal regions.

The high heart and liver activity also causes problem in imaging of breast cancer, especially when the lesion is located in the left lower zone and the right lower zone of the chest wall (Figure 39).

Our data suggest that Tl-201 scan has not proven useful in the local staging of breast cancer.

V(4) Thallium-201 imaging in malignant lymphoma

V(4)(a) Introduction

For Malignant lymphomas, the choice of treatment and the chance of survival are critically dependent on adequate pre-treatment staging of the disease [278].

In the assessment of the extent of the disease at the time of initial presentation, routine clinical and radiographic examination are insufficient [279]. Lymphoangiography has become an essential part of the examination. This technique is especially useful in detecting occult disease in those patients who have clinically limited involvement and few symptoms. The contrast material injected in the lower extremity enters the thoracic duct below the second lumbar segment and thus may fail to demonstrate the involvement of nodes above this level. Since the opaque material may remain in the nodes for weeks or months, repeating the study showing the effect of the treatment is difficult [279].

Enlarged lymph nodes in the retroperitoneal space or mediastinum can be identified accurately by CT imaging, but the presence of enlarged nodes does not mean metastatic involvement [204].

Ga-67 citrate can localize in malignant lymphoma, but is, however, non-specific and is also taken up in a variety of non-malignant conditions. The presence of bowel activity may obscure uptake in malignant disease in lymph nodes below the diaphragm [278].

For some lymphomas, the accuracy of Ga-67 citrate approaching 80-85 percent has been claimed, although its value in non-Hodgkin's lymphoma is doubtful [278]. It appears that gallium-67 image supplements, but cannot substitute for, lymphoangiography.

In the present study, I evaluated Tl-201 chloride images in the staging of malignant lymphoma.

V(4)(b) Patient Population

Fifteen patients with histologically proven malignant lymphoma were examined. Thirteen patients had mediastinal tumours (7 patients with Hodgkin's disease and 6 patients with non-Hodgkin's lymphoma), one patient had rectal lymphoma (plasmocytic lymphoma), and one patient had abdominal and pelvic lymphoma. Twelve patients were male and three were female. The mean age of the group($\pm$ SD) was 39.3 ($\pm$ 15.6) years. Patients were studied after a four hour fast, at rest and lying supine.

V(4)(c) Methods

A large field of view gamma camera fitted with a low energy, high sensitivity collimator and interfaced to a mini computer was positioned over the tumour site. Seventy-five MBq Tl-201 chloride was injected intravenously and flushed with 10 ml normal saline. Images were then acquired as mentioned in Chapter III. (A) 5 second frames for 5 minutes, 64 X 64 matrix size. (B) 30 seconds frames for 55 minutes, 128 X 128 matrix.

All images were stored on disk.

An early static image was created from the dynamic data obtained from 5 to 15 minutes post injection.

Images were displayed on polaroid images and interpretated visually.

V(4)(d) Results

In patients with mediastinal tumours, 11 cases (84.6%) were positive with Tl-201 scans. The two negative cases included one with Hodgkin's disease 5 cm in diameter (nodular sclerosing mixed cellular type) and one with non-Hodgkin's lymphoma 5 cm in diameter and with superior vena

caval obstruction (diffuse mixed lymphocytic type) (Table 22). The size of the tumour seen on Tl-201 scans were in between 4 and 9 cm in diameter.

Tl-201 chloride also was accurate in locating metastatic spread of the disease in six out of nine cases. Two patients with cervical lymph nodes, three with supraclavicular lymph nodes and one with proven metastatic lesion in the rib showed abnormal Tl-201 uptake (Figure 43). The size of the lesions detected by Tl-201 scans ranged between 2.5 - 5 cm in diameter. The remaining three patients had involvement of cervical or axillary lymph nodes which were less than 1.5 cm in diameter. All were negative.

The diagnostic evaluation of all above mentioned patients, CT scanning, lymphoanglography and laparotomy showed no evidence of subdiaphragmatic involvement of the disease.

The patient with abdominal lymphoma had extensive abdominal lymph node involvement with clinically palpable masses in the lower abdomen and a palpable mass in the right groin region. Tl-201 scan showed markedly increased tracer uptake in the abdomen (Figure 43). However, in view of the normal uptake of Tl-201 seen in the large bowel and kidneys, the exact extent of the intra-abdominal disease could not be assessed.

There were also multiple large and small areas of increased tracer uptake in both inguinal region representing the involved chains of lymph nodes and histological examination revealed non-Hodgkin's lymphoma (Figure 44).

The patient with rectal lymphoma had a large mass in the rectal region posteriorly which showed marked increased tracer uptake (Figure 45).

V(4)(e) Discussion

In a recent ~~simple~~ single case report, Linde and Basso (1987)[252] discussed the incidental finding of a Hodgkin's lymphoma in a patient undergoing Tl-201/Tc-99cm imaging of the parathyroids because of hypercalcaemia. The present study has allowed a more extended appraisal of Tl-201 imaging in a series of patients with lymphomas.

The application of Thallium-201 chloride scans as a staging tool in lymphoma has been disappointing because not all tumour sites were visualized with this technique. The data obtained from the study showed that the size of the lesion is critical. The chances of locating a tumour less than 2.5 cm in diameter is negligible even if it is in the supraclavicular or neck regions. This is due to normal (background) tracer accumulation in the muscular structures and thyroid gland. In addition, the photon attenuation within the overlying tissues serves to further degrade the image.

in patients with sub-diaphragmatic extension of the disease, the location of the tumour is also a problem. If the lesion is in the abdomen, it can lie in juxtaposition to the liver, spleen, kidney or spine, all of which normally contain high concentration of Tl-201 chloride. At the same time it will be surrounded by high gastrointestinal activity which causes confusion in interpretation.

The sensitivity of Tl-201 chloride in locating mediastinal lymphoma does not appear to depend upon the cell type. Similar sensitivity has been found in detecting primary tumours of Hodgkin's disease (85.7% versus 87.5% for non- Hodgkin's lymphoma). The sensitivity of Tl-201 chloride in detecting small nodal spread of the disease is disappointing.

The improved results of treatment for all stages of malignant lymphomas have followed the more accurate assessment of disease extent at presentation, together with advances in radiotherapy equipment and technique, and the introduction of effective combination chemotherapy for systemic disease [280].

V(5) Thallium-201 chloride imaging in brain tumours

V(5)(a) Introduction

Accurate localization of a brain lesion before surgery greatly facilities the operative procedure by permitting smaller craniotomics and reducing the incidence of negative biopsies. The sensitivity of con-

ventional radionuclide brain imaging for detection primary brain tumour or metastatic disease is relatively high. In the last ten years, however, CT scanning has become the preferred imaging modality for screening and detecting patients with suspected intracranial lesions (281).

Most comparative studies have shown better sensitivity with contrast-enhanced CT imaging than with conventional radionuclide imaging in the detection of intracranial tumour (282) (283).

Kaplan et al, 1987(247), observed that the damage incurred by the central nervous system as a result of initial tumour destruction which is compounded by surgical intervention and/or radiation therapy is permanent. On standard CT it is sometimes difficult to differentiate such damage from residual or recurrent tumour. They found that radionuclide study, particularly Tl-201 imaging, gave the most precise estimate of intracerebral tumour.

In this study, I evaluated Tl-201 chloride in detecting intracranial lesions.

V(5)(b) Patient population

We evaluated thallium-201 uptake in 18 patients with known brain lesions -- nine patients with primary brain tumours, two patients with cerebrovascular accident secondary to arteriosclerosis, and seven

patients with brain metastases. Eleven patients were male and seven female. The mean age for group (± SD) was 46.27(± 13.95) years. The medications of the patients were not altered.

V(5)(c) Methods

Seventy-five MBq thallium-201 chloride were injected intravenously. Static images were obtained ten minutes post- injection. The patient was positioned under a large field of view gamma camera interfaced to a mini-computer. Anterior, posterior and both lateral views of the brain (300 K counts) were obtained for each view. The 80 keV x-ray photopeak was utilized with a 20% window. Images were displayed on coloured television screen and coloured polaroid pictures were obtained. In three patients, flow studies of the brain were obtained at 5 seconds per frame for 2 minutes. In one patient with a primary brain tumour, dynamic acquisition was performed one minute per frame for one hour and time activity curves from the tumour and background were obtained.

Tl-201 images were compared to more standard imaging modalities including CT scanning, ^{99m}Tc-DTPA imaging and ^{99m}Tc-HMPAO imaging.

V(5)(d) Results

The flow studies obtained in ~~eight~~ three patients were not helpful due to poor count statistics.

In the patients from whom data was acquired throughout the first hour, Tl-201 uptake occurred rapidly, peak tumour uptake being achieved by 5 minutes post injection and then remaining constant throughout the imaging period. Tumour to background ratios were high (2.3/1) and there were no significant changes for the duration of the time of imaging, shown from the time activity curve obtained from an astrocytoma of the brain (Figure 47). The accumulation of Tl-201 in the neoplastic foci persisted and the lesions were well defined and easy to distinguish from normal anatomic structures such as the base of the skull and large venous sinuses.

The sensitivity of Tl-201 for primary and metastatic brain lesions was 100% (Table 23). All lesions detected with the gold standard method CT scanning were visualized with Tl-201 scans. Tumours with central necrosis showed a rim of increased uptake and central photopenia (Figure 50).

The images obtained by Tl-201 were similar in six cases, and better in two cases to those obtained in Tc ^{99m} -DTPA (Figures 53-54).

In two patients studied following surgical and radiation therapy, the Tl-201 abnormalities were smaller than those on CT and Tc ^{99m} - HMPAO (which reflect both residual tumour and surrounding oedema) (Figure 58).

In patients with CVA (2 cases), there was no abnormal trace accumulation in the insulted region resulting in normal scintiscans appearance (Figures 59-61).

V(5)(e) Discussion

The sensitivity of Tl-201 in detecting brain tumours was very high (100%), and because of the low blood background levels in the brain and high tumours uptake, cerebral lesions were well visualized with Tl-201.

Thallium-201 chloride accumulation within the neoplastic tissues persisted for the first one hour post-injection with no significant changes, and multiple views of the brain could be obtained. The procedure is noninvasive and the scanning time acceptably short at 5 to 8 minutes per view. Using Tl-201 chloride in the imaging of brain lesions, we could differentiate between cerebral vascular accident (CVA), which showed no abnormal Tl-201 uptake, from patients who had brain tumours which showed intense Tl-201 uptake.

In two cases with brain metastasis, Tc ^{99m} - DTPA showed only slightly increased tracer uptake first in the frontal region and second posteriorly. The thallium-201 abnormality appeared as a focal and well defined area of increased thallium uptake in these regions.

CT imaging is the generally accepted method for monitoring intracerebral tumours and is frequently used to assess the response of brain tumours therapies. However, it is often unable to differentiate between fibrotic, non-fibrotic and neoplastic tissue. Kaplan et al 1987[274], noted that in four of seven patients with brain tumour, this diagnostic modality was unable to precisely define neoplastic status when compared to histological findings. The CT scan could not differentiate central necrosis from viable tumour, and did not accurately define the degree of intracerebral oedema. In addition, the CT scanning did not always correlate well with the patient's subsequent clinical course. Tl-201 scans in brain tumours gave the most precise estimate of intracerebral tumour burden.

In the two patients studied following surgical and radiation therapy in the present series, Tl-201 scan showed a smaller and more focal area of increased tracer uptake than CT and Tc ^{99m} - HMPAO SPECT studies. These findings correlate with a comparative study made by Kaplan et al, 1987[247], of radionuclide and CT scan results with pathology. Closest agreement was noted between the thallium-201 images and persistent tumour. According to Kaplan et al, CT scans inconsistently defined the precise amount and location of active neoplastic tissue present. Tl-201 scans showed the precise viable residual tissue better than CT and other radionuclide studies [247].

All out-patients with brain tumours were on steroid therapy in spite of abnormal Tl-201 uptake seen in all tumours. This compares to the findings in Ga-67 scintigraphy for detecting brain tumour. Waxman et al, 1978[284] demonstrated the effect of steroids administration on the gallium and technetium glucoheptonate brain scan by comparing the relative sensitivity of both radiopharmaceuticals in patients both on and off steroids. Using Ga-67 citrate they demonstrated a significant steroid effect on the sensitivity of 95% to 64% following steroids. They also found the steroids did not alter the sensitivity of Tc ^{99m} - glucoheptonate study. In their series four patients who underwent gallium and Tc ^{99m} - glucoheptonate brain scans before steroid therapy and again after being on steroid therapy for one week, the gallium brain scan, in all cases, showed either a disappearance or reduction in gallium uptake by the tumour. The Tc ^{99m} - glucoheptonate brain scan was not affected (284).

In conclusion, Tl-201 brain scan is highly sensitive in detecting brain tumours, can be performed immediately following injection, does not appear to be affected by concomitant steroid administration and reflects viable tumour burden.

V(6) Thallium-201 imaging in bone and soft tissue tumours

V(6)(a) Introduction

Following the introduction of the technetium - 99m - labeled phosphate compounds for skeletal scintigraphy, isotope bone scanning has been widely applied to patients with primary bone tumours [285], and bone metastases [286]

The technetium phosphate complexes for skeletal imaging have been found to localize in a variety of skeletal lesions, including benign and malignant tumours, which made the bone scan less specific than the conventional radiology [286].

Ga-67 citrate [180], Bleomycin labeled with various radionuclide [287], and radionuclides labeled antibodies have been used also for detecting and localizing these tumours.

There are a large number of neoplasmatic and inflammatory lesions of the soft tissues are known to accumulate these traces.

Simon and Kirchner, 1980[288] tried to improve the specificity of scintigraphy in differentiating malignant from benign lesions by comparing the images with Tc-^{99m} phosphonate and Ga-67 citrate in 57 patients. They found that there were considerable differences in the degree of in-

tensity between malignant and benign tumours. With the exception of chondrosarcomas, almost all malignant tumours showed uptake of Ga-67 which was more intense than MDP. If a tumour showed no Ga-67 uptake it was always benign. It was also noted that continuous bone accumulation of gallium was not present in either malignant or benign bone tumours.

In the current study I have evaluated Tl-201 chloride in detecting bone and soft tissue tumours.

V(6)(b) Patient population

Four patients with primary bone tumours (1 Ewings sarcoma, and 3 osteogenic sarcoma), two patients with primary soft tissue tumours (1 liposarcoma and 1 osteogenic sarcoma), one patient with bone metastases, and one patient with chronic osteomyelitis examined with Tl-201 chloride.

Five were male patients and three were female. The mean age (± SD) was 28.25 (± 15.4) years.

V(6)(c) Methods

The patients were positioned under a large field of view gamma camera interfaced with a mini-computer 10 minutes after I.V. injection of 75 MBq of Tl-201 chloride. The field of view was centered over the tumour site. A 10 minute static image was performed. In two patients time ac-

tivity curves were generated over the tumour and background close to the tumour. Tl-201 images were compared to Tc ^{99m} - MDP images, standard radiology and CT findings.

V(6)(d) Results

From the time activity curves obtained from two patients with osteosarcoma, tumour to background ratio was found to be very high (6.3/1 and 7.2/1) (Figure 62).

All seven patients with malignant disease showed abnormal Tl-201 uptake in the lesion (Figures 63-64).

Thallium-201 chloride images in four patients with primary bone tumours were similar to those obtained with Tc ^{99m} - MDP bone scan. Tl-201 chloride was also accurate in determining the exact extent of the disease in comparison to the CT scan findings. Tl-201 scan was also able to delineate areas of necrosis by a distinct rim of activity surrounding an area of central photopenia.

In the two patients with soft tissue sarcoma, the Tc ^{99} MDP bone scans were normal and there was no extra osseous tracer uptake. Tl-201 images were accurate in demonstrating these tumours.

In the patient with bone metastasis, Tc ^{99m} MDP bone scan showed increased tracer uptake in the dorsal spine, ribs, and diffuse increase tracer uptake in the skull. Tl-201 scan showed focal area of increased uptake in the skull and dorsal spine, but failed to detect the small lesions in the ribs. In the patient with chronic osteomyelitis, there was diffuse increased Tc ^{99m} MDP uptake, but Tl-201 study showed a focal area of increased uptake in the recurrent site of infection.

V(6)(e) Discussion

Thallium-201 chloride scan was highly sensitive (100%) in detecting primary bone and soft tissue sarcomas and provided accurate differentiation of the tumour limits as determined by CT scan. Conflicting reports exist in literature about the correlation between pathology and Tc ^{99m} MDP bone scans. King et al, 1980[289], in a study of radiation induced osteosarcoma in rabbits, suggested that the tumour extension along the shaft of the bone was better detected by scanning than by radiography. Mckillop et al, 1981 [290], found a good agreement between bone scan, x-rays and pathological findings in 46 of 48 patient studied. Similarly, Papanicolaou et al., 1982[291] found an excellent correlation between pathology and bone scintigraphy, a length discrepancy of greater than 3cm being observed on two occasions only.

Goldman et al, 1975[292], found in 12 of 13 cases the area of abnormal radioisotopic uptake corresponded to the extent of radiological changes, but did not exceed them. In those cases operated on, the tumour involve-

ment in the gross specimens correlated well with the areas of abnormality seen by both diagnostic imaging modalities. Only in one patient the scan obtained demonstrated slight increase in isotopic uptake throughout the shaft of the femur proximal to the tumour. Pathological examination did not reveal intramedullary tumour spread [292]. By contrast, overestimation of the size of the tumour by bone scanning occurred in 11 of 18 osteogenic sarcomas studies by Chew and Hudson, 1987 [293].

Most soft tissue sarcomas will not demonstrate uptake of the bone scanning agent [290]. In two cases studied there was no abnormal extraskeletal uptake in the site of the tumour by Tc-99m MDP scan. The soft tissue tumours were accurately demonstrated by Tl-201 scans. The 99m Tc-MDP bone scan, however, has value on this condition because increased uptake in bone adjacent to a soft tissue sarcoma indicates bone involvement. Involvement may also be present when there is increased uptake in the soft tissue itself and is continuous with the bone. Adequate surgical treatment of these tumours needs complete resection of all contaminated structures [293].

Tl-201 scan was found to be a useful indicator of an acute exacerbation in one patient with chronic osteomyelitis. The abnormality was demonstrated by a focal area of increased Tl-201 uptake locally. The Tc-^{99m} MDP bone scan showed a large area of increased tracer uptake much more extensive than the Tl-201 uptake. Usually chronic osteomyelitis causes bone scan abnormalities, so that the technique cannot be used to

diagnose exacerbation [294]. Locally increased uptake of either gallium - 67 citrate or indium leukocytes may be useful indicators of an acute exacerbation.

In conclusion, Tl-201 scans is highly sensitive for detecting primary bone tumours, but not much use clinically. Tl-201 scan may be of more value in locating soft tissue sarcoma.

V(7) Thallium-201 chloride imaging in tumours of the liver

V(7)(a) Introduction

The conventional ^{99m}Tc-sulphur colloid liver scan is the method of choice for the initial evaluation of the liver for mass lesions. It is highly sensitive in detecting intrahepatic masses but non-specific (204).

It is difficult using non-invasive methods to determine the nature of a mass lesion presenting as a cold area on ^{99m}Tc-tin or sulphur colloid liver scan.

Ultrasound studies are very sensitive in detecting local lesions of the liver. A recent report indicated that focal lesions with a diameter of 1 cm could be detected [295]. In a report on 39 hepatomas, 11 (28%) were not detected. Two of the 28 cases detected by ultrasound were missed by liver colloid scan, and the liver colloid scan detected nine

of 11 cases missed by US. The poor US detection rate was attributed to lesions under two cm, lesions in the region of the porta, and patient obesity [296].

CT scanning had a significant false negative rate in the detection of hepatomas. This has been attributed to the small size or isodense appearance of the tumours. In addition, the CT scan appearance of hepatoma is non-specific [295].

Se-75 selenomethionine liver scanning has been reported as useful in distinguishing hepatoma from other causes of focal lesion in a non-cirrhotic liver. But in the presence of liver cirrhosis, this technique was unhelpful [297].

In an area which is cold on the colloid scan, uptake of gallium-67 which is equal to or greater than that of normal liver tissue has been considered strong evidence for hepatoma [298] [299]. Although the gallium-67 scan is sensitive for detection of hepatomas (90%) [300], it is relatively non-specific and has also been reported in metastatic disease and in abscess [301].

Broderick et al, 1980[298], compared the sensitivity and specificity of ^{99m}Tc-sulphur colloid and Ga-67 citrate scans to that of ultrasonography in 19 patients who had biopsy proven hepatomas. The ultrasound findings were non-specific showing echographic patterns that varied from discrete sonolucent or sonodense areas to diffusely abnormal parenchyma without

discrete lesions. Two showed a normal US pattern. All cases, including these two, showed a defect on ^{99m} Tc-sulphur colloid and relatively increased Ga-67 citrate uptake in the areas of decreased Tc-99m sulphur colloid activity.

Ga-67 citrate has been demonstrated to be highly useful in distinguishing hepatoma from "pseudotumour" of the liver. Pseudotumours are frequently present in patients with cirrhosis and hepatomas occur as a complication of advanced cirrhosis. Both lesions are seen as "cold" areas on sulphur colloid liver scan. The hepatoma accumulates Ga-67 but the pseudotumours do not (300).

We have evaluated Tl-201 chloride in detecting and classifying mass lesions in the liver.

V(7)(b) Patient Population

I evaluated Tl-201 chloride imaging in 21 patients with cold defects on the Tc-99m liver colloid scan. The histological diagnosis was known in each patient.

Eight patients had primary hepatocellular carcinoma, seven patients nodular cirrhosis of the liver, five patients liver secondaries from a variety of tumours and one patient a hydatid cyst of the liver. Eighteen patients were male and three female. The mean age of the group ($\pm$ SD) was 47.05 ($\pm$ 11.44) years.

V(7)(c) Methods

The conventional liver scan was performed 15 minutes after intravenous injection of 200 MBq of ^{99m}Tc-tin colloid. Static images were performed in anterior posterior and both lateral projections by obtaining 500 K count each view.

Tl-201 images of the liver were performed two to three days later after intravenous injection of 75 MBq of Tl-201 chloride. The patient was positioned under a large field of view gamma camera. The camera was peaked on Tl-201 68-85 keV photopeak with a 20 percent window. Imaging began ten minutes post injection and anterior, posterior and right lateral projections of the liver were obtained 500 K counts per projection.

With the exception of two patients (both with hepatoma), a gallium-67 citrate study was performed immediately following the Tl-201 study.

Two hundred MBq of Ga-67 citrate were injected intravenously following completion of Tl-201 imaging. The patient returned 48 hours later for Ga-67 imaging. They were positioned under a large field of view gamma camera fitted with a medium energy collimator. The 93, 184 and 300 keV photopeaks of Ga-67 with a 20 percent window were utilized. Again, 500 k counts images were collected in the same projections.

All images were stored on the computer disk and displayed on X-ray films and coloured polaroid pictures. Images were interpreted visually.

In areas which were cold on the colloid scan, uptake of Ga-67 or Tl-201 equal to or greater than that in normal liver was considered positive. Areas showing Ga-67 or Tl-201 uptake less than that in normal liver were considered negative.

V(7)(d) Results

The results are summarized in Table 25.

All patients with hepatoma had a focal defect at the site of the tumour on the liver tin colloid scans. Increased Tl-201 uptake in the tumour compared to normal liver was found in six patients with hepatoma, one patient had uptake equal to that in the surrounding liver tissue, and one patient had a rim of increased uptake surrounding central photopenia (Figures 71-81). In the six patients who underwent Gallium-67 imaging, five patients showed increased tracer uptake and one showed equivalent tracer uptake with the surrounding liver tissue (Figure 74).

Tl-201 uptake in patients with nodular cirrhosis was similar to that seen with tin colloid liver scan, multiple focal defects and patchy tracer distribution being found with Tl-201 in all cases (Figures 83, 86, 89). Ga-67 citrate showed homogenous tracer uptake in four cases,

with no focal defects (Figures 84, 87). In the remaining three patients, the uptake of Ga-67 showed focal defects in the areas which were cold on the colloid scan (Figures 88, 89).

All five patients with liver metastases showed multiple focal cold defects on Tl-201 imaging due to decreased Tl-201 uptake in metastases compared to normal liver (Figure 90 - 92). Similar findings were obtained on Ga-67 imaging in four patients, but one patient with metastases from lung cancer showed increased Ga-67 uptake in the metastases. Negative gallium and Tl-201 images were found in the patient with hydatid cyst (Figure 93).

V(7)(e) Discussion

Since Tl-201 chloride and Ga-67 citrate normally concentrates in the liver, the liver is thus prominent in all thallium-201 and gallium images. The use of these radionuclides for imaging tumours in this organ involves detecting a hot spot in a hot background field. Therefore, Tc^{99m}-tin colloid liver scan should always precede these procedures. The abnormality of Tl-201 or Ga-67 uptake in hepatic lesions is defined in relation to Tc^{99m}-tin colloid uptake in the same region.

Previous reports have noted that if the area of a cold defect on a Tc-^{99m} colloid liver scan showed Ga-67 uptake equal to or greater than that of adjacent normal liver, the correlation with hepatoma was very strong (Hoffer, 1986)[300].

Ga-67 imaging of the liver is useful in patients with cirrhosis where hepatic pseudotumours can have the same appearance as a hepatoma on the Tc-^{99m} tin colloid scan. However, pseudotumours or regenerative nodules of cirrhosis rarely have significant gallium uptake (204) (300).

Diplazzi et al., 1978(302), studied 31 cirrhotic and 25 patients with hepatomas on top of cirrhosis, using Ga-67 and Tc-99m sulphur colloid. Ga-67 citrate was concentrated in cold defects on the colloid scan in 23 out of 25 cancer-cirrhotic patients with eight percent false negative result. None of the 31 cirrhotic patients had Ga-67 accumulation in the cold regions on the colloid scans (302).

From the data obtained in seven cirrhotic patients studied, there was discordance between Tl-201 images when compared to Ga-67 images. The Ga-67 uptake was homogenous in four patients with liver cirrhosis with no focal defect evident (Figures 84,87). In three patients the Ga-67 uptake showed focal defects in the areas which were cold on Tc^{99m}-tin colloid scan. Tl-201 images showed multiple focal defects and the appearance was similar to that observed with tin colloid liver scan.

In the present study, all the hepatoma patients had similar appearances on Tl-201 and Ga-67 imaging with both showing significant uptake in areas cold on the Tc-99m scan.

In four of the five patients with metastases studied, the Ga-67 and Tl-201 images showed similar appearances with failure of the radiopharmaceuticals to accumulate in the cold spots on the colloid scan. In the remaining patient (with metastatic bronchial carcinoma), the Tl-201 did not show active uptake in the metastases but Ga-67 was positive.

The findings of the present study on Tl-201 imaging in hepatoma and liver metastases are in keeping with those of Tonami et al, 1977[243], who reported that Tl-201 accumulation occurred in three of four patients with hepatoma but none of eight with liver metastases.

Liver uptake of Ga-67 is not specific for hepatoma and may occur in liver abscess as well as Ga-67 avid metastases [204]. I did not have the opportunity to study any patient with liver abscess using Tl-201, though a single patient with hydatid cyst had a negative result. It is not possible, therefore, to comment on the ability of Tl-201 imaging to differentiate liver abscess from hepatoma.

I concluded that Tl-201 chloride is equally useful to gallium-67 for imaging primary hepatoma. It surpasses gallium imaging in distinction pseudotumours of the liver. In addition, it has the advantage over gallium-67 of early imaging.

Table 14

Thallium-201 Imaging In Primary Lung Cancer

	Tl-201 Scans			
	n	+ve positive	Sensitivity	-ve negative
Sq. cell ca	99	90	91 %	9
Adeno ca	25	21	84 %	4
Small cell	11	7	64 %	4
Anaplastic	6	4	67 %	2
Others	6	4	67 %	2
TOTAL	147	126	85.7 %	21

Table 15

Thallium-201 Scan In Benign Lung Disease

	Number	Positive (+ve)
Sarcoid	3	1
Fibrosing Alvealitis	1	0
COAD	2	0
T.B	3	2
Lung Abscess	1	0
TOTAL	10	3

Table 16

Mediastinal Imaging in Lung Cancer (Group A)

	Thallium-201 Scan n = 72	C T Scan n = 72
Positive	9	47
Negative	63	25

Table 17

Mediastinal Imaging in Lung Cancer (Group B)

	Thallium-201 n = 75	C T Scans n = 75
True +	3	16
True -	51	36
False +	0	14
False -	21	9

Table 18

Thallium-201 chloride and Gallium-67 citrate imaging in lung cancer - frequency of tracer uptake in primary tumour

	Number of Patients	Positive with Tl-201	Sensitivity %	Positive with GA-67	Sensitivity %
Squamous cell ca.	32	30	94%	27	84%
Adeno Ca.	7	6	86%	6	86%
Small cell ca.	4	2	50%	2	50%
Anaplastic ca.	2	1	50%	1	50%
TOTAL	45	39	87%	36	80%

Table 19

Scintigraphic Findings of Thallium-201 and Ga-67 Imaging in Tumours

	Tl-201 (+ve) Ga-67 (+ve)	Tl-201 (-ve) Ga-67 (-ve)	Tl-201 (+ve) Ga-67 (-ve)	Tl-201 (-ve) Ga-67 (+ve)
Number of Patients	29	4	3	2

Table 20

Comparative study of Tl-201 chloride and Ga-67 citrate in detecting mediastinal spread of the disease in lung cancer.

	Mediastinal Tracer Uptake			
	Tl-201 (+ve)	Tl-201 (-ve)	Ga-67 (+ve)	Ga-67 (-ve)
Mediastinal CT (+ve)	5	23	16	12
Mediastinal CT (-ve)	0	17	0	17

Table 21

The Sensitivity of Tl-201 in Detecting Breast Cancer

	n	Positive with Tl-201	Sensitivity
Primary breast Ca	20	20	100%
Recurrence breast Ca	6	4	67%
TOTAL	26	24	92.3%

Table 22

The Sensitivity of Tl-201 in Malignant Lymphoma

	Number of patients	Positive with Tl-201	Sensitivity
Mediastinal Lymphoma :			
Hodgkin's Disease	7	6	85.7%
Non Hodgkin's Disease	6	5	87.5%
Abdominal and Pelvic Lymphoma	1	1	
Rectal Lymphoma	1	1	
TOTAL	15	13	86.7%

Table 23

The Sensitivity of Tl-201 in Detecting Brain Lesions

	Number of patients	Positive with Tl-201
Primary Brain Tumours :		
Astrocytoma	3	3
Glioblastoma	4	4
Medulloblastoma	1	1
Brain Lymphoma	1	1
CVA	2	0
Brain Metastasis :		
Breast Cancer	3	3
Lung Cancer	3	3
Renal Cell Cancer	1	1
TOTAL	18	16

Table 24

The Sensitivity of Tl-201 in Detecting Bone and Soft Tissue Tumours

	Number of patients	Positive with Tl-201
Primary Bone Tumours :		
Ewing Sarcoma	1	1
Osteogenic Sarcoma	3	3
Primary Soft Tissue Tumours :		
Liposarcoma	1	1
Osteogenicc Sarcoma	1	1 *
Bone Secondaries :		
Breast Cancer	1	1
Benign Lesions :		
Osteomyilitis	1	1

Note :

* The lesions in the skull and dorsal spine were positive with Tl-201, but the small lesions in the ribs were not clearly visible.

Table 25

The Senstitivity of Tl-201 and GA-67 in Detecting Mass Lesion in the Liver

	Positive with Tl	Positive with GA
Hepatocellular Ca	8/8	6/6
Liver Cirrhosis	0/7	4/7 *
Liver Secondaries	0/5	1/5
Hydatid Cyst	0/1	0/1

Note :

* GA-67 citrate study in patients with nodular cirrhosis showed homogenous tracer uptake in 4 patients and cold focal defects in 3 patients.

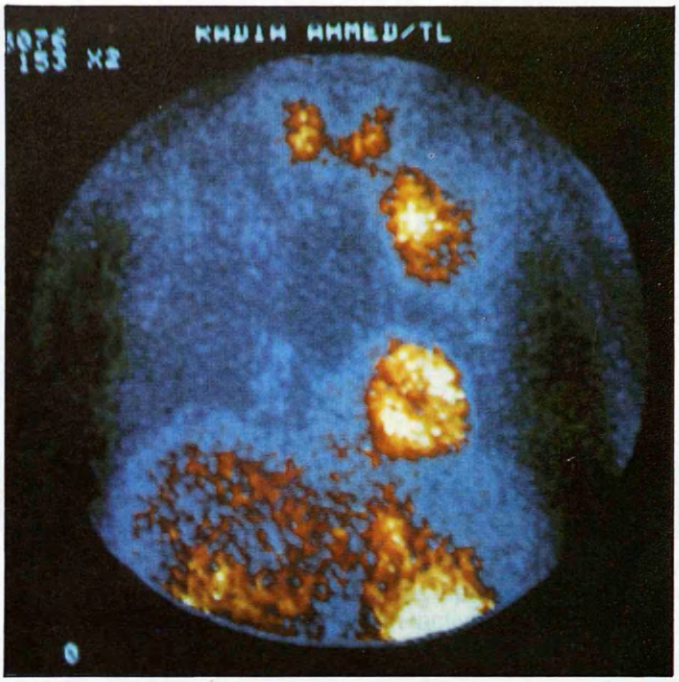

Figure (20): Increased Tl-201 uptake in a primary lung carcinoma.

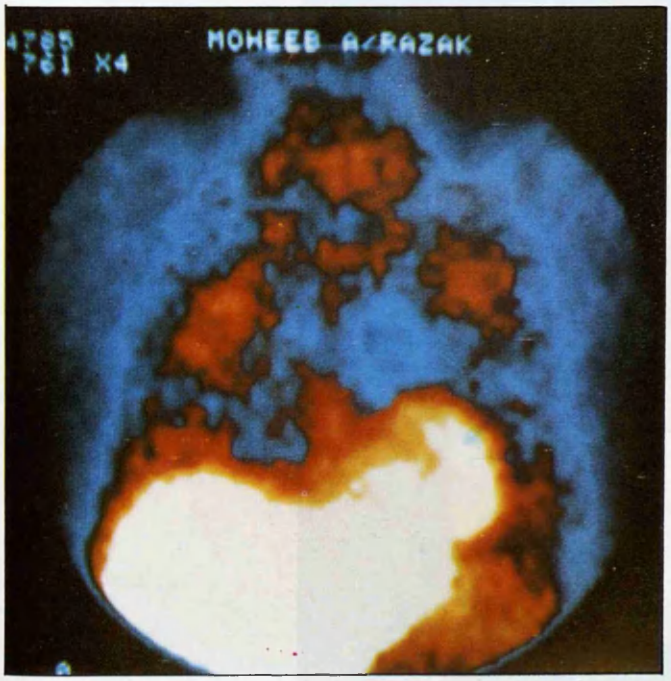

Figure (21): Diffuse increased Tl-201 uptake in a patient with active tuberculosis.

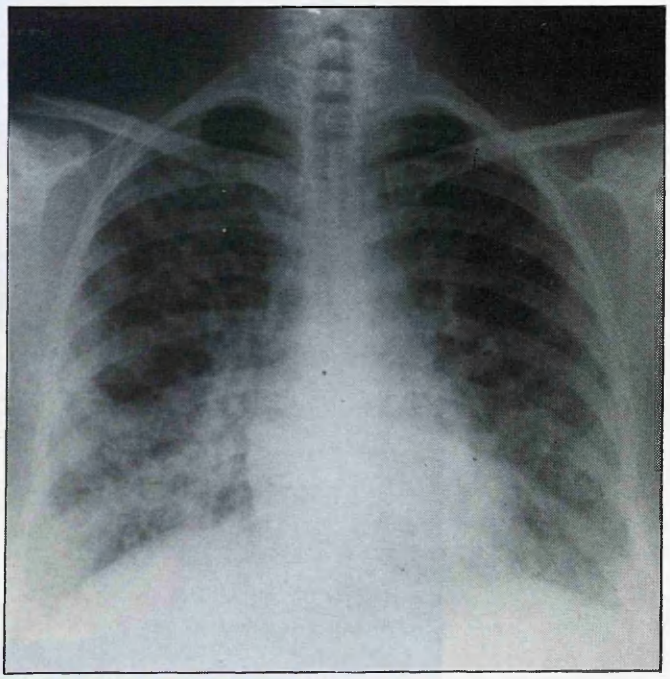

Figure (22): Chest X-ray of the same patient with diffuse active Tuberculosis.

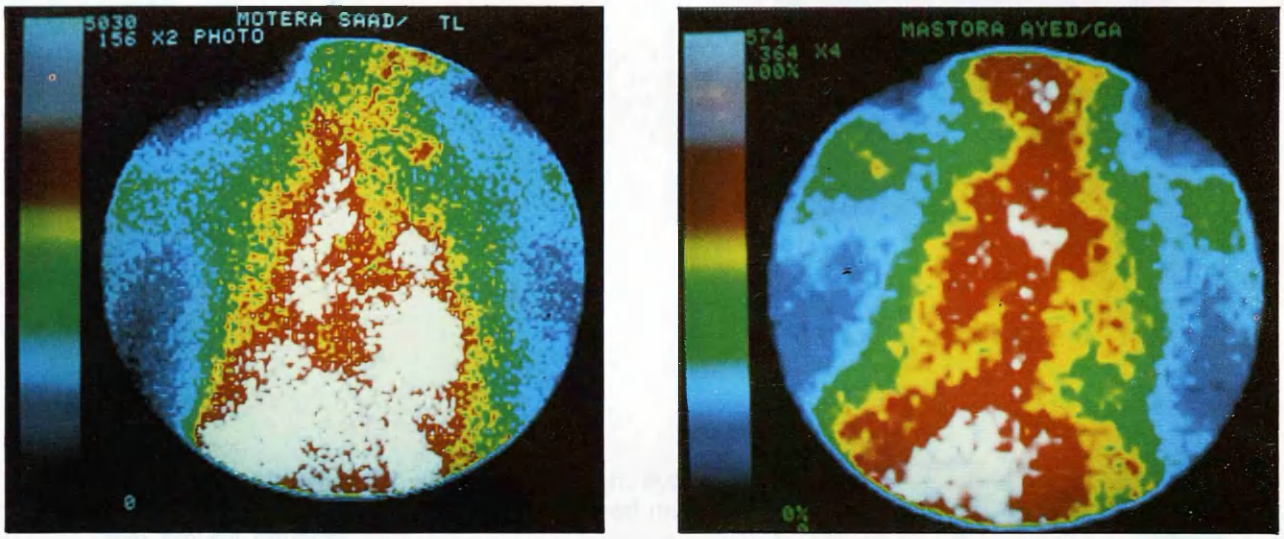

Figure (23): Tl-201 (a) and Ga-67 (b) scans show increaseed both radionuclides uptake in both para-hiler region, in patient with active sarcoidosis.

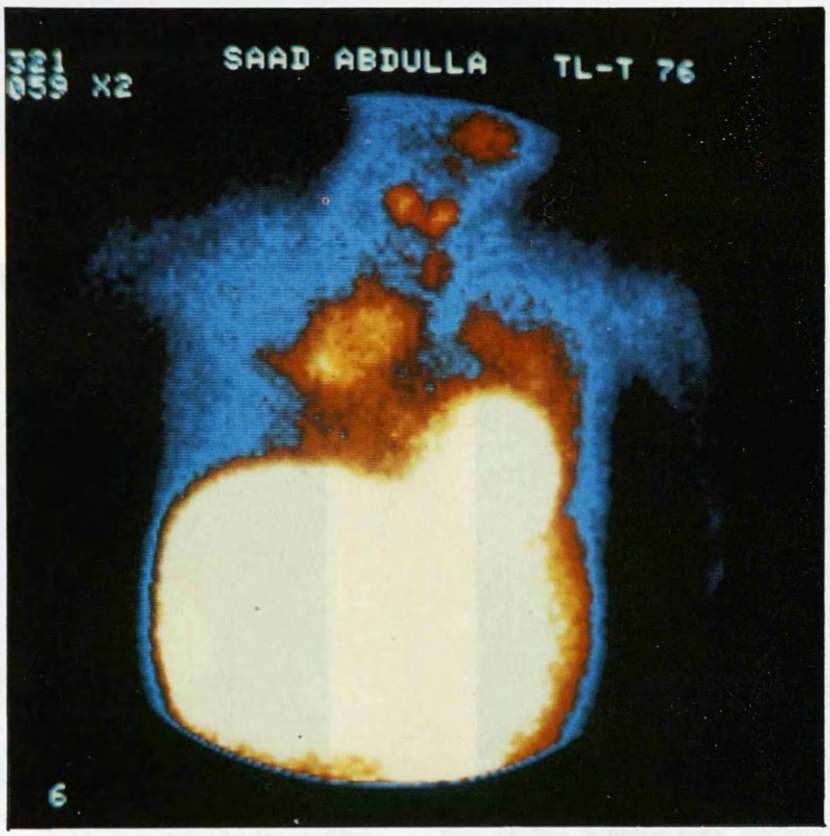

Figure (24): Abnormal Tl-201 uptake in the primary tumour and in the upper mediastinum region in patient with lung carcinoma.

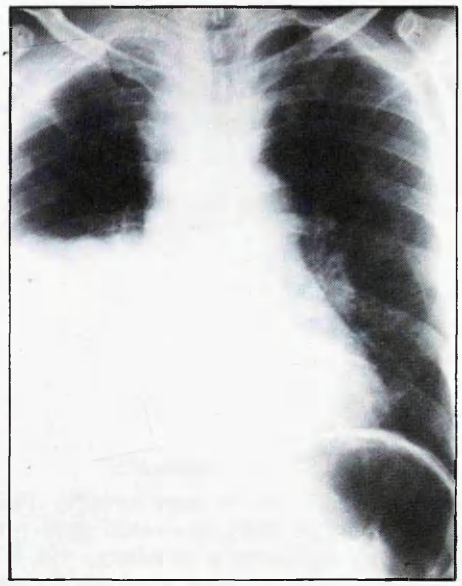

Figure (25): 59 years old with severe cough, dyspneoa and haemoptesis. Chest X-Ray showed massive pleural effusion.

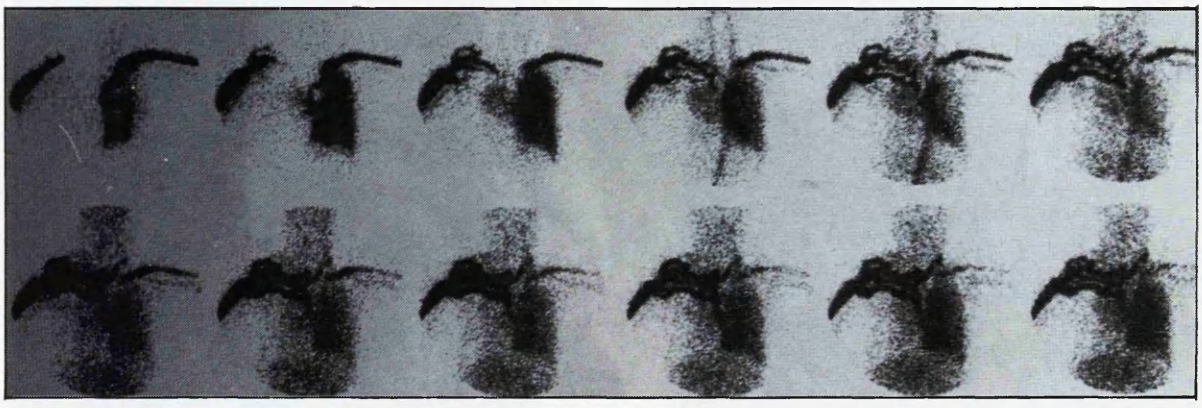

Figure (26): Bilateral venography showed obstruction in the right subclavian and inomminate veins.

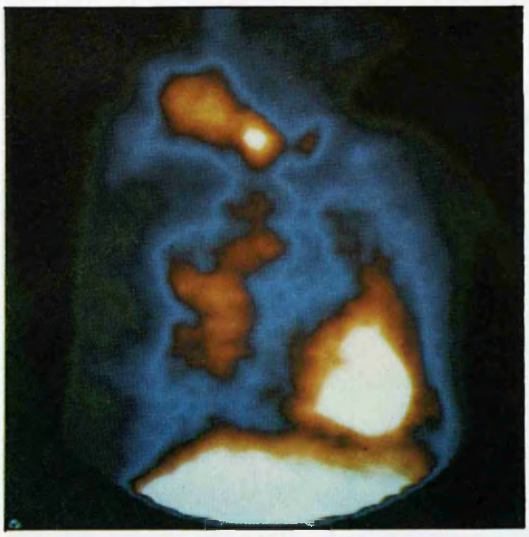

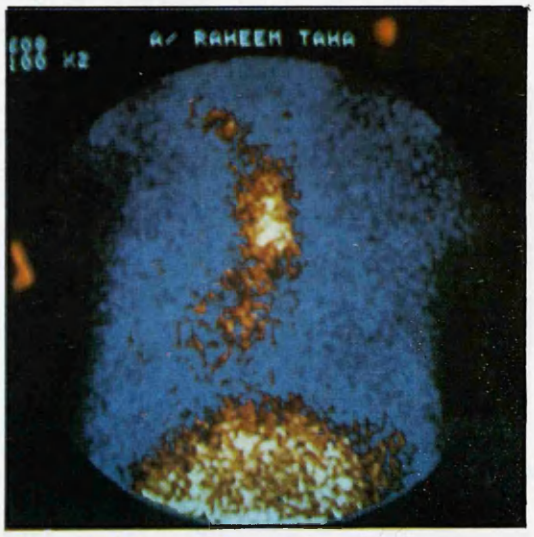

Figure (27): A. Thallium-201 scan demonstrates a large tumour in the right supraclavicular region involving the right lobe of the thyroid gland and extending to the mediastinum

b. Gallium scan demonstrates the mediastinal extention of the tumour with minimal increased tracer uptake in the supraclavicular region. histopathalogy: Squamous cell carcinoma.

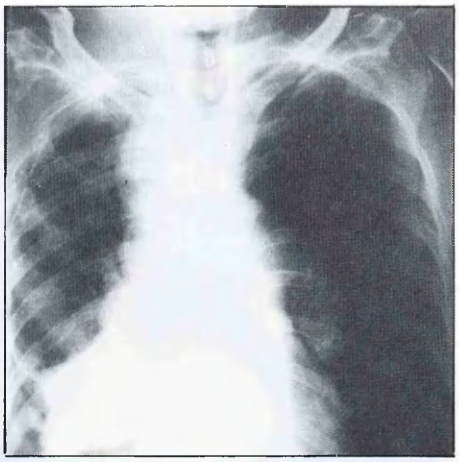

Figure (28): Chest X-Ray after therapy showing resolving of the pleural effusion.

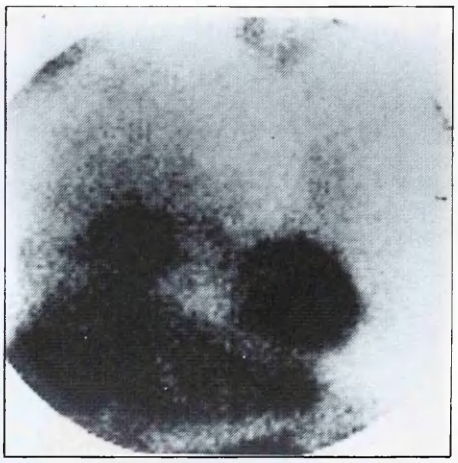

Figure (29): Anterior view of the chest. 15 minutes acquisition time obtaining 2300 K.count. It shows intense Tl-201 uptake in a bronchial carcinoma of lower lobe of the right lung.

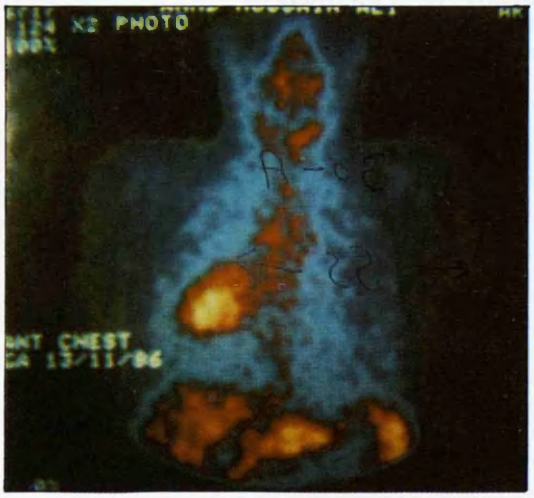

Figure (30): a) Shows abnormal Ga-67 citrate uptake in a patient with primary lung cancer.

b) shows abnormal Tl-201 uptake in the same patient.

a)

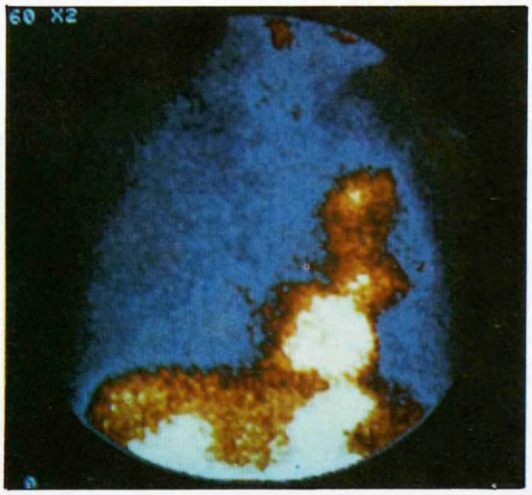

b)

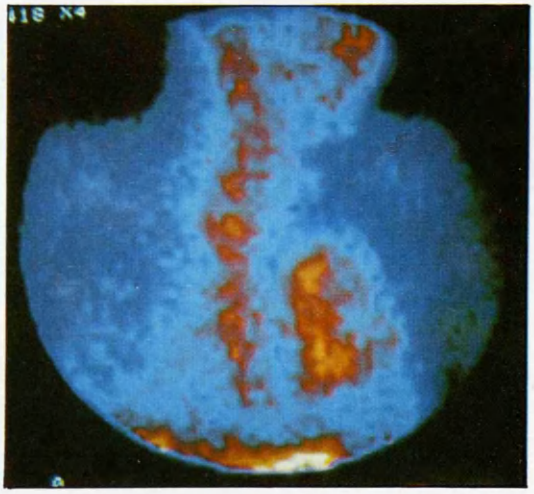

Figure (31): a) Shows abnormal Tl-201 chloride uptake in primary lung cancer
b) Shows abnormal Ga-67 citrate uptake in the same patient.

a) 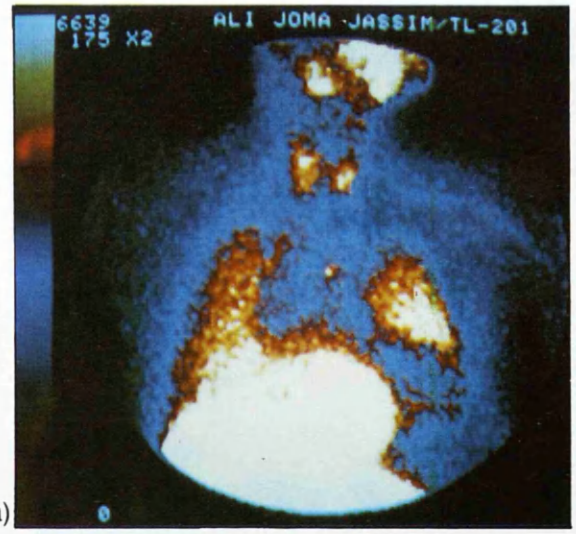

b) 

Figure (32): a) Thallium-201 (a) and Ga-67 (b) studies in a patient with lung cancer. Gallium scan demonstrates the primary tumour and mediastinal spread. a) Thallium failed to demonstrate the mediastinal spread of the disease.

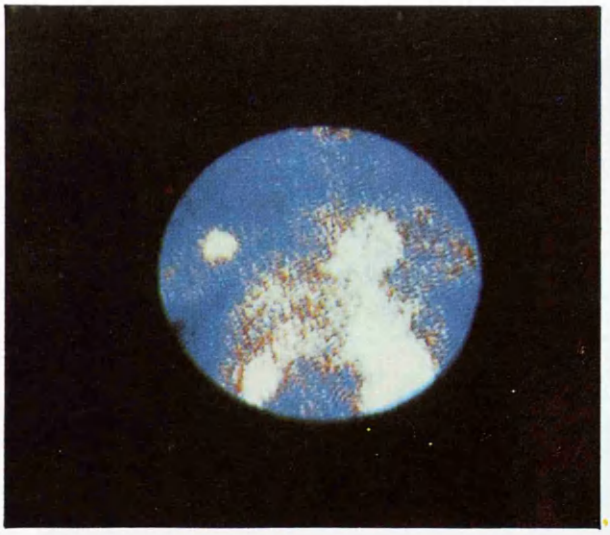

Figure (33) : Abnormal Tl-201 uptake in a primary adenocarcinoma of the right breast.

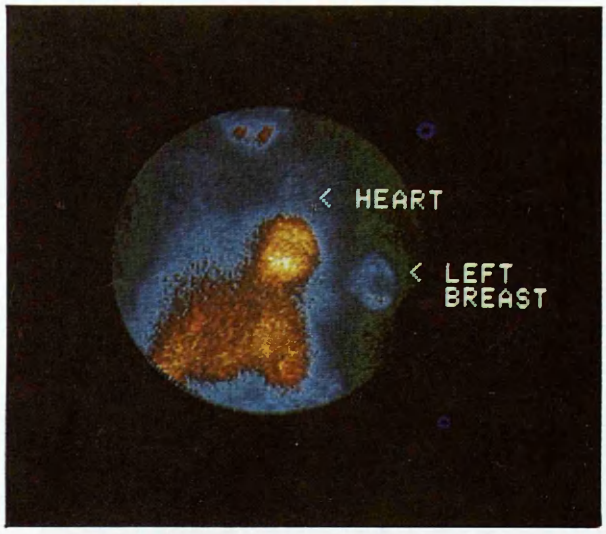

Figure (34) : Abnormal Tl-201 uptake in a primary breast carcinoma. Shows a rim of increased tracer uptake with central photopenia.

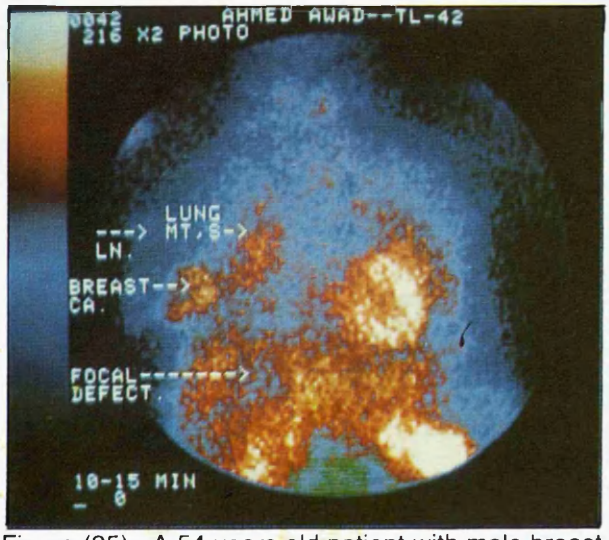

Figure (35) : A 54 years old patient with male breast carcinoma. Tl-201 scan showed abnormal tracer uptake in the right breast, lung metastasis and right axillary lymphnodes. The liver metastasis is seen as cold focal defect.

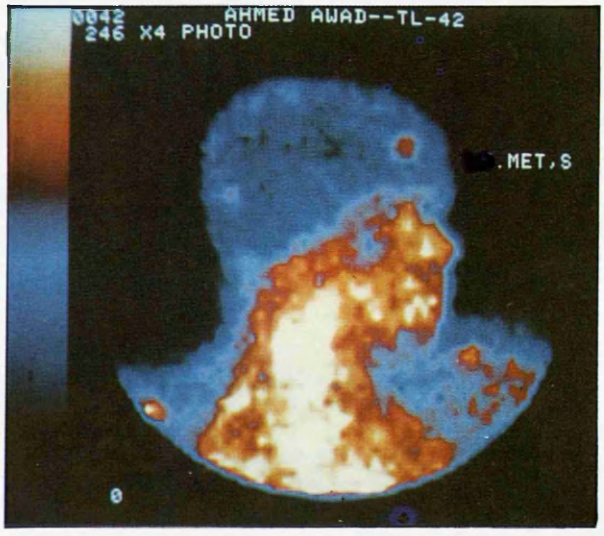

Figure (36) : Tl-201 scan demonstrates the brain metastasis in the above mentioned patient.

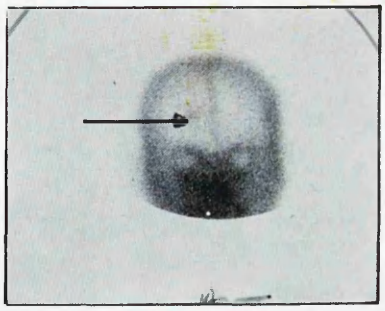

Figure (37) : Tc^{99m} DTPA brain scan shows small focal area of increased tracer uptake in the frontal lobe due to brain metastasis.

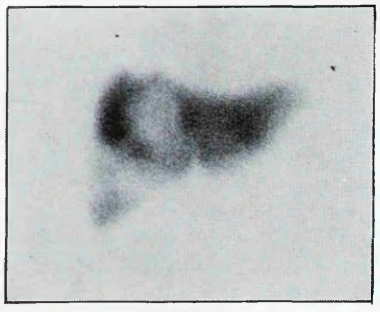

Figure (38) : Tc^{99m} tin colloid liver scan, anterior view, shows multiple focal areas of decreased tracer uptake in the liver.

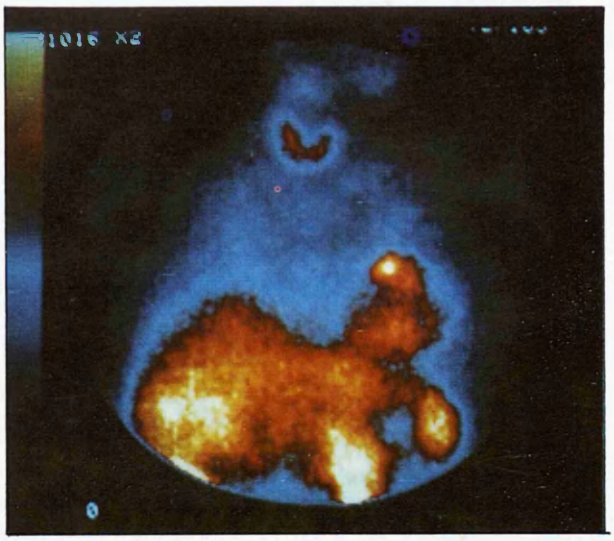

Figure (39) : Abnormally increased tracer uptake in the left breast. Activity seen is adjacent to the heart.

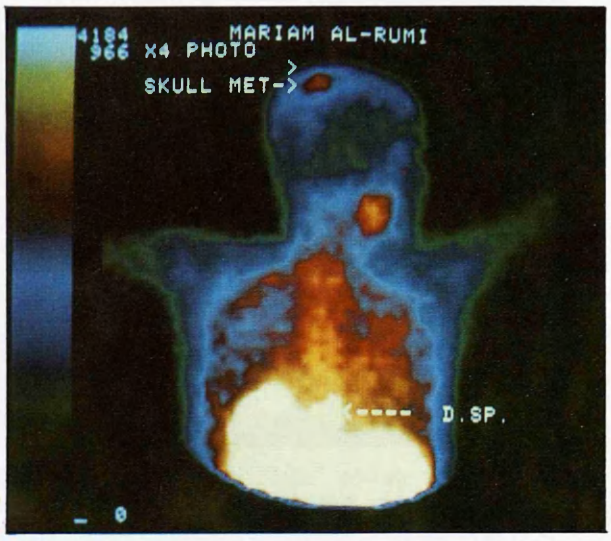

Figure (40) : 52 years old patient with breast carcinoma with bone metastases. Tl-201 scan shows the lesion in the skull and dorsal spine.

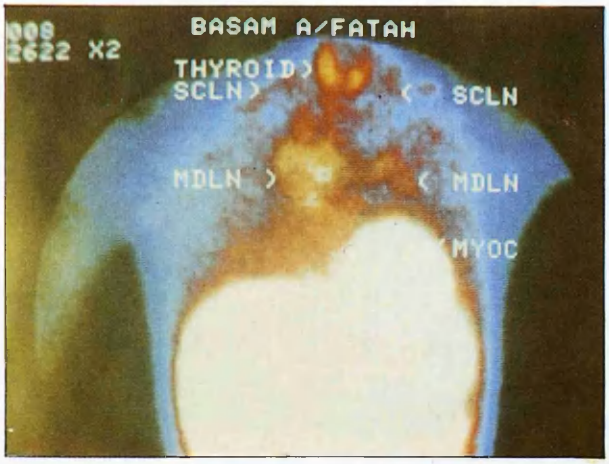

Figure (41) : Abnormal Tl-201 uptake in the upper mediastinum and in both supraclavicular regions in patient with mediastinal Lymphoma. Hodgkin's disease.

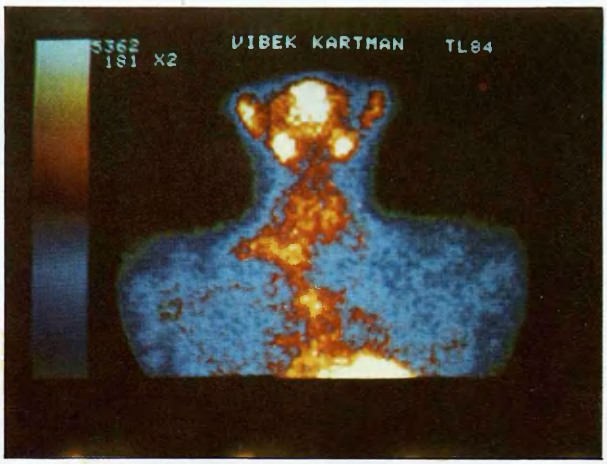

Figure (42) : Abnormal Tl-201 uptake in the upper mediastinum and in patient with mediastinal Lymphoma. Non-Hodgkin's disease.

Figure (43) : 45 years old male with abdominal lymphoma who had large masses in the abdomen and a mass in the Right groin region. Tl-201 scan of the abdomen showed massively increased tracer uptake in the abdomen and in the large bowel.

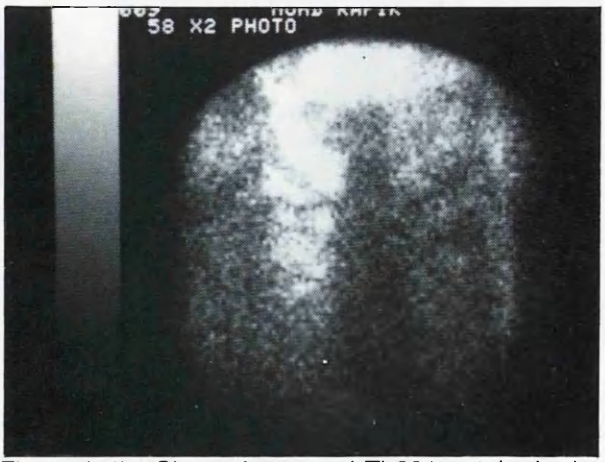

Figure (44) : Shows increased Tl-201 uptake in the Right groin region and multiple focal areas of increased tracer uptake in the Right thigh. There is also increased tracer uptake in the left groin region representing involved lymphatic chains.

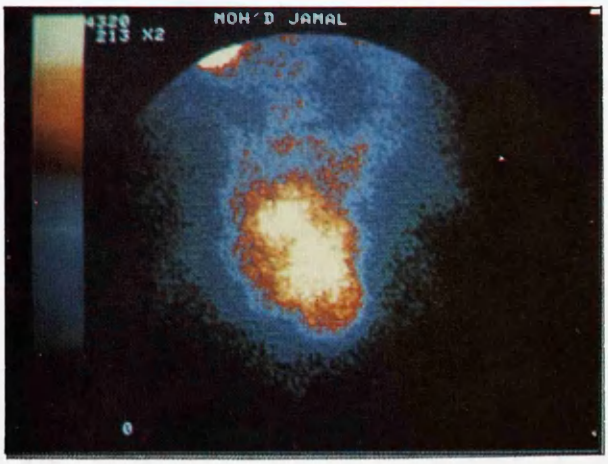

Figure (45) : Shows a large area of increased uptake of Tl-201 in the posterior pelvis in a patient with rectal lymphoma.

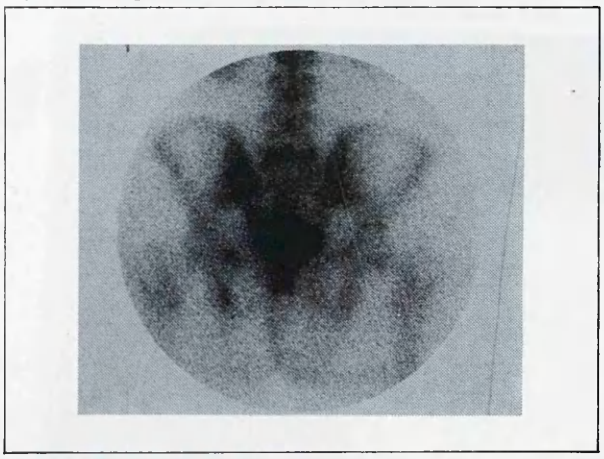

Figure (46) : Tc^{99m} MDP bone scan of the posterior pelvis shows pathologically increased tracer uptake in the sacral and pubic bones.

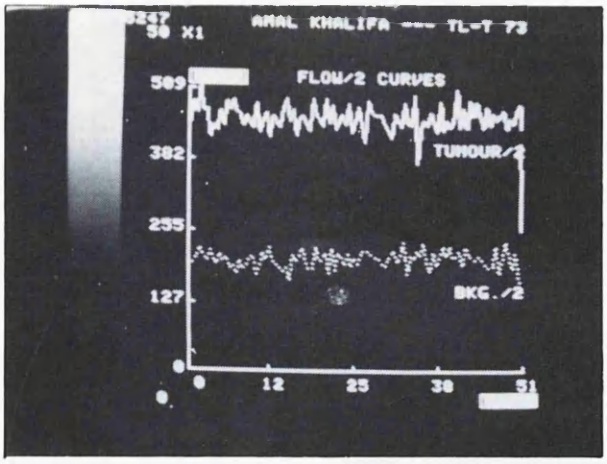

Figure (47) : Time activity curve of Tl-201 uptake in tumour and background from a patient with astrocytoma. The tumour background ratio is high and does not change during 51 minutes of the study.

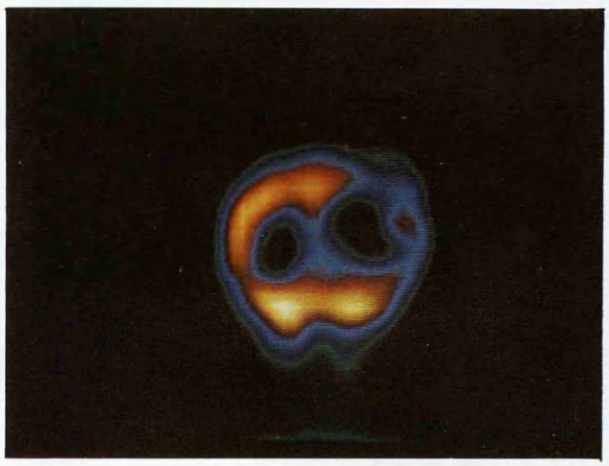

Figure (49) : Brain perfusion tomography using Tc^{99m} HM-PAO shows a large area of decreased perfusion in the right parietal lobe in the same patient with astrocytoma.

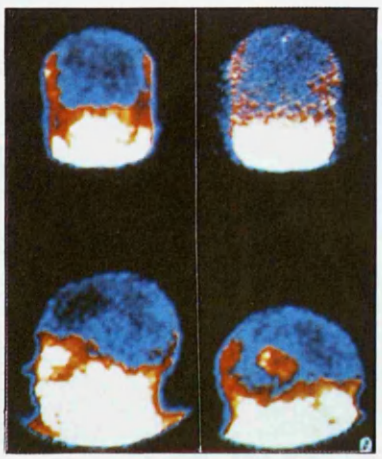

Figure (51) : Tl-201 brain scan shows increased tracer uptake in the left parieto temporal region in the above mentioned patient. Pathology revealed glioma.

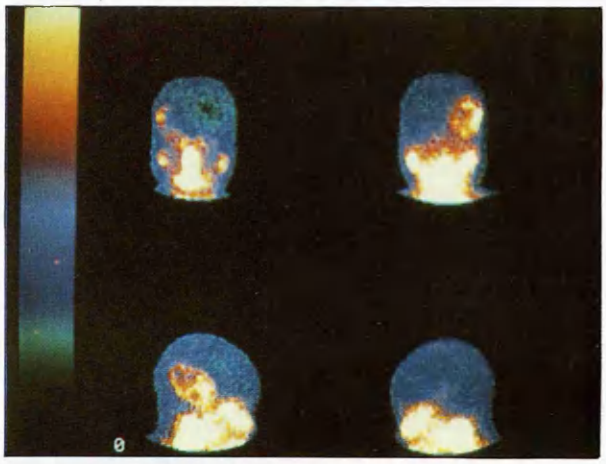

Figure (48) : Tl-201 brain scan shows abnormally increased tracer uptake in the Right parieto-occipital region of the brain in a patient with astrocytoma.

Figure (50) : 55 years old, male, diabetic. For the last 4 years on insulin therapy, since one month, started to forget even his daughter's name. Tc^{99m} DTPA brain scan shows a doughnut like focus of pathologically increased tracer uptake in the left parieto-temporal region with a central photopenia.

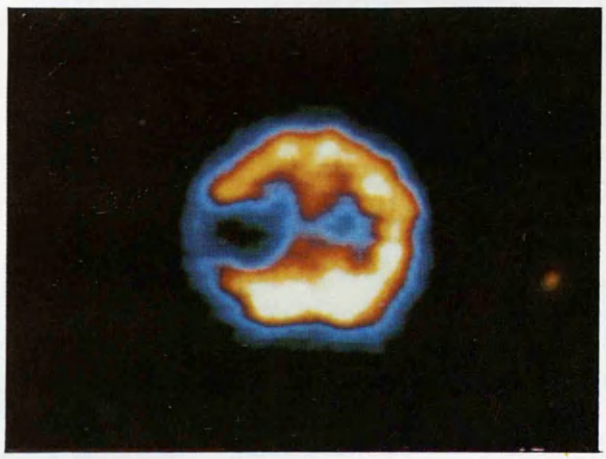

Figure (52) : Tc^{99m} HM-PAO brain perfusion tomography shows a large area of decreased perfusion in the left temporo-parietal region.

Figure (53) : Anterior and left lateral views of the brain using Tc^{99m} DTPA showed faint area of increased tracer uptake in the left frontal lobe.

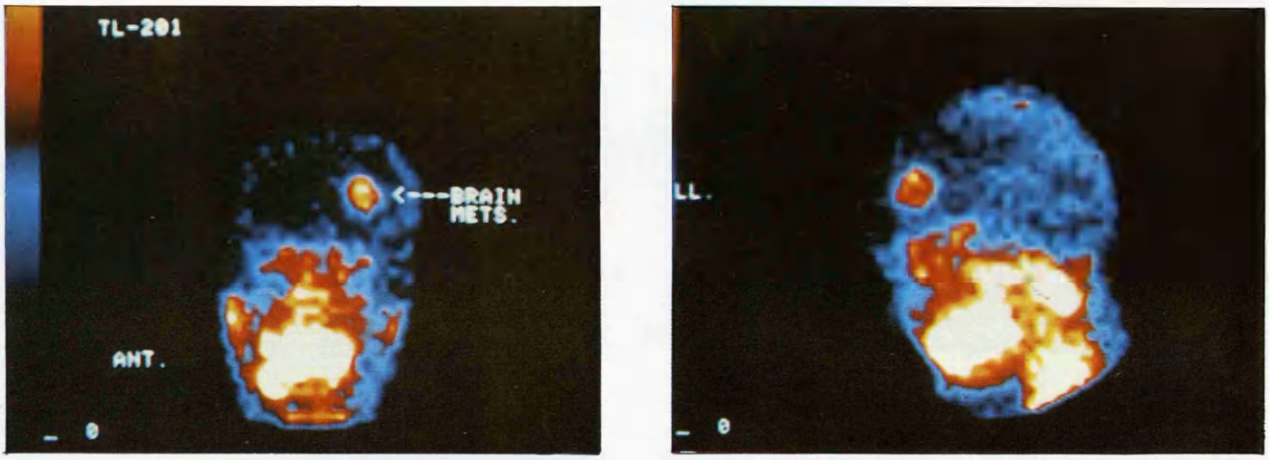

Figure (54) : Tl-201 brain scan shows clear visualization of the lesion in the brain. Metastasis from lung carcinoma.

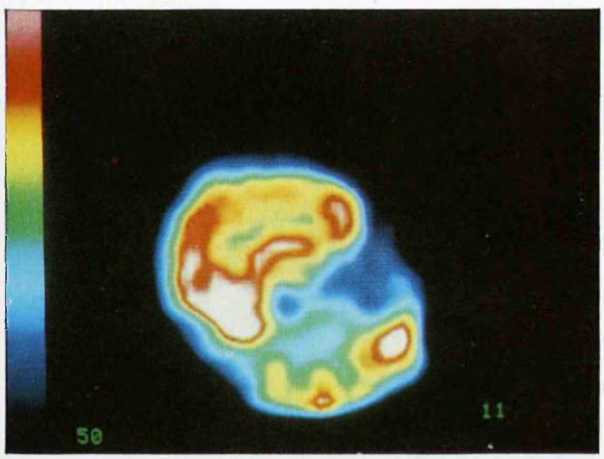

Figure (55) : Tc^{99m} HM-PAO brain perfusion tomography shows a large area of decreased perfusion in the frontal lobe.

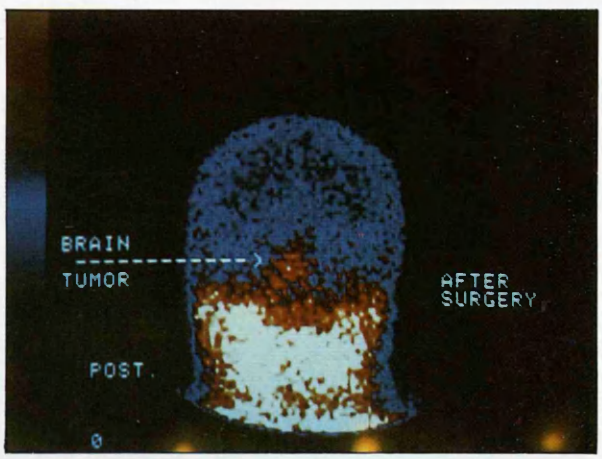

Figure (56) : Tl-201 brain scan shows increased tracer uptake in the occipital region in a patient with medulloblastoma after surgical intervention.

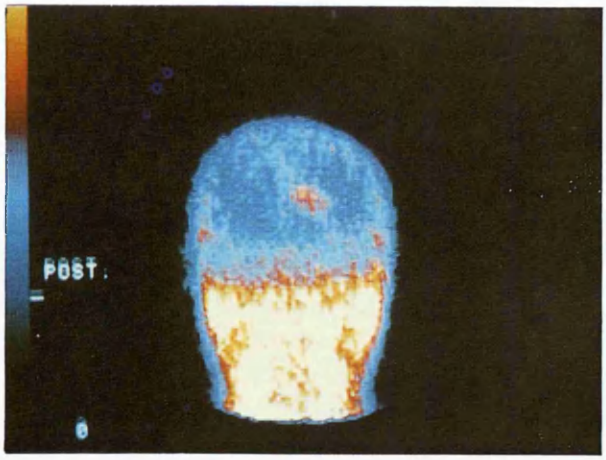

Figure (57) : 45 years old, patient with brain secondaries of unknown primary, received 40 Gy radiation therapy. Tl-201 brain scan shows focal area of increased tracer uptake.

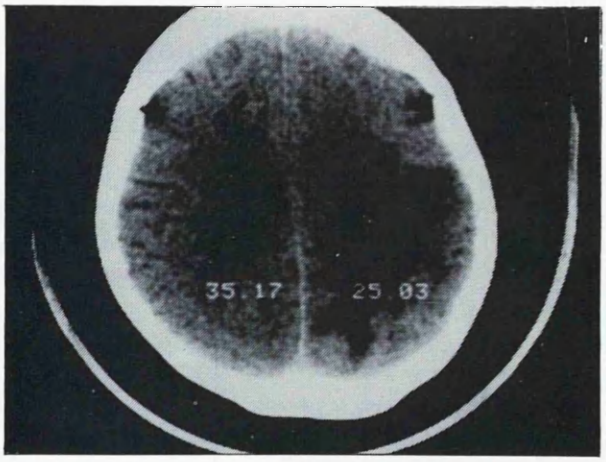

Figure (59) : A 54 years old female with breast cancer under control, developed right sided weakness in the upper and lower limbs. CT scan showed a large lesion in the left hemisphere dif. diagnosis CVA or metastasis.

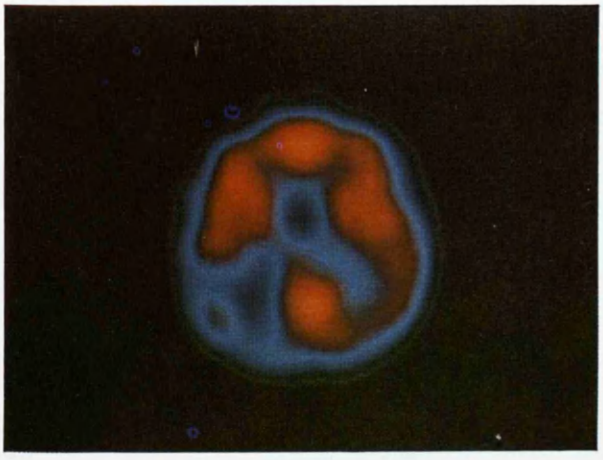

Figure (60) : Tc^{99m} HM-PAO brain perfusion tomography shows a large area of decreased perfusion in the left parietal lobe.

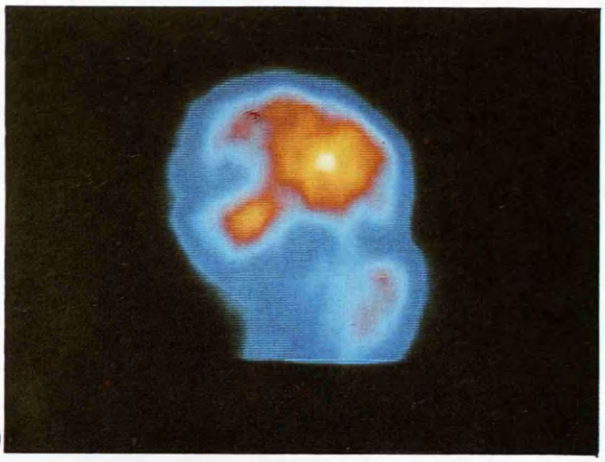

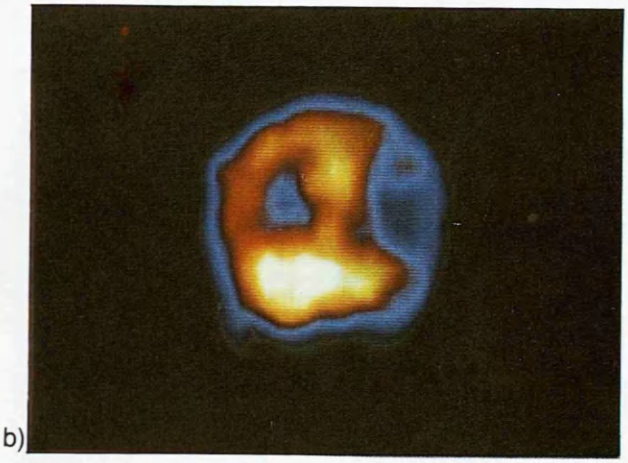

Figure (58) : Tc^{99m} HM-PAO brain perfusion tomography shows a large area of decreased perfusion in the occipital lobe which reflects both residual tumour and surrounding oedema. a) trans-axial section b) coronal section.

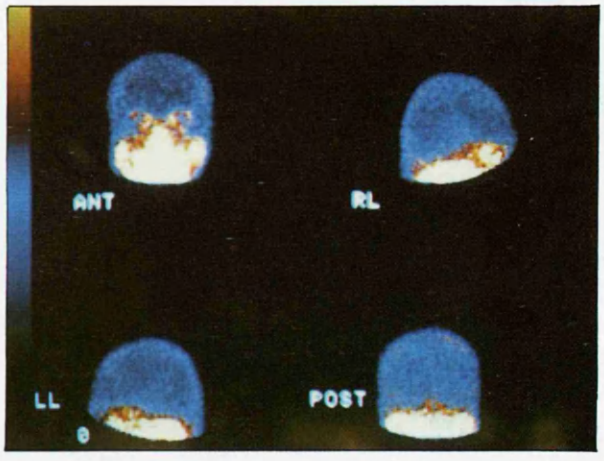

Figure (61) : Tl-201 study does not show any abnormally increased tracer uptake in the brain. CVA was diagnosed, patient improved after treatment.

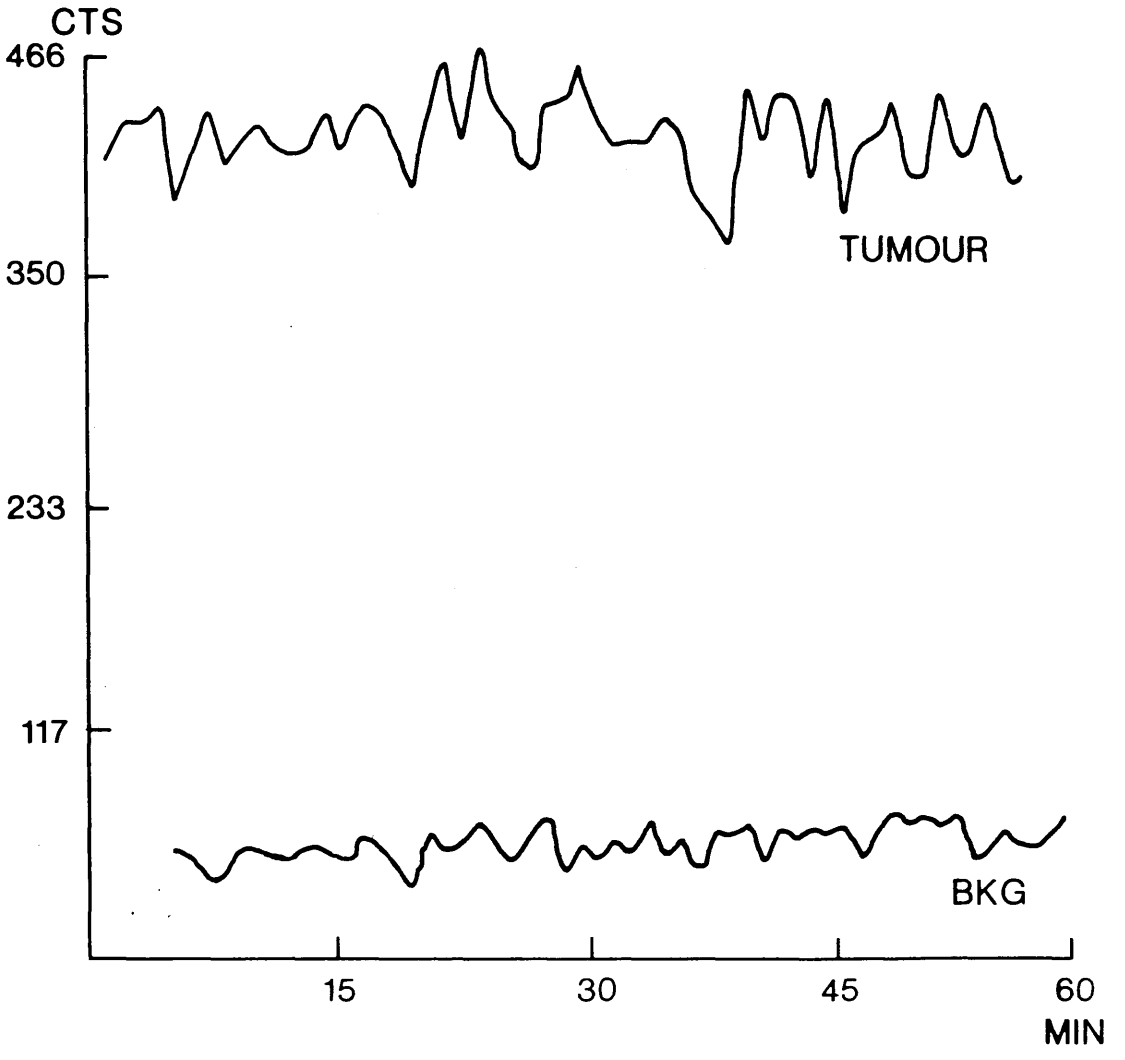

Figure (62): Activity-time curve from a patient with Ewing Sarcoma, obtained 60 minutes post injection (BKG = Background close to the tumour).

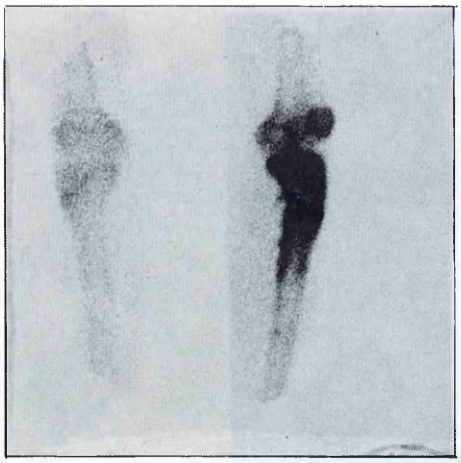

Figure (63): Tc^{99m} MDP bone scan shows increased tracer uptake in the upper 1/3 of the left tibia in a patient with osteosarcoma.

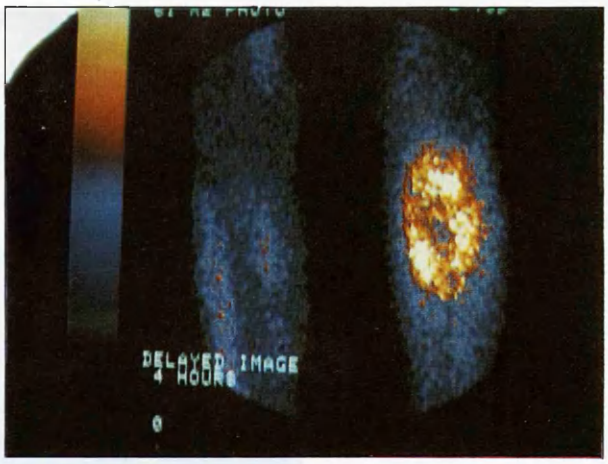

Figure (64): Tl-201 chloride scan shows intense increased tracer uptake in the same patient with osteosarcoma.

Figure (65): Tc^{99m} MDP bone scan shows increased tracer uptake in the proximal end of the right femur in a patient with osteosarcoma.

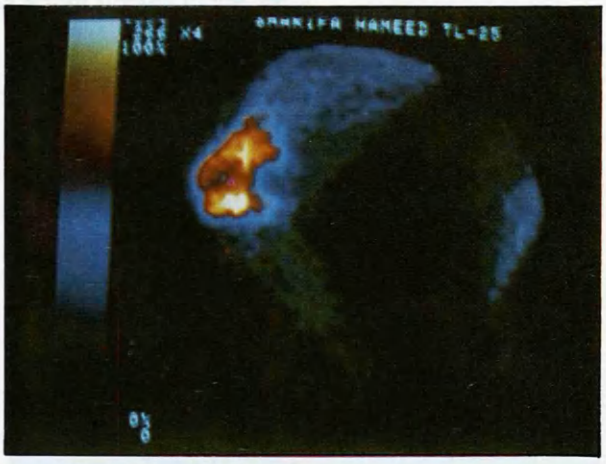

Figure (66): Tl-201 scan shows intense increased tracer utpake in the site of the tumour in the same patient.

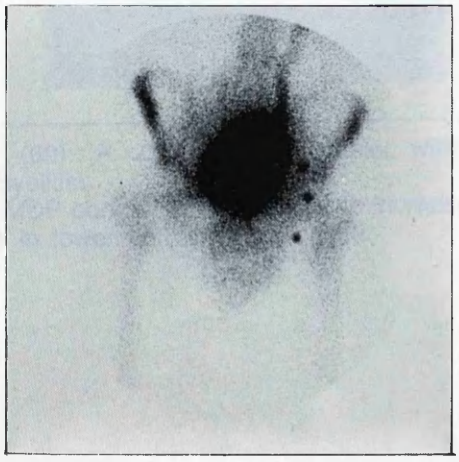

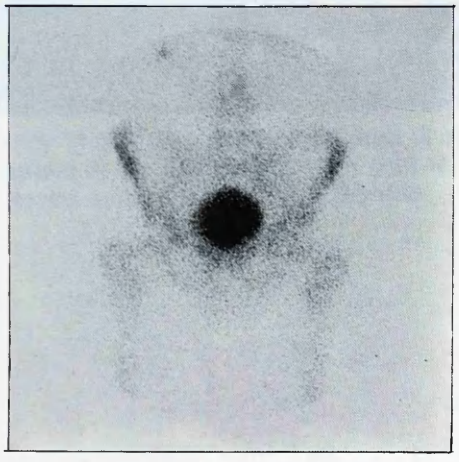

Figure (67): A 55 years old, male, had left groin swelling of 5 months duration. Pathology liposarcoma. Anterior view of the pelvis with marker and 24 hours after injection does not reveal abnormal tracer uptake, in the skeleton. There is slight increased tracer uptake in site of the tumour.

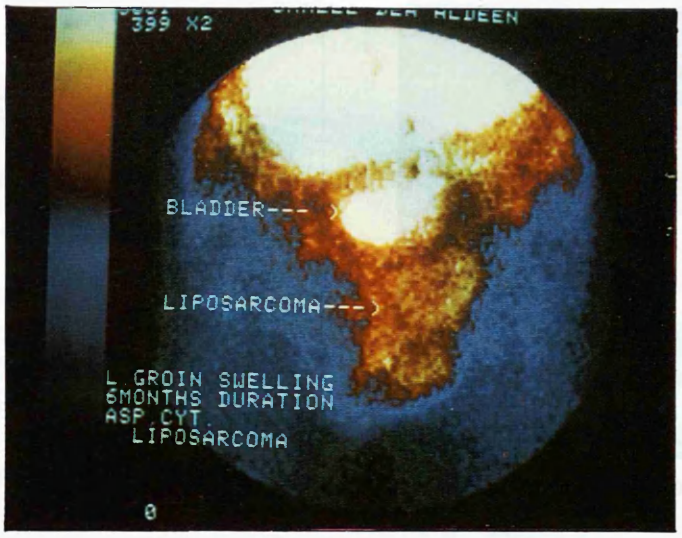

Figure (68): Tl-201 chloride scan of the pelvis shows a large area of intense increased tracer uptake in the left groin region.

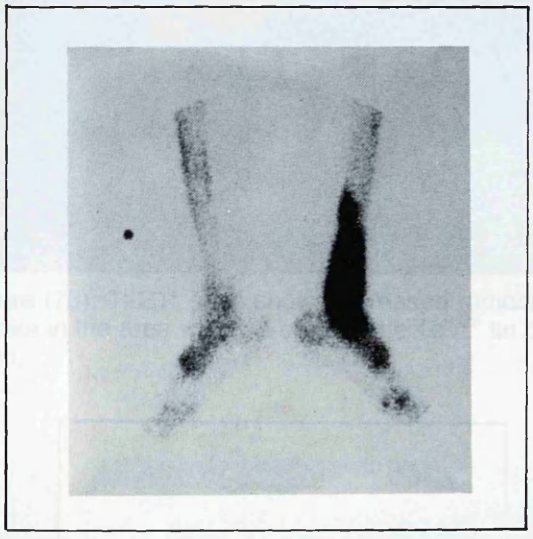

Figure (69): A 23 years old, male, with chronic osteomyelitis.
Tc^{99m} MDP bone scan shows diffuse increased tracer uptake in lower part of the left tibia.

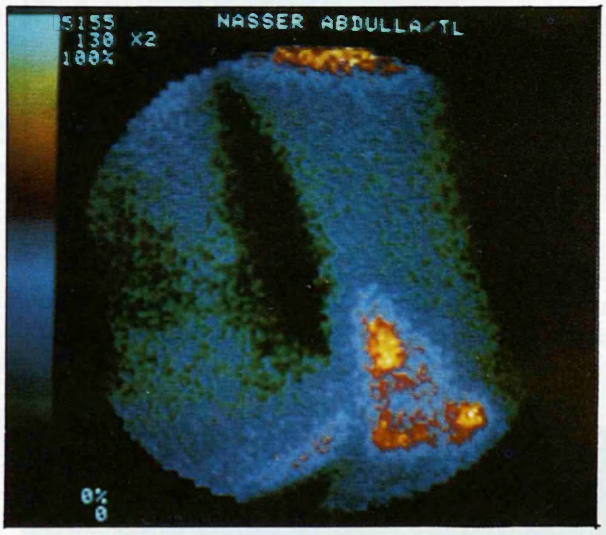

Figure (70): Tl-201 scan shows focal area of increased tracer uptake in the lower part of the right tibia which proved to be exacerbation of the disease.

Figure (71): Tc^{99m} tin colloid liver scan shows a large cold defect in the liver.

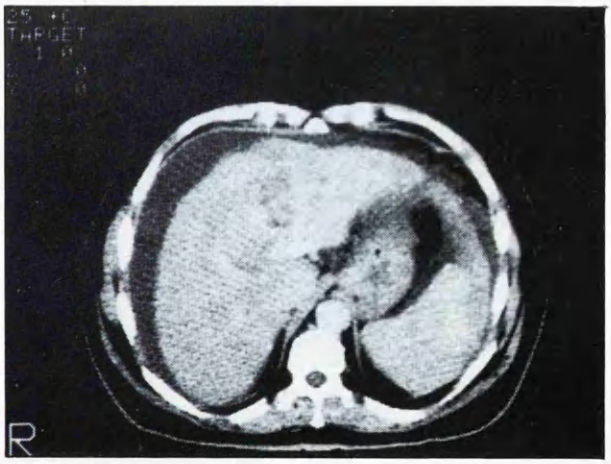

Figure (72): CT scan shows mass lesion in the liver.

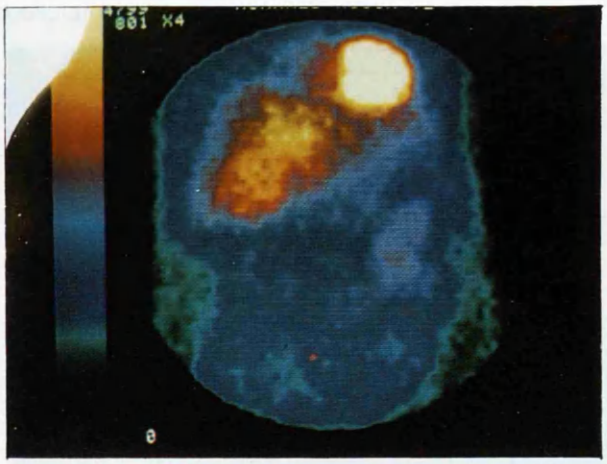

Figure (73): Tl-201 scan shows increased radionuclide uptake in the area which is cold on the Tc^{99m} tin colloid scan.

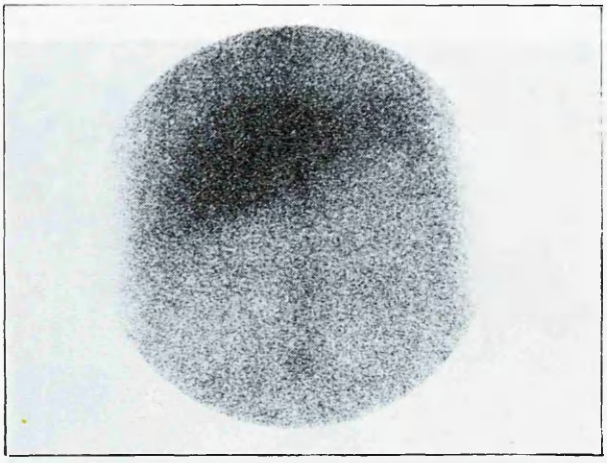

Figure (74): Ga-67 scan shows almost equivalent tracer uptake with surrounding normal liver tissue in the site of the tumour.

Figure (75): A 72 years old, female, had lost weight and appetite.
Anterior view of the liver with Tc^{99m} tin colloid shows a large focal defect involving mainly the right lobe of the liver. Biopsy showed hepatocellular carcinoma.

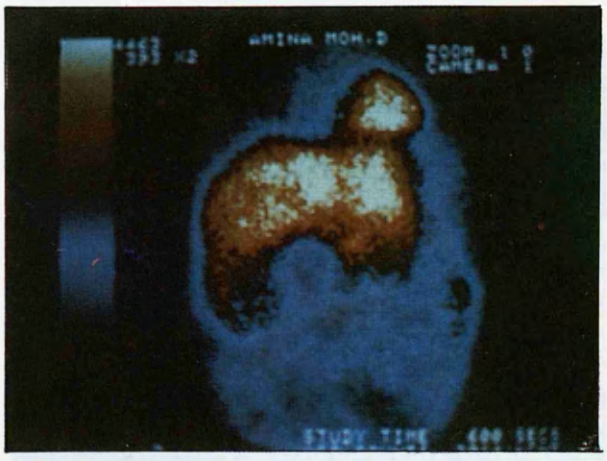

Figure (76): Tl-201 scan shows increased tracer uptake with a central photopenia in the area which is cold on the Tc^{99m} colloid scan.

Figure (77): Tc^{99m} tin colloid scan, anterior view, shows a large cold defect occupying almost the right and ieft lobes of the liver - pathology, revealed primary hepatocellular carcinoma.

Figure (78): Tl-201 scan shows increased tracer uptake in the site of the tumour.

Figure (79): Subtraction Tl-201 Tc^{99m} tin colloid images showed increased Tl-201 uptake in the primary hepatocellular carcinoma.

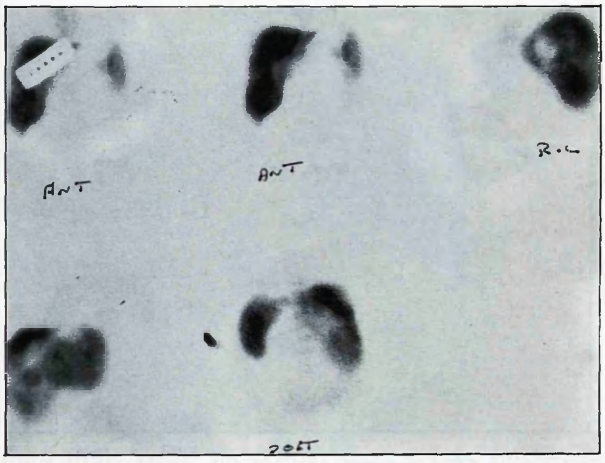

Figure (80): Tc^{99m} tin colloid scan shows a focal defect in the right lobe of the liver in a patient with hepatoma.

a)

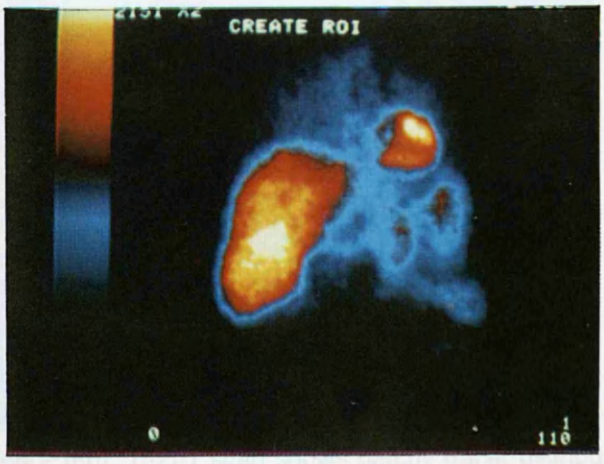

b)

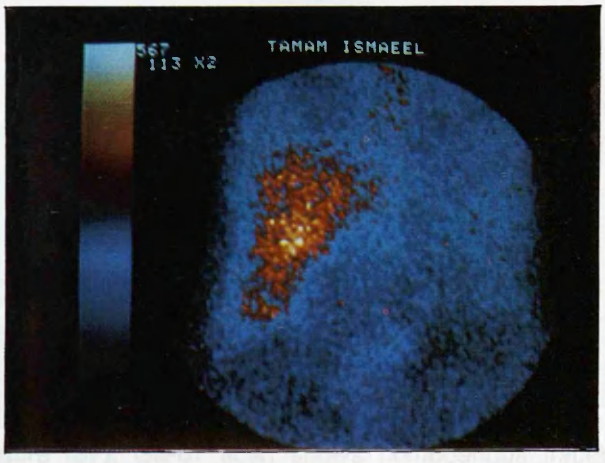

Figure (81): Tl-201 (a) and Ga-67 (b) images revealed increased uptake of both radionuclides in the site of the tumour.

Figure (82): Tc^{99m} tin colloid scan, anterior view shows poor and patchy tracer distribution in the liver with colloid shift to the spleen and bone marrow in a patient with micronodular cirrhosis.

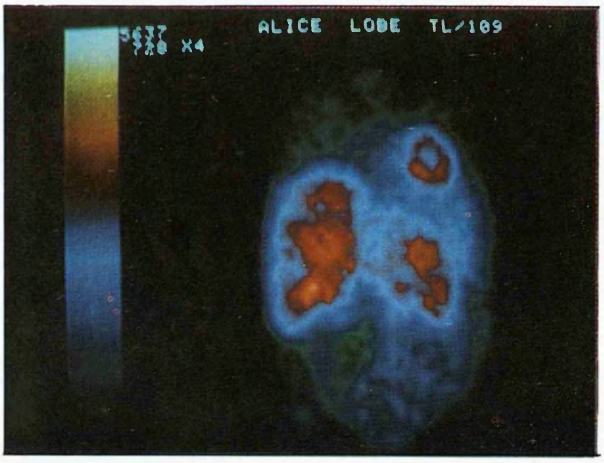

Figure (83): Tl-201 image shows patchy tracer distribution with multiple focal defects.

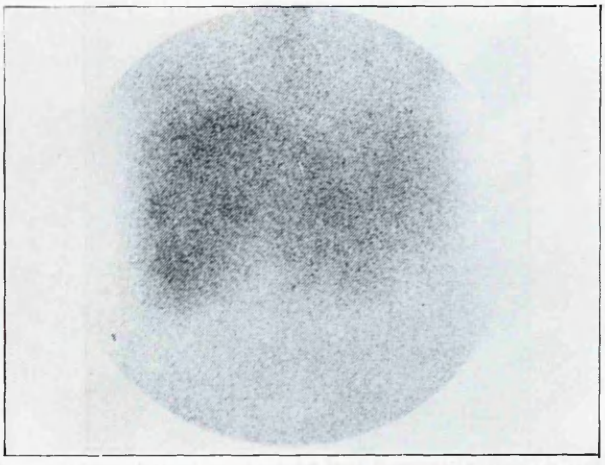

Figure (84): Ga-67 image of the liver shows homogenous tracer uptake in the liver.

Figure (85): Tc^{99m} tin colloid scan shows decreased and patchy tracer distribution in the liver.

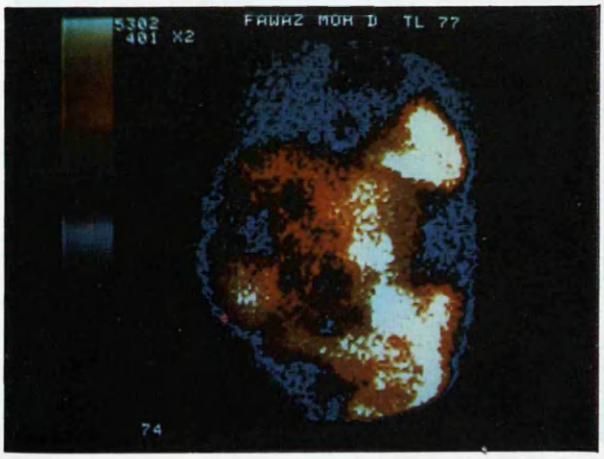

Figure (86): Tl-201 scan shows patchy tracer distribution in the liver.

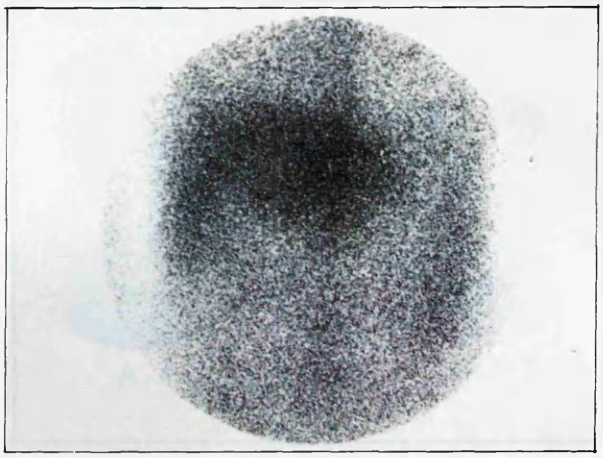

Figure (87): Ga-67 scan shows homogenous tracer uptake in the liver.

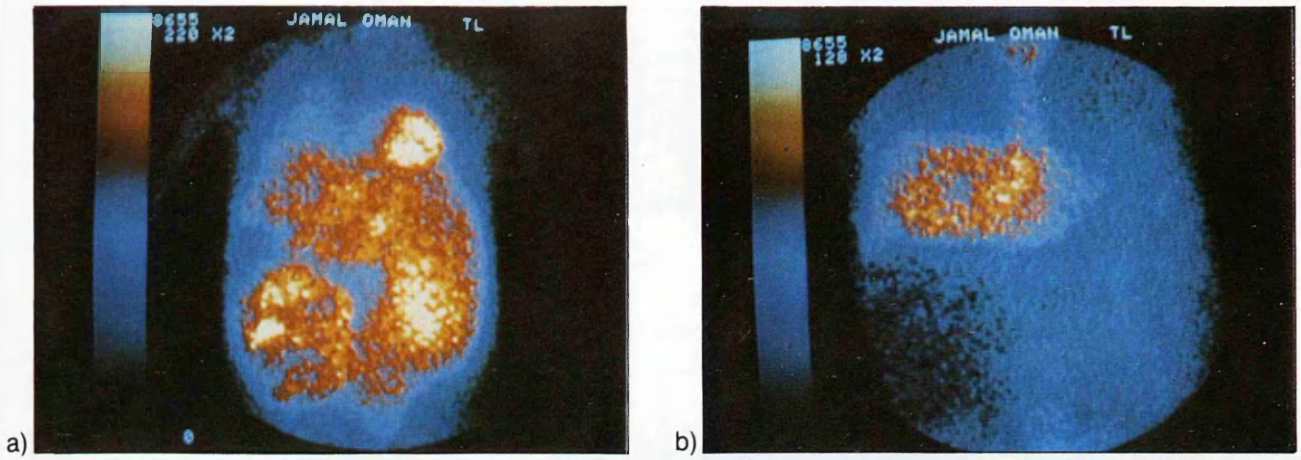

a) b)

Figure (88): (a) Tl-201 and (b) Gallium-67 scans show focal defects in the areas which are cold on the Tc^{99m} colloid scan in the patient with bilharzial cirrhosis.

Figure (89): Anterior view of the liver and spleen with Tc^{99m} colloid scan shows small liver with patchy tracer distribution and multiple focal defects. Grossly enlarged spleen in a patient with bilharzial cirrhosis.

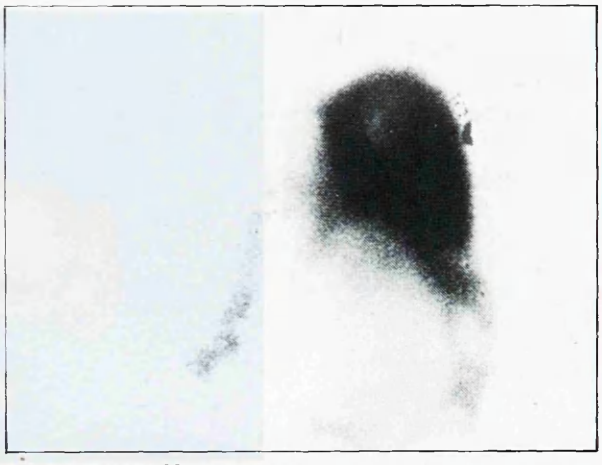

Figure (90): Tc^{99m} tin colloid scan, Anterior view in a patient with situs inversus — shows large focal defects in the Right and Left lobes of the liver. Liver metastasis from Liomyosarcoma of the stomach.

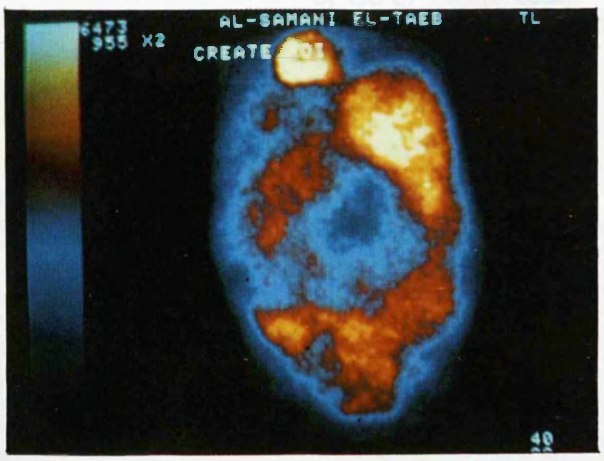

Figure (91): Tl-201 scan shows a large focal defect in the liver.

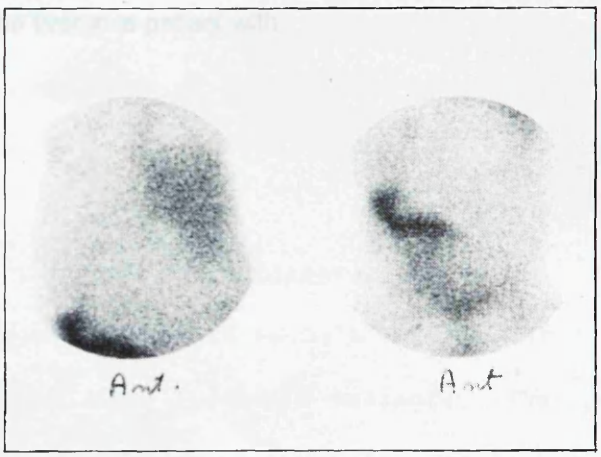

Figure (92): Ga-67 shows a large focal defect in the liver.

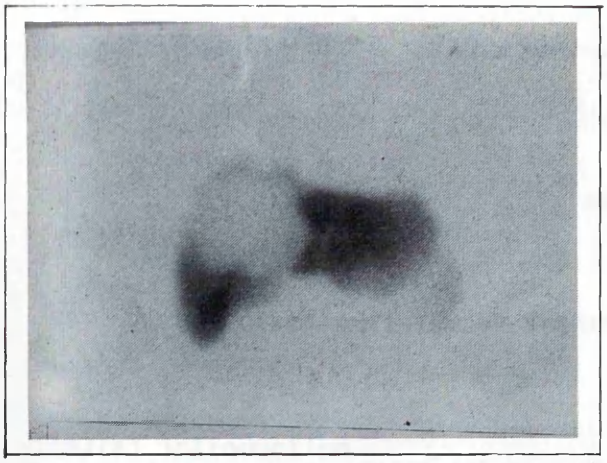

a)

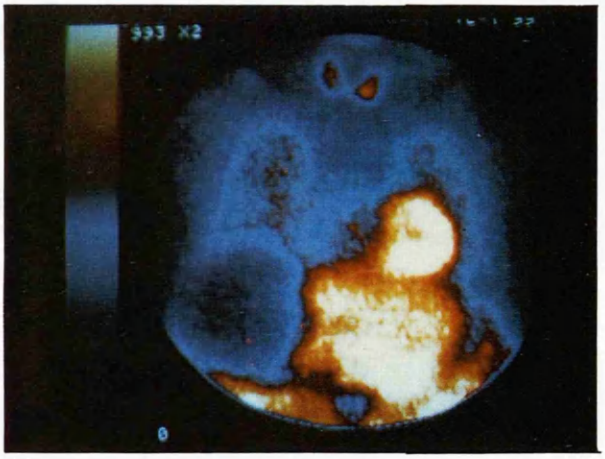

b)

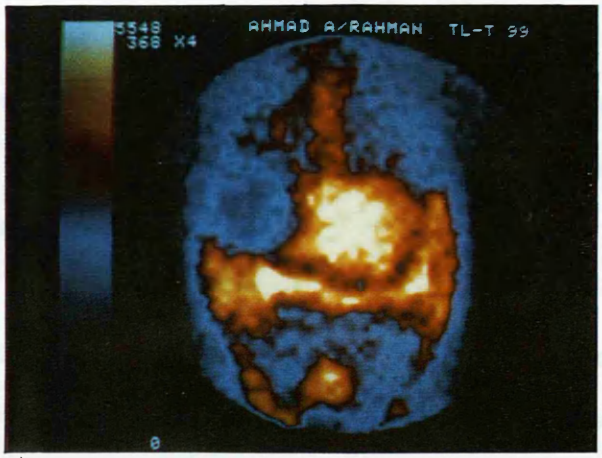

c)

Figure (93): a) Tc^{99m} tin colloid scan.
b) Tl-201 chloride scan.
c) Ga-67 citrate scan.
Show a large focal defect in the liver in a patient with hydatid cyst of the liver.

CHAPTER VI

EFFECT OF ANTI-TUMOUR THERAPIES ON THALLIUM-201 UPTAKE

VI(1)(a) Introduction

Anti-tumour therapies can achieve better results when there is adequate initial evaluation of location and extent of a tumour [303]. The subsequent management of a cancer patient is to assess response to treatment, to detect early relapse and to assist in making decisions concerning follow-up treatment [304].

The role of Tl-201 in predicting tumour responsiveness to anti-tumour therapies has not been fully evaluated. If a tumour site continues to demonstrate uptake after therapy, this indicates the presence of metabolic active tissue and may be evidence of the presence of residual viable tumours. A positive Tl-201 scan following treatment of known tumour sites of disease may be used as an index of persistence or recurrence of treated disease.

Terui, et al, 1984 [246], examined the effect of chemotherapy on Tl-201 uptake in four patients with primary bone tumours (2 Ewing's sarcoma and 2 osteogenic sarcoma). Of three out of four follow-up patients, the

post-therapy scans showed reduction in Tl-201 uptake more markedly than Tc-99m MDP uptake during effective chemotherapy. The remaining patient did not respond to the treatment and the scan showed no changes in the Tl-201 uptake.

Kaplan et al, 1987 [247], found that Tl-201 brain scans offered a more accurate assessment of response to therapy than other radionuclides and CT scanning.

I have evaluated the effect of radiotherapy and chemotherapy on Tl-201 uptake in patients with various malignant disease. A series of patients were studied before and after therapy.

VI(1)(b) Patient Population

Thirty three patients with lung carcinoma, 27 male and six female, the mean age group (± SD) 57.3 (± 8.7) years, had received prior lung irradiation. Eleven patients of these, two malignant lymphoma, one osteogenic sarcoma, two lung carcinoma and six breast carcinoma, had received prior chemotherapy; the mean age group was (± SD) 38.22 (± 10.3) years. Out of 16 patients with brain tumours, nine had primary brain tumours and seven metastases, 11 male and 5 female, the ~~main~~ mean age of the group (±SD) was 45.8 (± 13.2) years,were receiving steroid therapy at the time of imaging (see brain imaging).

VI(1)(c) Methods

As described in Chapter V, static Tl-201 imaging was performed ten minutes after administration of 75 MBq of Tl-201 chloride intravenously. The patient was positioned under a large field of view gamma camera interfaced with a mini-computer. The camera was peaked on Tl-201 photopeak 69-85 Ke V x-rays with a 20 percent window, and a 500K counts were obtained each view.

Sequential Tl-201 images were performed prior to therapy, within one week of end of therapy and after five months after therapy.

Tl-201 images were correlated with CT scanning findings. Chest x-ray anterioposterior and laterals were available in all cases. Gallium-67 imaging pre and after therapy was available for comparison in 21 cases with lung carcinoma. CT scanning of the thorax was performed using new generation scanner with a 20 S scanning times and with slice thickness of 13mm at slice distances of 15 mm to the tracheal bifurcation and 15mm or 20mm more caudally. The matrix was a 320 x 320 with individual pixel size of 1mm (figure 96).

The response of the tumour following irradiation was evaluated with tumour measurements on serial posteroanterior and lateral chest radiographs and CT scanning obtained before treatment, at the completion of irradiation and at 5 months follow up intervals. Complete regression of the tumour was described where there was a total disappearance of all

measurable masses (primary tumour and metastatic lymph nodes), partial regression was recorded when there was at least a 50 percent decrease in the cross-sectional areas of the measured masses and there was no progression of disease or new areas of malignant tumour appeared within the irradiated volume. The stable (no response) groups included patients without significant tumour regression. The response of the tumour following irradiation was assessed quantitatively. Thallium-201 images pre- and post-therapy were displayed on the computer screen. A region of interest around the tumour and the background surrounding the tumour was created over the pre-therapy image. The mean counts in the tumour and background were recorded. The same regions of the patient were recorded over the post-therapy image and the mean counts in the tumour and background were recorded. From these data, the true count in the tumour pre- and post-therapy was obtained. The percentage of loss of activity or changes of activity in the true count of primary tumour was obtained, and this may represent the degree of local response after treatment.

VI(1)(d) Results

Sequential Tl-201 scans were found to be useful in evaluating patients with malignant disease, especially when the scan was positive pre-treatment. In patients who had received chemotherapy, only one patient achieved complete regression of the tumour and Tl-201 scan showed no areas of increased tracer uptake (figure 97). Another patient achieved partial regression of the tumour, and Tl-201 scan showed reduction of

tracer uptake in the site of the tumour. Nine patients showed no significant changes of Tl-201 uptake and there was no response to treatment.

Table 26 shows the distribution and degree of local response after chemotherapy in individual patients.

Table 27 shows the sequential radionuclide studies and CT scanning with the distribution and degree of local response after radiation therapy in individual patients. Table 28 summarizes the distribution and degree of local response after radiation therapy.

In 33 patient who received about 50 Gy (5000 rads) on the tumour site, 30 patients were positive with Tl-201 and three patients were negative. No single patient achieved complete regression of the tumour after radiation therapy. Only nine patients (30 %) showed partial response to treatment and reduction of Tl-201 uptake of less than 50 percent in the site of the tumour (figure 94).

Twenty one patients (70%) showed no significant changes in tumour uptake in pre- and post-radiation therapy scans (figures 95-101). None of the three negative patients showed abnormal Tl-201 uptake in the site of the tumour in pre- and post-therapy scans.

In comparison to CT scanning, 33 patients were positive pre-radiation therapy, 13 (39%) patients achieved partial response to treatment, and 20 (60%) patients showed no response after radiation therapy.

Of these only 21 patients underwent gallium study before and after treatment, three patients were negative in pre- and post-therapy scans. Three patients (17%) showed partial response (figure 111) and 15 (83%) showed no response to treatment (figure 109).

Thirteen patients were followed up five months after treatment using Tl-201 scans. Of these, only two patients showed reduction of Tl-201 uptake in the site of the tumour. In the remaining the patients there were no significant changes from previous studies. Of these, 11 patients were also followed by Ga-67 imaging which showed only two patients had reduction of the tracer uptake in the site of the tumour.

VI(1)(e) Discussion

Anti-tumour therapy regimens may produce effective responses in patients with advanced malignant disease. Until clear survival advantages are shown for specific regimens, maintenance of a high quality of life must remain a very high priority.

Priestman and Baum, 1976 [305], suggested that obtaining a response improves a patient's quality of life and hence might be of great importance to individual patients. The correlation of tumour response with

anti-tumour therapies emphasizes the need to develop the most effective treatment regimens that will yield complete tumour regression, thus resulting in higher survival.

Since so many patients with malignant disease died with distant metastasis, survival alone may not be a reliable prognostic indicator and local tumour control must be carefully evaluated [306].

The response of tumour following anti-tumour therapies was evaluated with tumour measurement on serial radiological studies. In addition radionuclide studies have established roles in the follow up and management of patients with cancer [254]. Although radiographic modalities have superior spatial resolution, they cannot differentiate bulky fibrosis from active neoplastic disease [247].

Gallium-67 scanning was found to be useful for follow-up studies of the course of lymphomatous disease after therapy. A positive gallium-67 scan may be the only objective evidence of persistence or recurrence of treated disease [204]. It can distinguish between recurrent tumour and fibrosis secondary to post-irradiation therapy, since the former is usually gallium-positive and the later is usually gallium-negative [307].

During or shortly after therapy, gallium-67 uptake may be suppressed, even if the tumour is not completely obliterated. If the tumour site continues to demonstrate uptake after therapy, this is a strong indica-

tion of the presence of residual viable tumour. It is generally accepted that a positive scan is more reliable than a negative scan after therapy (204).

There is a good correlation between the change in gallium uptake and the change in tumour size after treatment, as determined radiographically (308). Changes in tumour uptake of gallium-67 have been correlated with radiation dose in patients with lung tumours. Bitran et al, 1978 (309), reported that after chest radiotherapy a gallium scan may show no abnormalities even though viable tumour is still present.

Gallium-67 scanning may be useful in detecting extra thoracic metastases from non-small cell lung cancer, but fails specifically within the brain, and it is less sensitive then bone scans in detecting osseous metastases. It does not supplant CT scans of the brain or bone scans when metastases are suspected (204).

In the present study, I found Tl-201 chloride useful in determining local tumour response after anti-tumour therapies. Complete suppression of Tl-201 uptake occurred after chemotherapy in one patient with Hodgkin's lymphoma. Decreased Tl-201 uptake occurred after radiation therapy in patients with primary lung cancer. There was a good correlation between the change in Tl-201 uptake and the change in the primary tumour size after treatment as determined radiographically.

Tl-20 scan is highly sensitive in detecting primary lung cancer but fails to identify mediastinal node involvement or small axillary or supraclavicular lymph node in patients with malignant disease.

Unfortunately, in none of these patients followed up with Tl-201 or Ga-67 scans were pathological correlation or autopsy data obtained because using Tl-201 as staging modality necessitates atleast an exploratory thoracotomy, which is impractical and sometimes medically contra-indicated in large number of patients with unresectable lesions treated by radiation or chemotherapy.

The role of radiation therapy in the management of unresectable or medically inoperable bronchogenic carcinoma remains undefined. Perez et al, 1980 (306) and Roswit et al, 1968 (310), reported a 22 percent one year survival rate for a large group of patients treated with 4000-5000 rads in four to five weeks in contrast to a 16 percent one year survival rate for a similar control group given a placebo. They found the survival rate also was the same whether the patients were treated with 4000, 5000, or 6000 rads. Other investigators questioned whether this was a true reflection of therapeutic effectiveness of irradiation since the patients in the irradiated group may have had more supportive care than those in the control group.

On the other hand, Bloedorn et al, 1964 (311), reported no histologic evidence of residual tumour at primary site in 54 percent of 26 patients receiving 6000 rad in six weeks preoperatively. The mediastinal lymph

nodes showed residual tumour in only 8 percent of the cases. Heilman et al, 1964 [312] described residual microscopic primary tumour in 17 of 24 patients treated with 5500-6000 rad for carcinoma of the lung four to six weeks prior to thoracotomy. Of 15 patients with pre-operative radiographic evidence of hilar or mediastinal adenopathy, only three had residual tumour in the pathologic specimen.

In the study herein, 33 patients received 5000 rad in four to five weeks to the tumour site. Thirty patients were positive with Tl-201 scans in pre- and post-radiation therapy. None of these had achieved complete regression of the tumour after therapy. Only 13 out of 30 were patients followed up five months after therapy, nine patients died during this period, five patients were critically ill and have developed extrathoracic metastases, and the remaining three patient were lost during follow up.

Finally, the administration of antineoplastic agents and steroid therapy prior to injection of Thallium-201 appeared not to affect the distribution of Tl-201 in the tumour. Any changes in the uptake of Tl-201 in post-treatment scans thus be assessed carefully if is to determine whether these changes represent tumour eradication, incomplete control, or recurrence of disease.

In conclusion, the changes of uptake of Tl-201 in the tumour site may appear highly specific, its use for measuring the extent of neoplastic disease has been disappointing due to insensitivity in detecting mediastinal and nodal spread of the disease.

Table 26

Distribution of Degree of Local Response After Chemotherapy Treatment

Name	Pre Therapy Tumour/Background Activities (K counts)	Post Therapy Tumour/Background Activities (K counts)	Degree of Local Response % *
M.J.	76.4/22.9	73.3/20.7	1.7
K.Y.	82.6/53.6	51.2/49.8	95.0
W.M.	209.2/103.5	225.0/109.0	- 9.7
F.A.	62.9/43.0	64.8/44.5	- 2.0
H.M.	47.2/22.7	55.3/25.6	-21.2
S.M.	56.9/34.2	48.9/31.4	- 4.8
M.M.	79.5/42.3	62.8/48.2	60.8
K.N.	54.2/33.0	49.8/31.0	11.3
S.A.	26.7/17.3	26.4/18.2	12.8
Z.A.	56.5/28.2	52.0/30.2	22.9
A.A.	20.3/12.3	19.2/11.9	8.7

* Tumour activity corrected for background in assessing response

Table 27

Distribution of Degree of Local Response After Radiation Therapy

	Pre Therapy Positive	Post Therapy No Response	Post Therapy Partial Response
Tl-201 (n = 33)	30	21	9
CT Scan (n = 33)	33	20	13
GA-67 Scan (n = 21)	18	15	3

Table 28

Distribution of Degree of Local Response After Radiation Therapy

Name	Pre Therapy Tumour/Background Activities (K counts)	Post Therapy Tumour/Background Activities (K counts)	Degree of Local Response * %
H.J.	40.8/25.9	41.5/27.2	4.0
S.M.	23.4/15.2	27.1/20.3	17.0
F.A.	64.7/45.4	58.2/39.5	1.5
N.S.	19.0/16.0	17.0/15.6	53.3
A.H.	67.7/52.2	117.0/104.0	16.0
M.R.	73.8/49.8	60.0/42.0	25.0
M.K.	88.2/45.0	80.3/61.2	55.7
W.A.	58.5/35.2	53.6/42.0	55.8
S.K.	46.3/32.0	38.2/27.5	25.1
L.H.	12.5/ 8.5	16.4/11.9	-12.5
A.T.	33.0/26.0	44.5/30.0	-107.0
A.F.	43.0/22.5	38.8/28.5	49.8
H.M.	19.0/13.0	8.0/ 6.0	66.6
M.A.	27.0/24.0	16.0/14.0	45.9
A.J.	29.0/21.0	34.0/26.0	0.0
A.M.	16.0/12.0	10.0/ 7.0	25.0
S.J.	18.0/16.0	23.5/21.6	5.0
A.S.	42.6/36.7	39.8/34.0	1.6
F.M.	42.0/40.0	36.0/35.0	50.0
F.A.	58.4/37.0	103.0/64.0	-82.2
M.K.	32.0/27.0	35.0/31.0	12.0
A.K.	52.0/37.0	47.0/35.0	53.3
M.A.	47.3/31.0	43.0/29.0	14.1
A.A.	25.8/22.3	17.3/15.0	34.0
S.K.	10.4/ 8.5	17.9/15.6	-21.0
A.S.	58.4/28.1	56.6/28.9	8.0
A.M.	19.5/16.2	22.0/18.9	6.0
S.S.	33.6/25.6	35.7/28.8	13.8
E.H.	57.0/31.8	64.3/41.2	12.0
A.K.	25.6/19.6	23.5/20.8	55.5

* Tumour activity corrected for background in assessing response.

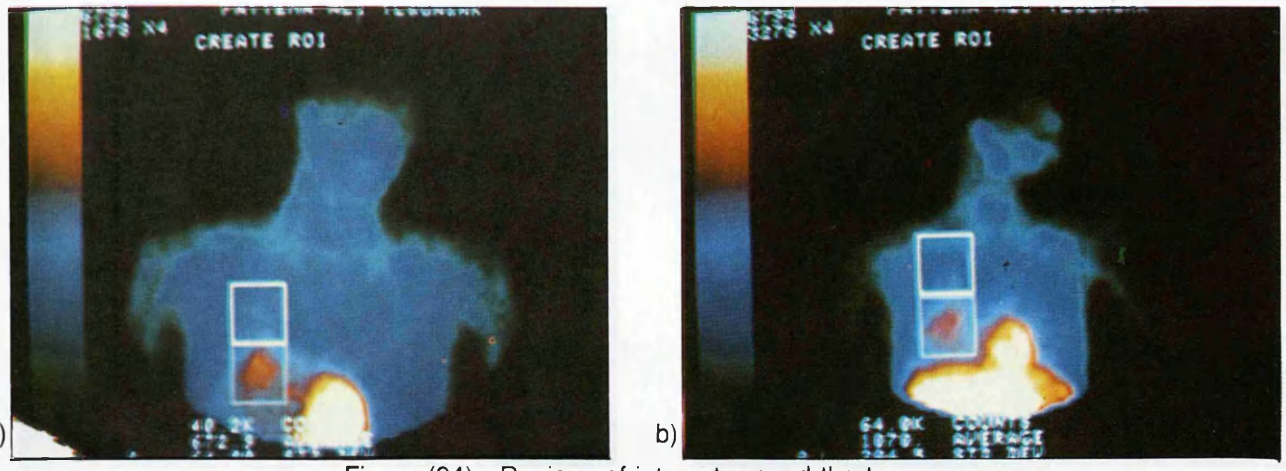

a) b)

Figure (94) : Regions of interest around the tumour and background were created in patient with lung carcinoma in pre-therapy scan (a) and post-therapy scan (b). The patient received 50 Gy and showed partial response to treatment.

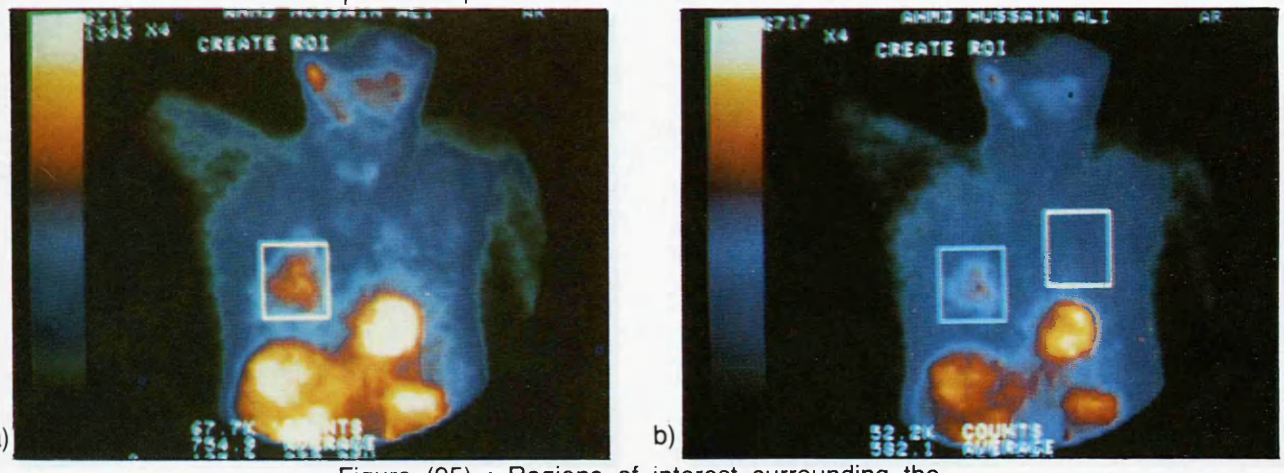

a) b)

Figure (95) : Regions of interest surrounding the tumour and background close to the tumour pre and post therapy in a patient with lung carcinoma received 50 Gy to the tumor site and showed no response after treatment.

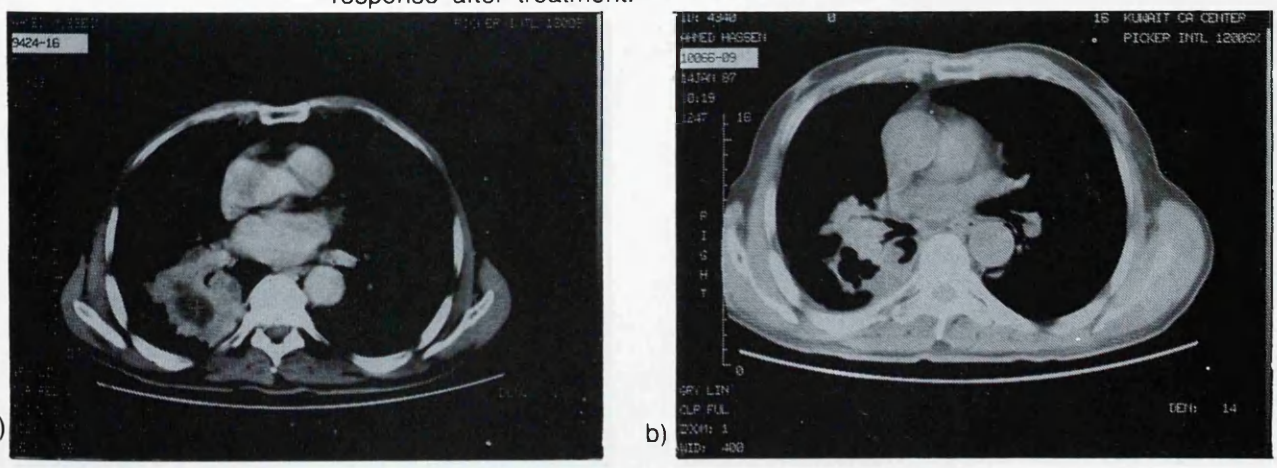

a) b)

Figure (96) : CT scans before therapy (a) and after therapy (b) do not show significant changes.

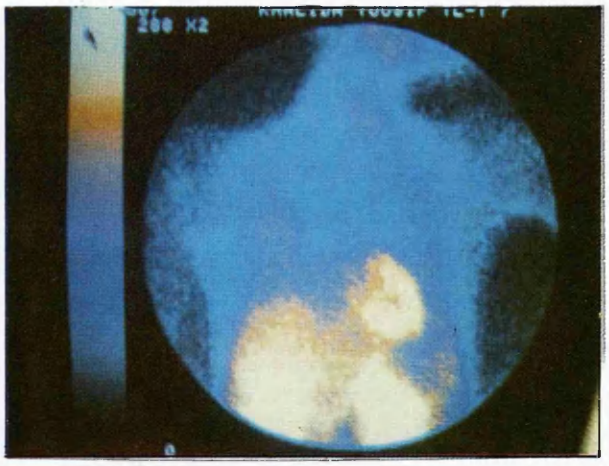

Figure (97) : a - Pre-therapy Tl-201 scan in a patient with mediastinal lymphoma (Hodgkin's lymphoma), shows increased Tl-201 uptake in the enlarged mediastinal lymphnodes.

b - Post-chemotherapy Tl-201 scan shows good response to treatment, and nearly complete regression of the disease (95%).

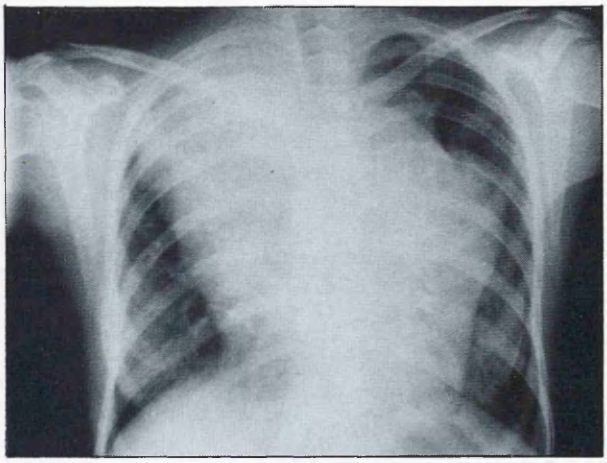

a)

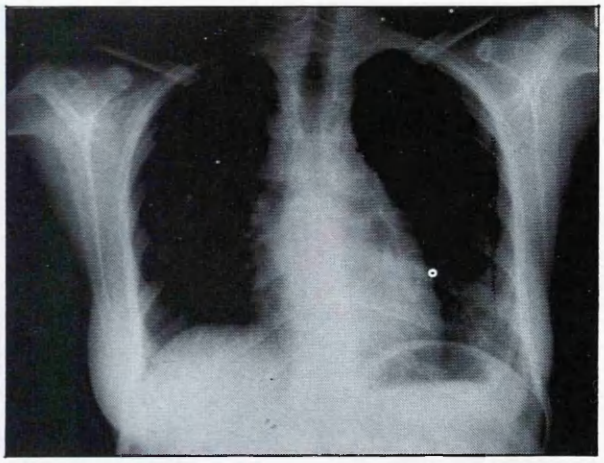

b)

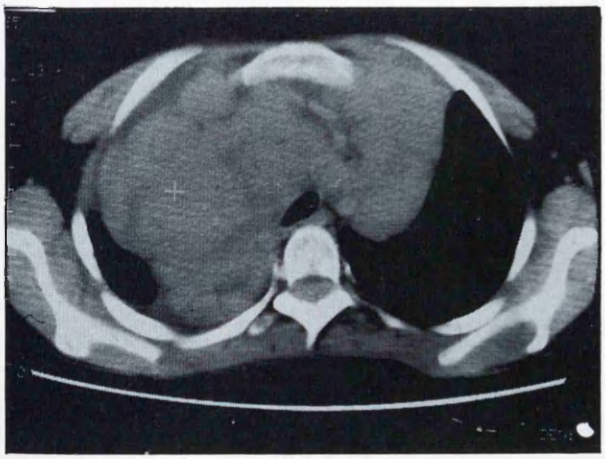

c)

d)

Figure (98) : Chest X-ray (a) Pretherapy (b) post therapy CT scan pre-therapy (c) CT scan post therapy (d) The large mass which occupies the whole upper mediastinum showed nearly complete regression after chemotherapy.

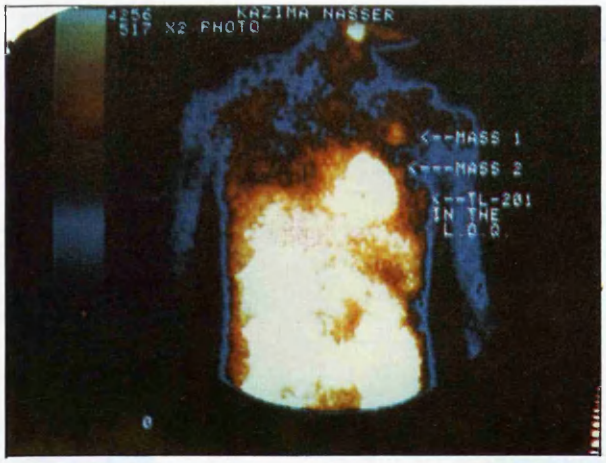

Figure (99): a) Pre-therapy Tl-201 scan in a patient with recurrent breast cancer, shows focal areas of increased tracer uptake in the left breast.

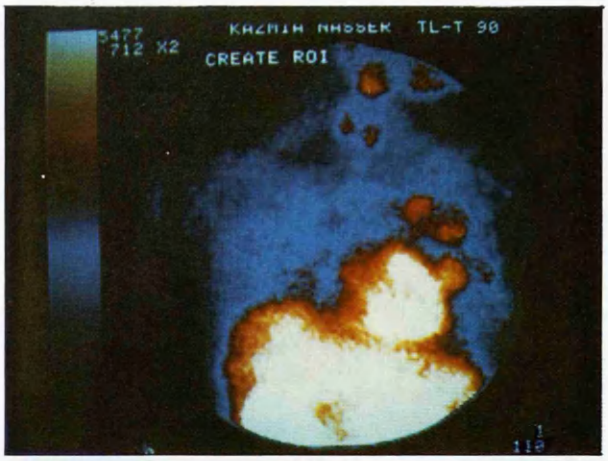

b) post chemotherapy Tl-201 scan shows more intense Tl-201 uptake in the site of the tumour and progression of the disease.

a)

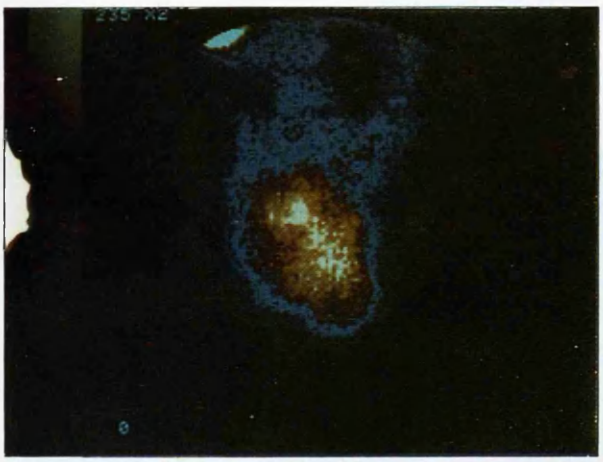

b)

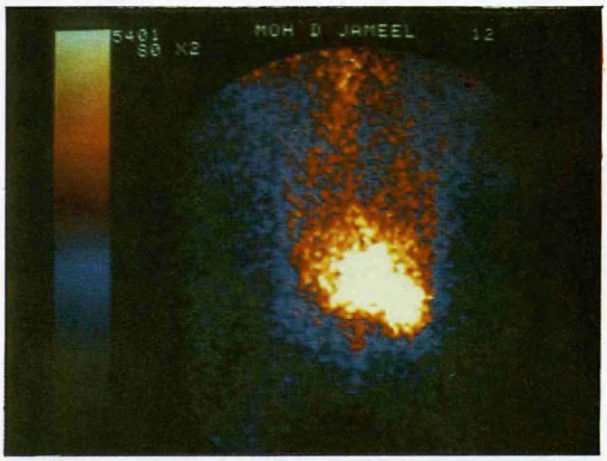

Figure (100): a) Pre-therapy Tl-201 scan b) post chemotherapy Tl-201 scan showed no significant changes in Tl-201 uptake in the site of the tumour of a patient with rectal lymphoma. The patient received 6 courses of VAC regime.

a)

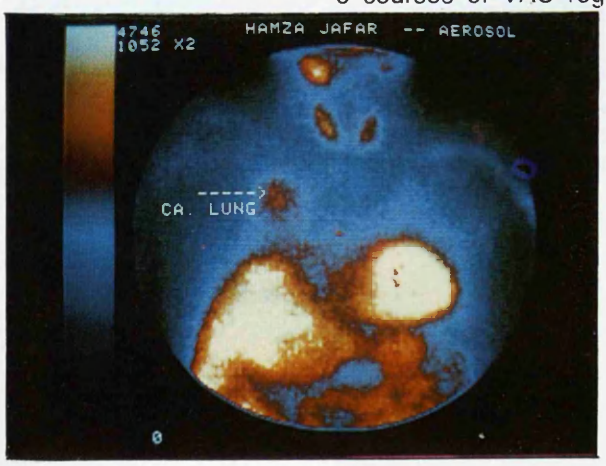

b)

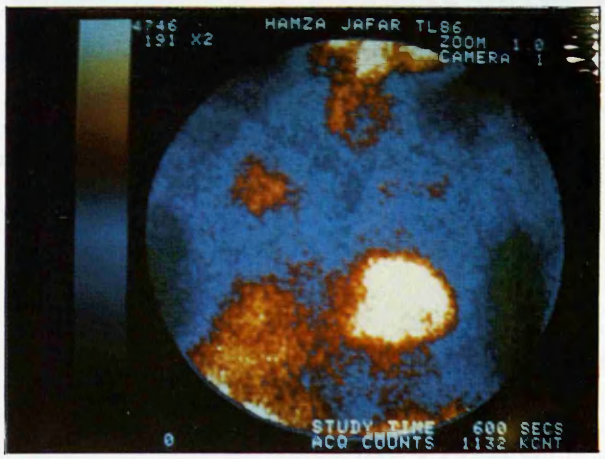

Figure (101): a) Pretherapy Tl-201 scan shows increased Tl-201 uptake in the upper lobe of the right lung. The patient received 50 Gy radiation therapy. b) Post therapy Tl-201 scan shows intense Tl-201 uptake in the site of the tumour and no response to treatment.

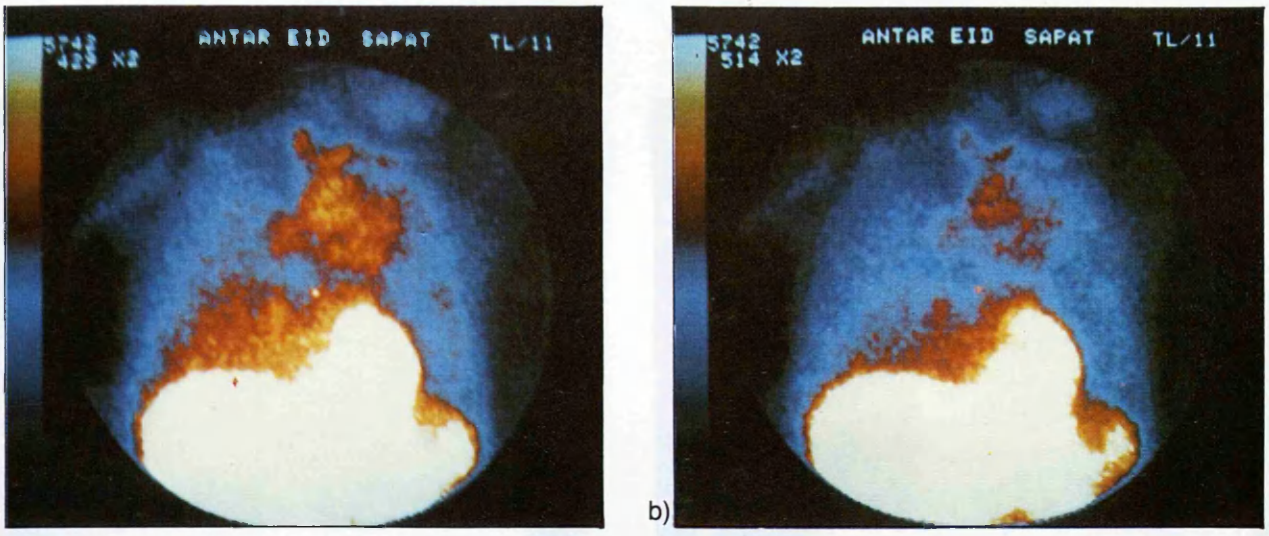

Figure (102): a) Pre-therapy Tl-201 scan
b) Post-therapy scan. The patient received 50 Gy of radiation therapy and showed partial response to treatment.

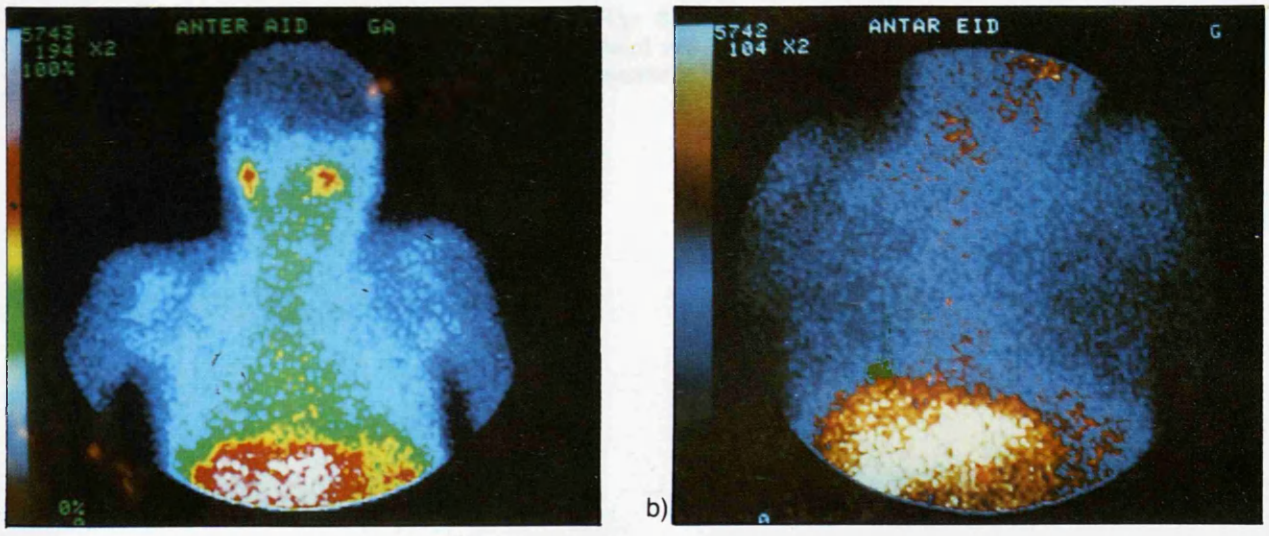

Figure (103): Ga-67 scans a) Pre-therapy b) post-therapy. The scans show no tracer concentration in the site of the tumour in both studies (negative).

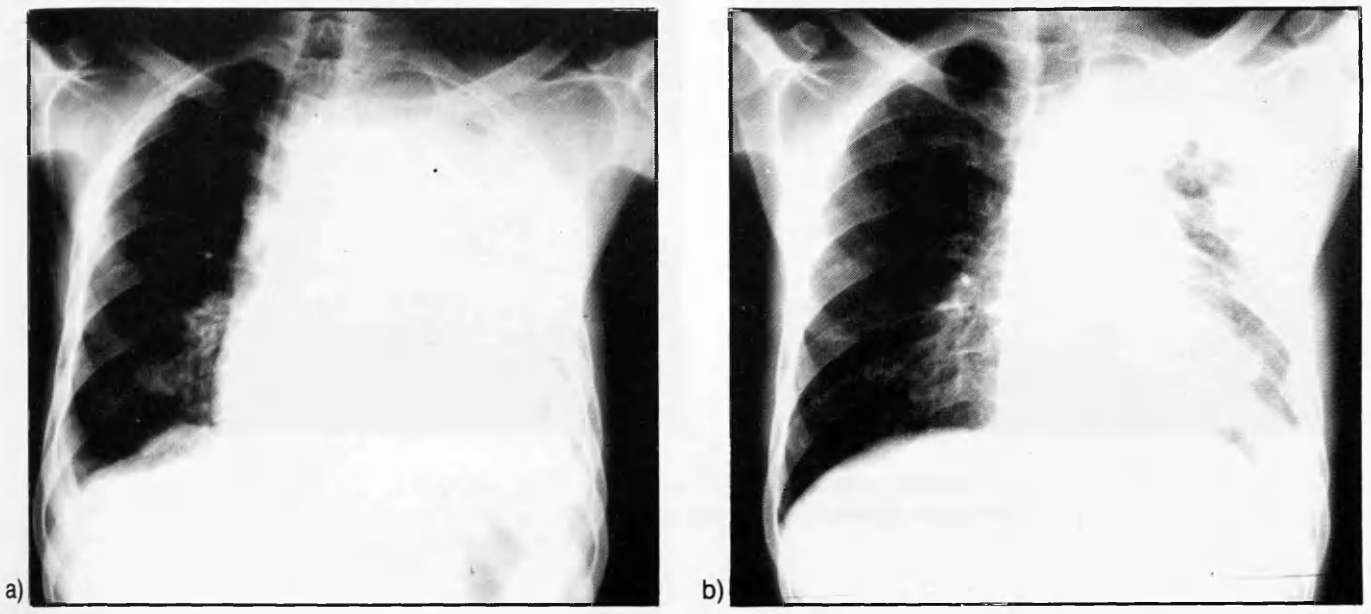

Figure (104) Chest X-Ray a) pre-therapy b) after therapy in the same patient with bronchial carcinoma. Regression of the disease is noted after 50 Gy of radiation therapy.

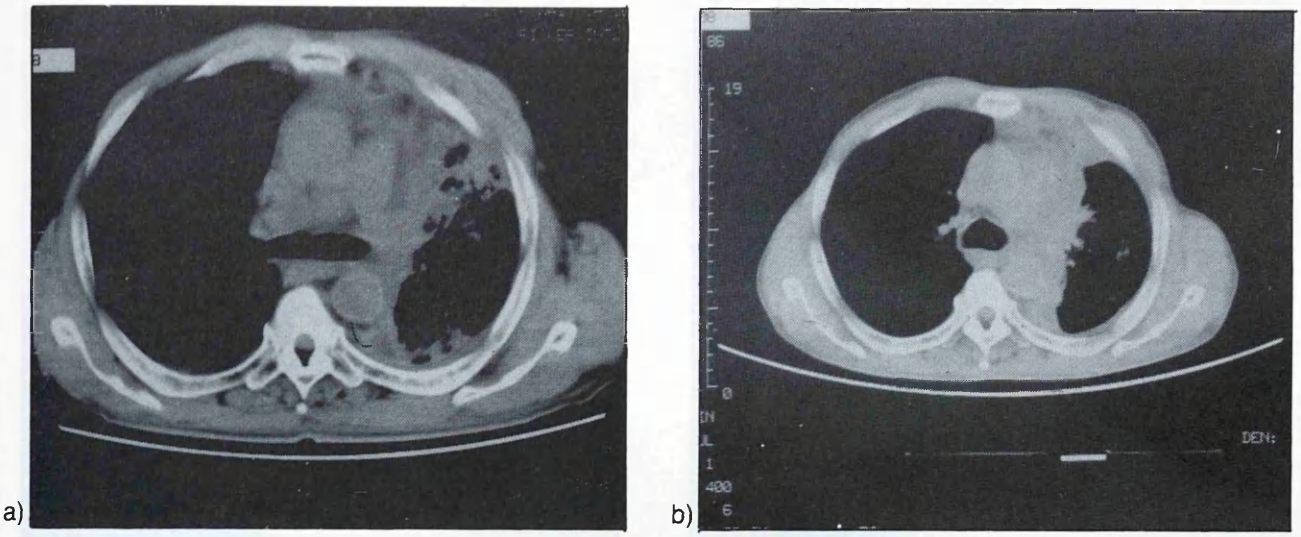

Figure (105) CT scan of the same patient a) pre-therapy b) post-therapy showed partial response to radiation therapy.

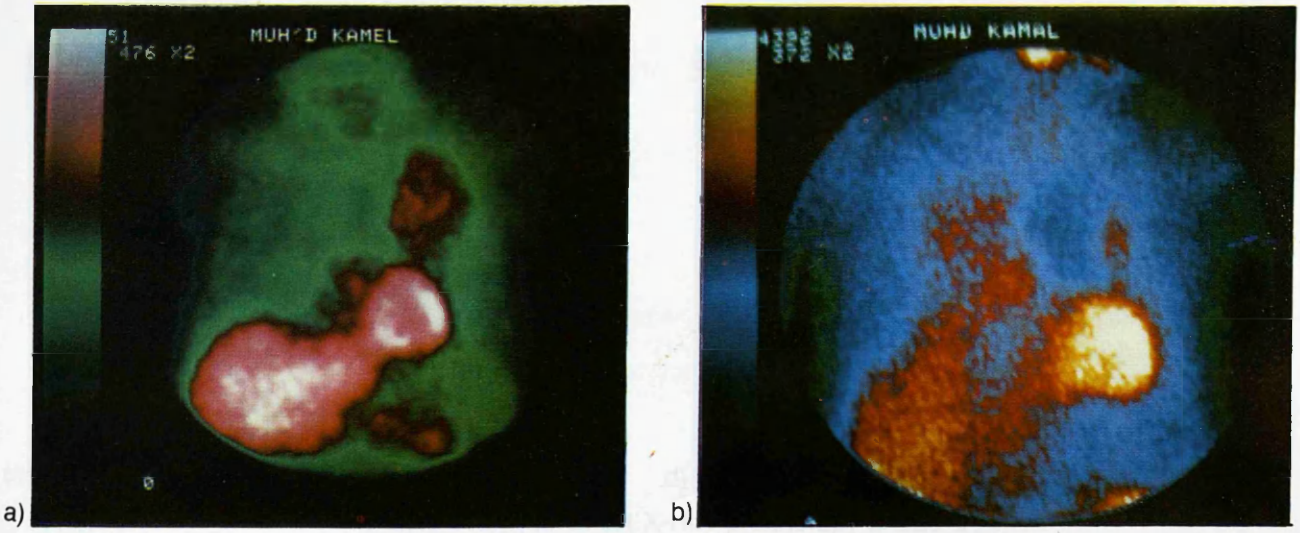

Figure (106): a) Pre-therapy Tl-201 scan shows a large area of increased Tl-201 uptake in the upper zone of the left lung. b) Post-therapy Tl-201 scan shows minimal increased Tl-201 uptake in the site of the tumour after receiving 50 Gy radiation therapy.

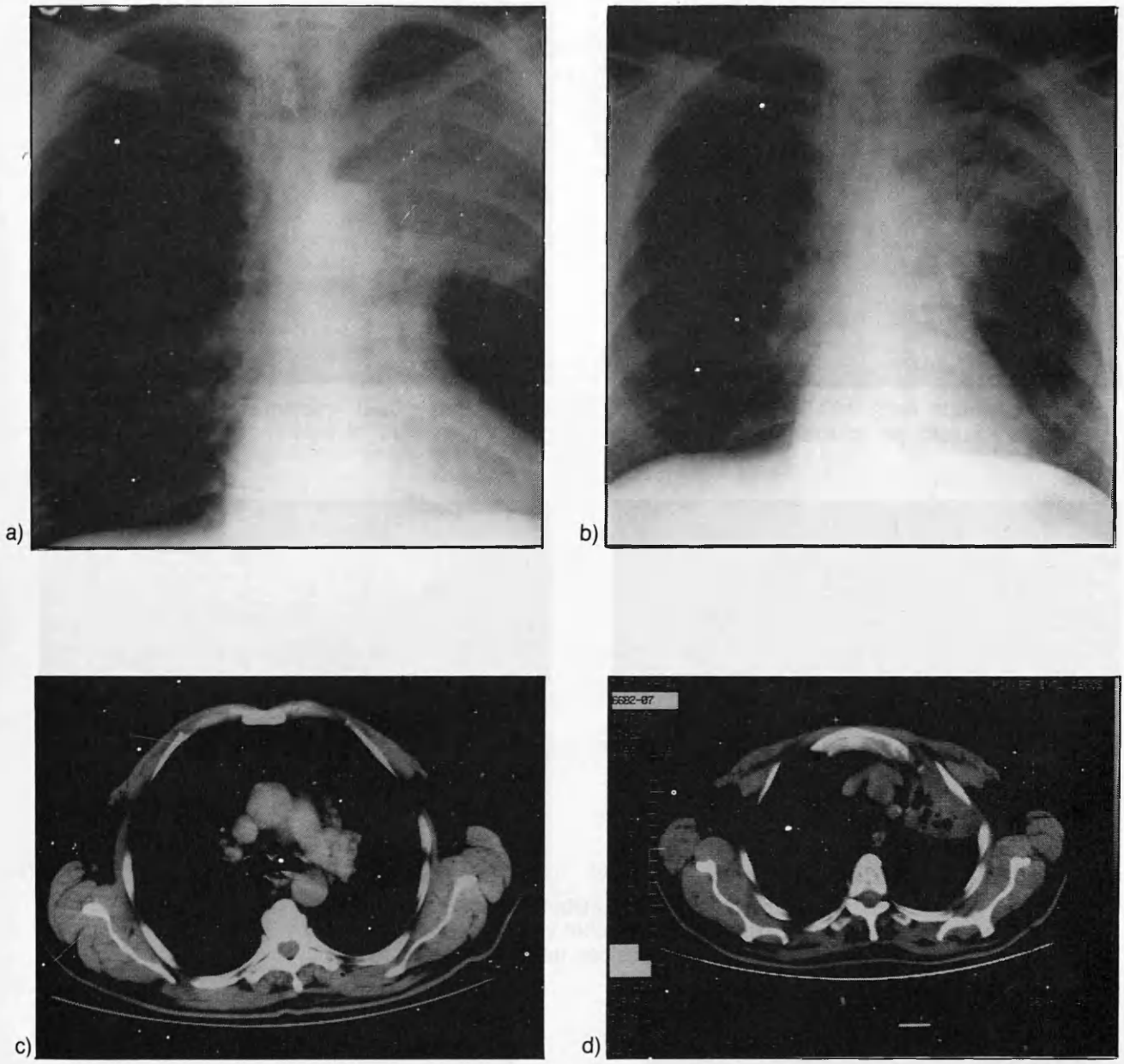

Figure (107): a) Chest X-Ray pre-therapy shows a large shadow in the upper zone of the left lung.
b) Chest X-ray post therapy shows partial response to treatment.
c) Pre therapy C.T. scan.
d) Post-therapy C.T. scan.

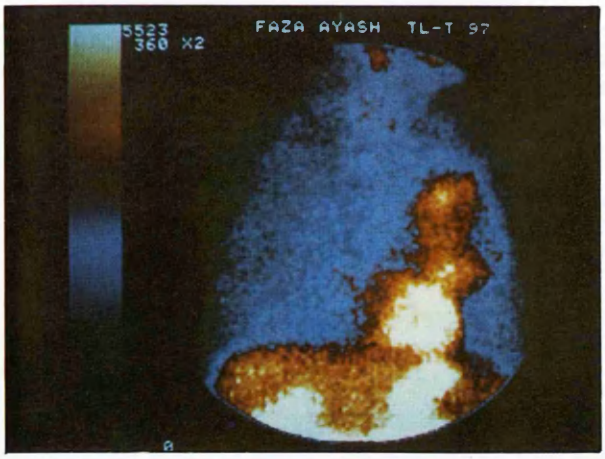

Figure (108): a) Pre-therapy Tl-201 scan shows intense Tl-201 concentration in the primary lung cancer of the left lung.

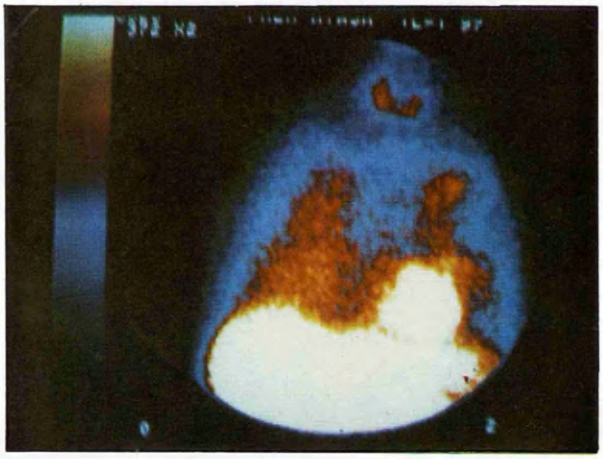

b) Post therapy Tl-201 scan shows slightly decreased tracer uptake in the site of the tumour.

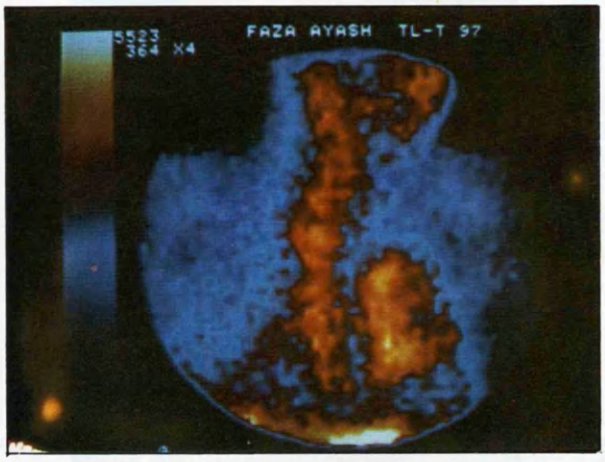

a)

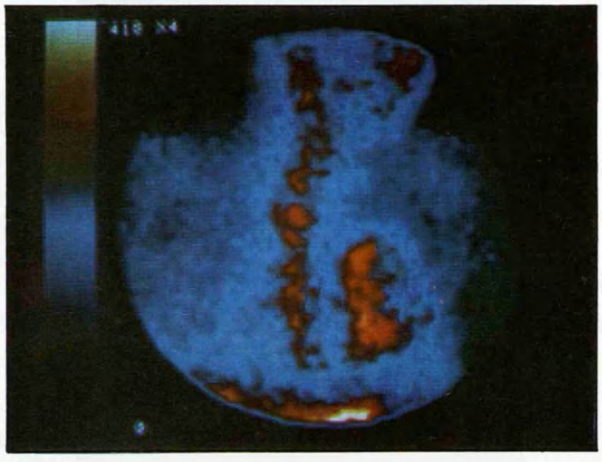

b)

Figure (109): Ga-67 studies a) Pre-therapy b) Post-therapy showed slightly reduced tracer uptake in the site of the tumour after radiation therapy.

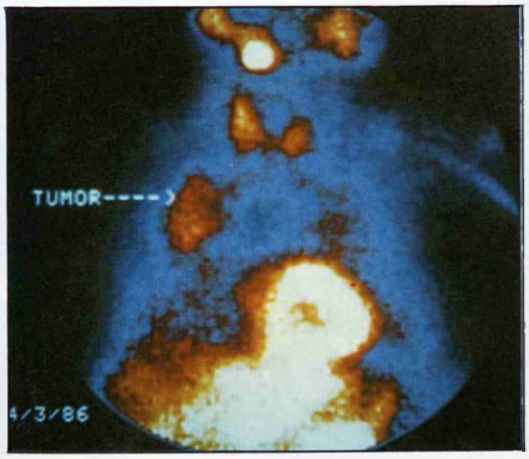

a)

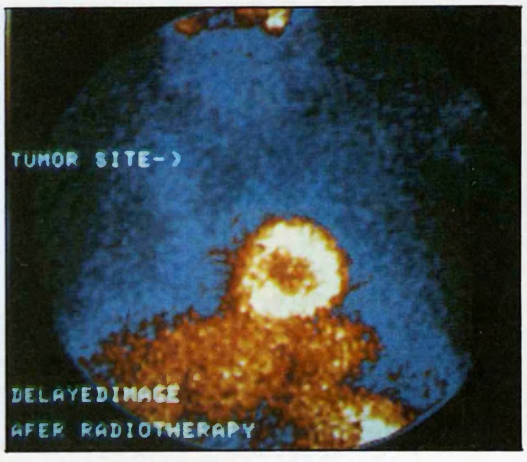

b)

Figure (110): Tl-201 scan a) Pre-therapy shows increased Tl-201 uptake in the primary tumour of the upper lobe of the right lung. b) Post-therapy scan shows minimal Tl-201 uptake in the site of the tumour.

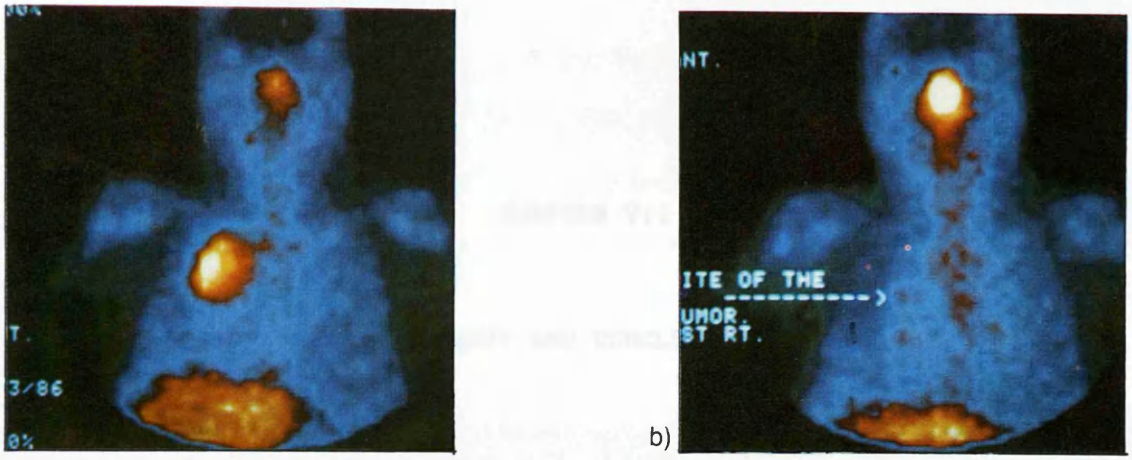

Figure (111): Ga-67 studies a) Pre therapy b) After 50 Gy radiation therapy showed minimal Ga-67 uptake in the site of the tumour.

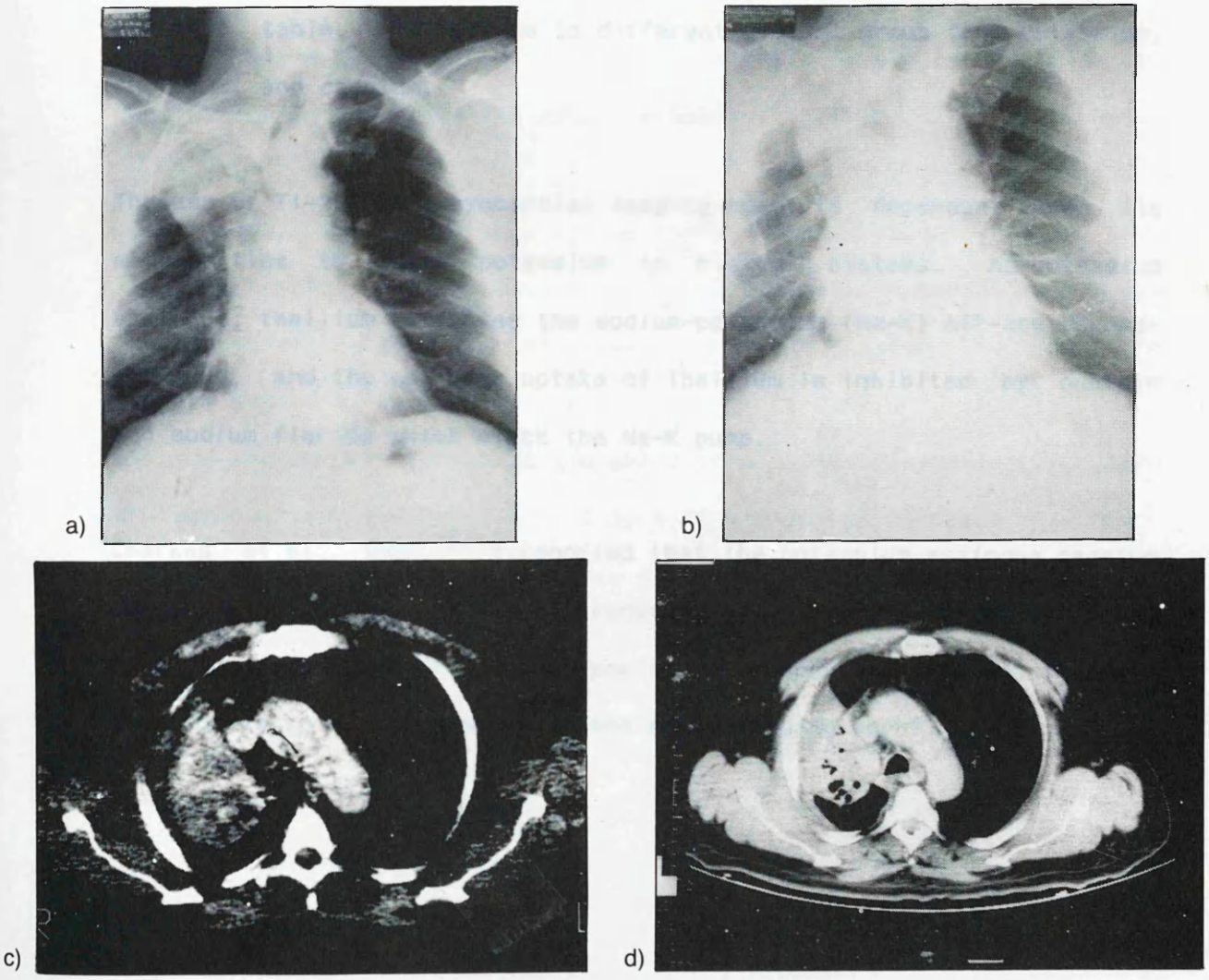

Figure (112): Radiographically a) Chest X-Ray before treatment b) Chest X-Ray after treatment. c & d) C.T. scanning of the same patient pre and post therapy reveal no significant changes in the size of the tumour. The patient showed clinical response to treatment.

CHAPTER VII

SUMMARY AND CONCLUSIONS

Thallium (atomic number 81) is a metallic element of group III A of the periodic table. It belongs to different element group from potassium, rubidium, and caesium.

The use of Tl-201 as a myocardial imaging agent is dependent upon its similarities to ionic potassium in biologic systems. As potassium analogue, thallium activates the sodium-potassium (Na-K) ATP-ase dependent pump, and the cellular uptake of Thallium is inhibited by ouabain and sodium floride which block the Na-K pump.

Charkes et al, 1965,[241] reported that the potassium analogue caesium concentrated in tumour and in introducing thallium-201, Lebowitz et al, 1975 suggested that it might be useful for tumour localization in addition to its role as a myocardial and renal imaging agent.

A number of reports appeared in literature dealing with Tl-201 uptake in tumours. The background of these few reports on Tl-201 tumour imaging led to this work which attempts to evaluate more systematically the role of Tl-201 as a tumour imaging agent in conditions other than Thyroid Carcinoma.

I studied the time course of Tl-201 uptake in various malignant diseases in order to assess the optimal time for tumour imaging with Tl-201. I determined the time of maximal tumour uptake of the tracer, and studied the changes in the tumour to background activity ratios in order to establish the optimal time for tumour imaging with Tl-201.

Ninety-seven patients with histologically proven malignant tumours were examined. After IV injection of 75 MBq of Tl-201, the patient was positioned under a large field of view gamma camera centered over the primary tumour site, two data acquisition were recorded, the first was every 5 seconds for 5 minutes and the second followed immediately every 30 seconds for 55 minutes. Then a 10 minute static image at 4 hours post injection was obtained. Time activity curves over the tumour surrounding background area and the myocardium were generated for both dynamic data acquisition. For each patient the time activity curves were analysed for the time of maximal tumour uptake of Tl-201. The tumour time activity curve was divided by the background curve and the time of maximal tumour to background ratios was estimated in each patient.

The changes in Tl-201 concentration between early and 4 hours delayed images were quantitatively assessed.

The results of this study show that uptake occurs rapidly in tumour with a peak value obtained 10 to 15 minutes post injection in most cases. There were no significant differences in different tumour types. Tumour to background ratios also rapidly attained peak values and remained relatively constant over the hour following injection. No significant changes in tumour to background ratio were found in the 4 hour post injection images compared to 1 hour post injection data. From the data I establish the time for tumour imaging with Tl-201 and is best performed 20 to 60 minutes post injection. Multiple views can be obtained in this period with no significant loss of lesion uptake. I did not find any evidence that the delayed (4 hour) imaging was advantageous because tumour to background ratio is not significantly changed. The short waiting period after injection with Tl-201 clearly offers a major potential advantage over alternative tumour imaging agents such as gallium-67 or radio-labeled monoclonal antibodies which require much longer delays from injection to image.

The mechanism of Tl-201 uptake in tumours has not been established. In the present study this mechanism was evaluated by comparison of the time course of Tl-201 uptake in tumours and myocardium in 88 patients with various malignant disease. The time course of tumour uptake was found to be similar and paralleled myocardial uptake with almost identical times of peak uptake being obtained in tumours and myocardium. The

range of times to peak activity that I found in tumour and myocardium (between 8-20 minutes) was very similar to that reported by Bradley-Moore et al, 1975 [48] for Tl-201 myocardial uptake in an animal model. The similarity in tumours and myocardial Tl-201 uptake may indicate a similar mechanism of tracer uptake. Myocardial Tl-201 uptake is generally accepted to reflect both blood-flow and sodium-potassium ATP-ase dependent pump activity.

Tumours often have abnormal vascularity and Tl-201 may accumulate rapidly in the extra cellular space either due to the increased permeability of new vessels with large intra-capillary pores[189] or simply due to increased vascularity. I was able to study in a single patient the role of blood flow in the initial distribution of Tl-201 by comparison ratios of uptake of Tl-201 and Tc^{99m} microspheres in tumour and normal tissues in a patient with hepatic metastasis from carcinoma colon. Biopsies were taken and samples were analysed using the 3 channel gamma counter and found that the distribution of Tl-201 in tumour tissues is not proportional to the microspheres distribution. I concluded that initial extraction of Tl-201 by tumour cells is not purely a flow dependent process.

I measured the Tl-201 activity under control conditions and after cardiac glycoside "digoxin" intervention which acts as a sodium-potassium pump blocker in non-small cell lung cancer line SK-MES. The data obtained in my in vitro study showed a large decrease in extraction of

Tl-201 by the tumour cell line following incubation with digoxin. This suggests that digoxin blocks the uptake of Tl-201 by the squamous lung carcinoma cells SK-MES.

Results of the studies indicate that Tl-201 uptake in tumours is not purely a flow dependent process. The mechanism of intracellular uptake of Tl-201 demonstrates the viability and metabolic activity of the pathological cells. It appears to be similar to the myocardium by substitution of Tl-201 for potassium in the ATP-ase dependent sodium-potassium pump.

I established the sensitivity and specificity of Tl-201 uptake in a variety of tumours. I carried out a clinical evaluation of this radionuclide in the diagnosis and staging of various common malignancies in evaluation of the Tl-201 chloride to detect primary lung cancer and to demonstrate mediastinal spread of the disease. Two groups of patients with histologically proven lung cancer were examined. Group A consisted of 72 patients with a diagnosis of irresectable lung cancer and group B consisted of 75 patients with potentially resectable lung cancer. In addition, 10 patients with proven benign lung disease were examined. Forty-five of the patients in the radiotherapy group A underwent both thallium-201 and gallium-67 citrate imaging. Tl-201 images were compared with the results of CT scanning and surgical mediastinal exploration.

Tl-201 chloride was accurate in locating 126 out of 147 (86%) patients examined, but disappointing in detecting mediastinal tumour spread (14%). Tl-201 chloride was also found to concentrate in active sarcoidosis (1 case) and active TB (2 cases) giving a specificity of 70%. In the comparison study of Tl-201 and gallium-67 citrate, both radionuclides showed nearly similar sensitivity in detecting primary lung cancer but gallium-67 showed higher sensitivity (57%) in determining mediastinal spread of the disease. Tl-201 scan does not detect primary tumours too small to be seen on chest x-ray. It cannot predict cell type; it is non-specific in uptake and does not prove chest x-ray shadow is malignant. In addition, Tl-201 scan is too insensitive in detecting mediastinal tumour spread.

I examined Tl-201 chloride in detecting primary breast cancer and tumour spread.

Twenty six patients with histologically proven breast cancer were examined. Tl-201 scans were found to be highly sensitive in detecting the primary site of the breast carcinoma, 20 out of 20 malignant primary breast lesions took up Tl-201 focally at the primary site while abnormal uptake was seen in 4 out of 6 patients in recurrent disease.

In patients studied before surgery the sensitivity in predicting nodal involvement was very poor. The sensitivity of Tl-201 scan was also very poor in comparison to the results of palpation in patients who had clinical evidence of nodal spread of disease. It failed to detect any

lesions less than 2.5cm in diameter. Tl-201 scan was not sensitive in demonstrating small distant metastasis especially in ribs, lungs and mediastinal regions.

The data suggest that Tl-201 scan has not proven useful in the local staging of breast cancer.

The application of Tl-201 chloride scans as a staging tool in lymphoma was disappointing because not all tumour sites were visualized with this technique. The data obtained from the study shows that the size of the lesion is critical, the chances of locating a tumour less than 2.5 cm in diameter are negligible even if it is in the supraclavicular or neck region.

In patients with sub-diaphragmatic extension of the disease the location of the tumour is also a problem due to normally high concentration of Tl-201 in abdominal organs.

I evaluated Tl-201 uptake in 18 patients with known brain lesions, 9 patients with primary brain tumour, 2 patients with cerebrovascular accident and 7 patients with brain metastasis. The sensitivity of Tl-201 chloride in detecting brain tumours was very high (100%). The cerebral lesions were well visualized with Tl-201 due to high tumour uptake and low blood background levels in the brain. Using Tl-201 chloride in im-

aging brain lesions we could differentiate between cerebral vascular accident (CVA) which showed no abnormal Tl-201 uptake from patients who had brain tumour which showed intense Tl-201 uptake.

In two patients studied following surgical and radiation therapy, Tl-201 scan showed a smaller and more focal area of increased tracer uptake than CT scanning and Tc^{99m} HM-PAO SPECT studies. According to other investigators Tl-201 scans showed the precise viable residual tissue better than CT and other radio-nuclide studies [247]. All our patients with brain tumour were on steroid therapy. In spite of abnormal Tl-201 uptake seen in all tumours, Tl-201 images does not appear to be affected by concomitant steroid administration. I found Tl-201 to be useful and highly sensitive in detecting brain tumours. It can be performed immediately following injection. It reflects viable tumour burden and does not appear to be affected by concomitant steroid administration.

I have evaluated Tl-201 chloride in detecting bone and soft tissue tumours in 4 patients with primary bone tumour, two patients with primary soft tissue tumours, one patient with bone metastasis and one patient with chronic osteomyelitis. Tl-201 chloride scan was highly sensitive (100%) in detecting primary bone and soft tissue sarcomas and provided accurate delineation of tumour limits as determined by CT scanning. The soft tissue tumours were accurately demonstrated by Tl-201 scans. I concluded that Tl-201 scans are highly sensitive in detecting primary bone tumour, but not much use clinically. Tl-201 scans may be of more value in locating soft tissue sarcomas.

I evaluated Tl-201 chloride in detecting and classifying mass lesions in the liver in twenty one patients with focal defects on the Tc^{99m} tin-colloid scan. The histological diagnosis was known in each patient. With the exception of two patients both with hepatoma, a gallium-67 citrate study was performed immediately following the Tl-201 study. The data obtained from the study shows all the hepatoma patients had similar appearance on Tl-201 and Ga-67 imaging with both tracers showing significant uptake in areas cold on the Tc^{99m} colloid scan. In four of the five patients with metastasis studied the GA-67 and Tl-201 images had similar appearances with failure of the radiopharmaceuticals to concentrate in the cold spot in the colloid scan. In the remaining patients the Tl-201 did not show active uptake in the metastasis, but the GA-67 was positive.

There was discordance between Tl-201 images when compared with GA-67 images. In 7 cirrhotic patients studied, the gallium-67 uptake was homogenous in four patients with liver cirrhosis with no focal defect evident. In three patients the gallium-67 uptake showed focal defects in the area which was cold in Tc^{99m} Tin colloid scan.

Tl-201 images showed multiple focal defects and appearance was similar to that observed with tin colloid liver scan. I concluded that Tl-201 chloride is equally useful to GA-67 citrate for imaging primary

hepatoma. It surpasses gallium imaging in distinction of pseudotumours of the liver. In addition it has the advantage over GA-67 of early imaging.

I investigated the changes in tumour uptake following chemotherapy and radiotherapy and to determine whether such changes are helpful in evaluating tumour response therapy. The role of Tl-201 in predicting tumour responsiveness to anti-tumour therapies has not been fully evaluated if a tumour site is continue to demonstrate uptake after therapy, indicating the presence of metabolic active tissue and possible evidence of the presence of residual viable tumours. A positive Tl-201 scan following treatment of known tumour sites of disease may be used as an index of persistence or recurrence of treated disease. Thirty-three patients with lung carcinoma had received prior lung irradiation. Eleven patients had received prior chemotherapy and 16 patients with brain tumours were receiving steroid therapy at the time of imaging. Sequential Tl-201 images were performed prior to therapy, within one week of completion of therapy and in some patients 5 months after therapy. Tl-201 images were correlated with radiological findings. Using the computer the mean counts in the tumour and background were recorded in pre- and post therapy images, from this data the true counts in the tumour pre- and post therapy were obtained. The percentage of changes of activity in the true counts of primary tumour was obtained which represent the degree of local response after treatment. The results of sequential Tl-201 scan were found to be useful in evaluating patients with malignant disease, especially when the scan was

positive pre-treatment. There was a good correlation between the change in Tl-201 uptake and the change in the primary tumour size after treatment as determined radiographically.

The administration of antineoplastic agents and steroid therapy prior to injection of thallium-201 appeared not to affect the distribution of Tl-201 in the tumour. The changes of uptake of Tl-201 in the tumour site appear highly specific and Tl-201 uptake may provide a useful means of studying tumour viability. However, the use of Tl-201 in measuring the extent of the neoplastic disease has been disappointing due to insensitivity in detecting mediastinal and nodal spread of the disease.

REFERENCES

1. Blumgart, H.L. & Yens, O.C.: Studies on the velocity of blood flow. I The method utilized. Journal of Clinical Investigation (1927); 4:1-13.

2. Blumgart, H.L. & Weiss, S.,: Studies on the velocity of blood flow. II The velocity of blood flow in normal resting individuals and a critique of the method used. Journal of Clinical Investigation (1927); 4:15-31.

3. Lawrence, E.O. & Livingston, M.S.: The production of high speed light ions without the use of high voltages. Physical Review (1932); 40:19-35.

4. Lawrence, E.O. & Cooksey, D.: On the apparatus for the multiple acceleration of light ions to high speeds. Physical Review (1936); 50:1311-1140.

5. Hamilton, J.G.: The rates of absorbtion of the radioactive isotopes of sodium, potassium, chlorine, bromine and iodine in normal human subjects. American Journal of Physiology (1938); 124:667-678.

6. Noonan, T.R., Fenn, W.O. and Haege, L.: The distribution of injected radioactive potassium in rats. American Journal of Physiology (1941); 132:474-488.

7. Burch, G.E., Threefoot, S.A. and Ray, G.T.: The rate of disappearance of Rb ^{86} from the plasma, The biological decay rates of Rb ^{86} and the applicability of Rb ^{86} as a tracer of potassium in man with and without chronic congestive failure. Journal of Laboratory and Clinical Medicine (1954); 45:371-394.

8. Love, W.D. & Burch, G.E.: A comparison of potassium ^{42}, rubidium ^{86} and caesium ^{134} as tracers of potassium in the study of cation metabolism of human erythrocytes in vivo. Journal of Laboratory and Clinical Medicine (1953); 41:351-362.

9. Carr, E.A., Beierwaltes, W.H., Patno, M.E., Bartlett, J.D. & Wegst, A.V.: The detection of experimental myocardial infarcts by photoscanning. American Heart Journal (1962); 64: 650-660.

10. Carr, E.A., Gleason, G., Shaw, J. & Krontz, B.: The direct diagnosis of myocardial infarction by photoscanning after administartion of caesium-131. American Heart Journal (1964); 68:627-636.

11. McKillop, J.H.: Is Thallium-201 imaging clinically valuable in coronary artery disease?. CRC Critical Review in Diagnostic Imaging (1982); 18:167-195.

12. Verani, M.S.: Thallium-201 Myocardial Scintigraphy: An Overview. Clinical Nuclear Medicine (1983); 8:276-287.

13. Lebowitz, E., Greene, M.W., Fairchild, R., Bradley-Moore, P.R., Atkins, H.L., Ansari, A.N., Richards, P. & Belgrave, E.: Thallium-201 for medical use I. Journal of Nuclear Medicine (1975); 16:151-155.

14. Mills, S.L., Basmadjian G.P. and Ice, R.D.: Radiopharmaceuticals used in myocardial imaging. Journal of Pharmaceutical Sciences (1981); 70:1-12.

15. Gerlings, E.D. Miller, D.T. & Gilmore, J.P.: Oxygen availability: a determinant of myocardial potasstium balance. American Journal of Physiology (1969); 216:559-562.

16. Poe, N.D.: Comparative myocardial uptake and clearance characteristics of potassium and cesium. Journal of Nuclear Medicine (1972); 13:557-560.

17. Poe, N.D.: Rationale and radiopharmaceuticals for myocardial imaging. Seminars in Nuclear Medicine (1977); 7:7-14.

18. Crookes, W.: Preliminary researches on thallium. Proceedings of the Royal Society (1862); 12:150-159.

19. Kawana, M., Krizek, H., Porter, J., Latrhrop, K.A., Charleston, D. & Harper, P.V.: Use of ^{199} T1 as a potassium analog in scanning. Journal of Nuclear Medicine (1970); 11:333 (abstarct).

20. Belgrave, E. & Lebowitz, E.: Development of ^{201} Tl for medical use. Journal of Nuclear Medicine (1972); 13:781 (abstract).

21. Wackers, F.J.Th. & de Jong, R.B.J.: Myocardial imaging with thallium-201, Medicamundi (1976); 21:103-113.

22. Atkins, H.L., Budinger, T.F., Lebowitz, E., Ansari, A.N., Greene, M.We in front of the lateral process close to the lateral margin of the long plantar ligament.

23. Botvinick, E.H., Dunn, R.F. Hattner, R.S., and Massic B.M: A consideration of factors affecting the diagnostic accuracy of Thallium-201 myocardial perfusion scintigraphy in detecting coronary artery disease. Seminars in Nuclear Medicine (1980(; X(2):157-167.

24. Botvinick E.H., Shames D.M.: Nuclear cardiology: Clinical applications. Baltimore, Williams & Wilkins, 1979. pp 1-8.

25. Johnstone D.E.., Wackers F.J.Th., Berger H.J., Kelly, P.B., Gottschalk M.J., and Zaret B.L.: Effect of patient positioning on left lateral thallium-201 myocardial images. J Nucl Med (1979); 20: 183-188.

26. Mullins, L.J. & Moore R.D.: The movement of thallium ions in muscle. Journal of General physiology (1960); 43:756-773.

27. Gehring, P.J. & Hammond, P.M.: The uptake of thallium by rabbit erythrocytes. Journal of Pharmacology and Experimental Therapeutics (1964); 145: 215-221.

28. Gehring, P.J. & Hammond, P.B. : The inter-relationship between thllium and potassium in animals. Journal or Pharmacology and Experimental Therapeutics (1967); 155: 187-201.

29. Britten, J.S. & Blank, M.: Thallium ectivation of the (Na+ - K+) activated ATP-ase of rabbit kidney. Biochemica et Biophysica Acta (1968); 159: 160-166.

30. Gelbert A., Doherty, P.W., McLaughlin P.R., et al: Na+ - K+ ATPase and coronary blood flow as determinants of Tl-201 uptake by ischemic myocardium. circulation (1976); 54:11-70 (abstract).

31. Cannon, P.J., Weiss, M.B. & Casarella, W.J.: studies of regional myocardial blood flow: results in patients with left anterior descending coronary artery disease. Seminars in Nuclear Medicine (1976); 6: 279-304.

32. Welch, H.F., Strauss, H.W. & Pitt, B.: Extraction of thallium-201 by the myocardium. Circulation (1977); 56: 188-191.

33. Pohost G.M., Zir L.M., Moore R.H., Mckusick K.A, Guiney T.E., Beller, G.A.: Differentiation of transiently ischamic from infarcted myocardium by serial imaging after a single dose of thallium-201. Circulation (1977); 55: 294-302.

34. Grunwald A.M., Watson D.D., Holzgrefe H.H., Irving J.F., Beller G.A.: Myocardial thallium-201 kinetics in normal and ischamic myocardium. Circulation (1971); 64(3): 610-618.

35. Ronald D, Carlin and Kung-Ming Jan.: Mechanism of thallium extraction in pump perfused canine hearts. Journal of Nuclear Medicine (1985); 26: 165-169.

36. Prokop, E.K., Strauss, H.W., Shaw, J., Pitt, B. & Wagner, H.N.: Comparison of regional myocardial perfusion determined by ionic potassium to that determined by microspheres. Circulation (1974); %0: 978-984.

37. Strauss, H.W., Harrison, K., Langan, J.K., Lebowitz, E. & Pitt, B.: Thallium 201 for myocardial imaging: Relation of thallium-201 to regional myocardial perfusion. Circulation (1975); 51: 641-645.

38. Nielson A, Morris K.G., Murdock R.H., Bruno F.P., Cobb F.R.: Linear relationship between distribution of thallium-201 and blood flow in ischemic and nonischemic myocardium during exercise. Circulation (1980); 61: 797-801.

39. Sapirstein, L.A.: Fractionation of the cardiac output of rats with isotopic potasium. Circulation Research (1956); 4: 689-692.

40. Maseri, A.: Pathophysiologic studies of the pulmonary and coronary circulation in man. Am J Cardiol (1976); 38(6): 752-760.

41. Maseri, A., Mancini, P., Continic, et al: Method for the estimate of total coronary flow by Tc 99m tagged albumin microspheres. J Nucl Med (1971); 15:58-60.

42. Donato, L., Bartholomei, G. & Giordani, R.; Evaluation of myocardial blood perfusion in man with radioactive potassium or rubidium and external counting circulation 91964); 29: 195-203.

43. Zierler, K.L.: Equations for measuring blood flow by external monitoring of radioisotopes. Circulation Research (1965); 16: 309-321.

44. Nishiyama, H., Adolph, R.J., Gaber, M., Lukes, S.J., Franklin,D., and williams. C .: Effect of coronary blood flow on Thallium-201 uptake and washout. Circulation

45. Selwyn, A.P., Welman, E., Pratt, T.A., Clark, J., McArther C, and Lavender J.P.: The interpretation of Thallium-201 cardiac scintigrams. Studies in experimental ischemic heart disease in dogs. Circulation Research (1978); 43: 287-293.

46. Strauer, B.E., Berger, S., and Bull U.: Multifactorial determination of Thallium-201 uptake of the heart: an experimental study concerning the influence of ventricular mass, perfusion and oxygen consumption. Basic Research Cardiology (1978); 73: 298.

47. Pohost G.M., Alpert N.M., Ingwall J.S., and strauss W.: Thallium redistribution: Mechanisms and clinical utility. Seminars Nucl Med (1980); X(1):70-93.

48. Bradley-Moore, P.R., Lebowitz, E., Greene M.W., Atkins, H.L. & Ansari A.N.: Thallium-201 for medical use. II: Biologic behaviour. Journal of Nuclear Medicine (1975); 16:156-160.

49. Schelbert, H.R., Henning H., Rigo, P. Chauncey, D., O'Rourke, R.A> & Ashburn, W.L.: Consideration of 201 Tl as myocardial radionuclide imaging agent in man. Investigative Radiology (1976); 11:163-171.

50. Hamilton, G.W., Narahara, K.A., Yee, H., Ritchie, J.L., Williams, D.L. & Gould, K.L.: Myocardial imaging with thallium-201: Effect of cardiac drugs on myocardial images and absolute tissue distribution. Journal of Nuclear Medicine (1978); 19:10-16.

51. Strauss. H.W., & Pitt, B.: Thallium-201 as a myocardial imaging agent. Seminars in Nuclear Medicine (1977); 7:49-58.

52. Nishiyama, H., Sodd, V.J., Adolph, R.J., Saenger, E.L., Lewis, J.T. & Gabel, H.: Intercomparsion of myocardial imaging agents 201 Tl, 129Cs, 43K, 81Rb. Journal of Nuclear Medicine (1976); 17:880-889.

53. Kambara, H., Ishii Y, Kadota K, Yonekura Y, Torizuka K and Kuwai C.: Thallium-201 myocardial scintography: Fractional uptake by the myocardium at rest and during excersice in patients with coronary artery disease and Hypertrophic cardiomyopathy. Europ journal of Nuclear Medicine (1980); 5: 493-498.

54. Pitt, B. & Strauss, H.W. Myocardial imaging in the noninvasive evaluation of patients with suspected heart disease. American Journal of Cardiology (1976); 37: 797-806.

55. Abbate, A., Maseri, A., Biagini, A., Parodi, O., Severi. S. & Michelassi S.: study of early and late myocardial Kinetics of 201Tl in man at rest. Presented at Symposium on "Radionuclide in the diagnosis of myocardial infarction", Lund, Sweden, June 1977.

56. Strauer, B.E., Buller, and Burger, S.: Clinical studied concerning the determination of myocardial Thallium-201 uptake. Basic Res Cardiol (1978); 73: 365-379.

57. Domenech, R.J. Hoffman, J.I.E., Noble, M.I.M., Saunders, K.B., Henson J.R. & Subljanto, S.: Total and regional coronary blood flow measured by radioactive microspheres in conscious and anaesthetised dogs. Circulation Research (1969); 25: 581-596.

58. Griog D, The George E. Brown Memorial lecture. Physiclogy of the coronary circulation. Circulation 1963, 27, 1128-1137.

59. Gould K.L., Westcott, R.J., Albro P.C., and Hamilton G.W.: Noninvasive assessment of coronary stenosis by myocardial imaging during pharmacological coronary vasidilation, II Clinical Methology and Feasibility. Am J Cardiol (1978); 41: 279-287.

60. Albro, P.C., Gould K.L., Westcott, R.J. & Hamilton, G.W. : Myocardial perfusion imaging during pharmacologic coronary vasodilatation in assessing coronary disease. American Journal of Cardiology (1978); 41: 378 (abstract).

61. Harris D.N., Taylor N.N., Ackery D.M., and Conway N.: Imaging for myocardial ischemia with dipyridamole. Tl-201 and gated wall motion. Nucl Med Comm; 1980; 1:74-79.

62. Hetzel, K.R., Westerman, B.R., Quinn, J.L. III., Meyers, S. & Barresi, V.: Myocardial uptake of thallium-201 augmented with bicarbonate: concise communication. Journal of Nuclear Medicine (1977); 18:24-25.

63. Cook, D.J., Bailey, I., Strauss, H.W., Rouleau, J., Wagner, H.N. Jr., & Pitt B.: Thallium-201 for myocardial imaging: appearance of the normal heart. Journal of Nuclear Medicine (1976); 17:583-589.

64. Oster, Z.H., Strauss, H.W., Harrison, K., Burns, H.D. & Pitt B.: Thallium-201 distribution in the thyroid: relationship to thyroidal trapping function. Radiology (1978); 126:733-734.

65. Johnson, S.R., Wallace, E.Z., Bitton, R.N., Watkins, J. and McGann, P.: J.N. Medicine (1984); 25:20 (abstract).

66. Bingham, J.B., McKusick, K.A., Strauss, H.W., Boucher, C.A., Pohost, G.M.: Influence of coronary artery disease on pulmonary uptake of Thallium-201. Am J Cardiol (1980); 46:821-826.

67. Narahara, K.A., Hamilton, G.W., Williams, D.L., Gould, K.L.: Myocardial imaging with thallium-201: an experimental model for analysis of the true myocardial and background image components. J Nucl Med (1977); 18:781-786.

68. Boucher, C.A., Zir, L.M., Beller, G.A., Okada, R.D., Mekusick, K.A., Strauss H.W., Pohost, G.M.: Increased lung uptake of thallium-201 during excercise implications in patients with coronary artery disease. Am J Cardiol (1980); 46:189-196.

69. Kushner, F.G., Okada, R.D., Kirshenbaum, H.D., Boucher, C.A., Strauss, H.W., Pohost, G.M.: Lung thallium-201 uptake after stress testing in patients with coronary artery disease. Circulation (1981); 63:341-347.

70. Gibson, R.S., Watson, D.D., Carabello, B.A., Holt, N.D., Beller, G.A.: Clinical implications of increased lung uptake of Thallium-201 during exercise scintigraphy 2 weeks after myocardial infarction. Am J Cardiol (1982); 49:1586-1593.

71. Brown, K.A. and Okada, R.D.: Significance of Thallium-201 lung uptake after radionuclide excersie stress testing. Practical Cardiology (1984); 10:68-77.

72. Bingham, J.B., Strauss, H.W., Pohost, G.M., McKusick, K.A.: Mechanism of lung uptake of thallium-201. Circulation (1978); 58(11):11:62 (abstract).

73. Minamiji, K., Maede, K., Nakashima, Y., Kajiya, T., Ohmori, Y., Fukuzaki, H.: Assessment of left ventriculur dysfunction by thallium-201 lung uptake during excercise in coronary artery disease. Jpn Circ J (Japan) (1983); 47:381-390.

74. Christenson, J., Larsson, I., Svensson, S-E., & Westling , H.: Distribution of intravenously injected 201 thallium in the legs during walking. A new test for assessing arterial insufficiency in the legs. European Journal of Nuclear Medicine (1977); 2:85-88.

75. Feller, P.A., & Sodd, V.J.: Dosimetry of four heart imaging radionuclides ^{43}K, ^{81}Rb, ^{129}Cs and ^{201}Tl. Journal of Nuclear Medicine (1975); 16:1070-1075.

76. Budinger, T.F. & Rollo, F.D.: Physics and instrumentation. Progress Cardiovascular Diseases (1977); 20:19-53.

77. Adelstein, S.J. & Maseri, A.: Radio-indicators for the study of the heart: Principles and applications. Progress Cardiovascular Diseases (1977); 20:3-17.

78. Munch, J.C.: Human thallotoxicosis. Journal of the American Medical Association (1934); 102:1929-1934.

79. Reed, D., Crawley, J., Faro, S.N., Pieper, S.J. & Kurland, L.T.: Thallotoxicosis. Acute manifestations and sequelae. Journal of the American Medical Association (1963); 183: 516-522.

80. Cavanagh, J.B., Fuller, N.H., Johnson, H.R.M. & Rudge, P.: The effects of thallium salts with particular reference to the nervous system changes. Quarterly Journal of Medicine (New Series) (1974); 43:293-319.

81. Browning, E.: Toxicity of Industrial Metals. Ch. 39, Thallium London: Butterworths (1961); 282-287.

82. Cannon, P.J., Dell, R.B. & Dwyer, E.M. Jr.: Regional myocardial perfusion rates in patients with coronary artery disease. Journal of Clinical Investigation (1972); 51:978-994.

83. Schwartz, L., Froggart, G., Corvey, H.D., Taylor, K. & Morch, J.E.: Measurement of left anterior descending coronary arterial blood flow. Technique, methods of blood flow analysis and correlation with angiography. American Journal of Cardiolog (1973); 32:679-685.

84. Zaret, B.L., Martin, N.D., McGowan, R.L., Strauss, H.W., Wells, H.P. & Flamm, M.D.: Rest and exercise potassium-43 myocardial perfusion imaging for the noninvasive evaluation of aortocoronary bypass surgery. Circulation (1974); 49: 688-695.

85. Strauss, H.W., Zaret, B.L., Martin N.D., Well, H.P. and Flamm M.D.: Noninvasive evaluation of regional myocardial perfusion with potassium technique in patients is the exercise induced transient myocardial ischaemia. Radiology (1973); 108:85-90.

86. Bailey, I.K., Griffith, L.S.C., Rouleau, J., Strauss, H.W., & Pitt, B.: Thallium-201 myocardial perfusion imaging at rest and during exercise. Comparative sensitivity to electrocardiography in coronary artery disease. Circulation (1977); 55:79-87.

87. Wackers, F.J. Th., Sokole, E.B., Samson, G., vd Schoot, J.B., Lie, K.I., Liem, K.L. & Wellens, H.J.J.: Value and limitations of thallium-201 scintigraphy in the acute phase of myocardial infarction. New England Journal of Medicine (1976); 295:1-5.

88. Wackers, F.J. Th., Becker, A.E, Samson, G., Sokole, E.B., vd Schoot, J.B., Vet, A.J.T.M., Lie, K.I., Durrer, D. & Wellens, H.: Location and size of acute transmural myocardial infarction estimated from thallium-201 scintiscans. A clinicopathological study. Circulation (1977); 56:72-78.

89. Wackers, F.J., Lie, K.I., Sokole, E.B., Res J, van der Scott, J.S., Durrer, D.: Prevelance of right ventricular involvement in inferior wall infarction assessed with myocardial imaging with thallium-201 and technitium-99-pyrophosphorate. Am J Cardiol (1978); 42:358-362.

90. Blood, D.K., McCarthy, D.M., Sciacca, RR, Cannon, P.J.: Comparison of single-dose and double-dose thallium-201 myocardial perfusion scintigraphy for detection of coronary artery disease and prior myocardial infarction. Circulation (1978); 58:777-778.

91. Schwartz, J.S., Ponto, R., Carlyle, P., Forstrom, L., Cohn, J.N.: Early redistribution of thallium-201 after temporary ischaemia. Circulation (1978) 57:332-335.

92. Beller, G.A., & Pohost, G.M.: Time course and mechanism of resolution of thallium-201 defects after trasnient myocardial ischaemia. American Journal of Cardiology (1978); 41: 379 (abstract).

93. Grunwald, A.M., Watson, D.D., Holzgrefe, H.H., Irving, J.F., Beller, G.A.: Myocardial thallium-201 kinetics in normal and ischaemic myocardium. Circulation (1981); 64:610-618.

94. Khaw, B.A., Strauss, H.W., Pohost, G.M., Fallor, J.T., Katus, H.A., Haber, E.: Relation of immediate and delyaed thallium-201 distribution to localization of iodine-125 antimyosin antibody - acute experimental myocardial infarction. Am J Cardiol (1983); 51:1428-1432.

95. Iskandrian, A.S., Wasserman, L., Segal, B.L..: Thallium-201 myocardial scintigraphy, advantages and limitation. Arch Intern Med (1980); 140:320-327.

96. McLaughlin, P.R., Martin, R.P., Doherty, P., Daspit, S., Coris, M., Haskell, W., Lewis, S., Kriss, J. & Harrison, D.: Reproducibility of thallium-201 myocardial imaging. Circulation, 1977, 55: 497-503.

97. Berger, B.C., Watson, D.D., Taylor, G.J., Graddock, G.B., Martin, R.P., Teates, C.D., Beller, G.A.: Quantitative thallium-201 exercise scinetigraphy for detection of coronary artery disease. J Nucl Med (1981); 22:585-593.

98. Berger, B.C., Watson, D.D., Burwell, L.R., Corsby, I.K., Wellons, H.A., Teates, C.D., Beller, G.A..: Redistribution of thallium at rest in patients with stable and unstable angina and the effect of coronary artery bypass surgery. Circulation (1979); 60:1114-1124.

99. Alderson, P.O., Wagnar, H.N., Gomez-Mociras, J.J., Rehn, T.Q. Becker, L.C., Douglas, K.H., Manspeaker, H.F., and Schindledecker, G.R.: Simultaneous detection of myocardial perfusion and wall motion abnormality by cinematic T1-201 imaging. Radiology (1978); 127:531-533.

100. McKillop, J.H., Fawcett, H.D., Baumart, J.E., McDougall, I.R., DeBusk, R.F., Harrison, D.C. and Goris, M.L.: ECG gating of Thallium-201 myocardial images, effect on detection of ischaemic heart disease. J Nucl Med (1981); 22:219-225.

101. Vogel, R.A., Kirch, D.L., LeFree, M.T., Ramivates, J.O., Jensen, D.P., Steele, P.P.: Thallium-201 myocardial perfusion scintigraphy: results of standard and multi-pinhole tomographic techniques. Am J Cardiol (1979); 43:787-793.

102. Vogel, R.A., Kirch, D.L., LeFree, M.T. and Steele, P.: A new method of multiplanar emission tomography using a seven pinhole collimator and an Anger scinlitation camera. J Nucl Med (1978); 19:648-654.

103. Francisco, D., Go, R., Kirk, O.V., Erhardt, J., Marcus, M.: Tomographic thallium-201 perfusion scintigrams following maximal coronary vasodilation with dipyridamole. Circulation 60 (suppl II), 1979, II-174 (abstract).

104. Ritchie, J.L., Williams, D.L., Caldwell, J.H., Stratton, J.R., Harp, G.D., Vogel, R.A., Hamilton, G.W.: Seven-pinhole emission tomography with thallium-201 in patients with prior myocardial infarction. J Nucl Med (1981); 22:107-112.

105. Budinger, T.E.: Physical attributes of single photon tomography. J Nucl Med (1980); 21:579-592.

106. Murphy, P.H., Thompson, W.L., Moore, M.L., Burdine, J.A.: Radionuclide computed tomography of the body using routine radiopharmacuticals. I system characterization. J Nucl Med (1979); 20:102-107.

107. Tamaki, N., Mukai, T., Ishii, Y., Yonekura, Y., Kambara, H., Kawai, C., Torizaka, K.: Clinical evaluation of thallium-201 emission myocardial tomography using a rotating gamma camera: comparison with seven-pinhole tomography. J Nucl Med (1981); 22:849-855.

108. Maublant, J., Cassagnes, J., Le Jeune, S.S., Mestas, D., Veyre, A., Juliut, H., Mcyniel, G.: Comparison between emission tomography and conventional scintigraphy in the detection of myocardial infarction. J Nucl Med (1981); 22:79 (abstract).

109. Nohara, R., Kambara, H., Zuzuki, Y., Tanaki, S., Kadota, K., Kawai, C., Tanaki, N. and Torizuka, K.: Stress scintigraphy using single-photom emission computed tomography in the evaluation of coronary artery disease. Am J Cardio (1984); 53:1250-1254.

110. Fletcher, J.W., Walter, K.E., Witztum, K.F., Daly, J.L., Herbig, F.K., Meuller, H.S., Donati, R.M.: Diagnosis of coronary artery disease with ^{201} Tl. Computer analysis of myocardial perfusion images. Radiology (1978); 128:423-427.

111. Verani, M.S., Jhingran, S., Attar, M., Rizk, A., Quinones, M.A., Miller, R.R.: Poststress redistribution of thallium-201 in patients with coronary artery disease, with and without prior myocardial infarction. Am J Cardiol (1979); 43:1114-1122.

112. Burow, R.D., Pond, M., Schafar, A.W., Becker, L.: "Circumferential profiles": a new method for computer analysis of thallium-201 myocardial perfusion images. J Nucl Med (1979); 20:771-777.

113. Leppo, J., Rosenkrantz, J., Rosenthal, R., Bontemps, R., Yipintson, T.: Quantitative thallium-201 redistribution with a fixed coronary stenosis in dogs. Circulation (1981); 63: 632-639.

114. Nichols, A.B., Weiss, M.B., Sciacca, R.R., Cannon, P.J., Blood, D.K.: Relationship between segmental thallium-201 uptake and regional myocardial blood flow in patients with coronary artery disease. Circulation (1983); 68:310-320.

115. Goris, M.L., Daspit, S.G., McLaughlin, P., Kriss, J.P.: Interpolative background subtraction. J Nucl Med (1976); 17: 744-747.

116. McKillop, J.H., Murray, R.G., Turner, J.G., Bessent, R.G.: A comparison of visual and semiquantitative analysis of stress thallium-201 myocardial images in patients with suspected ischaemic heart disease. Radiology (1980); 136:187-190.

117. Lenaers, A., Block, P., van Thiel, E., Lebedella, M., Baccquevort, P., Erbsmann, F., Ermanns, A.M.: Segmental analysis of Tl-201 stress myocardial scintigraphy. J Nucl Med (1977); 18:509-516.

118. Walnwright, R.J., Maisey, M.N., & Sowton, E.: Quantitative thallium scintigraphy in the assessment and follow up of coronary artery bypass grafts. Journal of Nuclear Medicine (1977); 18:594 (abstract).

119. Meade, R.C., Bamrah, V.S., Horgan, J.D., Ruetz, P.P., Kronenwetter, C., Yeh, E.L.: Quantitative methods in the evaluation of thallium-201 myocardial perfusion images. J Nucl Med (1978); 19:1175-1178.

120. McKillop, J.H., Turner, J.G., Gray, H.W., Bassent, R.G., Greig, W.R.: Clinical value of delayed thallium-201 myocardial imaging in suspected acute myocardial infarction. Br Heart J (1978); 40:870-873.

121. Garcia, E., Maddahi, J., Berman, D., Waxman, A.: Space/time quantitation of thallium-201 myocardial scintigraphy. J Nuc Med (1981); 22:309-317.

122. Maddahi, J., Garcia, E.V., Berman, D.S., Waxman, A., Swan, H.J.C., Forrester, J.: Improved non-invasive assessment of coronary artery disease by quantitative analysis of regional stress myocardial distribution and washout of thallium-201. Circulation (1981); 64:924-935.

123. Massie, B., Botvinick, E.H., Brundage, B.H.: Correlation of thallium-201 scintigrams with coronary anatomy: factors affecting region by region sensitivity. Am J Cardiol (1979); 44:616-622.

124. McKillop, J.H., Murray, R.G., Turner, J.G., Bessent, R.G., Lorimer, A.R., Grieg, W.R.: Can the extent of coronary artery disease be predicted from thallium-201 myocardial images? J Nucl Med (1979); 20:715-719.

125. Gould, K.L.: Quantitative imaging in nuclear cardiology. Circulation (1982); 66:1141-1146.

126. Hamilton, G.W., Trobaugh, G.B., Ritchie, J.L. et al: Myocardial imaging with intravenously injected Thallium-201 in patients with suspected coronary artery disease. Analysis of technique and correlation with electrocardiographic, coronary anatomic and ventriculographic findings. Am J Cardiol (1977); 347-354.

127. Botvinick, E.H., Taradash, M.R., Shames, D.M. and Parmley, W.M.: Thallium-201 myocardial perfusion scintigraphy for the clinical clarification of normal, abnormal and equivocal electrocardiographic stress tests. Am J Cardiol (1978); 41: 43-51.

128. Leppo, J., Yipintsoi, T., Blankstein, R. et al: Thallium-201 myocardial scintigraphy in patients with tripple vessel disease and ischaemic exercise stress tests. Circulation (1979); 59:714-721.

129. Verani, M.S., Marcus, M.L., Spoto, G., Rossi, N.P., Erhardt, J.C. and Razzak, M.A.: Myocardial perfusion imaging in the evaluation of saphenous aorto-coronary bypass graft surgery. J Nucl Med (1978); 19:1032-1035.

130. Trogaugh, G.B., Wackers, F.J., Sokole, E.B., Deroven, T.A., Ritchie, J.L., Hamilton, G.W.: Thallium-201 myocardial imaging: An interinstitutional study of observer variability. J Nucl Med (1978); 19:359-363.

131. Zir, L.M., Miller, S.W., Dinsmore, R.E.: Interobserver variability in coronary angiography. Circulation (1976); 53: 627-632.

132. Chairman, B.R., McMots, H., Bristow, J.D. et al: Objective and subjective analysis of left ventricular angiograms. Circulation (1975); 52:420-425.

133. Yervshalmy, J.: The statistical assessment of the varibility in observer perception and description of roentgenographic pulmonary shadows. Radiol Clin North Am (1969); 7:381-392.

134. Nishiyama, H., Lewis, J.T., Ashare, A.B. et al: Interpretation of radionuclide liver images: Do training and experience make a different? J Nucl Med (1975); 16:11-16.

135. Okada, R.D., Boucher, C.A., Strauss, H.W., Pohost, G.M.: Exercise radionuclide imaging approaches to coronary artery disease. Am J Cardiol (1980); 46:1188-1204.

136. Amsterdam, E.A., Joye, J., Glass, E., Berman, D., DeNardo, G., Mason, D.T.: Accuracy of thallium-201 myocardial exercise scintingraphy to detect coronary artery disease in patients with abnormal resting electrocardiograms. Clin Res (1979); 27:147 (abstract).

137. Rehn, T., Griffith, L., Achuf, S., Bulkley, B., Pond, M., Becker, L.: Rest and stress thallium-201 imaging in left main coronary disease: Sensitive but not specific. Am J Cardiol (1978); 41:413 (abstract).

138. Rigo, P., Becker, L.C., Griffith, L.S.L. et al.: Influence of coronary collateral vessels on the results of thallium-201 myocardial stress imaging. Am J Cardiol (1979); 44:452-458.

139. Pohost, G.M., Boucher, C.A., Zir, L.M., McKusick, K.A., Beller, G.A., Strauss, H.W.: The thallium stress test: the qualitative aproach revisited Circulation (1979); 59- 60: Suppl II:II-49 (abstract).

140. Bruscke, A.V.G., Proudfit, W.L. and Sones, F.M.: Progress study of 590 consecutive cases of coronary disease followed 5-9 years. I Arteriographic correlations. Circulation (1973); 47:1147-1153.

141. Rigo, P., Bailey, I.K., Griffith, L.S.C., Pitt, B., Burrow, R.D., Wagner, H.N. and Becker, L.C.: Value and limitations of segmented analysis of stress thallium myocardial imaging for localization of coronary artery disease. Circulation (1980); 61:973-81.

142. Lenaers, A.: Thallium-201 myocardial perfusion scintigraphy during rest and exercise. Cardiovasc Radiol (1979); 2:195-202.

143. Dash, H., Massie, B.M., Botvinick, E.H., Brundage, B.H.: The noninvasive identification of left main and three-vessel coronary artery disease by myocardial stress perfusion scintigraphy and treadmill exercise electrocardiography. Circulation (1979); 60:276-84.

144. Beller, G.A., Watson, D.D., Berger, R.D., Taylor, G.J.: Detection of multivessel disease by exercise thallium-201 scintigraphy Am J Cardiol (1980); 45:482 (abstract).

145. Garcia, E., Maddahi, J., Berman, D.S., Waxman, A., Swan, H.J.C.: A comprehensive method for space-time quantitation of sequential thallium-201 myocardial scintigrams. Circulation (1980); 62:Suppl III:III-75 (abstract).

146. Maseri, A., Parodi, O., Severi, S., Pesola, A.: Transient transmural reduction of myocardial blood flow, demonstrated by thallium-201 scintigraphy, as a cause of varient angina. Circulation (1976); 54:280-288.

147. Uthurralt, N., Davis, G.J., Parodi, O. et al: Comparative study of myocardial ischaemia during angina at rest and on exertion using thallium-201 scintigraphy. Am J Cardiol (1981); 48:410-714.

148. Fuller, C.M., Raizner, A.E., Chahine, R.A. et al: Exercise-induced coronary arterial spasm: angiographic demonstration. documentation of ischaemia by myocardial scintigraphy and results of pharmacologic intervention. Am J Cardiol (1980); 46:500-506.

149. Wackers, F.J., Schoot, J., Sokole, E.B., Samson, G., Niftrik, G., Lie, K.I., Durrer, D. and Wellens H,J.: Noninvasive visulization of acute myocardial infarction in man with thallium-201. Br Heart J (1975); 37:741-745.

150. Wackers, F.J., Lie, K.I., Liem, K.L., Sokole, E.B., Samson, G., van der Schoot, J. and Durrer, D.: Potenstial value of thallium-201 scintigraphy as means of selecting patients for the coronary care unit. Br Heart J (1979); 41:111-117.

151. Silverman, K.J., Becker, L.C., Bulkley, B.H. et al: Value of early thallium-201 scintigraphy for predicting mortality in patients with acute myocardial infarction. Circulation (1980); 61:996.

152. Turner, J.D., Schwartz, K.M., Logic, J.R. et al.: Detection of residiual jeopardized myocardium 3 weeks after myocardial infarction by exercise testing with thallium-201 myocardial scintigraphy. Circulation (1980); 61:729.

153. McKillop, J.H., Billingham, M., ~~Schooder~~ Schroeder, J.S. and McDougall, I.R.. Correlation of an abnormal rest Tl-201 myocardial image; pathological findings in cardiac transplant recipients. Eur J Nucl Med (1982); 7:243-247.

154. McCarthy, D.M., Blood, D.K., Sciacca, R.R. and Cannon, D.J.: Single dose myocardial perfusion imaging with thallium-201: application in patients with nondiagnostic stress tests. Am J Cardiol (1979); 43:899-906.

155. Tweddel, A.C., Pearson, D., McKillop, J.H. and Murray, R.G.: Stress thallium-201 scintigraphy in patients with equivocal exercise electrocardiograms. Scott Med J (1980); 25:174 (abstract).

156. Carlilo, A.P., Marks, D.S., Pickard, S.D., Khaja, F. and Goldstein, S.: Correlation of exercise ^{201} Thallum myocardial scan with coronary arterlograms and the maximal exercise test. Chest (1978); 73:321-326.

157. Gaffney, F.A., Wohl, A.J., Blomquist, C.G., Parkey, R.W. and Willerson, J.T.: Thallium-201 myocardial perfusion studies in patients with the valve prolapse syndrome. Am J Med (1978); 64:21-26.

158. Padmanabhan, V., Margouleff, D., Binder, A., Morrison, J., Pizzardlo, R. and Gulotta, S.: Thallium-201 myocardial imaging during exercise in mitral valve prolapse. Circulation (1977); 56:217 (abstract).

159. Stanlloff, H.M., Huckell, V.F., Morch, J.E., Buda, A.J., Feiglin, D.H., Wigle, D. and McLaughlin, P.R.: Abnormal myocardial perfusion defects in patients with mitral valve prolapse and normal coronary arteries. Am J Cardiol (1978); 41:433 (abstract).

160. Tresch, D.D., Soin, J.S., Siegel, R., Love, M. and Keelan, M.H.: Mitral valve prolapse-evidence for a myocardial perfusion abnormality. Am J Cardiol (1978); 41:441 (abstract).

161. Massie, B., Botvinick, E.H., Shames, D., Taradash, M., Werner, J. and Schiller, N.: Myocardial perfusion scintigraphy in patients with mitral valve prolapse. Its advantage over stress electrocardiography in diagnosing associated coronary artery disease and its implications for the aetiology of chest pain. Circulation (1978); 57:19-26.

162. Klein, G.J., Kostuk, W.J., Boughner, D.R. and Chamberlain, M.J.: Stress myocardial imaging in mitral valve leaflet prolapse syndrome. Am J Cardiol (1978); 42:746.

163. Greeberg, B.H., Hart, R., Botvinick, E.H., Werner, J.A., Brundage, B.H., Shames, D.M., Chaterjer, K. and Parmley, W.W.: Thallium-201 myocardial perfusion scintigraphy to evaluate patients after coronary bypass surgery. Am J Cardiol (1978); 42:167-176.

164. Ritchie, J.L., Narahara, K.A., Trobaugh, G.B., Williams, D.L. and Hamilton, G.W.: Thallium-201 myocardial imaging before and after coronary revascularization: Assessment of regional myocardial blood flow and graft patency. Circulation (1977); 56:830-836.

165. Iskandrian, A.S., Scherer, H., Croll, M.N., Bemis, C.E., Segal, B.L., Kimbris, D. and Wallner, R.: Exercise ^{201} Thallium myocardial scans in patients with disease limited to the secondary branches of the left coronary system. Clin Cardiol (1979); 2:121-125.

166. Verani, M.S., Marcus, M.L., Spoto, G., Rossi, N.P., Erhardt, J.C. and Razzak, M.A.: Thallium-201 myocardial perfusion scintigrams in the evaluation of aortocoronary saphenous bypass surgery. J Nucl Med (1978); 19:765-772.

167. Bulkley, B.H. and Hurchins, G.M.: Myocardial consequences of coronary artery by-pass garft surgery. The paradox of necrosis in areas revascularisation. Circulation (1977); 56: 906.

168. Kollbash, A.J., Call, T.D., Bush, C.A., Tetalman, M.R. and Lewis, R.P.: Myocardial perfusion as an indicator of graft patency after coronary artery by-pass surgery. Circulation (1980); 61:882.

169. Murray, R.C., McKillop. J.H., Bessent, R.G., Turner, J.G., Lorimer, A.R., Hutton, L., Greig, W.R. and Lawrie, T.D.V.: An evaluation of thallium-201 exercise scintigraphy in coronary heart disease. Br Heart J (1979); 41:568-574.

170. Rehn, T., Griffith, I., Achuff, S., Pond, M. and Becker, I.: Value and limitations of thallium-201 imaging to detect by-pass graft patency. Am J Cardiol (1979); 43:434 (abstract).

171. Sbarbaro, J.A., Karunaratne, H., Cantez, S., Harper, P.V. and Resnekov, I.: Thallium-201 imaging in a assessment of aorto-coronary bypass garft patency. Br Heart J (1979); 42: 553-561.

172. Walnwright, R.J., Brennand-Roper, D.A., Maisey, M.N. and Sowton, E.: Exercise Thallium-201 myocardial scintigraphy in the follow-up of aortocoronary bypass graft surgery. Br Heart J (1980); 43:56-66.

173. Hirzel, H.O., Neusch, K., Gruentzig, A.R. et al: Short and long term changes in myocardial perfusion after percutaneous transluminal coronary angiography assessed by thallium-201 exercise scintigraphy. Circulation (1981); 63:1001.

174. Scholl, J.M., Chaitman, B.R., David, P.R. et al: Exercise electrocardiography and myocardial scintigraphy in the serial evaluation of the results of recutaneous transluminal coronary angioplasty. Circulation (1982); 66:380.

175. Verani, M.S., Tortoledo, F.A., Van Reet, R.E. et al: Quantitative analysis of regional myocardial perfusion after transluminal coronary angiography. Am J Cardiol (1983); 1: 589 (abstract).

176. Lavender, J.P., Lowe, J., Baker, J.R. et al: Gallium-67 citrate scanning in neoplastic and inflammatory lesions. Br J Radiology 1971; 44:361-366.

177. Littenburg, R.I., Taketa, R.M., Alazraki, N.P. et al: Gallium-67 for localization of septic lesions. Ann Intern Med (1973); 79:403-406.

178. Hoffer, P.B.: Mechanisms of localization. In: Hoffer, P.B., Bekerman, C., Henkin, R.E., ed. Gallium-67 imaging. New York: Wiley (1978); 3-8.

179. Tsan, M.F.: Mechanism of gallium-67 accumulation in inflammatory lesions. J Nucl Med (1985); 26:88-92.

180. Pinsky, S.M. and Henkin, R.E.: Gallium tumour scanning, Seminars in Nuclear Medicine (1976); 6:397-410.

181. Fogh J: Gallium-67 accumulation in malignant tumors and in pre-lactating or lactating breast. Proc. $oc. Exp. Biol. Med., 1971,138, 1086-1091.

182. Hoffer, P.B., Huberty, T., Khayam-Bushitt. The association of -67 and Lactoferrin. J Nucl Med (1977); 18:713-717.

183. Bennet, R.M., Mohla, C.: A solid phase radioimmunoassay for the measurement of lactoferrin in human plasma: Variations with age, sex and disease. J Lab Clin Med (1976); 88:156-166.

184. Hoffer, P.B., Miller-Catchpole, R., Turner, D.A.: Demonstration of lactoferrin in tumor tissue from two patients with positive gallium scans. J Nucl Med (1979); 20:424-427.

185. Hoffer, P.: Gallium: Mechanisms. J Nucl Med (1980); 21:282-285.

186. Gelrud, L.G., Arseneau J.C., Milder M.S. et al. The kinetics of gallium-67 incorporation into inflammatory lesions: Experimental and clinical studies. J Lab Clin Med (1974); 83:489-495.

187. Wright, D.G., Pizzo, P.A., Jones, A.E. et al.: Studies of Ga-67 uptake at sites of neutrophil exudation. Clin Res (1979); 27:360A (abstract).

188. Menon, S., Wagner, H.N. Jr, Isan, M.F.: Studies on gallium accumulation in inflammatory lesions: II uptake by staphylococcus aureas: Concise communication. J Nucl Med (1978); 19:44-47.

189. Winchell, H.S.: Mechanism for localization of radiopharmaceuticals in neoplasms. Semin Nucl Med (1976); 6:371-378.

190. Hayes, R.L., Brown, B.H.: Biokinetics of radiogallium. In Nuklear-medizinelsche Fortschritte, Gesellschaft fur Nuklearmedizin, Munich. Pabst HW, Hoer G, Schmidt HAE, eds. Schattauer Verlag. Stuttgart. (1975); 837-847.

191. Hayes, R.L.: The tissue distribution of gallium radionuclides. J Nucl Med (1977); 18:740-741.

192. Hayes, R.L., Rafter, J.J., Byrd, B.L. et al. Studies of the in vivo entry of Ga-67 into normal and malignant tissue. J Nucl Med (1981); 22:325-332.

193. English, D., Clairoux-Moreau, S., McPherson, T.A.: Uptake of Ga-67 citrate by physiologically-impaired cells in vitro. Clin Res (1977); 25:693 Abstract.

194. Anghileri, L.J.: Studies on the accumulation mechanisms of radioisotopes used in tumor diagnostic. Strahlentherapie (1971); 142:456-462.

195. Anghileri, L.J.: Mineral metabolism in tumours and ^{67}Ga accumulation. J Nucl Med (1974); 13:272.

196. Anghileri, L.J., Heidbreder, M.: On the mechanism of accumulation of ^{67}Ga by tumors. Oncology (1977); 34:74-77.

197. Sephton, R.G. and Harris. Brief communication: Gallium-67 citrate uptake by cultured tumor cells stimulated by serum transferrin. J Nat'l Cancer Inst (1976); 54:1263-1266.

198. Larson, S.M., Rasey, J.S., Allen, D.R. et al. A transferrin mediated uptake of gallium-67 by EMT-6 sarcoma. II studies in vivo (BALB/c mice): concise communication. J Nucl Med (1979); 20:843-846.

199. Camargo, E.E., Wagner, H.N. Jr., Tsan, M.F.: Studies of gallium accumulation in inflammatory lesions. IV. Kinetics of accumulation and role of polymorphonuclear leukocytes in the distribution of gallium in experimental inflammatory exudates. Nucl Med (1979); 18:147-150.

200. Vallabhajosula, S.R., Harwig, J.F., Siemsen, J.K. et al.: Radiogallium localization in tumors: Blood binding and transport and the role of transferrin. J Nucl Med (1980); 21:650-656.

201. Scheffel, U., Tsan, M.F.: Effect of serum unbound iron-binding capacity on the tissue distribution of ^{67}Ga in abscess-bearing rabbits. J Nucl Med (1980); 19:274-277.

202. Tsan, M.F. and Scheffel, U.: Mechanism of Gallium-67 accumulation in tumors. J Nucl Med (1986); 27:1215-1219.

203. Edwards, C.L., Hayes, R.L.: Tumour scanning with Ga-67 citrate. J Nucl Med (1969); 10:103-105.

204. Beckerman, C., Hoffer, P.B. and Bitran, J.D.: The role of Gallium-67 in the clinical evaluation of cancer. Seminars in Nucl Med (1985); 1:72-103.

205. Johnston, G.S., Go, M.F., Benua, R.S. et al.: Gallium-67 citrate imaging in Hodgkin's disease: final report of cooperative group. J Nucl Med (1977); 18:692-698.

206. Andrews, G.A., Hubner, K.F., Greenlaw, R.H.: Gallium-67 citrate imaging in malignant lymphoma: final report of a cooperative group. J Nucl Med (1978); 19:1013-1019.

207. Lanteri, R.L., Fawcett, H.D., McKillop, J.H. and McDougall, I.R.: Ga-67 or In-111 white blood cell scans for abscess detection: 4 case for In-111. Clin Nucl Med (1980); 5:185-188.

208. Waxman, H.D.: The role of nuclear medicine in pulmonary neoplastic processes. Seminars in Nucl Med (1986); 4:285-295.

209. Grove, R.B., Reba, R.C., Eckelman, W.C., et al.: Clinical evaluation of radiolabeled bleomycin (bleo) for tumor detection. J Nucl Med (1974); 15:386-390.

210. Nieweg, O.E., Beckhuis, H., Piers, D.A. et al: Scintigraphy with ^{57}Co-bleomycin in the detection of lung cancer: a review of 268 well-documented patients. Cancer (1984); 53:1675-1681.

211. Goodwin, D.A., Meares, C.F., DeRiemer, L.H. et al: Clinical studies with In-111 BLEDTA: a tumor conjugate of bleomycin with a bifunctional chelating agent. J Nucl Med (1981); 22:323-325.

212. Ohta, H., Yamamoto, K., Endo, K. et al.: A new imaging agent for medullary carcinoma of the thyroid. J Nucl Med (1984); 25:323-325.

213. Ohta, H., Endo, K., Fujita, T. et al.: Imaging of soft tissue tumors with Tc(V)-99m dimercaptosuccinic acid: a new tumor-seeking agent. Clin Nucl Med (1984); 9:568-573.

214. Watkenson, J., Clarke, S. and Sheheen, O.: An assessment of Technitium-99m (v) dimercaptosuccinic acid uptake in patients with head and neck squamous carcinoma. Nucl Med Communication (1987); 8:265 (abstract).

215. Hilditch, T.F., Connel, J.M., Elliott, A.T., Murry, T. and Reed, N.S.: Poor results with Technitium-99m (V) DMSA and Iodine-131 MIBG in imaging of medullary thyroid carcinoma. J Nucl Med (1986); 27:1150-1153.

216. Nostrand, D.V., Neutze, J. and Atkins, F.: Side effects of rational dose Iodine-131 therapy for metastatic well differentiated thyroid carcinoma. J Nucl Med (1986); 27:1519-1527.

217. Woolner, L.B.: Thyroid carcinoma, pathological classification with data on prognosis. Seminars Nucl Med (1971); 1:481.

218. Mansfield, C.M. and Park, C.H.: Contribution of radionuclide imaging to radiation oncology. Seminars of Nucl Med (1985); 1:28-43.

219. Shapiro, B,. Copp, J.E., Sisson, C.S., Eyre, P.L., Wallis,J. and Beierites, W.: Iodine-131 Metaiodobenzylquanidine for the locating of suspected pheochromocytoma: experience in 400 cases. J Nucl Med (1985); 26:576-585.

220. Ansari, A.N., Siegel, M.F., Dequattro, V. and Gazarian, L.: Imaging of medullary thyroid carcinoma and hyperfunctioning adrenal medulla using iodine-131 metaiodobenzynquanidine. J Nucl Med (1986); 27:1858-1860.

221. Kalff, V., Sisson, J.C., Beierwaltes, W.H. et al.: Adrenal gland identification: pre-operative assessment. Surgery (1982); 91:374-376.

222. Sisson, J.C., Shapiro, B., Beierwaltes, W.H. et al.: Radiopharmaceutical treatment of malignant pheochromocytoma. J Nucl Med (1984); 24:197-206.

223. Ikekubo, K., Habuchi, Y., Jeong, S., Yanaguchi, H., Saiki, Y. et al.: A follow-up study using iodine-131 metaiodobenzylguanidine imaging in patients with neuroblastoma. Clinical Nuclear Medicine (1986); 11:777-780.

224. Feldman, J.M., Frankel, N., Coleman, R.F.: Platelets uptake of pheochromocytoma scanning agent (I^{131}) metaiodobenzylguanidine. Metabolism (1984); 33:397-399.

225. Feldman, J.M., Blinder, R.A., Lucas, K.J. and Coleman, R.F.: Iodine-131-Metaiodobenzylguanidine scintigraphy of carcinoid tumours. J Nucl Medicine (1986); 27:1691-1696.

226. Lewington, V., McEwan, A.J., Fin, D. et al.: An evaluation of MIBG uptake by metastatic carcinoid tumour. Nucl Med Communications (1987); 8:266 (abstract).

227. Clarke, S., Lazarus, C., Edwards S., Roden T., and Melsey M.N.: A comparison of 1^{131} MIBG and Tc^{99m} pentavalent DMSA for imaging patients with medullary carcinoma of the thyroid. Nuclear Medicine (1986); 475-476.

228. Conry, B.G., Bomanji, J., Britton, K.E., Reznek, R.H. and Besser, G.M.: Comparison of the roles of ultrasound, U$, x-ray computed tomography, CT and ^{123}1-meta-iodobenzylguanidine, MIBG in neuroendocrine tumours. Nuclear Medicine Communications (1987); 8:266 (abstract).

229. Keenan, A.M., Harbert, J.C. and Larson S.M.: Monoclonal antibodies in Nuclear Medicine. J Nuclear Medicine (1985); 26: 531-537.

230. Kohler, G., Milstein, C.: Continuous cultures of fused cells secreting antibody of predefined specificity. Nature (1975); 256:495-497.

231. Carrasquillo, J.A., Krohn, K.A., Beamier, P. et al.: Diagnosis of and therapy for solid tumours with radiolabeled antibodies and immune fragments. Cancer Treat Rep (1984); 68: 317-328.

232. Mach, Y.P., Buchegger, F., Forni, M. et al.: Use of radiolabeled anti-CEA for the detection of human carcinomas by external photoscanning and tomoscintigraphy. Immunol Today (1981); 2:239-249.

233. Order, S.E., Klein, J.L., Ettinger, D. et al.: Use of isotopic immunoglubulin in therapy. Cancer Res (1980); 40: 3001.

234. Larson, S.M. and Carrasquillo, J.A.: Nuclear oncology : Current perspectives. Nuclear Medicine Annual, edited by Leonard, M., Freeman and Heidi Weismann. Raven press, New York (1983); 167-197.

235. Morrison, R.T., Lyster, D.M., Alcorn, L.N. et al.: Gamma scintigraphy using TC-99m labeled antibody to human chronic ganadotropin. Clin. Nuclear Medicine (1984); 9:20-24.

236. Rockoff, S.D, Goodenough, D.J., Mcintyre, K.R.: Theoretical limitations in the immunodiagnostic imaging of cancer with computed tomography and nuclear scanning. Cancer Res (1980); 40: 3054-3058.

237. Ott, R.J., Grey, L.J., Zivanovic, M.A. et al.: The limitations of the dual radionuclide subtraction technique for the external detection of tumours by radioiodine-labelled antibodies. Br J. Radiol (1983); 56:101-108.

238. Sharkey, R.M., Primus, F.J., Goldenberg, D.M.: Second antibody clearance of radiolabeled antibody in cancer radioimmuno detection. Proc Natl Acad Sci USA (1984); 81:2843- 2846.

239. Bradwell, A.R. and Dykes, P.W.: Wither tumour imaging using radiolabelled antibodies? ~~Communication in press.~~ Nuclear Medicine Communications, (1988) 9, 328-330.

240. Britton, K.E. and Granowska, M.: Radioimmunoscintigraphy : A way ahead. ~~Communication in press.~~ Nuclear Medicine Communications (1988) 9, 330-332

241. Charkes, N.D., Sklaroff, D.M., Gersohn, C.J. et al.: Tumour scanning with radioactive 131-Ceasium. J Nuclear Medicine (1965); 6:300-306.

242. Cox, P.H., Belfer, A.J. and Vander Pompe, W.B.: Thallium-201 chloride uptake in tumours, a possible complication in heart scintigraphy. British Journal of Radiology (1976); 49:767-768.

243. Tonami, N., Michigishi, T., Bunko H., et al.: Clinical tumour scanning with Tl-201 chloride. J Nuclear Medicine (1977); 18:617 (abstract).

244. Ochi H., Sawa H., Fukuda T, et al.: Thallium-201 chloride thyroid scintigraphy to evaluate benign and/or malignant nodules - usefulness of the delayed scan. Cancer (1982); 50:236-240.

245. Hoefngal, C.A., Delpart, C.C., Marcuse, H.R.: The role of Tl-201 total body scintigraphy in follow up of thyroid carcinoma. J Nuclear Medicine (1985); 26:31 (abstract).

246. Terui, S., Oyamada, H., Nishikawa, K. et al.: Tl-201 chloride scintigraphy for bone tumours and soft part sarcomas. J Nuclear Medicine; 25:114 (abstract).

247. Kaplan, W.D., Takvorian, T., Morris, J.H. et al.: Thallium-201 brain tumour imaging : A comprehensive study with pathological correlation. J Nuclear Medicine (1987); 28:47-52.

248. Senga, O., Miyakawa, M., Shirota, H. et al.: Comparison of Tl-201 chloride and GA-67 citrate scintigraphy in the diagnosis of thyroid tumour : Concise communication. J Nuclear Medicine (1982); 23:225-228.

249. Beller, G.A. and Watson, D.D.: Myocardical thallium kinetics in ischemia and infarction. Prog Nuclear Medicine (1980); 6:35-55.

250. Carlin, R.D., Jan, K.: Mechanism of Thallium extraction in pump perfused canine hearts. J Nuclear Medicine (1985); 26: 165-169.

251. Gewirtz, H., O'Keefe, D.D., Pohost, G.M. et al: The effect of ischemia on thallium-201 clearance from the myocardium. Circulation (1978); 58:215.

252. Linde, R., and Basso, L.: Hodgkins Disease with hypercalcemia detected by thallium-201 scintigraphy. J Nucl Med (1987); 28:112-115.

253. Ziada, G., Mohammed, M., Bahr, R., Abdel-Dayem, H.: Background subtraction in quantitative Thallium-201 analysis, normal voluntar study. Nucl compact, 1986, 16, 285-290.

254. Jones, S.E. and Salmon, S.E.: The role of radionuclides in clinical oncology. Sem Nucl Med (1976); 6:331-346.

255. Kaplan, H.S. and Rosenberg, S.A.: The management of Hodgkin's disease. Cancer (1976); 36:796.

256. Alarazki, N.P., Ramsdell, J.W., Taylor, A., Friedman, P.L., Peters, R.M., Tisi, G.M.: Reliability of gallium scan chest radiography compared with mediastinoscopy for evaluating mediastinal spread in lung cancer. Am Rev Respir Dis (1978); 117:415-420.

257. Alarazki, N.P.: Usefulness of gallium imaging in the evaluation of lung cancer. CRC Crit Rev Diagn Imaging (1980); 13:249-267.

258. Salvatore, M., Carratu, L., and Porta, E.: Thallium-201 as a positive indicator for lung neoplasms. Preliminary experiments. Radiology (1976); 121:487-488.

259. Hisada, K., Tonami, N., Myiamae, T., Hiraki, Y., Yamazaki, T., Maeda, T., Nakajo, M.: Clinical evaluation of tumour imaging with Tl-201 chloride. Radiology (1978); 129:497-500.

260. Spiro, S.G. and Goldstraw, P.: The staging of lung cancer. Thorax (1984); 39:401-407.

261. Ashraf, M.H., Nilson, P.L., Walesby, R.K.: Selection by mediastinoscopy and long-term survival in bronchial carcinoma. Ann Thorac Surg (1980); 30:208-214.

262. Rigler, G.: Earliest roentgenographic signs of carcinoma of the lung. JAMA (1966); 195:655.

263. Fosburg, R.G., Hopkins, G.B., Kan, M.K.: Evaluation of mediastinum by gallium-67 scintigraphy in lung cancer. J Thorac Cardiovasc Surg (1979); 77:76-82.

264. Lumia, S.L., Ruckdeschel, J.C., McKneally, M.F.: Noninvasive evaluation of mediastinal metastases in bronchogenic carcinoma: A prospective comparison of chest radiography and gallium-67 scanning. Cancer (1981); 47:672.

265. DeMeester, T.R., Golomb, H.M., Kirchner, P. et al.: The role of gallium-67 scanning in the clinical staging and pre-operative evaluation of patients with carcinoma of the lung. Ann of Thorac Surg (1979); 28(5):451-464.

266. Richardson, J.V., Zenk, B.A., Rossi, N.P.: Pre-operative noninvasive mediastinal staging in baronchogenic carcinoma. Surgery (1980); 88:382-385.

267. Neumann, R., Merino, M., Hoffer, P.B.: Gallium-67 in hilar and mediastinal staging of primary lung carcinoma. J Nucl Med (1980); 21:32.

268. Hirleman, M.T., Yiu-Chiu, V.S., Chiu, L.C.: The resectability of primary lung carcinoma. A diagnostic staging review. CT:J Compat Tomography (1980); 4:146.

269. Milroy, K., Smith, M.L., Farchney, A. et al.: Mediastinal imaging in lung cancer. Quarterly Journal of Medicine (1986); 231:715-723.

270. Julian, P., Waxman, A.D., Birnbirg, F.: The staging lung cancer: A comparison of chest x-ray, linear tomography, computer tomography and gallium scintigraphy. J Nucl Med (1982); 23:20 (abstract).

271. Okerlund, M.D., Sheldon, K., Corpuz, S. et al.: High sensitivity localization of parathyroid tumours by nuclear imaging in 50 proven cases. J Nucl Med (1984); 25:19 (abstract).

272. Winzelberg, G.G., Melada, G.A., Hydovitz, J.D.: False positive thallium-201 parathyroid scan of the mediastinum in Hodgkin's lymphoma. Am J Roentgenol (1986); 147:819-821.

273. Togawa, T., Suzuki, A., Kato, K. et al.: Relation betwen Tl-201 to Ga-67 uptake ratio and histological type in primary lung cancer. Eur J Cancer Clin Oncol (1985); 28:925-930.

274. Gravelle, I.H.: Diagnosis imaging in breast cancer. Clinics in Oncology. W.B. Saunders Company Ltd. (1982); 1:795-820.

275. McLean, R.G. and Ege, G.N.: Prognostic value of auxillary lymphoscintigraphy in breast carcinoma patients. J Nucl Med (1986); 27:1116-1124.

276. Ege, G.N.J: Internal mammary lymphoscintigraphy: A rational adjunct to the staging and management of breast carcinoma. Clinical Radiology (1978); 29:453-456.

277. Matsuo, S.: Studies on the metastasis of brast cancer to lymph nodes. Diagnosis of metastasis to internal mammary nodes using radiocalloid. Acta Med Okayama (1974); 28:361-371.

278. Berry, R.J. and Ek, P.I.: Pretreatment assessment of cancer. Clinical Nuclear Medicine edited by Maisey, M.N., Britton, K.T. and Gilday, D.L. (1983); 365-370.

279. Lee, B.J., Nelson, J.H. and Schuarz, G.: Evaluation of lymphoangiograp[hy, inferior vena cava graphy and intravenous pyleography in the clinical staging and management of Hodgkin's disease and lymphosarcoma. New Eng J Medicine (1964); 271:327-337.

280. Timothy, A.R., Sutcliffe, S.B., Lister, T.A., Wrigley, P.F. and Jones, A.E.: The management of stage III A Hodgkins disease. Int J Radiation Oncology Biol Phys (1980); 6:135-142.

281. Cowan, R.J.: Conventional radionuclide brain imaging in the era of transmission and emission tomography. Seminars in Nucl Med (1986); 63-73.

282. Buell, U., Niendorf, H.P., Kazner, E., Lanksch, W., Wilske, J., Steinhoff, H., Gahr, H.: computerized tranaxial tomography and cerebral serial scintigraphy in intracranial tumours - rates of detection and tumour type identification. J Nucl Med (1978); 19:476-479.

283. Baker, H.L., Houser, O.W., Campbell, J.K.: National cancer institute study: Evaluation of computerized tomography in the diagnosis of intra cranial neoplasms. Radiology (1980); 136:91-96.

284. Waxman, A.D., Beldon, J.R., Richll, W. et al: Steroid induced suppression of gallium uptake in tumours of the central nervous system: Concise communication. J Nucl Med (1978); 480-482.

285. McKillop, J.H.: The bone scan in primary bone tumours and marrow disorders. Bone scanning in clinical practice. Ed. Ignac Fogelman Springer-Verlag, (1986); 61-70.

286. McKillop, J.H; Bone scanning in metastatic disease. Bone scanning in clinical practice. ED. Ignac Fogelman, springer-verlag, 1986; 41-60.

287. Goodwin, D.A. and Mear, S: Radiolabeled antitumour agents. Sem. Nucl. Med., 1976, 389-409.

288. Simon, M.A., Kirchner, P.T.: Scintigaphic evaluation of primary bone tumours. J Bone Joint Surg, 62, 758-764.

289. King, M.A., Casarett, G.W., Weber, D.A., Burgener, F.A., O'Mara, R.E., Wilson, G.A.: A study of irradiated bone. III Scintigraphic and radiographid detection of radiation induced osteosarcoma. J Nucl Med (1980); 21:426-431.

290. McKillop, J.H., Etcubanas, E. and Goris, M.L.: The indication for and limitations of bone scintigraphy in osteogenic sarcoma. A review of 55 patients. Cancer (1981); 48:1133-1138.

291. Papanicolaou, N., Kozakewich, H., Teves, S., Goorink, A., Emans, J.: Comparison of the extent of osteosarcoma between surgical pathology and skeletal scintigraphy. J Nucl Med (1982); 23:7 (abstract).

292. Goldman, A.B., Becker, M.H., Braunstein, P., Francis, K.C., Genieser, N.B. and Firooznia, H.: Bone scanning - osteogenic sarcoma. Correlation with surgical pathology. Radiology (1975); 124:83-90.

293. Chew, F.S., Hudson, T.M., Enneking, W.F.: Radionuclide imaging of soft tissue neoplasms. Seminars of Nucl Med (1981); 4:266-276.

294. McKillop, J.H. and Fogelman, I.: Bone scintigraphy in benign bone disease. British Med J (1984); 28:264-266.

295. Cornelius, E.A. and Atterbury, C.E.: Problems in the imaging diagnosis of hepatoma. Clinical Nucl Med (1984); 9:30-38.

296. Kawasaki, H., Sakaguchi, S., Toshitake I.: The value of B-scan ultrasonography in the diagnosis of liver cancer. Am J Gastroenterol (1978); 69:436.

297. Coakley, A.J. and Wright, E.D.: Selenomethionine liver scanning in the diagnosis of hepatoma. Br J Radiol (1980); 537-538.

298. Broderick, T.W., Gosink, B., Menuck, L., Harris, R and Wilcox, J.: Echographic and radionuclide detection of hepatoma. Radiology (1980); 135:149-151.

299. Waxman, A.D., Richmond, R., Juttner, H. et al: Correlation of contrast angiography and histologic pattern with gallium uptake in primary liver-cell carcinoma: non-correlation of alpha fetoprotein. J Nucl Med (1980); 21:324-327.

300. Hoffer, P.B.: Clinical investigation with receptor-specific and other tumour-seeking radiopharmaceuticals. Clinic in Oncology (1986); 5:183-198.

301. Halpern, S. and Hagan, P.H.: Gallium-67 citrate imaging in neoplastic inflammatory disease. Nuclear Medicine Annual ed. by Leonard M. Freeman and Heidi S. Weismann, Raven Press, New York, (1980); 219-265.

302. Diplazzi S, Conti, F, Cottone, M., et al: Scintiscanning with Ga-67 in detection of primary carcinoma of the liver associated with cirrhossis. Radio Med (Torino); 64:53-56.

303. Mansfield, C.M. and Park, C.H.: Contribution of radionuclide imaging to radiation oncology. Seminars in Nucl. Med. 1985, 1:28-45.

304. Kim, E.E and Haynie, T.P.: Role of nuclear medicine in chemotherapy of malignant lesions. Seminars in Nucl Med., 1985, 1:12-20.

305. Priestman, T.J and Baum, M.: Evaluation of quality of life in patients receiving treatment for advanced breast cancer. Lancet, 1976, I:899-901.

306. Perez, C.A., Stanley, K., Rubin, P. et al.: A prospective randomized study of various irradiation doses and fractionation schedules in treatment of inoperable non-Oat-cell carcinoma of the lung. Cancer, 1980; 45:2744-2753.

307. Patterson, A.H.G. and McReady, V.R.: The current status of gallium-67 scanning Br. J. Radiol, 1975, 48,944 (abstract).

308. Kinoshita, F., Ushio, T., Maetawa, A.: Scintiscanning of pulmonary diseases with Ga-67 citrate. J. Nucl. Med. 1974; 15:227.

309. Bitran, J.D., DeMeester, T.R., Rezaizadeh, K. Clinicopathologic correlations demonstrating the failure of gallium-67 scanning in determining response in radiotherapy. Chest, 1978; 73:356.

310. Roswit, B., Patno, M.E., Rapp, R., Vienbergs, A., Feder. B., Stuhlbarg, J. and Reid, C.B.: The survival of patients with inoperable lung cancer. A large scale randomized study of radiation therapy versus placebo. Radiology, 1968; 90:688-697.

311. Bloedorn, F. G., Cowley, R. A., Cuccia, C.A, Mercado, R. Jr., Wizenberg, M.J, and Linberg E J.: Preoparative irradiation in bronchogenic carcinoma Am. J. Roentgenol. Radium. Ther. Nucl. Med., 1964; 92:77-87.

312. Hellman, S., Kligerman, M.M., von Eassen, C.F. and Scibetta, M.P. Sequelae of radical radiotherapy of carcinoma of the lung. Radiology, 1964; 82:1055-1061.